

The copyright of this thesis vests in the author. No quotation from it or information derived from it is to be published without full acknowledgement of the source. The thesis is to be used for private study or non-commercial research purposes only.

Published by the University of Cape Town (UCT) in terms of the non-exclusive license granted to UCT by the author.

4

**RAINFALL VARIABILITY OVER WESTERN AND  
SOUTHWESTERN TANZANIA, THE MONSOON  
AND POTENTIAL INDIAN AND ATLANTIC  
OCEAN INFLUENCES**

**Amin Twazhirwa Mapande**

**A thesis submitted in fulfilment of the  
degree of Master of Science**

**Department of Environmental and Geographical Sciences,  
University of Cape Town**

**July 2003**

## **CONTENTS:**

### **List of Figures / Tables:**

### **Acknowledgements**

### **Abstract**

## **CHAPTER 1: Introduction:**

### **1.1 Monsoon**

### **1.2 Monsoon definition and monsoon regions**

### **1.3 Onset and withdrawal of the monsoon and related activity**

### **1.4 Causes of the monsoons**

### **1.5 Climatic seasons of Tanzania and Literature Review**

## **CHAPTER 2: Data and Methodology**

### **2.1 Data used in the study**

### **2.2 Methodology**

#### **2.2.1 Rainfall index**

#### **2.2.2 Composite analyses**

#### **2.2.3 Cross sectional analyses**

## List of Figures

<b>Figure</b>	<b>Description</b>
2.0	Tanzania Map showing the study area and 6 rainfall stations
2.3.1	Mean annual area averaged rainfall distribution over western and southwestern Tanzania
2.3.2	Mean annual rainfall distribution of six stations used for study
3.1.1(a-h)	Mean monthly climatological field pattern
4.1(a-c)	Seasonal rainfall time series of stations used in the study
4.2.1 (a-h)	Monthly wet years composite anomaly evolution
4.2.2 (a-h)	Monthly dry years composite anomaly evolution
5.2(a)	CMAP pentad averaged rainfall time series for the wet and dry years over western and southwestern Tanzania

## **Abstract**

Potential linkages between the monsoon regions of the Atlantic and Indian Oceans and seasonal rainfall variability in western and southwestern Tanzania are investigated. Rainfall over this region is characterized by large intraseasonal and interannual variability. This fluctuation of rainfall can significantly affect rain-fed agricultural production and other hydrological applications. Anomalies in the monsoon circulations over Atlantic and Indian oceans contribute to the rainfall variability over the region. A spatially rainfall index was used to delineate anomalous wet/dry seasons during the 1968 – 1998 period. Various composite fields (i.e. sea surface temperature (SST), winds, latent heat fluxes, outgoing longwave radiation (OLR), velocity potential and divergent wind, moisture flux and precipitation) were used to understand the evolution of the wet and dry years over the region and associated monsoon circulation over these oceans.

Result show that wet years are associated with lower tropospheric westerly anomalies from the tropical southeast Atlantic Ocean and the Congo basin converging over the study zone with weak easterly anomalies from the tropical western Indian Ocean. An anticyclonic anomaly over the central Indian ocean is another prominent feature, which tends to weaken the mean easterly wind flow from this ocean to the region. At upper levels during the wet season, easterly anomalies build up over the tropical western Indian Ocean which enhance the convective instability at low levels, a necessary condition for low-level convergence and precipitation to occur over the region.

In addition, wet years are associated with positive latent heat flux and negative OLR anomalies over the region, which imply increased local evaporation and convection. The composite velocity potential anomaly indicates a strong low-level convergence at 850hPa with associated upper level divergent anomaly.

In contrast, lower tropospheric southeasterly to easterly anomalies from the tropical South Indian Ocean during November to February and upper level westerly anomalies over Tanzania are evident during the dry seasons. This upper level feature suggests a weaker Walker circulation and unfavourable conditions for low-level ascent and convection since it implies upper level convergence and subsidence. A lower tropospheric cyclonic anomaly over the tropical Southeast Atlantic and an anticyclonic anomaly over the southwestern Indian Ocean are prominent features during dry seasons. These circulations act to weaken mean easterly flow across the tropical southern African and reduce the flux of moisture into Tanzania from these oceans (Atlantic and Indian). Another notable feature during the dry years is a cyclonic anomaly over the tropical central Indian Ocean which tends to weaken the northeast monsoon flow towards Tanzania from the Indian Ocean. Positive OLR and negative latent heat flux anomalies are apparent which indicate reduced evaporation and convection consistent with rainfall decrease during the dry seasons. Velocity potential and divergent wind plots show a strong low-level divergence at 850hPa and upper level convergent anomaly.

It is also noteworthy that during the wet seasons over western and southwestern Tanzania, rains normally began earlier and end later whilst for dry seasons, rains are associated with late onset and early cessation. During wet seasons, rains are more evenly distributed over the region with strong wet spells occurring during the season. The opposite is true for dry seasons. Often the latter experience late onset of the rains with an extended dry spell occurring early after the onset, and relatively few wet spells.

## CHAPTER 1

### Introduction

In many tropical countries, the economy is essentially dependent on agriculture, which in turn depends mostly on the seasonal rains. Hence, the concept of season, seasonal rains; monsoon, etc. are found in all traditions dealing with economic, social, political and religious aspects of life in the tropical regions.

The annual cycle of the monsoon systems has led the inhabitants of monsoon regions to divide their lives, customs, and economies into two distinct phases; the "wet" and the "dry" (Webster et al., 1998). The wet phase refers to the rainy season during which warm, moist, winds blow inland from the tropical oceans. The dry phase refers to the other half of the year when winds bring cool and dry air from the winter continents. This distinct variation of the annual cycle occurs over southern Asia, northern Australia, West Africa, and in tropical America. In some locations for example, in the Asia-Australia sector, the dry winter air flows across the equator towards the summer continents, picking up moisture from the warm tropical oceans to become the wet monsoon of the summer continent. In this manner, the dry winter monsoon is linked to the wet summer monsoon and vice versa. All monsoons are influenced by three basic physical mechanisms; differential heating between the land and oceans; the Coriolis force; and the role of water which stores and releases energy as it changes from liquid to vapour and back (Latent heat). It is the combined effect of these three mechanisms, which produces the monsoon's characteristic reversals of winds and precipitation. In contrast, regions closer to the equator possess two rainy seasons.

For example, in equatorial East Africa, two rainy seasons occur during March to May (long rains) and October to December (short rains) as the Inter-tropical Convergence Zone (ITCZ) crosses the equator. The rainy seasons are sometimes referred to as the Southeast (SE) and the northeast (NE) East African monsoon (Okoola, 1996).

Agrarian-based communities have developed in the monsoon regions because of abundant solar radiation and precipitation, the two essential ingredients for successful agriculture. Agricultural practices have traditionally tied strictly to the annual cycle of monsoons. Although the regularity of the warm, moist and cool, dry phases of the monsoon would seem to be ideal for agricultural communities any small variations in the timing and quality of seasonal rainfall have the potential for significant consequences, such as droughts and floods.

A weak monsoon season typically results in less total rainfall than average and generally corresponds to low crop yields production and famine (Mhita, 1990; Webster et al., 1998). A strong monsoon usually produces abundant crops, although too much rainfall may produce devastating floods. A late or early onset of the monsoon, or an extended breaks in the monsoon rains may have devastating effects on the agriculture even if the mean annual rainfall is near average. As a result, forecasting monsoon variability on time-scales ranging from days to month is an issue of immense importance. The economy of Tanzania largely depends on agriculture, which in turn is highly vulnerable to variability in rainfall amount and distribution.

The spatial and temporal distribution of rainfall is sometimes poor while the intensity may vary from minimal to extreme amounts. Extremes in rainfall occurrence may result in droughts and floods, which are often associated with food, energy, and water shortage, loss of life and property and many other socio-economic disruptions. Two distinct circulations are experienced in northern and coastal Tanzania, the Northeast (NE) and the Southeast (SE) monsoon. The former is dominant during austral summer (December to February) while the Southeast (SE) monsoon occurs during boreal summer (June to August) feeding flows into the Southwest (SW) Indian monsoon, with transition seasons during September -November and March to May. The Inter-tropical Convergence Zone (ITCZ) passes over the region twice a year and associated with its passage are the two main rainfall seasons over northern Tanzania of March to May and October to December.

The complex topography and the existence of large lakes modify the monsoonal circulation and give rise to large spatial and temporal variation in precipitation over the region. This modification leads to a diffuse expression of the Inter tropical convergence Zone (ITCZ) near the surface and thus the ITCZ over East Africa is observed most clearly in the wind field near 700hPa (Anyamba, 1983; Mukabana and Pielke 1996). Over this region, the ITCZ is the major large-scale system controlling seasonal rainfall (Asnani, 1993).

Observational evidence suggests that strengthening of convection and latent heat release over the warmer oceanic areas occurs at the expense of convergence over Africa (Jury, 1992).

A strengthening of upper easterly flows over the tropical East African region during El Nino events results in increase (decrease) in moisture flux over Eastern (Southern) Africa (Hastenrath et al., 1993).

Nakamura, (1968), Johnson and Morth (1961) and Camberlin and Wairoto (1997) studied the origins and nature of the equatorial westerlies over East Africa and they showed that the existence of westerlies in the middle and lower troposphere was associated with rainfall in the region. Nieuwolt (1978) and Minja (1982) found droughts in East Africa to be associated with weak monsoons. In a case study during December/January season over southwestern Tanzania, Mpetta and Jury (2001) found that convective rainfall events were associated with an influx of Northeasterly Indian Ocean monsoon flow followed by increased westerly flow from the Guinea / Congo region.

Other research conducted to investigate various causes of rainfall variability in East Africa, include Ogallo (1989), Kabanda (1995), Mpetta and Jury (2001) who established that the El Nino/Southern Oscillation (ENSO) phenomenon has an influence on the occurrence of droughts in Tanzania. Research carried out in Tanzania (Ogallo, (1989)) to explore rainfall variability relationships with sea surface temperature (SST) have concentrated on inter-annual variability, teleconnections to other parts of Africa and its adjacent oceans, mechanisms of rainfall variability and extreme rainfall conditions.

However, relatively less research has been directed towards investigating the influence of the neighbouring (Atlantic and Indian) oceans on intra-seasonal, seasonal and inter annual rainfall variability in specific sub-regions of Tanzania.

In this study, rainfall variability of the western and southwestern area of Tanzania, lying between 4.75°S and 11.5°S and 29°E and 37°E is considered. Lake Tanganyika is to the west of this region while Lake Malawi lies to the south respectively. The area experiences one main prolonged rainy season (uni-modal regime), which usually begins in October and continues until April with the highest total around January and early February (Alusa and Mushi, 1973; East African Meteorological Department (EAMD), 1963a; Mhita, 1990).

### **1.1 Monsoon**

The word 'Monsoon' is believed to be derived from the Arabic word "Mausim" or from the Malayan word "Monsin", which means 'season'. Generally, it refers to the seasonal reversal of wind direction along the shores of the Indian Ocean, especially in the Arabian Sea, that blow from the southwest during one half of the year and from northeast during the other. In India for example, the summer monsoon rain along the west coast are referred to as the southwest monsoon because the surface winds are southwesterly. For the same reason, the winter rains along the east coast of India are referred to as the Northeast monsoon. In East and West Africa also, the word monsoon is associated with the wind direction. As monsoons have come to be better understood, the definition now denotes climatic systems in which the moisture increases dramatically in the warm season.

## 1.2 Monsoon definition and Monsoon regions

Attempt has been made (Khromov, 1957) to define the monsoon quantitatively and to separate monsoon regions from non-monsoon regions.

All the definitions are based on changes in surface wind direction between summer and winter seasons. The most widely accepted of these definitions is that given by Ramage (1971) who defines the monsoon from the following criteria:

- The prevailing wind direction shifts by at least  $120^\circ$  between January and July.
- The average frequency of the respective prevailing wind directions in January and July exceeds 40%.
- The mean resultant wind in at least one of the months exceeds 3m/s.
- Less than one cyclone- anticyclone alteration occurs every two years in either month in 5-degree latitude - longitude region.

For northern Australia, Holland (1986) defined the onset of the monsoon as the first occasion on which the smoothed 850hPa zonal wind components flow at Darwin ( $12^\circ 26'S$ ,  $130^\circ 52'E$ ) changes from easterly to westerly. Holland (1986) further showed that this definition of the monsoon over northern Australia corresponds well with rainfall over a large part of northern Australia.

Similar definitions based on the 'first' occurrence of the lower tropospheric westerlies have been suggested for other monsoon regions. Mean summer winds and moisture flux in these regions are westerly in the lower levels.

With the notable exception of western South America and Southwestern Africa, which have cool coastal SST due to upwelling, large areas within the belt between latitude 25°S and 35°N and longitude 30°W and 150°E satisfy this definition.

The monsoon region includes significant areas of tropical Africa, Southern Asia, Northern Australia and Central America (Ramage, 1971). It turns out to be essentially that region in which the ITCZ exhibits a large annual oscillation in position. In areas like West Africa, northern Australia and Southern Asia, the monsoon is defined in terms of equatorial lower tropospheric westerlies of the summer hemisphere. Those regions closer to the equator such as equatorial East Africa and Indonesia experience two rainy seasons which coincide with the transitions between the summer and winter monsoons of the Asian landmass / Indo-Pacific ocean regions. For example, in equatorial East Africa and Indonesia, the two rainy seasons occur in March to May and October to December, falling between the monsoon rainy periods at higher latitudes.

In East Africa, these semi-annual rainy periods are referred to as the "long" and "short" rains. The northward movement of the rain belt in March is rather slower than its southward movement in October. Thus, the rainy season of March to May is longer than the October-December season in Tanzania.

### **1.3 Onset and withdrawal of the monsoon and related activity**

The monsoon is one of the most dramatic climate phenomenon on the planet. The large areas involved in monsoons and the associated large-scale weather patterns suggest that they play an important role in global climate.

Delays in the onset of the monsoon rains generally cause alarm in the affected countries since the arrival of the monsoon usually heralds the end of the dry hot season. People usually look forward to the onset of rains to moisten the parched land, to fill the water reservoirs, to sow the seeds for their annual crops and to reduce the intensity of heat and corresponding physical discomfort.

Once the monsoon has arrived, it rarely runs in a consistent or constant manner since there is considerable intra-seasonal of dry and wet spells and interannual variability.

There are frequent departures from average conditions. Spells of very heavy rain cause floods and associated with outbreaks of epidemic and zoo endemic diseases (e.g. malaria, diarrhoea, rift-valley fever etc) and spells of very little rain cause withering of the traditional crops leading into droughts. Spells of very little rainfall are frequently referred to as 'breaks' in the monsoon.

A prolonged break generally causes alarm in the farming community. Typically there is some quasi-periodicity in the fluctuations of monsoon activity during the usual monsoon season. Five-day (pentad) oscillations have been known for nearly a century, Quasi-biweekly oscillation has been revealed by many authors (Murakami et al., 1986, Krishnamurti and Bhalme, 1976 while 30-50 day or Madden Julian oscillations are also well recognized (Madden and Julian, 1971, 1972). Very early withdrawal of the rains is a source of anxiety; very late withdrawal may also damage crops. Vagaries of the monsoon in respect of its arrival, intensity and withdrawal are perpetual source of concern for the farmers and indeed for the entire nation of Tanzania whose economy is mainly based.

#### **1.4 Causes of the monsoons**

The annual oscillation in the overhead position of the sun between the tropics of Cancer and Capricorn causes a corresponding oscillation in the position of the thermal equator on the earth's surface.

This is associated with the annual fluctuation of not only temperature but also pressure, winds, ITCZ, cloudiness, rains etc. This oscillation in solar maximum associated with differential heating between land and oceans is the main cause of the global monsoons.

Within this framework of global monsoons, there are regional variations. On the earth's surface, there are zonal asymmetries of land and sea. The distribution of land and sea in the monsoon areas leads to differential heating rates and drives the monsoonal circulations. Mountainous regions (e.g. the Himalayas, the Burma highlands and the East African highlands) influence the atmospheric response to the solar heating gradient by elevating the land surface heating of the atmosphere to the middle troposphere or by creating barriers to the atmospheric flow. The earth's rotation changes the relative trajectories of the air parcels as they move from the winter to the summer hemisphere. The response of the ocean to both the annual cycle of solar radiation and the winds induced by the differential heating of the land and the ocean is a critical element of the monsoon.

Temporal variations in the heating gradients are induced by the large heat capacity of water, the ability of the ocean to store heat in the mixed layer, changes in upwelling and revolution of heat by currents. These asymmetries in SST and upper ocean heat content cause variations in the intensity of the annual oscillation of the thermal equator and hence variations in the intensity of the monsoon oscillations over different regions.

Generally, it is not only spatial variations in the character of the monsoon but also large variations in the monsoon activity on interannual, decadal and large scales that are important. In one year, the monsoon gives heavy rains over a place but in another year, the same place gets very little rain in the monsoon season. Again, during the monsoon season there are fluctuations in the intensity of the monsoon activity, the periods of such fluctuations ranging from a few days (synoptic) to several weeks (intra seasonal).

### **1.5 Climatic Seasons of Tanzania and Literature Review**

Tanzania is one of three countries in East Africa and is located just south of the equator between latitude 12°S to 1°S and longitude 29°E to 41°E. The country lies within the seasonally arid tropics and includes high altitude areas, lowlands and many large water bodies. Synoptic features and wind flow patterns, which produce rains in East Africa are complex and are often influenced by topographical features. Several authors have studied rainfall patterns in East Africa (e.g. Griffiths, 1959; Nyenzi, 1992; and Ogallo, 1989) and generally have found that the ITCZ is the major source of rainfall in the region as it moves North and South of the equator lagging behind the solar angle.

The sun is approximately overhead in Tanzania at around 23rd of March, and again at around 22nd of September so that the ITCZ becomes most effective about a month later in April/May, and October/November. This ITCZ migration leads to the peak of the two main rainy seasons in Northern Tanzania including the Northern Coast. April is the rainfall peak of the March-May season and November, the peak of October -December season.

During this time, the pressure is high in the subtropical latitudes of northern and southern Africa and there is a general movement of air mass from these high-pressure belts towards the trough of low pressure in the equatorial region. At times this may result in well-organized southeasterly and northeasterly winds meeting in a zone of convergence (ITCZ) or more often, winds which are not well organized but which converge locally. Both convergences result in vertical upward motion of air, condensation into cloud and precipitation.

As the sun moves south in October and north in April, the western, southwestern, central and southern areas of Tanzania expect an onset of rain in October and cessation in April. Thus, western and southwestern Tanzania ( $4.75^{\circ}\text{S}$ - $11.5^{\circ}\text{S}$ ,  $29^{\circ}\text{E}$ - $37^{\circ}\text{E}$ ) experiences one prolonged rainy season (uni-modal regime) from mid-October until early April. However, in many years, there are frequently considerable variations in the position of the rain belt and large day-to-day variations in amount and distribution of rain exist, which are caused by changes in the area of low level convergence.

From December to March, high land surface temperatures give rise to a large low-pressure area centred between 10°S and 15°S with high pressure over North Africa and the Arabian Peninsula. This situation leads to a northeasterly dry air-stream over northern parts of the Tanzania bringing little rains in those areas. However, when this air-stream reaches southern Tanzania it tends to have a westerly direction that converges with moist southeasterly trade winds from the South Indian Ocean to produce upward motion and seasonal rainfall over those areas.

In July, the overhead position of the sun reaches the tropic of Cancer. During this time, surface high pressure exists over southern Africa and low pressure to the north. With this pressure pattern, the wind flow over Tanzania is southeasterly. These winds cross the South Indian Ocean and are moist in the lower layers and feed into the southwesterly monsoonal flow towards India. The circulation is mostly divergent in the austral winter over the region. The large area of low pressure over the Arabian peninsula and India has a controlling influence, such that the southeast trade winds curving across the equator into the southwest monsoon over the western Indian Ocean, and East African coast form a distinct low level jet called the Findlater or low level East African jet (Findlater, 1971)

East Africa topography is also important for directing flow of Findlater jet. Although little rain falls in Tanzania during this period, a considerable amount of stratiform clouds form on the eastern slopes over the coastal belt. Local circulations caused by topographic features, land-water contrasts (e.g. mountains and valleys, wind, lake and seas breezes) are superimposed on the synoptic circulation of the Tanzanian region.

The time space variability of the rainfall in Tanzania depend not only on the monsoon winds system and the associated behaviour of the ITCZ but also on tropical easterly/westerly waves perturbations and subtropical anticyclones.

Numerous studies (e.g. Charney, 1975; Charney and Shukla, 1981) have illustrated that gradually varying surface boundary forcing conditions, such as Sea Surface Temperature (SST), soil moisture and vegetation cover, influence tropical circulation patterns on seasonal and longer time scales. The role of global and regional SST anomalies in tropical rainfall variability is widely recognized and has been the subject of intensive study in recent years (e.g. Ropelewski and Halpert, 1987; Reason et al., 2000)

Previous studies have used principal component analysis techniques to examine the temporal and spatial variability in East Africa (Atwoki, 1975; Ogallo, 1988, 1989; Barring, 1988; Nyenzi, 1990; Semazzi et al, 1996). Ogallo (1989) investigated rainfall variability using the rotated principal component analysis (RPCA) method, to characterize the seasonal rainfall over East Africa for the period 1922-1983.

The results showed seasonal shifts in the patterns of the dominant RPCA modes that were similar to the seasonal migration of the rainfall patterns associated with ITCZ.

Hyden (1999) found dry / wet southern summers to be associated with Northward / Southward shift of the ITCZ from its average position. This is consistent with increased / decreased weather activity over Southern Tanzania during such periods. Nicholson and Nyenzi (1990) and Nicholson (1996a) observed strong quasi-periodic fluctuations in the East African with a time scale of five to 6 years corresponding to the ENSO and SST fluctuations in the equatorial Indian and Atlantic Oceans. On inter-annual time scales, El Nino / Southern Oscillation (ENSO) events are important for SST variability over the Indian Ocean which shows responses varying from simultaneous to about one season lag.

SST may evolve in response to changes in cloud cover and wind strength over the north and south Indian Ocean (Reason et al, 2000). Other important SST patterns in the Indian Ocean, whose potential relationship with ENSO is still to be clarified, include the Indian Ocean Zonal mode (Saji et al., 1999; Webster et al., 1999) and subtropical south Indian Ocean dipole patterns (Behera and Yamagata, 2001; Reason, 2001)

The stratospheric QBO could play a role in modulating rainfall (Mason and Tyson, 1992; Jury et al., 1994). The Walker circulation cell connecting Africa and the Indian Ocean may interact with the QBO, and during its westerly phase, rising motion occurs in the troposphere over East and Southern Africa.

During the QBO easterly phase, tropical cyclones and convection are most intense near Madagascar (Jury et al., 1995).

The space-time structure of Eastern African rainfall is fairly complicated. Stations located in northern Tanzania (along the coast, in the northern highlands and around lake Victoria) exhibits an annual bimodal rainfall distribution, with maxima in the March-May and October to December seasons. This bimodality is absent for the stations located in southern, central and western Tanzania where only one maximum rainfall season in October to April/May is experienced.

Studies of rainfall variability in Tanzania have mainly focused on the long time scale, i.e. seasonal and inter-annual variability. Attempts have been made to establish statistical model for forecasting seasonal rains over the country (Kabanda, 1995).

The inter-annual rainfall variability in the October-December season and its connections to the large-scale climate forcing have been recently investigated (Kabanda and Jury, 1999), who found some associations with the ENSO phenomenon and Quasi-biennial Oscillations (QBO). As mentioned earlier, other authors (Webster et al., 1999) include East African rainfall variability of the October-December (OND) season in the framework of a proper large-scale oscillation in the Indian Ocean. In a case study during December/January season over southwestern Tanzania, Mpeta and Jury (2001) found that convective rainfall events were associated with an influx of Northeasterly Indian Ocean monsoon flow followed by increased westerly flow from the Guinea / Congo region.

Further work is needed on the uni-modal regime of (October – April) rain season at the intra-annual and intra-seasonal scale.

This thesis aims at filling the gap by improving understanding of rainfall variability during the October to April rain season over western and southwestern Tanzania, the monsoon and potential influences from Indian and Atlantic Oceans. The evolution of anomalously Wet and dry years over this region will be investigated as with the nature of the intra seasonal variability during these years.

In the next Chapter, data and methods used in the study are briefly discussed together with seasonality and distribution of rainfall over western and southwestern Tanzania.

In Chapter 3, mean monthly climatological patterns for various fields presented.

Results of rainfall analyses i.e. Rainfall Time series and mean monthly composite anomaly evolutions for the wet and dry years are introduced in Chapter 4.

In Chapter 5, the intraseasonal variability over the western and southwestern Tanzania for the wet and dry years is discussed. The summary and conclusions are presented in Chapter 6.

## **CHAPTER 2**

### **Data and Methodology**

#### **2.1 Data used in the study**

The data used in this study to investigate the evolution of wet and dry spells over Western and Southern Western Tanzania and the dynamics of monsoon circulation over Atlantic and Indian Ocean, include pentad and monthly rainfall, NCEP/NCAR reanalyses, NOAA outgoing long wave radiation (OLR) and monthly Reynolds Reconstructed SST (Smith et al., 1996). The rainfall data used consists of mean monthly records at six stations within the period 1968–1998 from Tanzania Meteorological Agency and pentad (5 day mean) rainfall for the CMAP gridded product (Xie and Arkin, 1997). The latter is a merge of satellite, model and raingauge data. Zonal and meridional components of wind at 850, 700 and 200hPa levels, moisture flux calculated from the winds, divergence, velocity potential and divergent winds are used.

Some limitations of this study should however, be mentioned. The period of the CMAP rainfall data set are extends only from 1979, this tends to affect the sample size for composite as well as pattern stability and also presents consideration of long time scale variability. The spatial grid resolution of CMAP and NCEP/NCAR data set of  $2.5^{\circ} \times 2.5^{\circ}$  and lack of enough observations over tropical Africa (Kalnay et al., 1996), may be too coarse to capture the localized regional forcing due to topography, soil and vegetation and local water bodies

Another limitation of this study is the relatively short record length employed (i.e.29 years). In this case, decadal variability cannot be considered and thus the results found in this thesis need to be viewed with caution.

## 2.2 Methodology

The methods used in this study include determination of anomalous rainfall years by means of average rainfall indices, monthly composite analysis, and cross section analysis.

### 2.2.1 Rainfall index

The rainfall index is used to delineate anomalous wet and dry years during the 1968 - 1998 period for October - April season over the Western and South-western Tanzania. This period was selected because of quality and continuous data coverage available at all stations needed for analysis. Six stations were used in this study namely, Kigoma, Tabora, Sumbawanga, Iringa, Mbeya and Songea [Figure 2.0].

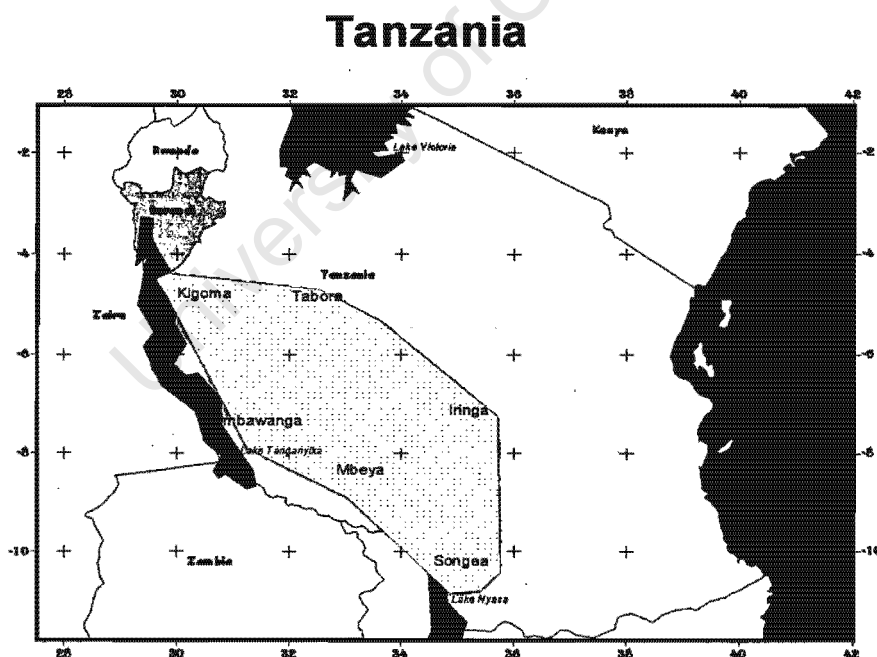


Figure (2.0) The Network Stations used for study

The anomalous rainfall (wet / dry) years were computed by subtracting the climatological mean based on the 1968 –1998 period from the monthly rainfall total and normalized by dividing each record by the corresponding standard deviation for each record. At each station, the normalized rainfall index is calculated as:

$$P_{ij} = \frac{R_{ij} - M_j}{S_j} \dots\dots\dots(\text{Eqn.1})$$

where  $P_{ij}$  = the normalised departure,  $R_{ij}$  is seasonal rainfall total at station  $j$  and in year  $i$ , and  $M_j$  and  $S_j$  are the mean and standard deviation of the rainfall at the given station respectively.

The computed value of  $P_{ij}$ , as a time series provides immediate information about the significance of a particular deviation from the mean and is used to delineate the anomalous wet and dry scenarios for the respective season and years over western and southwestern Tanzania. CMAP gridded time series for the gridpoint nearest to each gridded rainfall station were derived for the 1979-1999 period available and compared with the station data in order to check for consistency. The results from CMAP data were found to be consistent with those of the rainfall station data used over the study region in the specified period

The occurrences of the wet and dry years were then identified. The major wet and dry seasons were first delineated, and the averaged values (composites) for the circulation field were derived to represent wet and dry years. The composite were used to study the space and time evolutions of the monsoon circulation over the region during these anomalous wet and dry seasons.

### **2.2.2 Composite Analyses**

Composite analysis involves identifying and averaging one or more categories of fields of a variable selected according to their association with 'key' conditions (Folland, 1983). The results of these composites are then used to generate hypotheses for patterns, which may be associated with the individual scenarios (Folland, 1983). In this study, the 'key' conditions for the composite analysis are the anomalous wet and dry seasons. A number of studies have indicated that the results obtained from composite analysis usually agree closely with correlation methods (e.g. Ward, 1992). The main advantage of composite fields is that they are easy to interpret and are often presented in meteorological units.

Another important advantage of composite analysis is that the common features and patterns are better indicated than individual cases. This approach has been used many times before in climate research in the African / Indian Ocean region (e.g. Cadet, 1985; Murakami, 1988; Matarira and Jury, 1992; Park and Schubert, 1993; Levey, 1993; Nassor, 1994 and Makarau, 1995).

In this study, the wet and dry years delineated from the station monthly data were composited in order to isolate the associated circulation patterns and identify potential mechanisms.

The individual selected wet / dry years were further analysed using CMAP pentad (5-day) rainfall in order to investigate intra-seasonal variability. Individual cases of gridded parameters such as winds, SST and OLR were also selected and averaged for the specified wet and dry seasons in monthly basis.

### **2.2.3 Cross- Sectional Analyses**

Latitude height and longitude height cross-sections of zonal and meridional moisture flux for the selected anomalous wet and dry years were used to study the monsoon circulation changes over the area of study. Latitude height sections of moisture flux were used to examine the strength and magnitude of moisture circulation over the region associated with the influence of the Atlantic and Indian Oceans during the wet and dry years. Longitude-height sections were used to examine meridional circulations of moisture during the wet and dry years over the study region. Two latitude-height sections were produced and studied, one along 20°E (Atlantic side over Angola) and another along 40°E (over western Indian Ocean), while longitude height section is averaged between 15 – 5°S over the study region.

### 2.3 Seasonality and Distribution of Rainfall over Western and South Western Tanzania

Mean Annual Rainfall distribution Western and South-Western Tanzania (1968 - 1998)

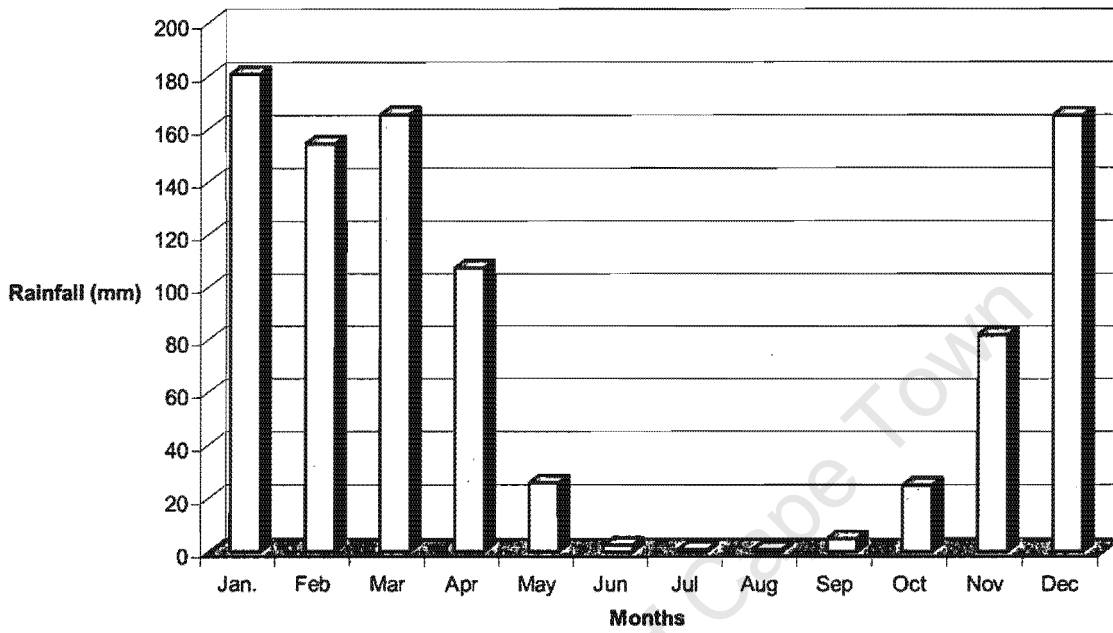
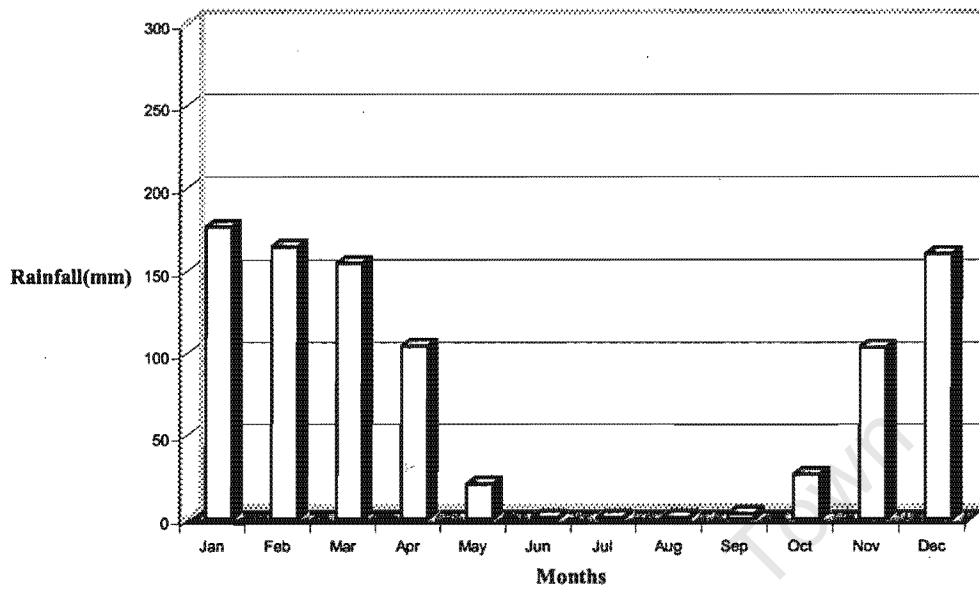


Figure 2.3.1 Mean annual area averaged rainfall distribution over western and southwestern Tanzania (1968-1998)

Figure (2.3.1) illustrates the monthly mean averaged rainfall for the six stations used in this study, namely Kigoma, Tabora, Sumbawanga, Iringa, Mbeya and Songea. It is evident from this figure that November to April may be considered the wet season, June to September the dry season and October and May are transition months.

Sumbawanga Mean Annual Rainfall distribution(1968-1998)



Songea Mean Annual Rainfall distribution(1968-1998)

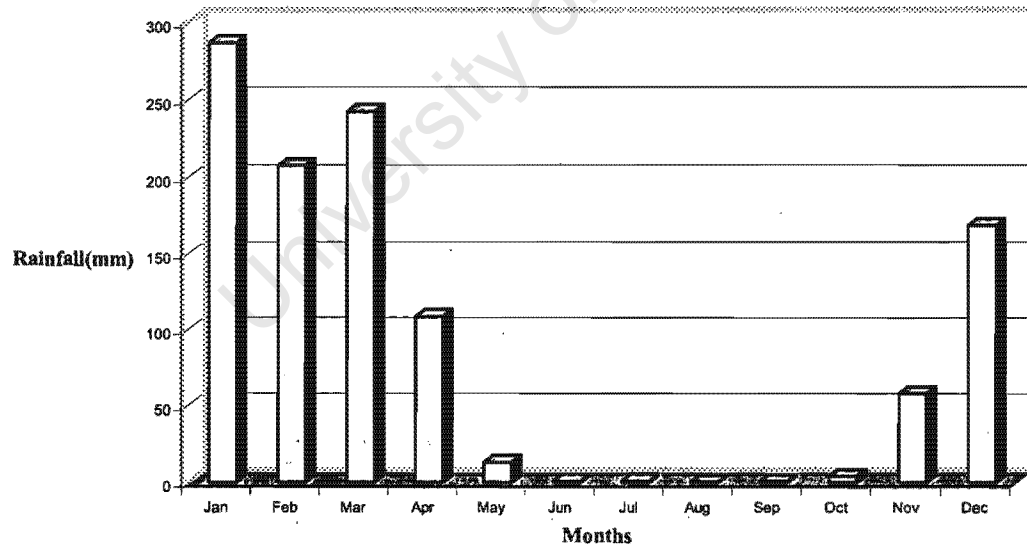
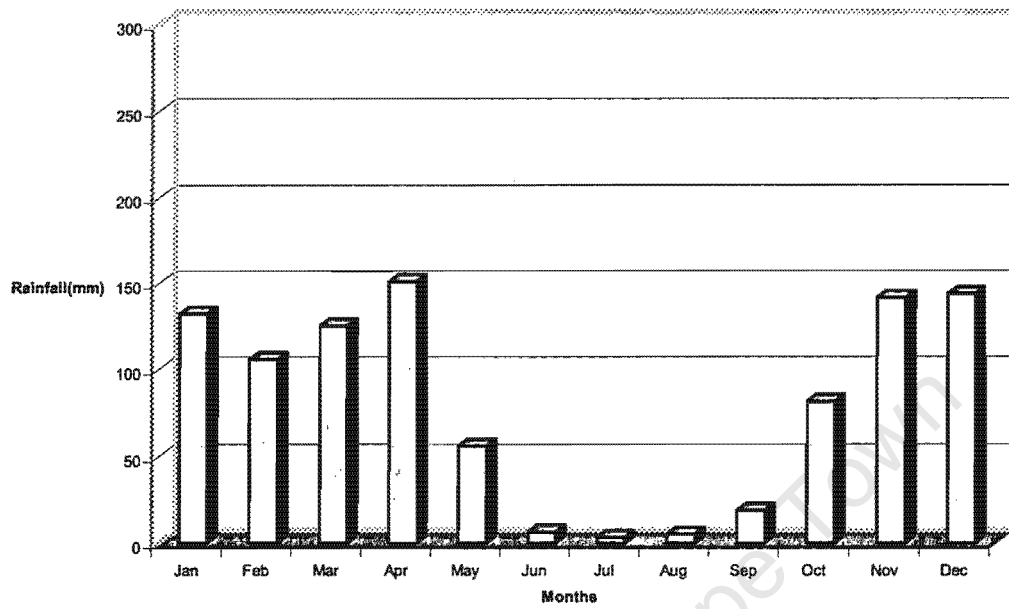
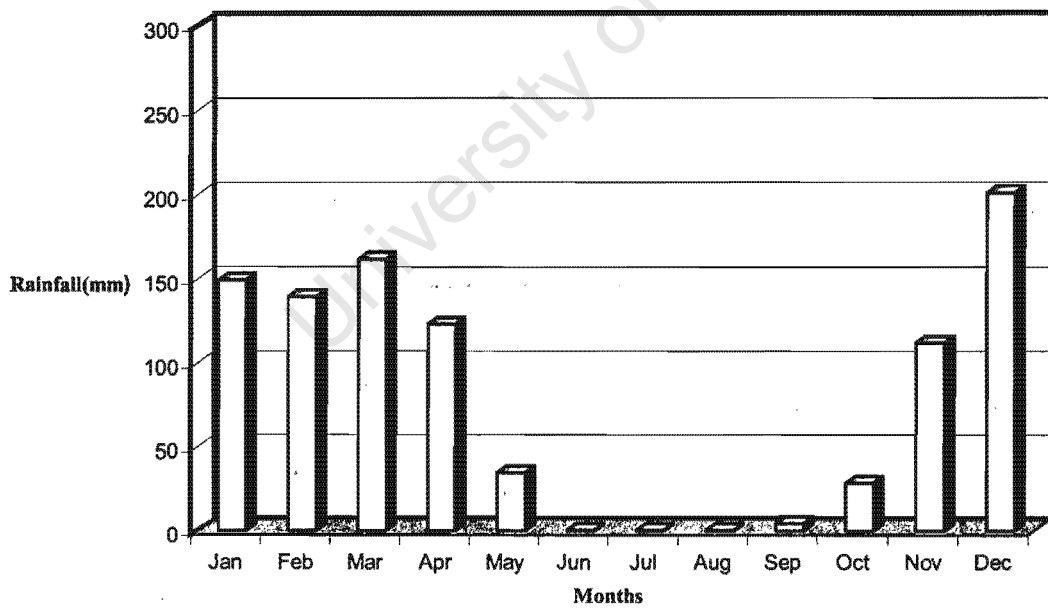


Figure 2.3.2: Mean annual rainfall distribution of six stations used for research (1968-1998): Scale interval is 50mm in y-axis.

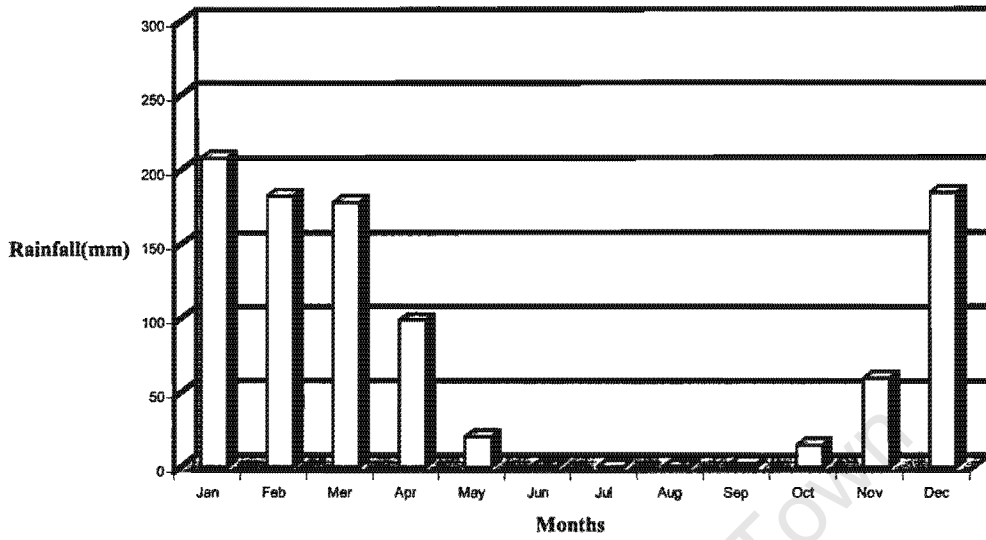
**Kigoma Mean Annual Rainfall distribution(1968-1998)**



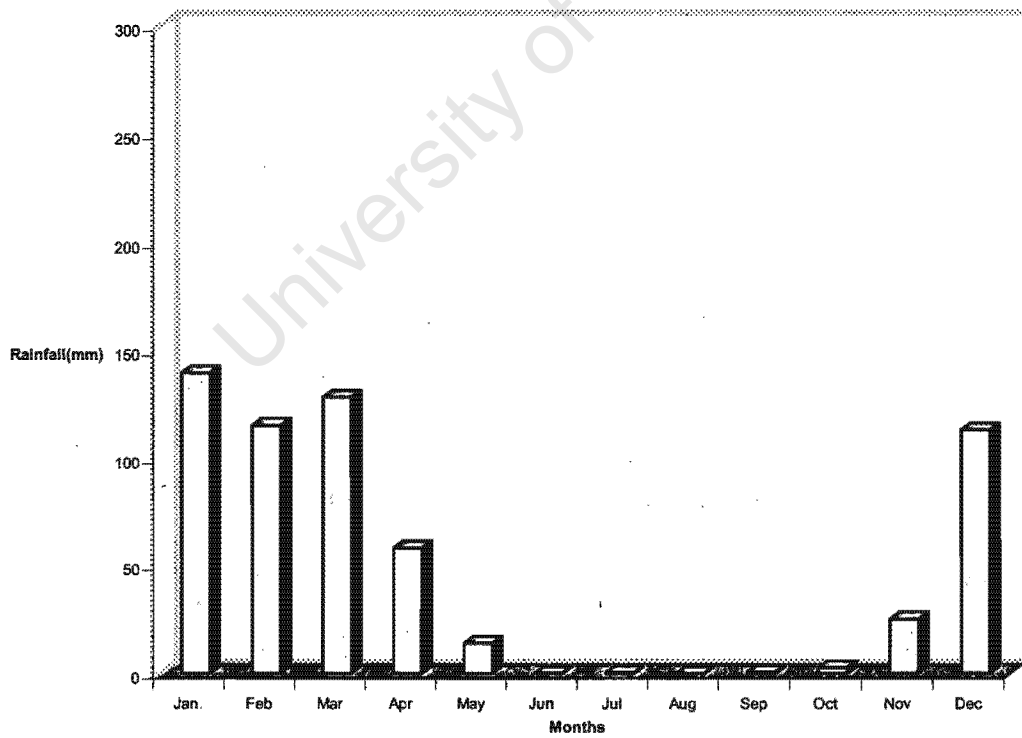
**Tabora mean annual Rainfall distribution(1968-1998)**



Mbeya Mean Annual Rainfall distribution(1968-1998)



Iringa Mean Annual Rainfall distribution(1968-1998)



In figure (2.3.2), there are however, some differences between the six stations in the monthly distribution and in the seasonal duration from one station to another. In all cases, a core-wet season of November to April is clear. A number of different topographic, soil and vegetation characteristics affect the various parts of the region for example, lake effects (local water bodies), altitude of the topography, local wind regimes and interactions associated with meso-scale circulations and large-scale weather systems may be important. Kigoma and Sumbawanga stations over the Western area report higher rainfall mainly due to moisture advection from Congo basin coupled with Lake Tanganyika effects. Mbeya and Songea stations over south western Tanzania may receive increased rain due to orographic effects caused by mountainous ranges of Livingstone, Ufipa and Lake Malawi. However, due to the variable orography some stations (e.g. Iringa) may receive lower totals due to rain shadow effects.

During February, most stations receive less rains, which may be associated with the climatological position of the ITCZ being furthest south. The increased rains in March are consistent with the ITCZ migrating north back towards Tanzania. In general, orographic effects and meso-scale circulations associated with the lakes and other water bodies may influence seasonal rainfall distributions over the southwestern, and these tend to modify the impacts of the large-scale monsoon circulations over the region. Such meso-scale and local effects are not considered in this thesis however.

## **CHAPTER 3**

### **3.1 Mean monthly climatology**

The synoptic features and wind flow patterns which produce rains in the tropics are complex, especially in East Africa. Within East Africa, and especially Tanzania, vertical motion can be induced by ascent of air over topography, horizontal convergence and unequal heating of land and water bodies. There are diurnal variations due to insolation and seasonal rainfall variations, which result from the north and south movement of the inter-tropical convergence zone (ITCZ) or the heat trough in sympathy with the overhead sun (e.g. Griffith, 1959; Nyenzi, 1988 and Ogallo, 1989).

There are also inter-annual variations, which may be linked to the El Niño/Southern oscillation (ENSO) (Nicholson and Chervin, 1983, Ogallo, 1988, Hastenrath et al., 1993). Local water bodies and mountainous ranges surround western and southwestern Tanzania with Lake Tanganyika and Ufipa plateau to the west; Lake Malawi and Livingstone mountainous ranges to the south. Synoptic features and wind flow patterns all affect rain-producing systems in the region.

As the sun is moving south in October and north in April, western and southwestern Tanzania experience an onset of the rain in October and withdrawal of rains in April. However, there are frequently considerable jumps in the position of rain belt and large day-to-day variations in amount and distribution caused by changes in the local areas of moisture convergence and instabilities in local flows. In this section, mean monthly climatological patterns for various fields (i.e. sea surface temperature (SST), winds, latent heat fluxes, outgoing long wave radiations (OLR), velocity potential and divergent wind, moisture flux and precipitation) are analysed.

These analyses are used to understand the evolution of composite anomalies of the monsoon circulation over the adjacent Indian and Atlantic oceans, which are associated with wet and dry spells over western and southwestern Tanzania. The monthly means are calculated for the 1968-1998 period for October season to May [Figure 3.1.1(a-h)].

During October [Figure 3.1.1(a)], the ITCZ starts to move south and its position is evident from convergent low-level wind and low value of OLR over the Indian Ocean. During this time, the dominant wind flow over western Tanzania is low level southeasterly from the adjacent tropical South Indian Ocean and westerlies from the Congo basin. These flows converge over the Lake Victoria basin and northern part of Lake Tanganyika in the region of Kigoma. This moisture convergence is also consistent with the eastward extent of OLR value of less than  $240\text{Wm}^{-2}$  over those areas, which indicates deep cumulus convection and precipitation. Velocity potential and divergent wind plots also reflect this region of strong convective activity, and indicates a strong low-level convergence at 850hPa with associated divergence at the 200hPa level. The strong convergence over Kigoma region and Lake Victoria basin is indicated by westerly winds, which draw moisture over Congo basin, and this is reflected by the increased latent heat flux over the region. Similarly the strong southeasterly flow at 850hPa over the tropical South Indian Ocean is reflected in the large latent heat flux northeast of Madagascar.

These two moisture sources help maintain the convection over the region in October as reflected by the moisture flux and precipitation plots. Along 20°E, the zonal moisture flux plot indicates the dominantly low level westerlies in the latitude range of 3°S to 3°N with easterlies further south between 21°S and 12°S. These easterlies are inclined northward with altitude up to 500hPa level with maximum intensity at 700hPa level. Along 40°E, low-level easterlies exist between 15°S and 3°N and extend vertically up to 700hPa.

The longitude height section of moisture flux reveals a region of strong low- level easterlies observed to extend westwards up to 32°E. These easterlies increases with height up to 500hPa level with maximum intensity at 850hPa level.

It is worth noting that these westerly and easterlies may be quite important in transporting moisture from the Congo rainforest and from Indian Ocean into western Tanzania. This could partly explain the relatively large amount of rainfall shown in the precipitation plot over the Lake Victoria basin and northern part of the Lake Tanganyika at Kigoma region during this period.

In November [Fig.3.1.1 (b)], the 28°C SST isotherm is observed to extend slightly south of the equator over the western Indian Ocean accompanied by a southward shift of the ITCZ. The northeasterly monsoon and tropical easterlies over the region begins to strengthen during this period. The enhancement of these flows is associated with the establishment of the Arabian winter anticyclone over the northern hemisphere and the southeastwards shift of the South Indian Ocean anticyclone.

The increased equatorial westerlies over the northern Congo basin converge over western Tanzania with easterlies from tropical Indian Ocean. This convergence follows the southeastward extent of the OLR values of less than  $240\text{Wm}^{-2}$  there and marks the region of increased convective rainfall over the western part of Tanzania. In general, patterns of November follows those of October, an increase of rainfall over western Tanzania during this month is associated with southward shift of the ITCZ over western Indian Ocean compared to October. Significant moisture sources are the tropical South Indian Ocean and the Congo basin.

In December [Fig. 3.1.1 (c)], the ITCZ is well established over southern Tanzania / northern Mozambique, the South Indian Ocean anticyclone weakens and the Arabian winter anticyclone intensifies. Tanzania, and in fact most of East Africa, is characterised by northeast (NE) monsoonal flow. Westerlies from the Congo basin expand southwards in association with land surface latent heat fluxes. Near the western Tanzanian border, the northeasterlies from the Indian Ocean and westerlies from the Congo basin converge. This convergence is consistent with the southeastward distribution of the OLR flux of less than  $240\text{Wm}^{-2}$  as well as increase in land surface evaporation with strong convective precipitation apparent. Velocity potential and divergent wind plots confirm this region of strong convective activity, which indicates a strong low-level convergence there with associated divergence aloft. The zonal section of moisture fluxes along  $20^{\circ}\text{E}$  indicates that the low level westerlies increase and extend further southward from between  $4^{\circ}\text{N}$  and  $6^{\circ}\text{S}$  in November to between  $3^{\circ}\text{N}$  and  $10^{\circ}\text{S}$  in December. Easterlies exist both north and south of these westerlies and they increase with height from the surface to 700hPa level.

Along 20°E, the zonal section of moisture flux shows strong low-level easterlies dominating between 12°S and 3°N with weak westerlies south of these easterlies. The longitude height section of moisture flux indicates a region of strong low-level easterlies extending westward from 38°E to 33°E. These easterlies increase with altitudes from the surface to 500hPa with maximum intensity at 850hPa level.

The negative vertical shear of moisture flux existing over the region suggests the presence of baroclinic instability, which may be associated with active convective periods. These low-level westerlies and easterlies, which converge over the region reflects the increased rainfall shown over western and southwestern Tanzania during this period.

During January [Fig.3.1.1 (d)], the position of ITCZ moves further south to about 12°S and the 28°C SST contour is observed to expand further south over the South Indian Ocean compared to December. Significant warming occurs over the southeast Atlantic Ocean and the Angola low, which draws moisture from this ocean region starts to deepen.

The wind flow at 850hPa over interior Tanzania during this period reflects the northeasterly monsoon from the western Indian Ocean with westerlies from the tropical southeast Atlantic Ocean penetrating as far as Lakes Victoria and Tanganyika. These two main moisture sources converge over western Tanzania near 10° S and mark the seasonal rainy peak in the southwest during this month.

Further south, displacement of the ITCZ is also consistent with the expansion and distribution of the OLR values of less than  $240\text{Wm}^{-2}$  and rain belt further southeastward over Southern Africa and Madagascar. The increased latent heat flux over Mozambique, northern Zimbabwe, southern Zambia, Madagascar and Botswana indicates regions of large thermal low pressure associated with deep cumulus convection, moisture convergence and increased precipitation. These regions of strong convection are also reflected by velocity potential and divergent wind, which indicates a strong low-level convergence there at 850hPa level associated with upper level divergence.

The zonal section of moisture flux along  $20^{\circ}\text{E}$  indicates a southward increase of the low level westerlies between  $3^{\circ}\text{S}$  and  $10^{\circ}\text{S}$ , with strong easterlies to the north and south of these westerlies. Easterlies to the south between  $24^{\circ}\text{S}$  to  $15^{\circ}\text{S}$  increase with height from the surface to 500hPa level with maximum intensity at 850hPa level, while those to the north of  $3^{\circ}\text{N}$  latitude band become stronger at 700hPa level. The zonal section of moisture flux over western Indian Ocean along  $40^{\circ}\text{E}$  shows that the low level easterlies have retreated northward from between  $12^{\circ}\text{S}$  and  $3^{\circ}\text{N}$  in December to between  $10^{\circ}\text{S}$  and  $3^{\circ}\text{N}$  in January. To the south of this flow, westerlies increase along the  $15^{\circ}\text{S}$  latitude band.

The longitude height section of moisture flux indicates a region of strong low level easterlies extending further westward from  $33^{\circ}\text{E}$  in December to  $31^{\circ}\text{E}$  in January, while a region of weak low level westerlies observed to the west near  $28^{\circ}\text{E}$ .

It is evident that the strong westerlies along 20°E between 10°S and 3°S and easterlies along 40°E between 10°S and 3°N can partly explain the moisture convergence and significant increase of rainfall over western and southwestern Tanzania in January.

During February [Fig. 3.1.1(e)], the ITCZ is near its southernmost position and SST continues to warm over the tropical South Indian and Southeast Atlantic Oceans. The Angola low continues to deepen. The wind flow over most of Tanzania during this period is still the northeasterly monsoon from the western Indian Ocean and weak westerly flows from the tropical southeast Atlantic near 10°S. Recurving of the northeasterly monsoon along the coast of Tanzania leads to increased westerly flow over tropical western Indian Ocean during this month compared to December and January.

Rainfall decrease over western and southwestern Tanzania in February is associated with the deepening of the Angola low which draws moisture away from western Tanzania towards Zambia. Another cause of this decrease is due to the shift of the ITCZ and maximum convergence further south. This can be seen in the distributions of OLR values of less than  $240\text{Wm}^{-2}$  over Mozambique and Zambia. The increased land evaporation contributes further to strong convection, maximum moisture convergence and increased rainfall there. The velocity potential and divergent wind plots confirm these regions of strong convective activity of southern Africa by indicating a strong low-level convergence at 850hPa level. The zonal section of moisture flux along 20°E and 40°E shows similar patterns to January. A slight increase of the low level westerlies along 40°E over western Indian Ocean near 15°S is evident.

The longitude height section of moisture flux reveals an intrusion of westerlies at middle levels that extends westward to about 29°E, while at lower levels strong easterlies are dominant. Taken together, the deepening of the Angola low, which draws moisture towards southern Angola and western Zambia and therefore away from Tanzania, coupled with the southernmost position of ITCZ, leads to the substantial decrease of rainfall over the study region in February.

March [Fig. 3.1.1(f)] represents the end of the northeast monsoon over western Indian Ocean and the transition towards the southeast monsoon over tropical South Indian Ocean. This transition period is associated with the ITCZ moving north, weakening of the winter Arabian anticyclone and strengthening of the South Indian Ocean anticyclone. The 29°C SST isotherm over the tropical western Indian Ocean indicates the position of the heat trough over Tanzania. Over the tropical Atlantic Ocean, the ITCZ starts to move north together with warming both south and north of the equator. The Angola low weakens and there is little westerly flow from the southeast Atlantic into the Congo basin.

Over the western Indian Ocean, westerly flow at 850hPa is weaker than February and the dominant flow over interior Tanzania is easterlies from the tropical southeast Indian Ocean. Shifting north of the ITCZ over Tanzania is also consistent with the southwestward extent of the OLR values of less than  $240\text{Wm}^{-2}$  over northern Mozambique, Tanzania and central Africa, which indicates the regions of deep cumulus convection, moisture convergence and

increased precipitation. This region of convection is reflected by large latent heat fluxes there, which implies a large land surface evaporation and precipitation. The velocity potential and divergent winds support this by indicating a weak low-level convergence over the southern part of the country and strong convergence over northwestern parts of the country at 850hPa level. The increased low level moisture convergence and precipitation over northern Tanzania suggest the onset of the long rainy season of March to May during this period.

The zonal section of moisture flux along 20°E indicates the northward shift of strong low level westerlies to lie between 3°S and 4°N while easterlies to the south of these westerlies extend northwards to lie between 21°S and 12°S. These easterlies increase with height up to 600hPa level and cross the equator with maximum intensity at 850hPa to the south and at 700hPa level to the north of these westerlies. Over the western Indian Ocean along 40°E, weak westerlies are observed between 21°S and 12°S with strong low-level easterlies to the north between 3°S and 4°N. These low level westerlies between 3°S and 4°N along 20°E and easterlies between 3°S and 4°N along 40°E explain the low level moisture convergence over the northern parts of Tanzania consistent with increased precipitation over northern Tanzania, Lake Victoria, Uganda and western parts of Kenya during this period. The longitude height section of moisture flux indicates a region of strong easterlies extending westwards and upwards to 700hPa with maximum intensity at 850hPa level.

In April [Figure 3.1.1 (g)], the ITCZ moves further north to lie near 2°S over northern Tanzania. This northward displacement of the ITCZ follows the collapse of the winter Arabian anticyclone and northwest shift of the strengthened South Indian Ocean anticyclone. Over the western Indian Ocean, the heat trough is observed to expand more to the north with SST warming to 29°C over much of the tropical Indian Ocean. In the Atlantic, the Gulf of Guinea also shows SST of 29°C and warmer although the ITCZ seems to be quasi-stationary there compared to March. The dominant flow over interior Tanzania in April is mainly southeasterly from the tropical South Indian Ocean with some southerly flow from Mozambique Channel. OLR values of less than  $240\text{Wm}^{-2}$  extend northwestward from northeast Tanzania to the Lake Victoria basin and the neighbouring regions of Kenya and Uganda. This indicates the location of deep cumulus convection and increased precipitation over those regions. April is the seasonal rainy peak over northern Tanzania and early withdrawal of the rainy season over western and southwestern Tanzania.

The northward shift of the convective rain belt and latent heat source is apparent in the velocity potential and divergent wind plots, which indicate low-level divergence over the southern sectors of the country and strong convergence over the northern sectors at 850hPa level in association with opposing patterns at the 200hPa level. This is consistent with the increased rainfall over northern coast of Tanzania, northeastern highlands, Lake Victoria basin, and the relative rainfall decrease over southwestern and western Tanzania as depicted from the moisture flux and precipitation plots.

The zonal section of moisture flux along 20°E reveals strong low-level easterlies dominating between 21°S and 5°S. These easterlies increase with height up to 600hPa with maximum intensity at 850hPa and 700hPa level. Between 3°S and 4°N, low level westerly flow is observed to extend northward over the equator compared to March.

Along 40°E over the western Indian Ocean, the zonal section of moisture flux shows strong low-level easterlies dominating south and north of the equator between 12°S and 5°S and from the Equator to 4°N with weak westerlies further south between 18°S and 15°S. The longitude height section of moisture flux over the region (15°S – 5°S) reveals a westward shift of the strong low level easterlies at 850hPa level from 34°E - 30°E in March to 33°E – 29°E in April which extends vertically upwards with height up to 600hPa level. This strong convergence of westerly and easterlies occurs along the equator reflecting the major convective rain belt moving north over the region and marks the transition toward winding up of the rainy season over western and southwestern Tanzania during this period.

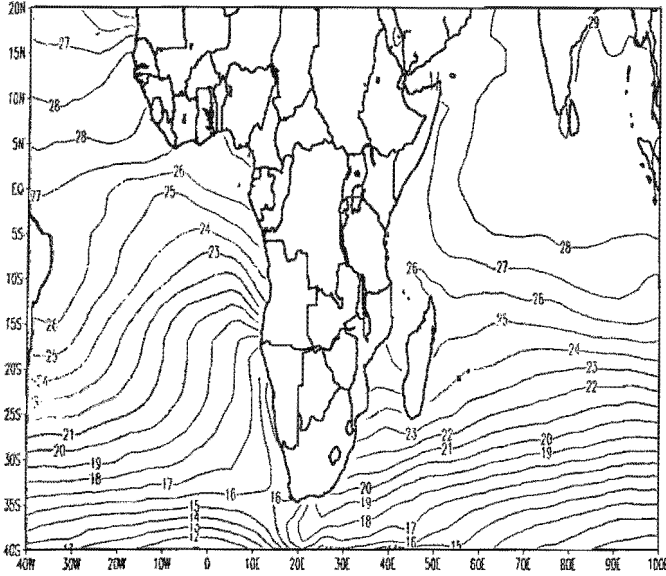
In May [Fig. 3.1.1(h)], the position of the ITCZ moves north of the equator together with northward displacement of the South Indian Ocean anticyclone. SST reaches 30°C in parts of the tropical North Indian Ocean. During this period, the wind flow over Tanzania is southeasterly and feeds into the developing East African low-level jet. Increasing monsoonal convection over South East Asia leads to the strong westerlies developing over the equatorial Indian Ocean.

Although little rain falls in the interior of northern Tanzania, a considerable amount of stratiform cloud forms on the eastern slopes over the northern coastal belt. The land surface evaporation decreases over most of the country during this period leading to less convection and less rainfall. The major convective rain belt moves further north with the region of the OLR values less than  $240\text{Wm}^{-2}$  nearly symmetric with respect to the equator.

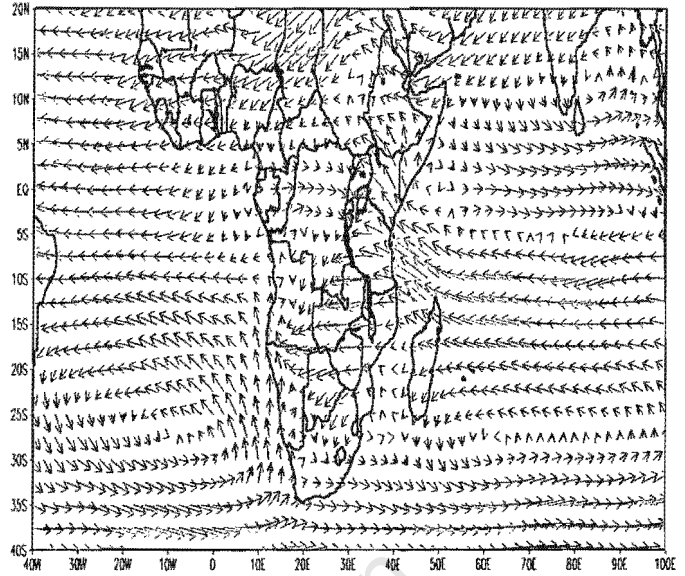
Significant convection, moisture convergence and increased rainfall occur north of equator over Uganda, Kenya and Ethiopia. May is the final month of the long rainy season of March to May over northern Tanzania and the transition period towards the southwest (SW) monsoon over the Indian subcontinent.

The ending of the long rainy season over northern Tanzania and transition towards the Southwest monsoon over India is reflected by the velocity potential and divergent wind, which indicates strong low-level divergence extending northward from Mozambique to Tanzania. The zonal section of moisture flux along  $20^{\circ}\text{E}$  and  $40^{\circ}\text{E}$  portrays almost the same patterns as April with a few significant differences. There is a northward shift of easterlies along  $20^{\circ}\text{E}$  between  $21^{\circ}\text{S}$  and  $6^{\circ}\text{S}$  in April to between  $18^{\circ}\text{S}$  and  $6^{\circ}\text{S}$  in May. Along  $40^{\circ}\text{E}$ , the easterlies which dominated over the equator in April are replaced by weak westerlies in May extending vertically up to 500hPa level. These westerlies feed into the developing East African low level jet and reduce the flux of moisture from the Indian Ocean into the region consistent with rainfall decrease in this month. The longitude height section of moisture flux between the surface and 500hPa level in May shows weakening of easterlies at 850hPa level over the region.

Oct Sea Surface Temperature (°C) Climatology

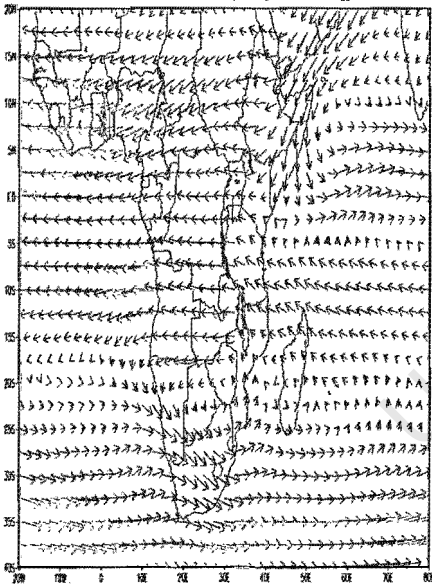


850 hPa Oct Wind (m/s) Climatology



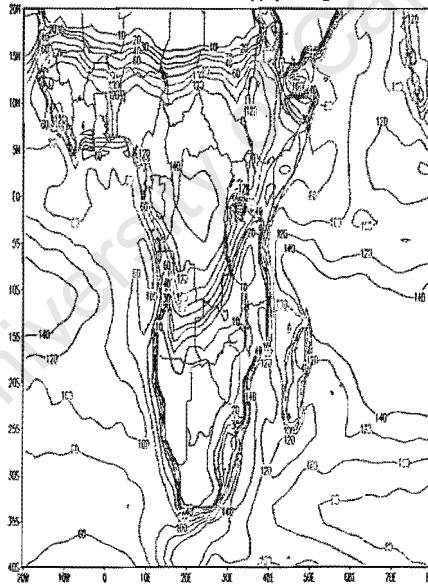
→  
10

700 hPa Oct Wind (m/s) Climatology

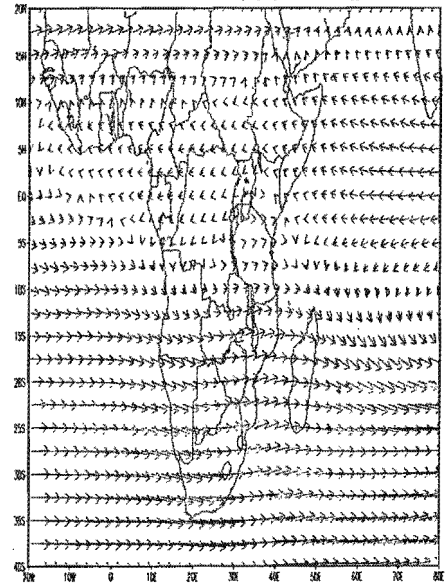


→  
10

Oct Surface latent heat flux (W/m²) climatology



200 hPa Oct Wind (m/s) Climatology



→  
30

Figure 3.1.1(a): October mean climatology of SST(contour interval 1°C ), wind at 850,700 and 200hPa (scale vector is shown at the bottom), latent heat flux (contour interval is 20Wm<sup>-2</sup>). Colour on wind vectors indicate their magnitude from low (purple) to high (red).

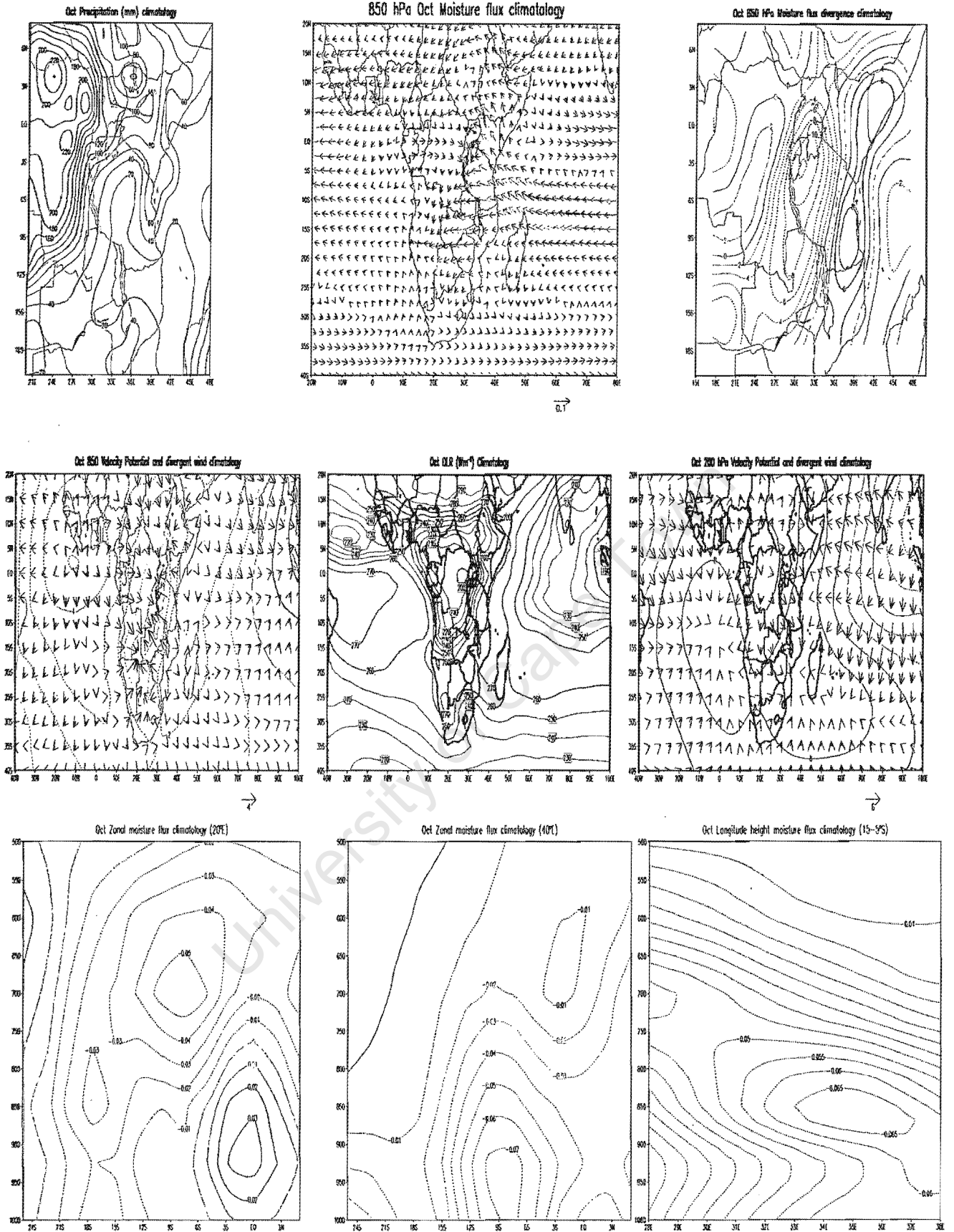


Fig.3.1.1(a) cont.

Moisture flux in  $\text{g/kg.ms}^{-1}$  and scale vector is shown at the bottom of the figures ;  
 Velocity potential in  $10^{-6} \text{m}^2\text{s}^{-1}$  and contour interval is  $2 \times 10^{-6} \text{m}^2\text{s}^{-1}$ ;  
 Divergent wind in  $10^{-6} \text{s}^{-1}$  and contour interval is  $2 \times 10^{-6} \text{s}^{-1}$ . Positive means westerlies and negative easterlies.

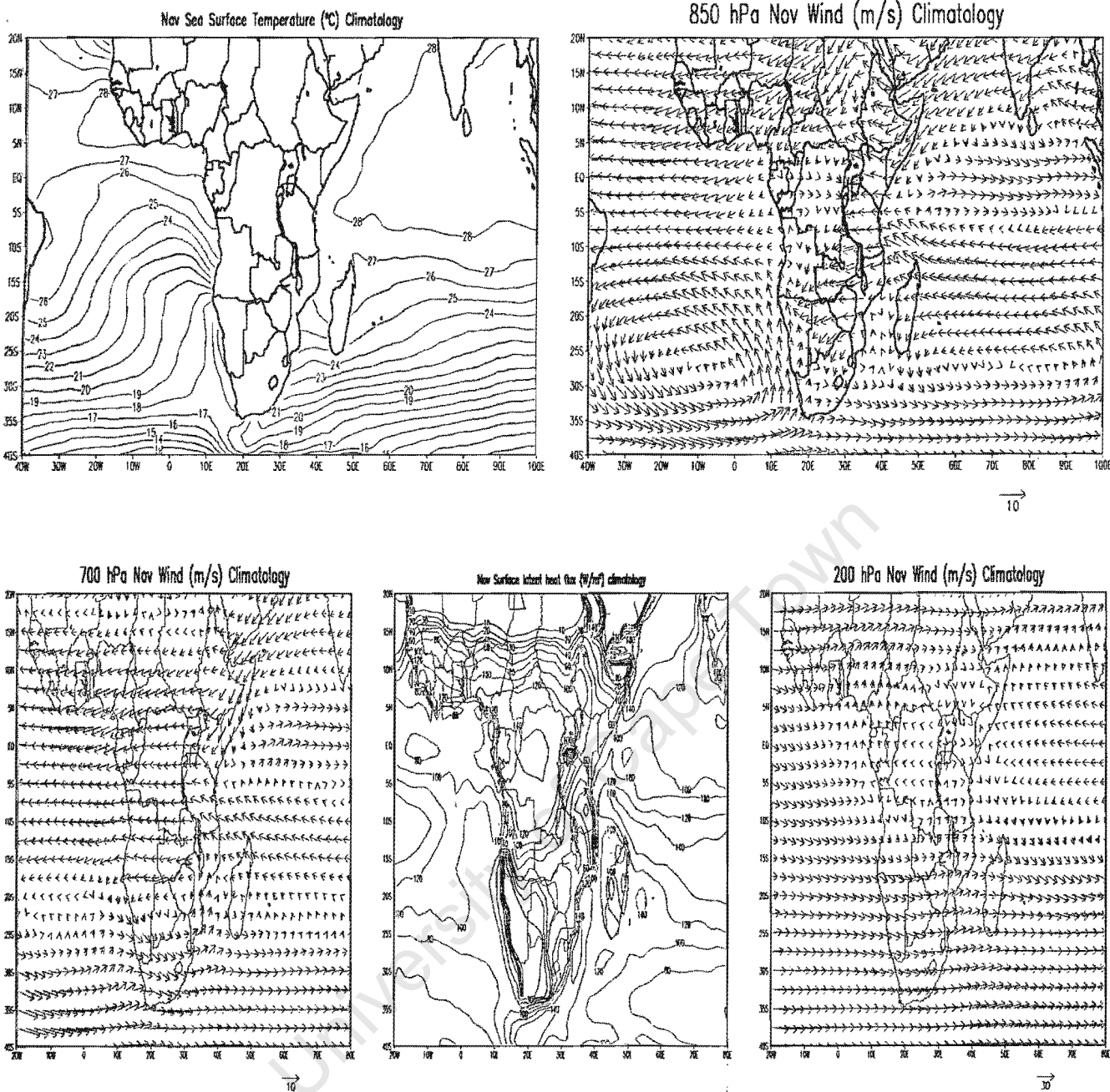
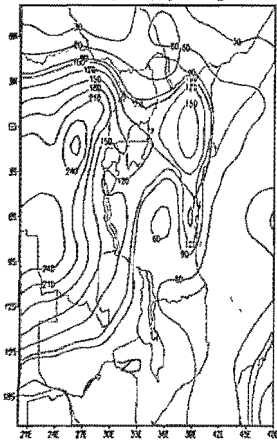
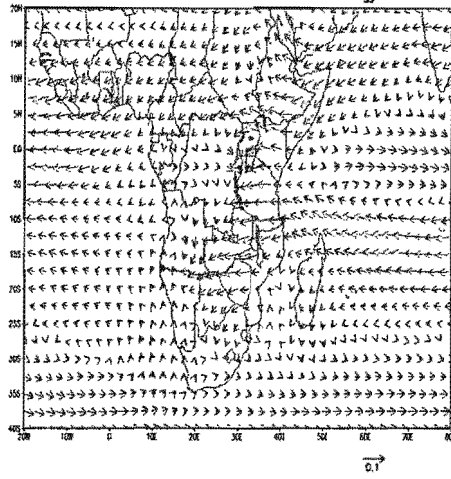


Figure 3.1.1(b): as figure 3.1.1(a) but for November

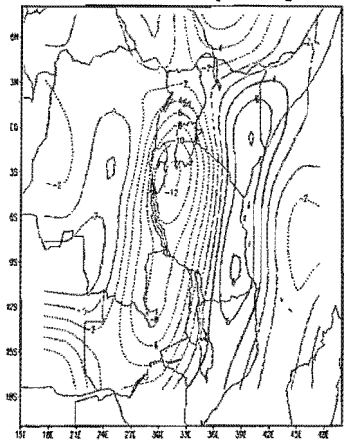
Nov Precipitation (mm) climatology



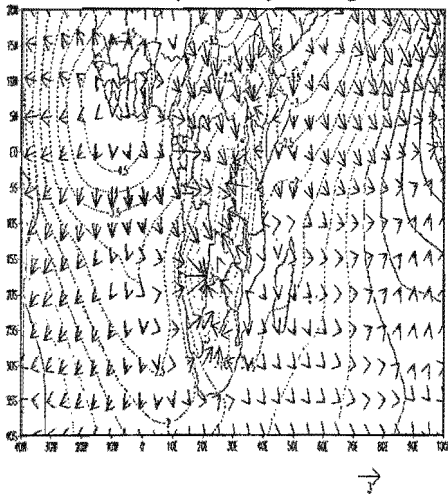
850 hPa Nov Moisture flux climatology



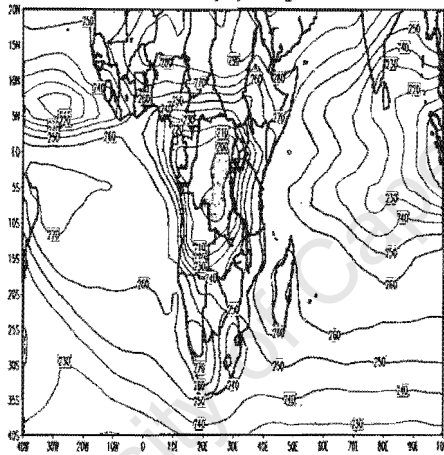
Nov 850 hPa Moisture flux divergence climatology



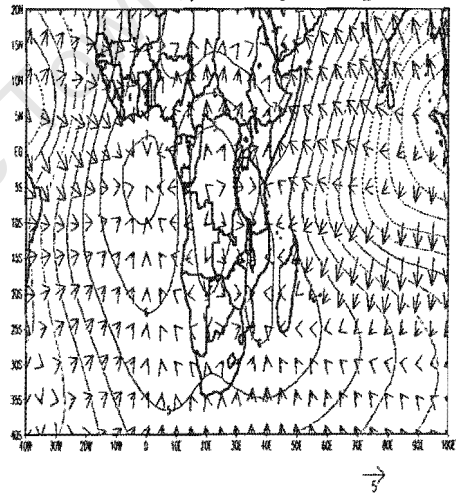
Nov 850 Velocity Potential and divergent wind climatology



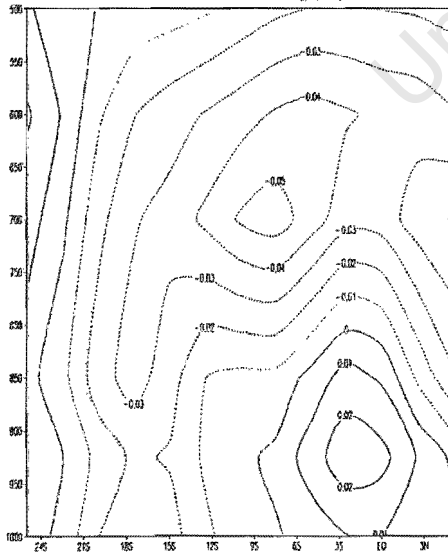
Nov QLR (Wm<sup>-2</sup>) Climatology



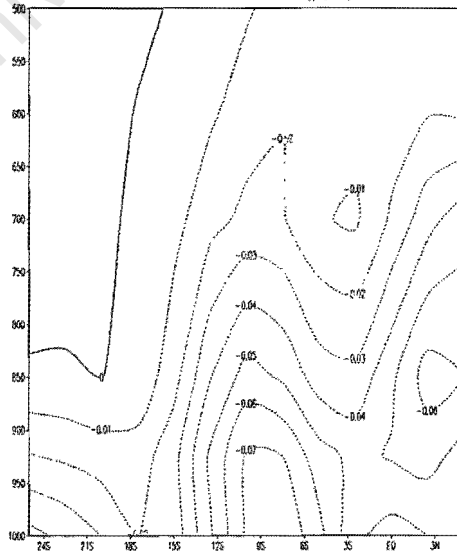
Nov 200 hPa Velocity Potential and divergent wind climatology



Nov Zonal moisture flux climatology (20E)



Nov Zonal moisture flux climatology (40E)



Nov Longitude height moisture flux climatology (15-5S)

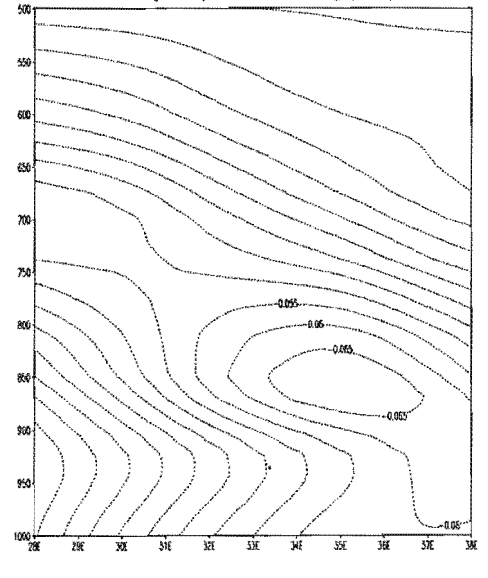
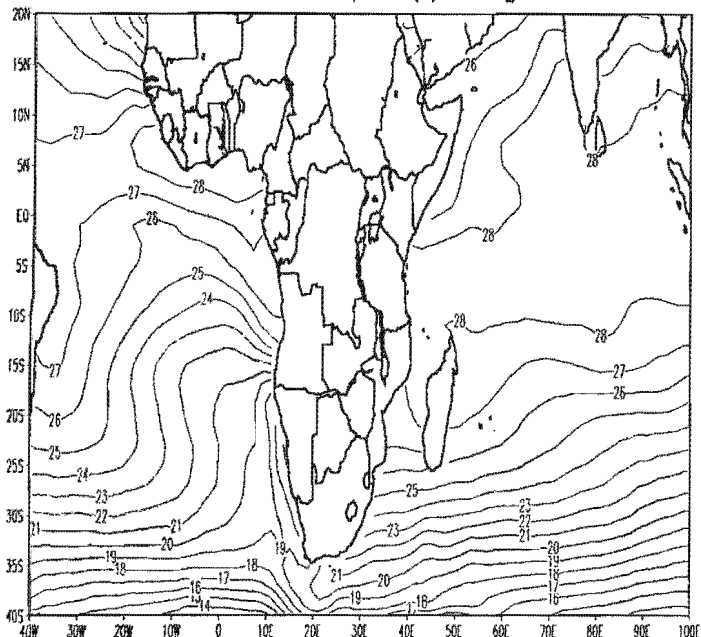
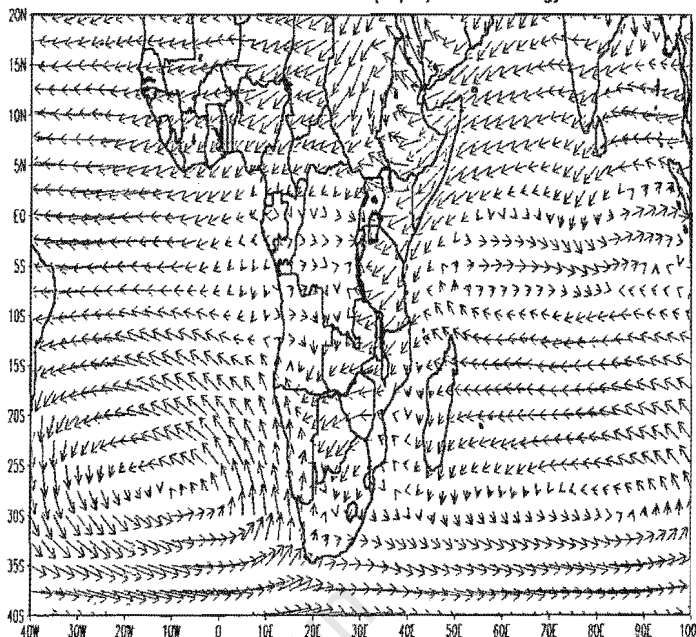


Fig.3.1.1(b) cont...

Dec Sea Surface Temperature (°C) Climatology

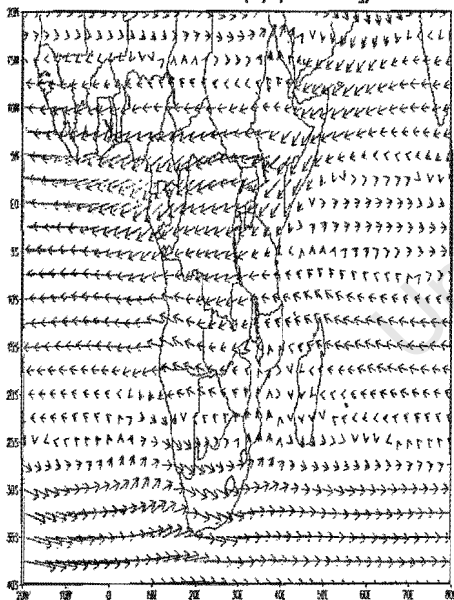


850 hPa Dec Wind (m/s) Climatology



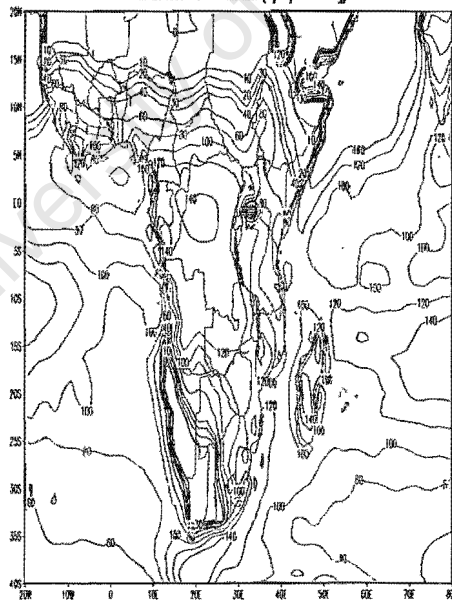
10

700 hPa Dec Wind (m/s) Climatology

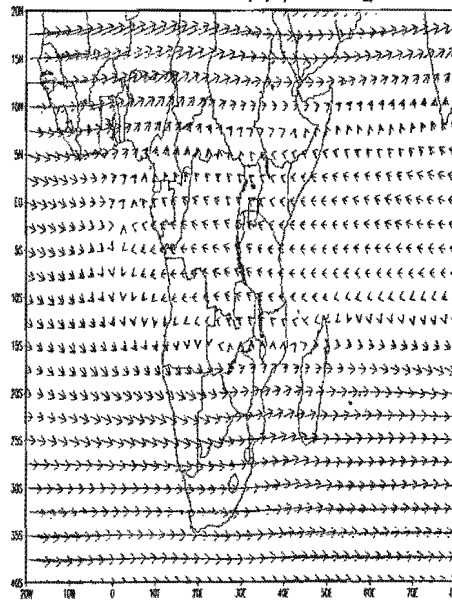


10

Dec Surface latent heat flux (W/m²) climatology



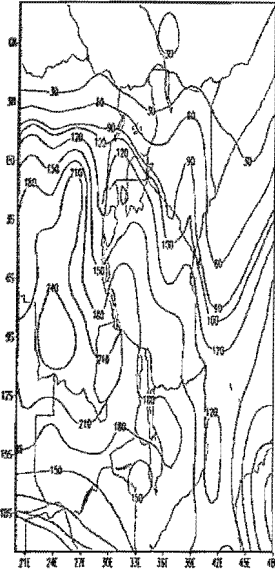
200 hPa Dec Wind (m/s) Climatology



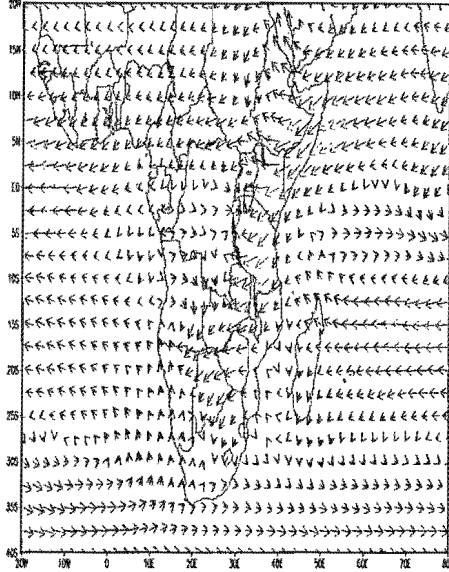
30

Figure 3.1.1(c): as figure 3.1.1(b) but for December

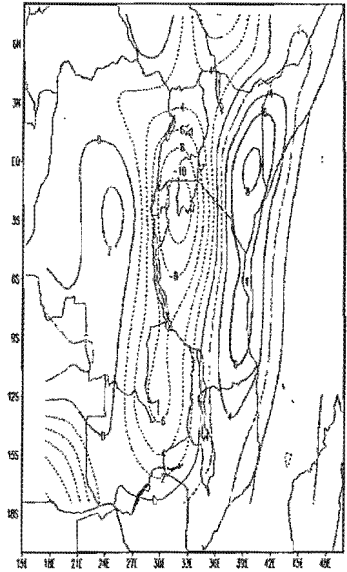
Dec Precipitation (mm) climatology



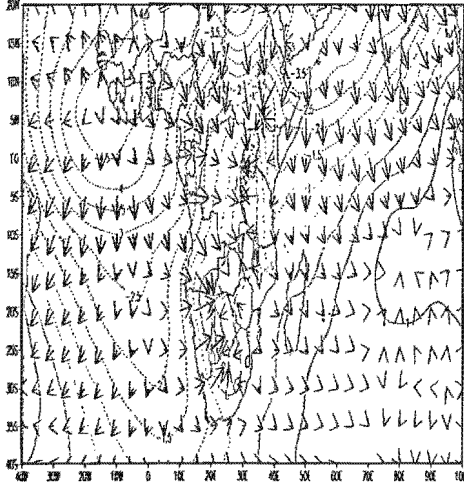
850 hPa Dec Moisture flux climatology



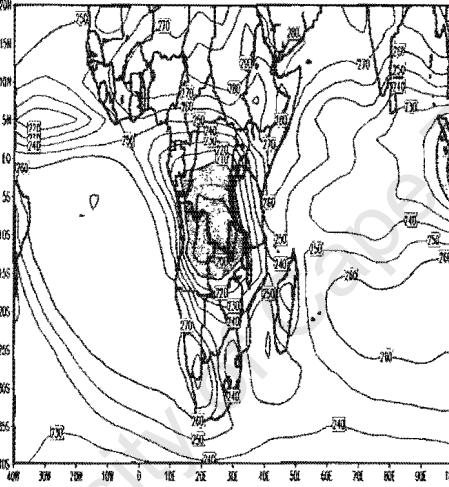
Dec 850 hPa Moisture flux divergence climatology



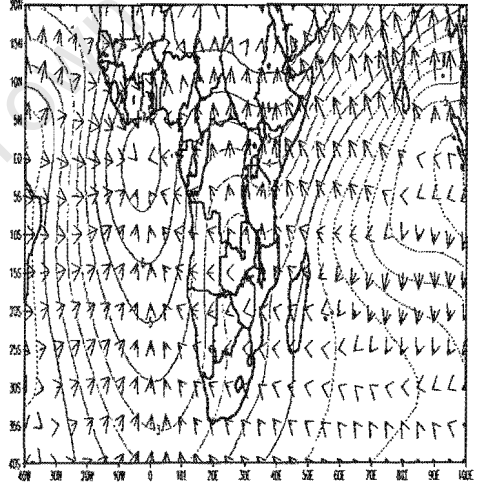
Dec 850 Velocity Potential and divergent wind climatology



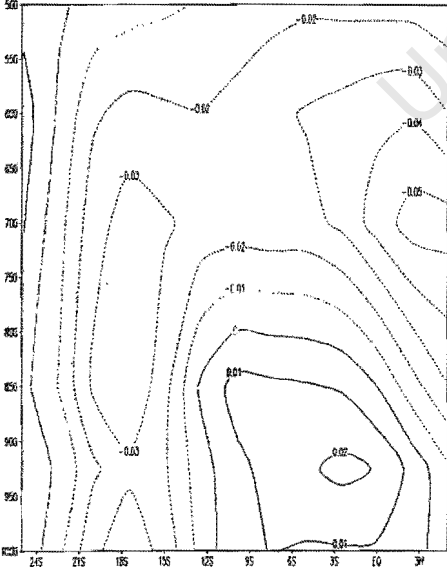
Dec DLR (Wm<sup>-2</sup>) Climatology



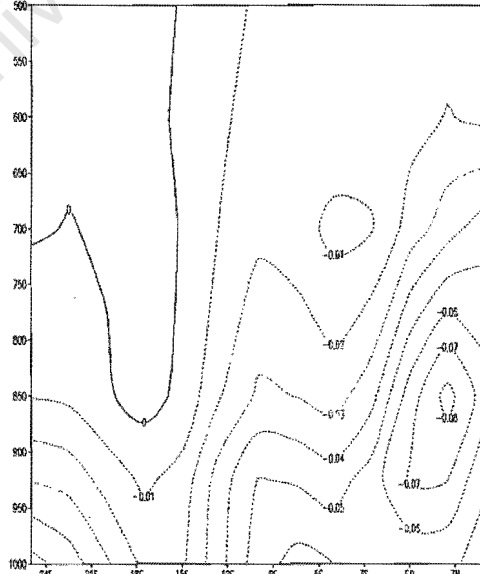
Dec 200 hPa Velocity Potential and divergent wind climatology



Dec Zonal moisture flux climatology (20°E)



Dec Zonal moisture flux climatology (40°E)



Dec Longitude height moisture flux climatology (15-5°S)

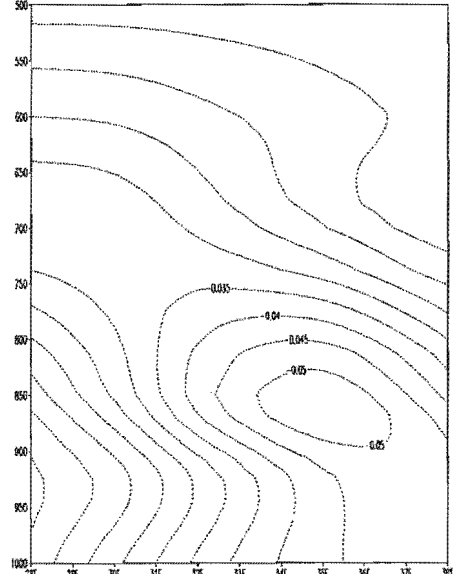
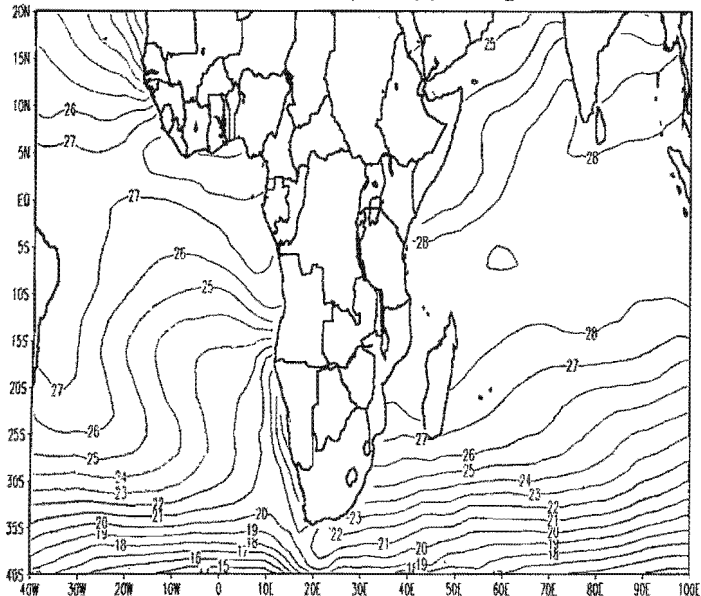
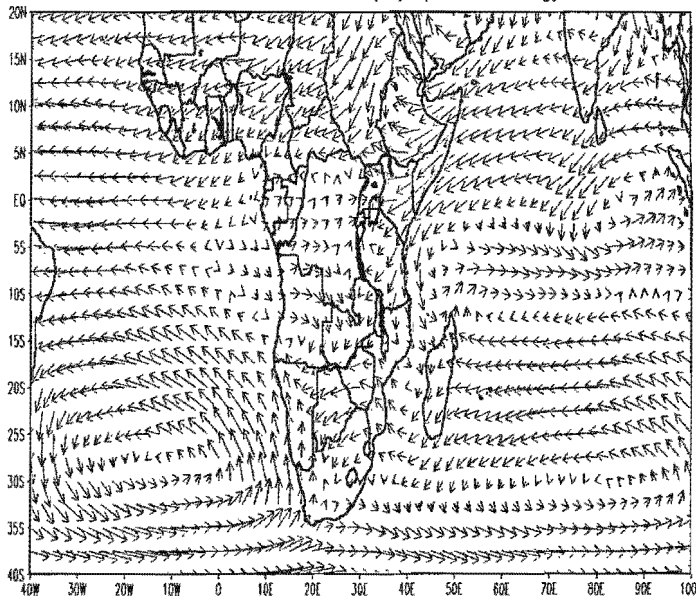


Fig. 3.1.1(c) cont...

Jan Sea Surface Temperature (°C) Climatology

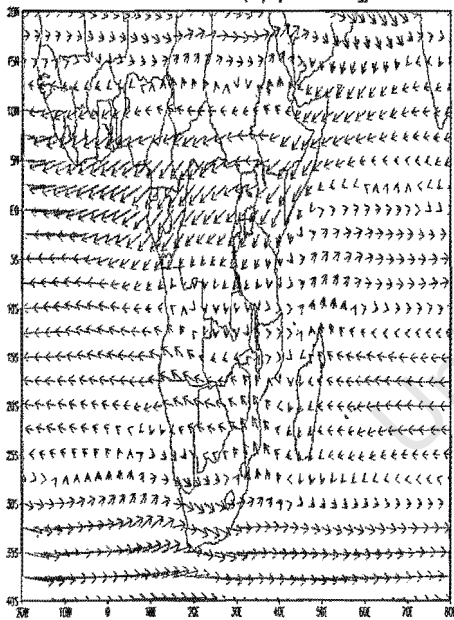


850 hPa Jan Wind (m/s) Climatology



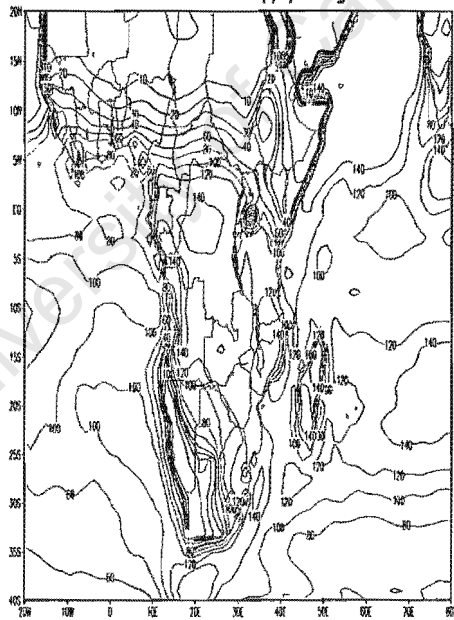
→  
10

700 hPa Jan Wind (m/s) Climatology

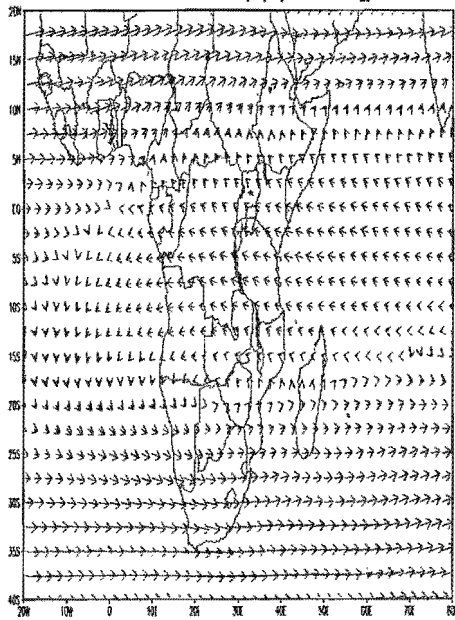


→  
10

Jan Surface latent heat flux (W/m²) climatology



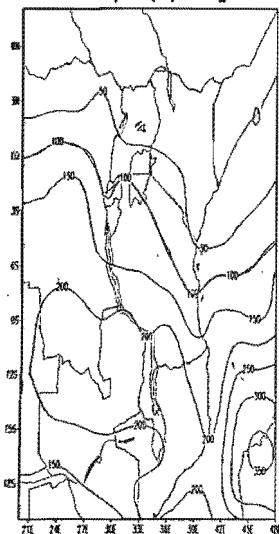
200 hPa Jan Wind (m/s) Climatology



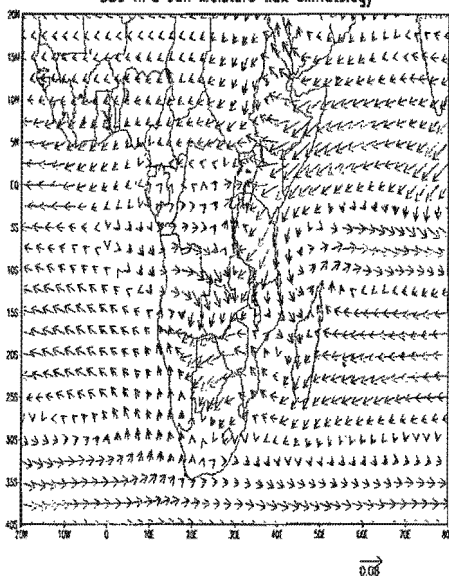
→  
40

Figure 3.1.1(d): as figure 3.1.1(a) but for January

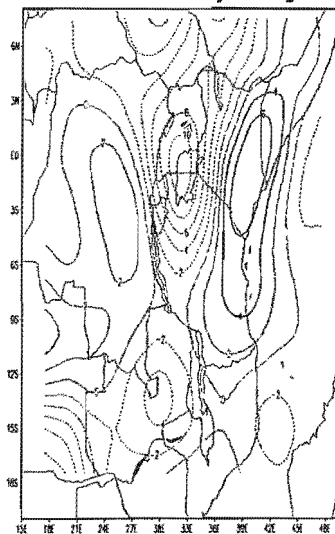
Jan Precipitation (mm) climatology



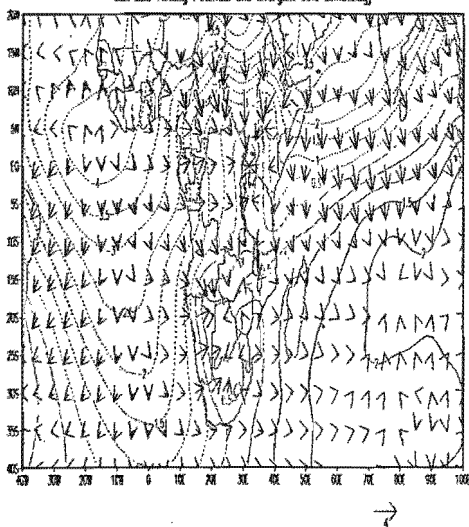
850 hPa Jan Moisture flux climatology



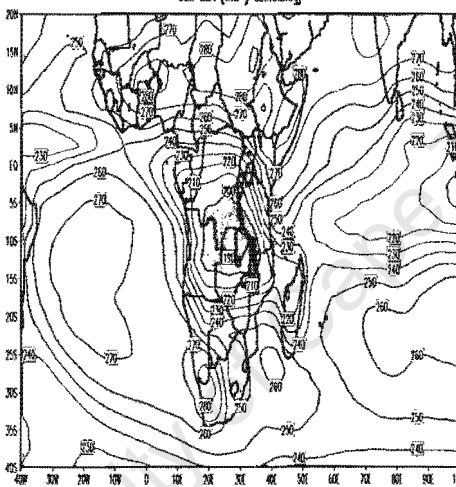
Jan 850 hPa Moisture flux emergence climatology



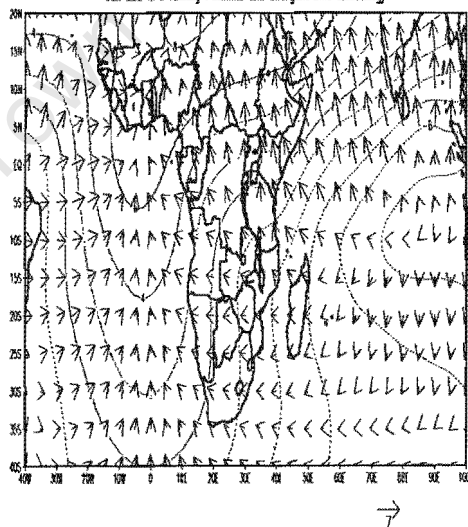
Jan 850 Velocity Potential and divergent wind climatology



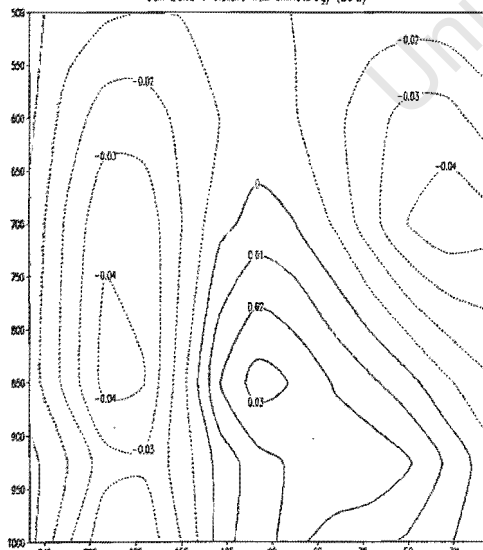
Jan CLR (Wm<sup>-2</sup>) Climatology



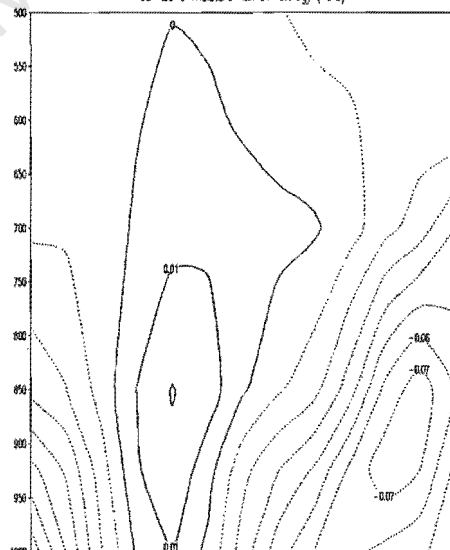
Jan 200 hPa Velocity Potential and divergent wind climatology



Jan Zonal moisture flux climatology (20°E)



Jan Zonal moisture flux climatology (40°E)



Jan Longitude height moisture flux climatology (15-5°S)

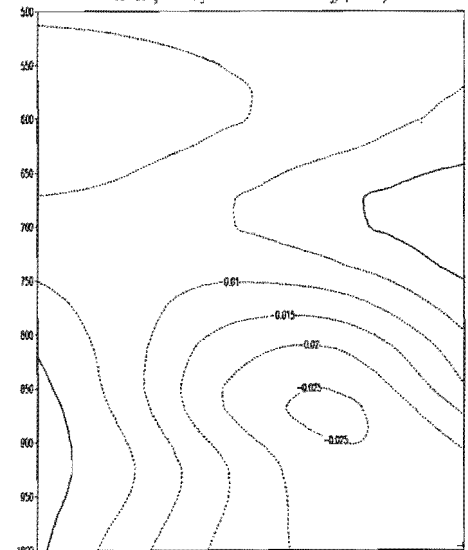
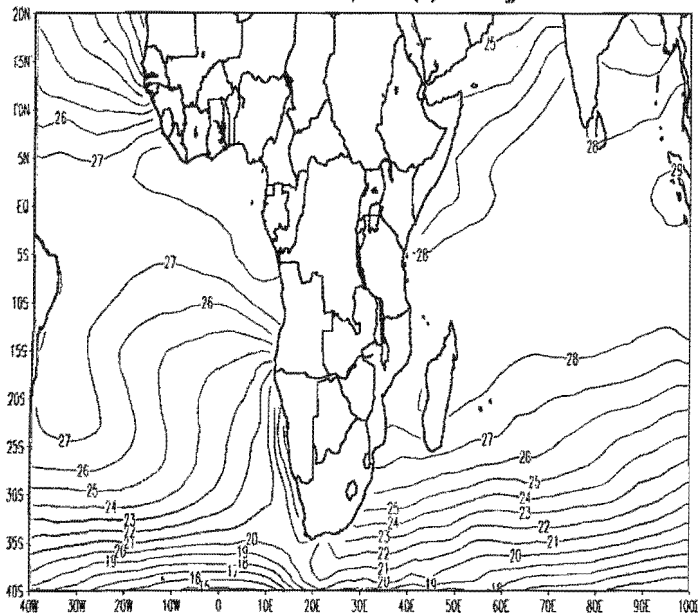
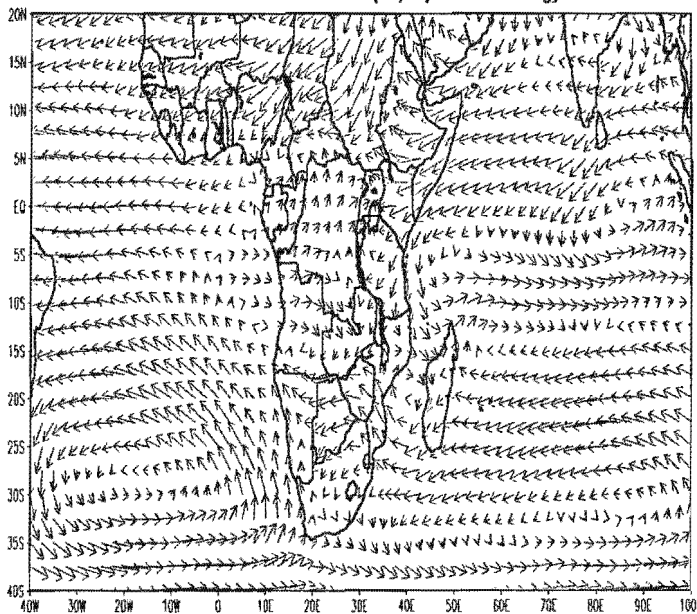


Fig.3.1.1(d) cont...

Feb Sea Surface Temperature (°C) Climatology

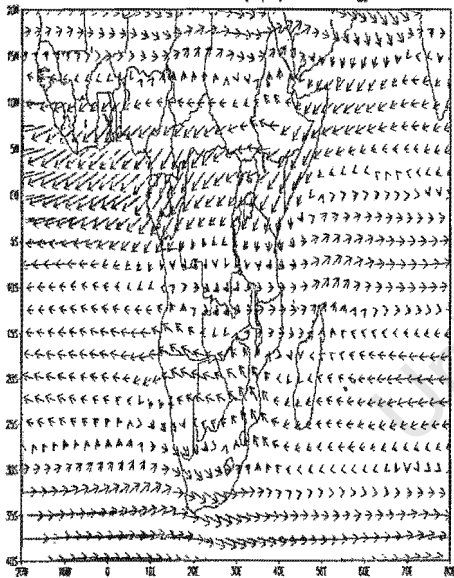


850 hPa Feb Wind (m/s) Climatology



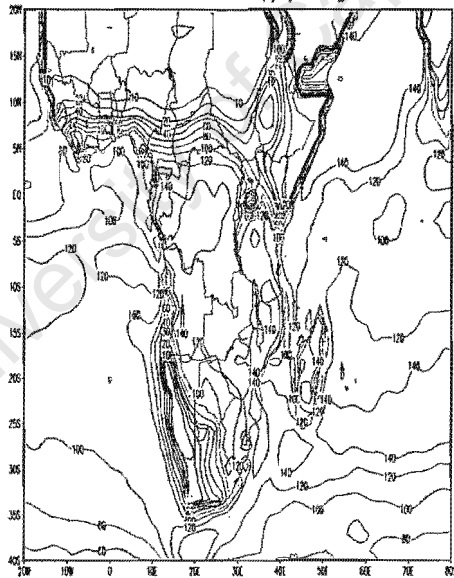
10

700 hPa Feb Wind (m/s) Climatology

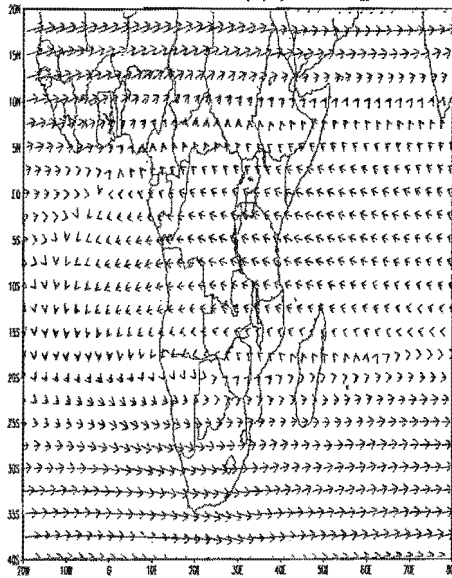


10

Feb Surface latent heat flux (W/m²) climatology



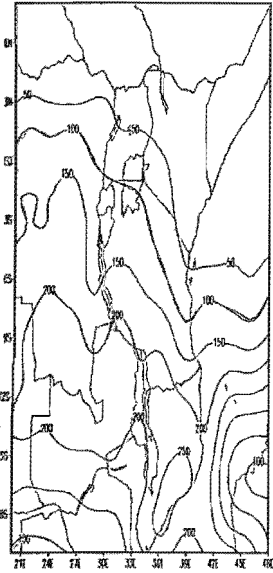
200 hPa Feb Wind (m/s) Climatology



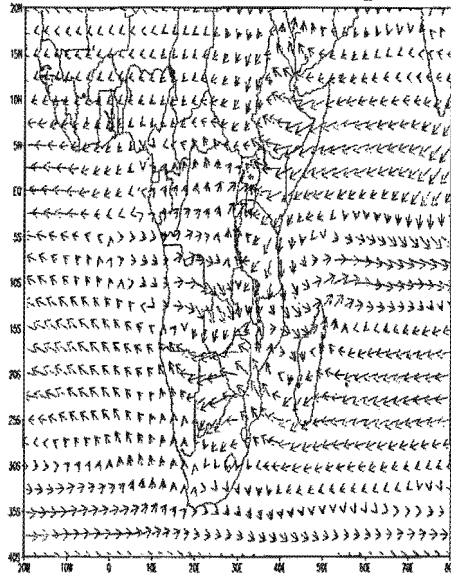
40

Figure 3.1.1(e): as figure 3.1.1(a) but for February

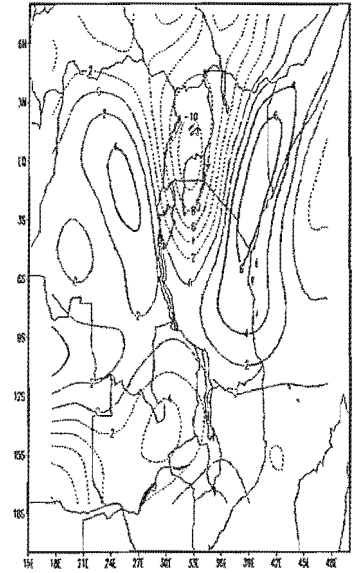
Feb Precipitation (mm) climatology



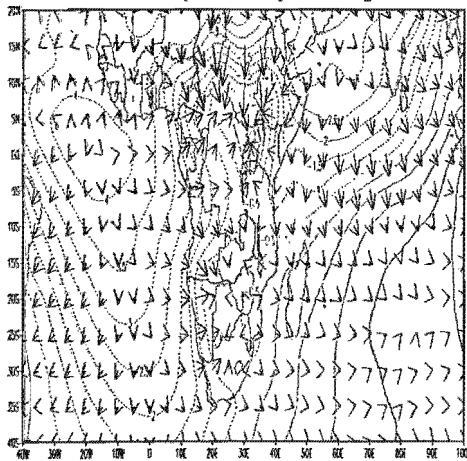
850 hPa Feb Moisture flux climatology



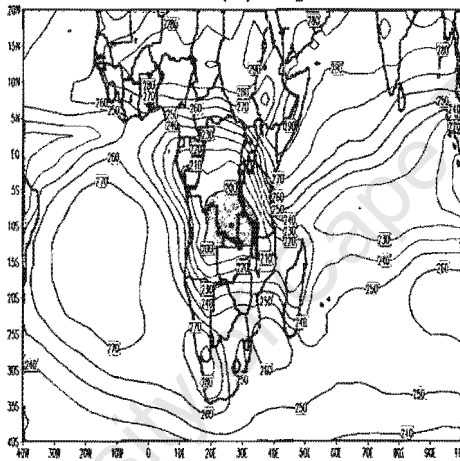
Feb 850 hPa Moisture flux divergence climatology



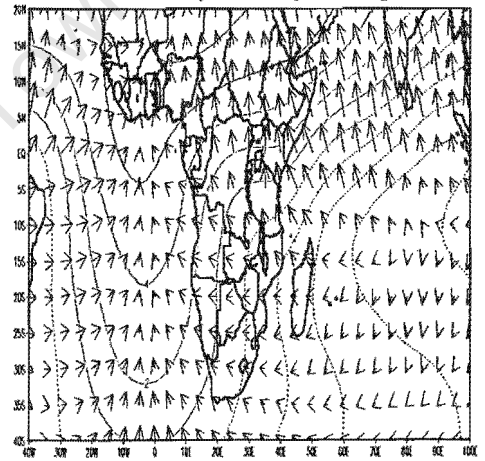
Feb 850 Velocity Potential and divergent wind climatology



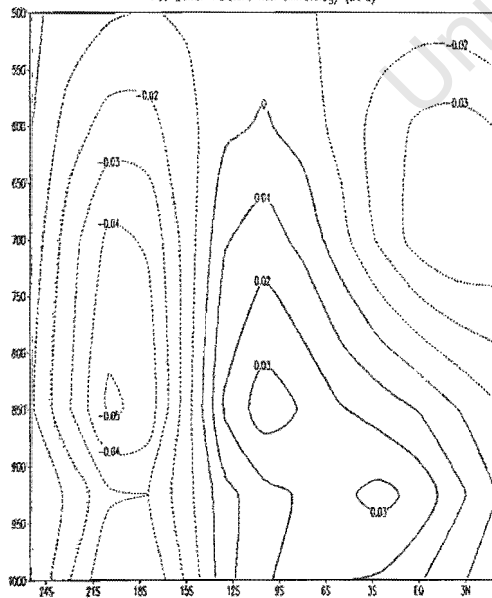
Feb OLR (Wm<sup>-2</sup>) Climatology



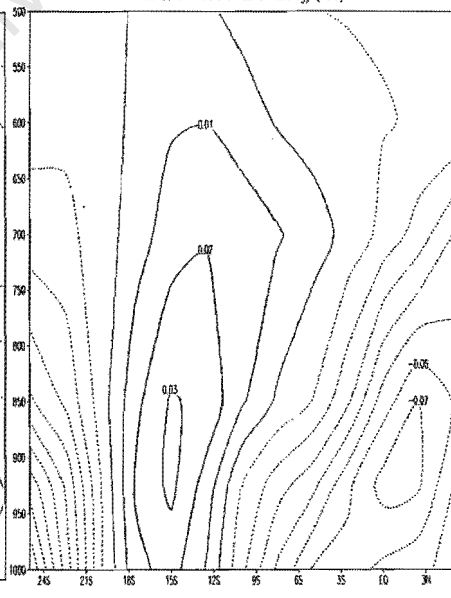
Feb 200 hPa Velocity Potential and divergent wind climatology



Feb Zonal moisture flux climatology (20°E)



Feb Zonal moisture flux climatology (40°E)



Feb Longitude height moisture flux climatology (15-5°S)

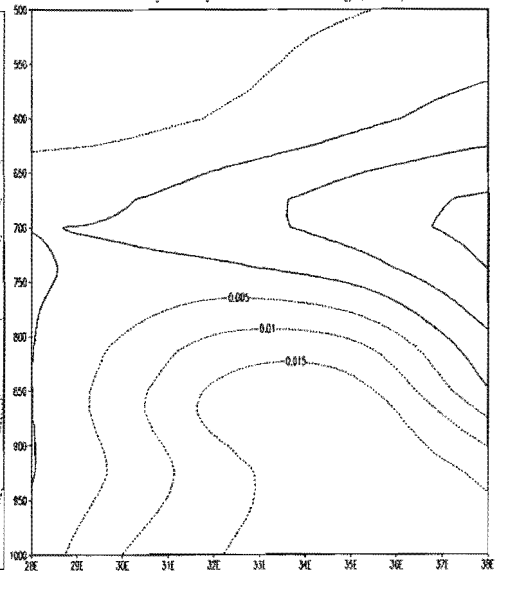
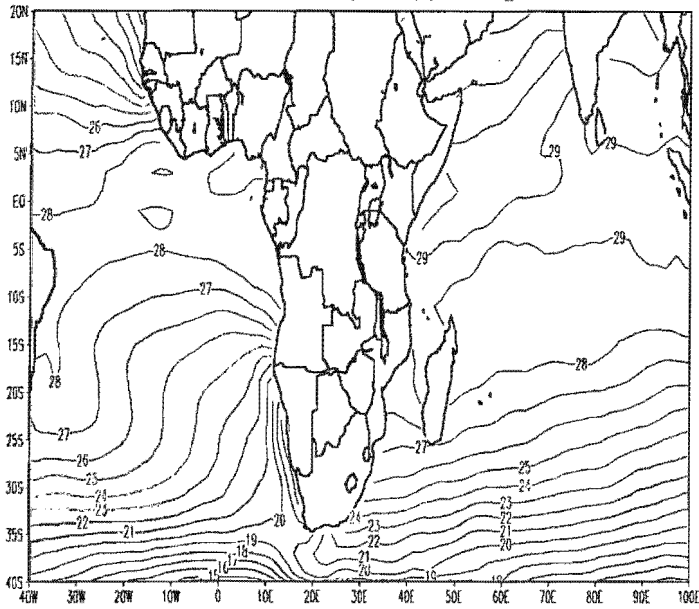
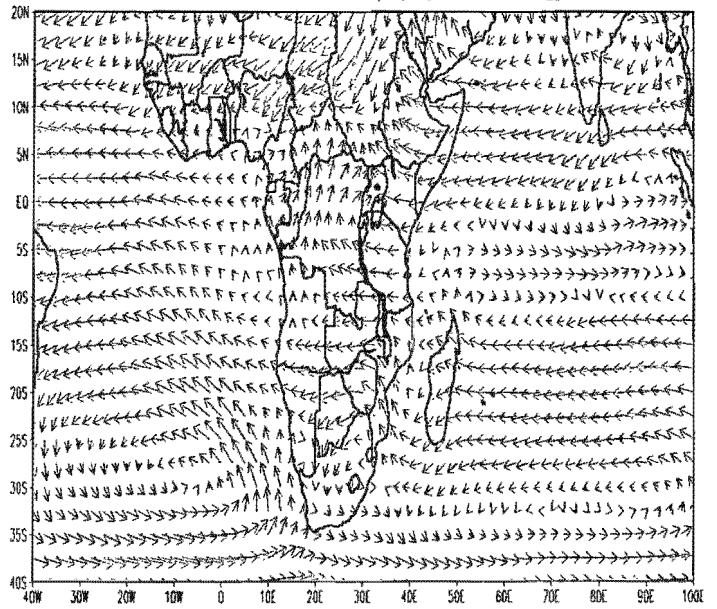


Fig. 3.1.1(e) cont..

Mar Sea Surface Temperature (°C) Climatology

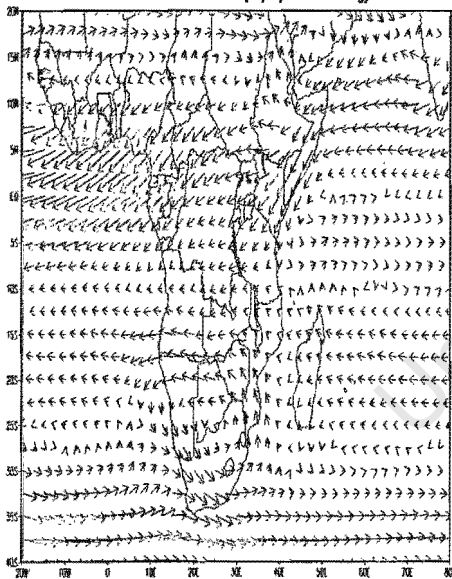


850 hPa Mar Wind (m/s) Climatology



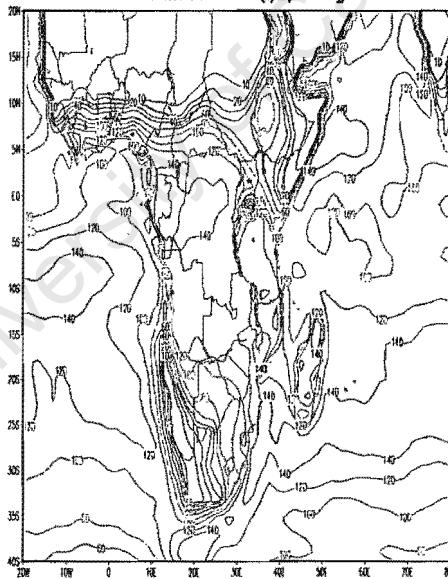
10

700 hPa Mar Wind (m/s) Climatology

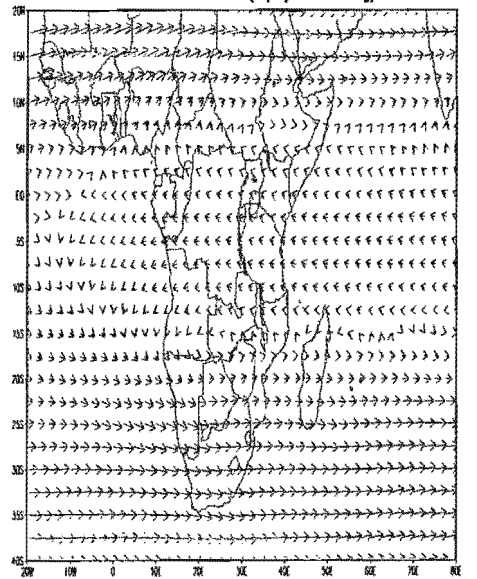


10

Mar Surface latent heat flux (W/m²) climatology



200 hPa Mar Wind (m/s) Climatology



40

Figure 3.1.1(f): as figure 3.1.1(a) but for March

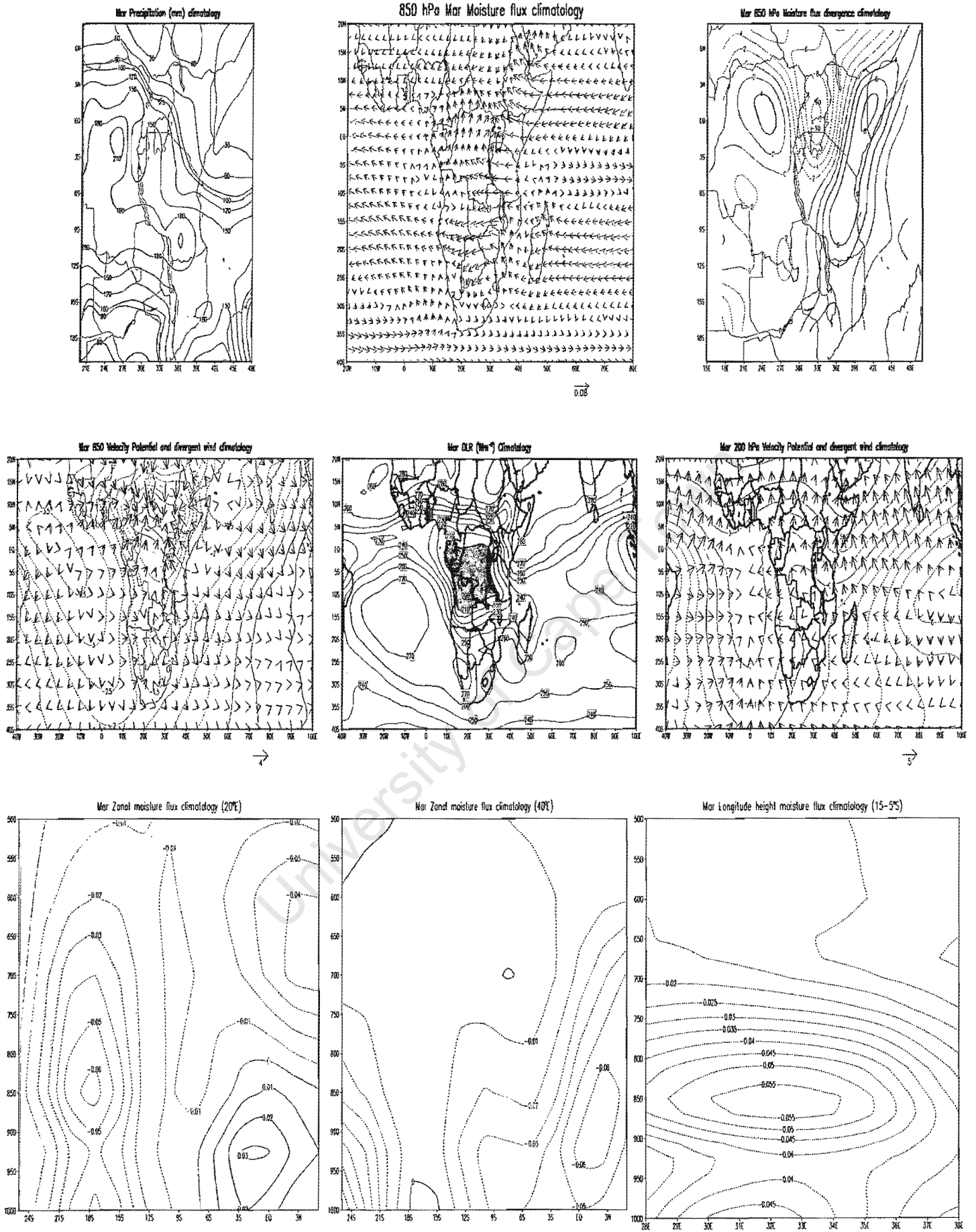
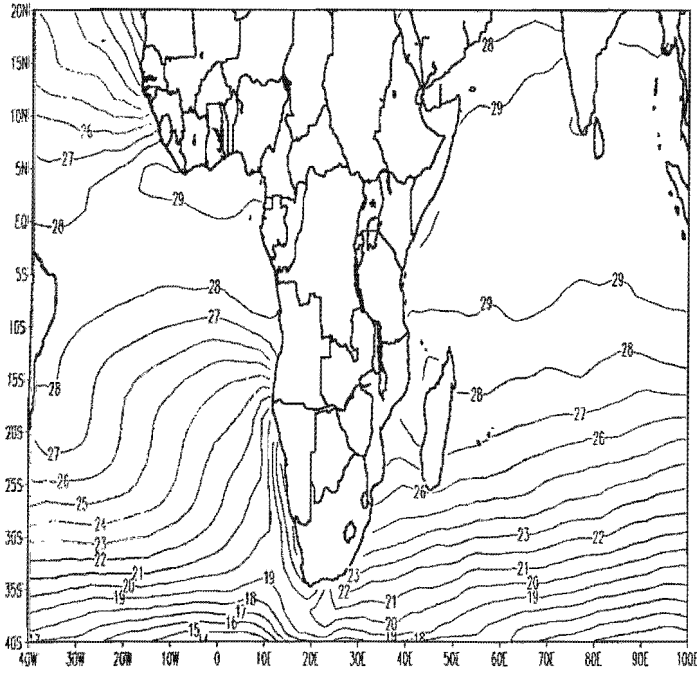
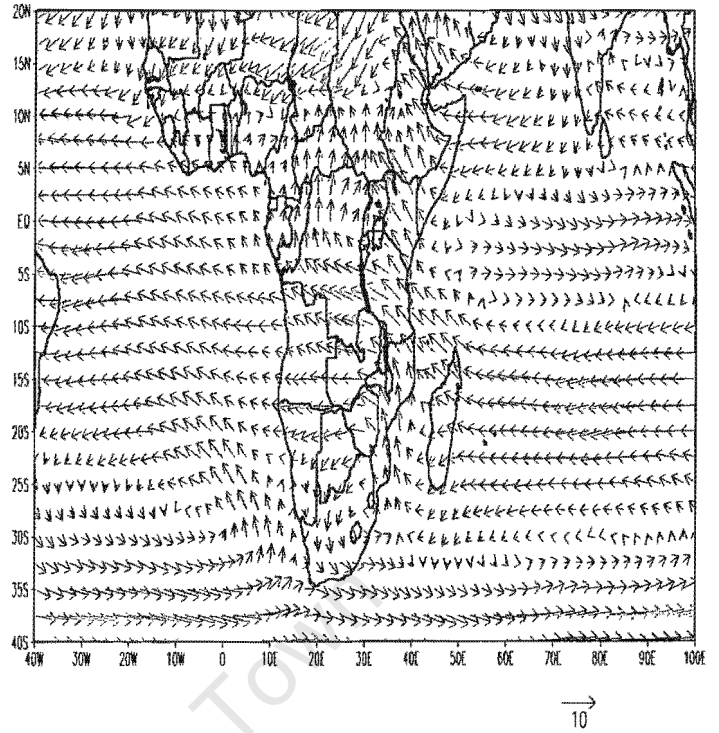


Fig. 3.1.1(f) cont..

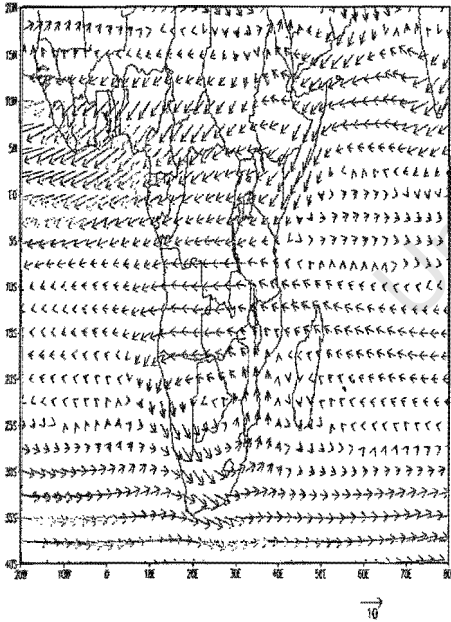
Apr Sea Surface Temperature (°C) Climatology



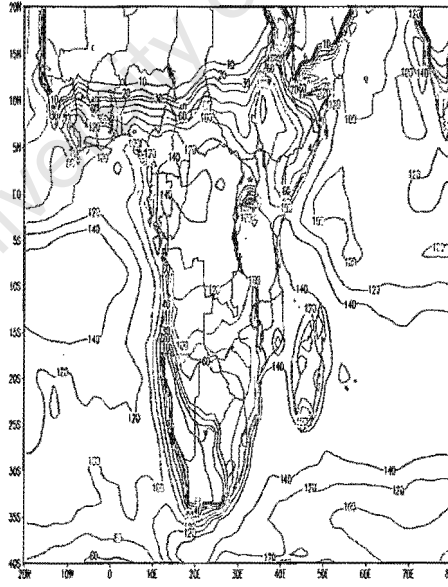
850 hPa Apr Wind (m/s) Climatology



700 hPa Apr Wind (m/s) Climatology



Apr Surface latent heat flux (W/m²) climatology



200 hPa Apr Wind (m/s) Climatology

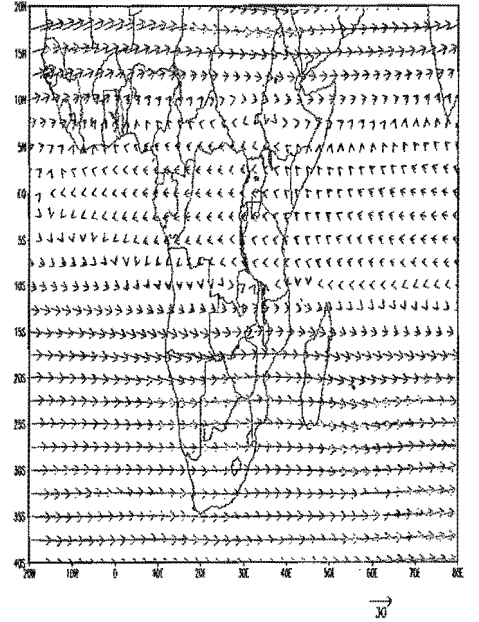


Figure 3.1.1(g): as figure 3.1.1(b) but for April

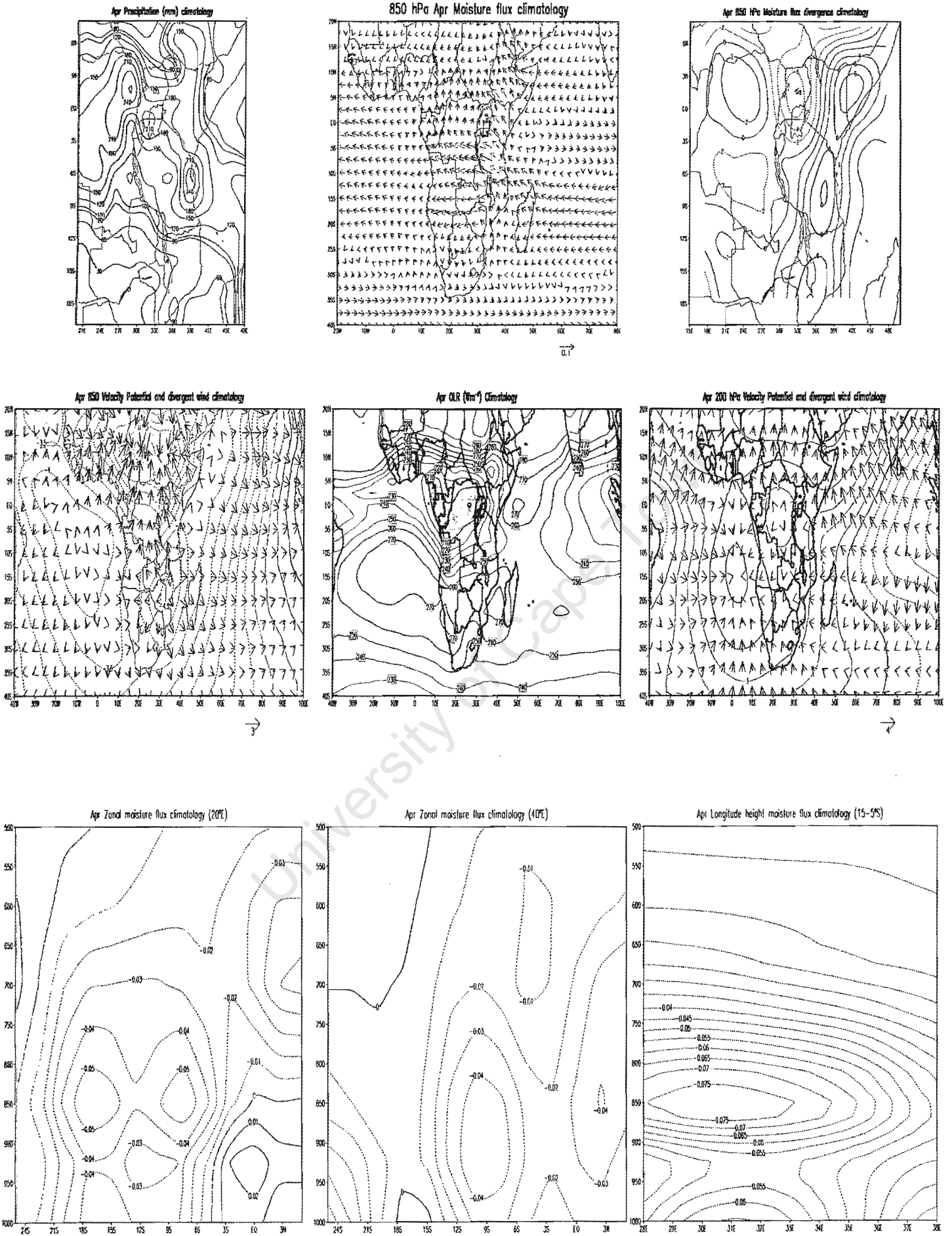
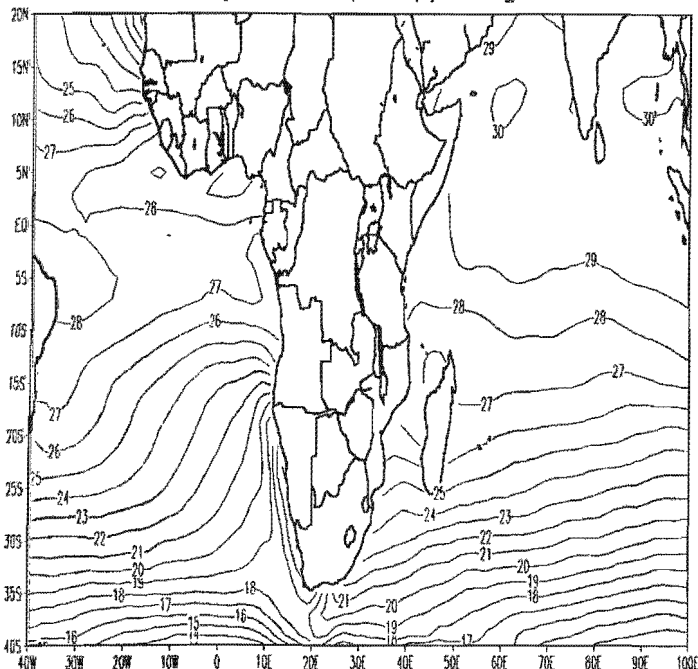
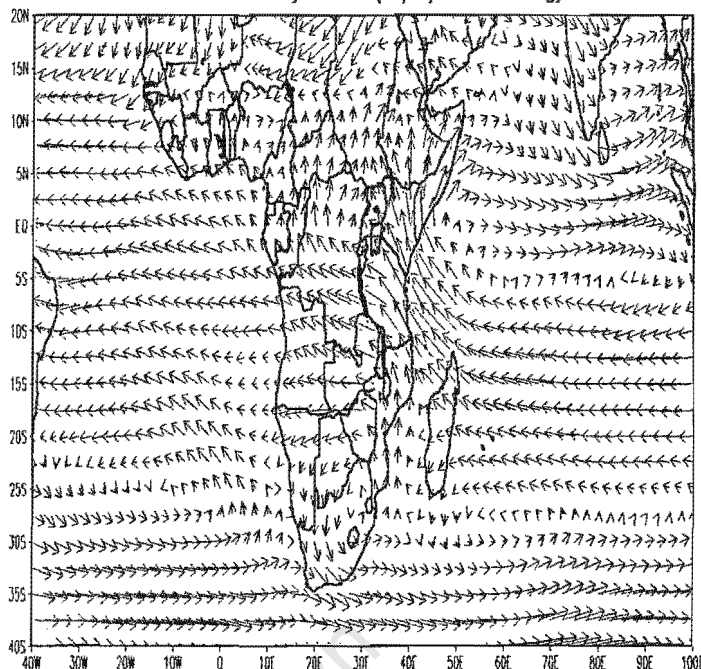


Fig. 3.1.1(g) cont..

May Sea Surface Temperature (°C) Climatology

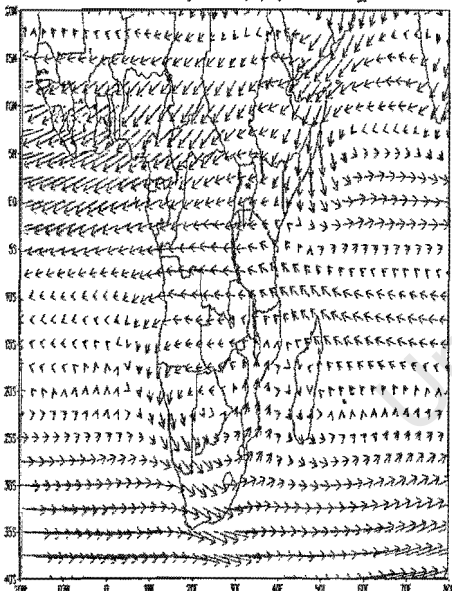


850 hPa May Wind (m/s) Climatology



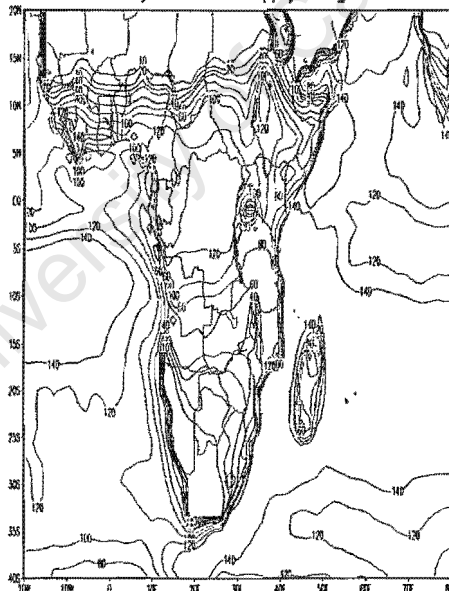
→  
10

700 hPa May Wind (m/s) Climatology

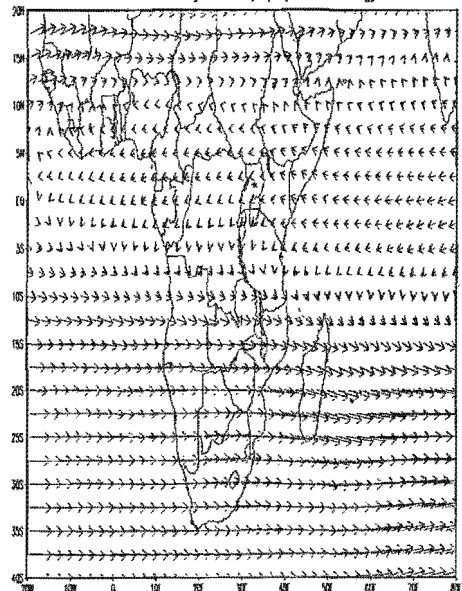


→  
10

May Surface latent heat flux (W/m²) climatology



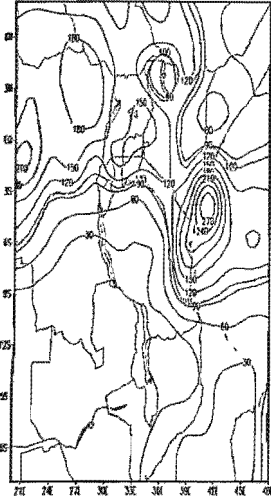
200 hPa May Wind (m/s) Climatology



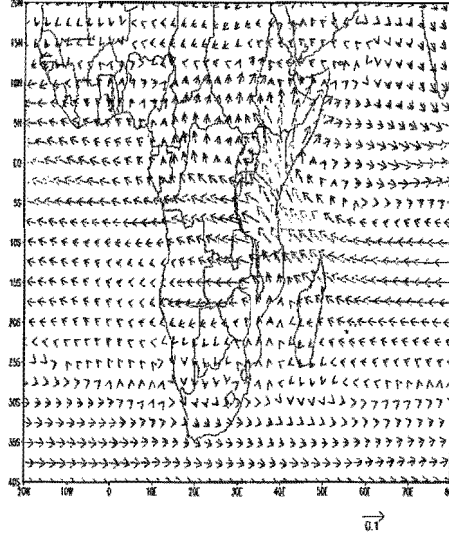
→  
30

Figure 3.1.1(h): as figure 3.1.1(d) but for May

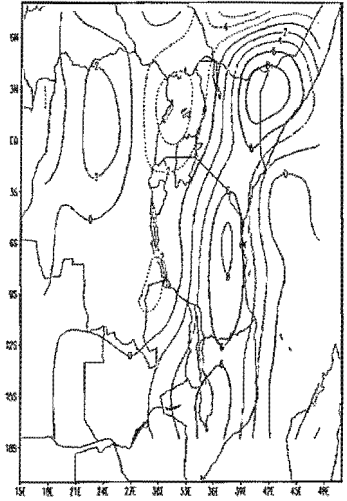
May Precipitation (mm) climatology



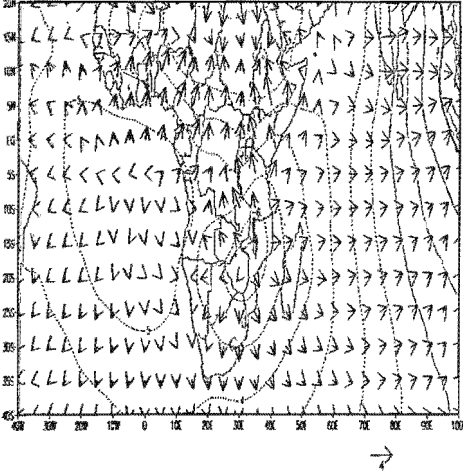
850 hPa May Moisture flux climatology



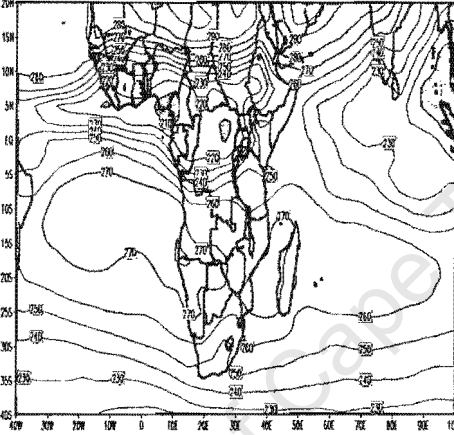
May 850 hPa Moisture flux divergence climatology



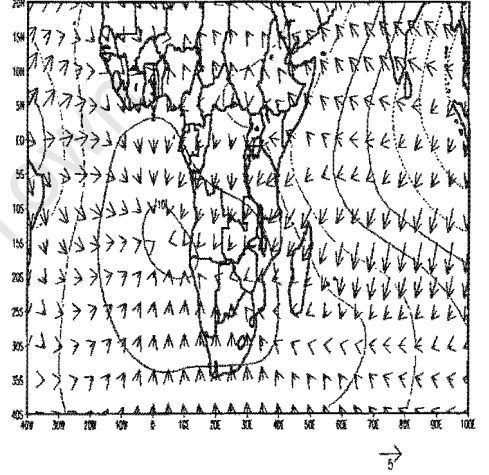
May 850 Velocity Potential and divergent wind climatology



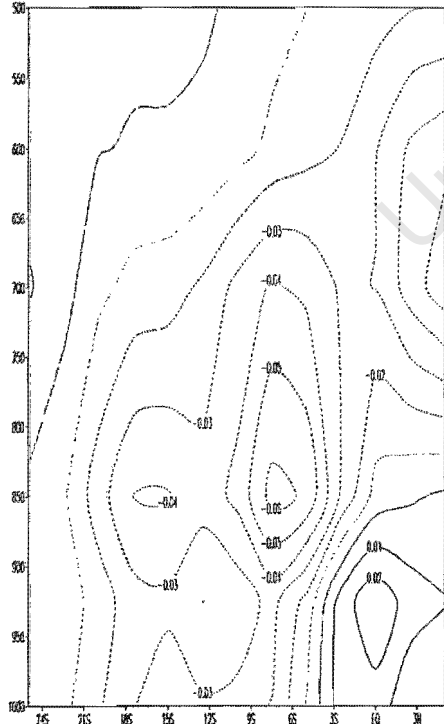
May CLR (Wm<sup>-2</sup>) climatology



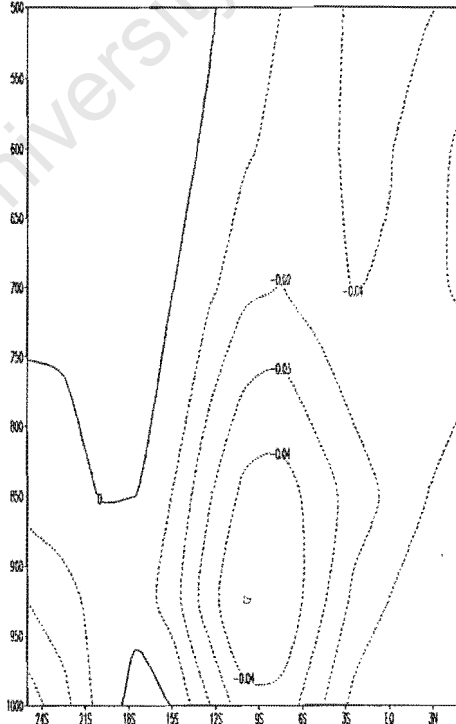
May 200 hPa Velocity Potential and divergent wind climatology



May Zonal moisture flux climatology (20°E)



May Zonal moisture flux climatology (40°E)



May Longitude height moisture flux climatology (15-5°S)

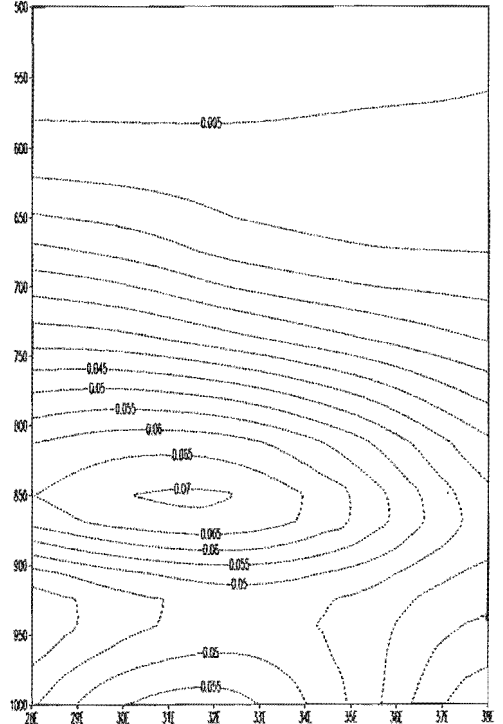


Fig.3.1.1(h) cont..

## **CHAPTER 4: Results of Rainfall Analyses**

### **4.1 Rainfall Time series**

Equation 1 in chapter 2 was used to normalise the October –April seasonal rainfall at each of the six stations used over western and southwestern Tanzania. Figures 4.1(a-c) shows the normalized rainfall departure for the six stations considered over the region. Years which are significantly wet or dry at each station are then chosen for composites. A criterion of at least  $\geq 0.8$  deviations above (below) the mean is required at each station for that particular year to be considered wet (dry) over western and southwestern Tanzania. This means that some years which are rather wet or dry at some stations but not at others are in fact excluded from the composite. An example is 1988, which at Tabora and Kigoma shows rainfall almost 1 standard deviation above average but at Iringa the rainfall for this year is less than 0.5 deviations above average.

Resulting for this procedure, the following years are included in the wet composite: 1968, 1970, 1978, 1979, 1982 and 1986. Similarly, the dry composite years are determined to be 1969, 1976, 1987, 1992, 1993 and 1998. The selected years are consistent with CMAP-Area averaged rainfall time series constructed for each gridded rainfall station used over 1979-1999 period.

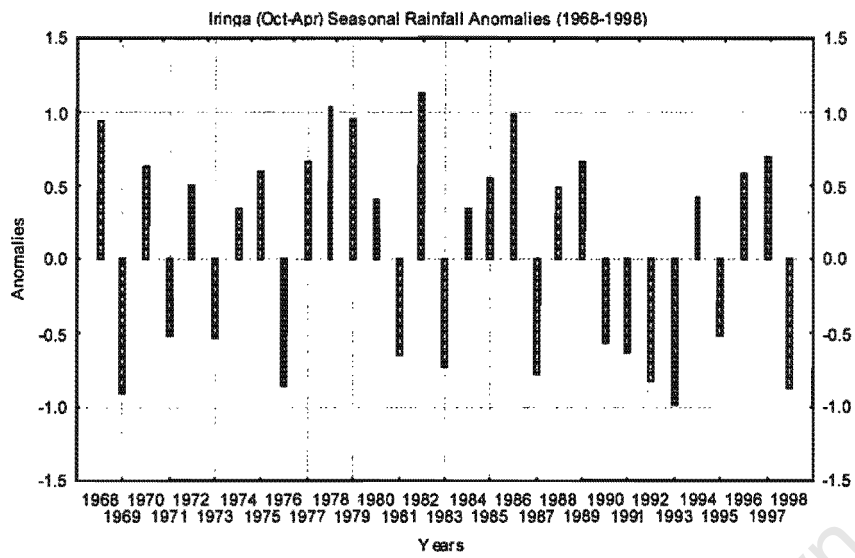
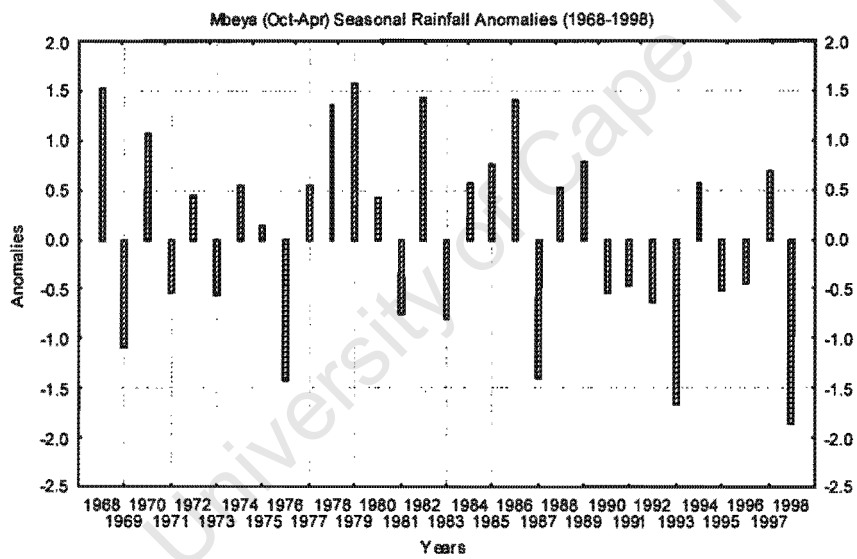


Figure 4.1 (a): Iringa and Mbeya (Oct-Apr) Seasonal rainfall Time series



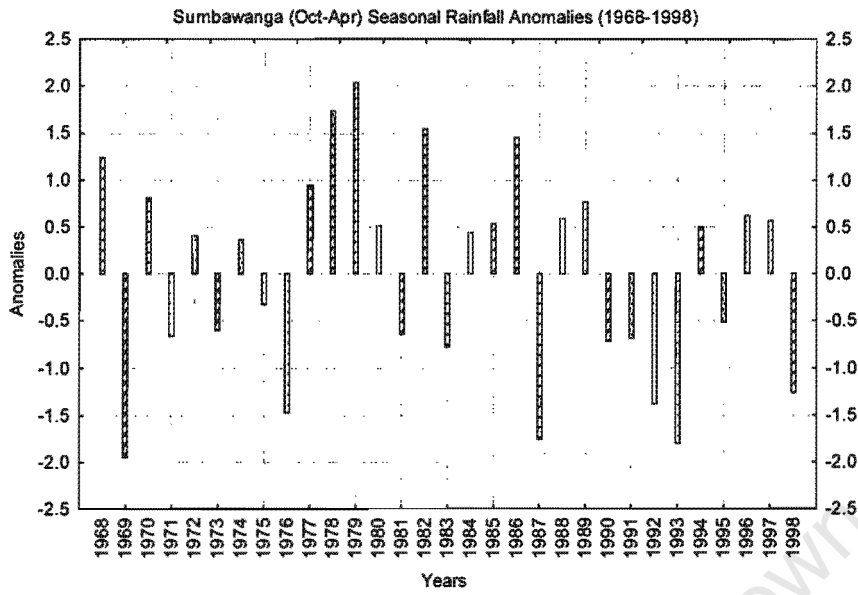
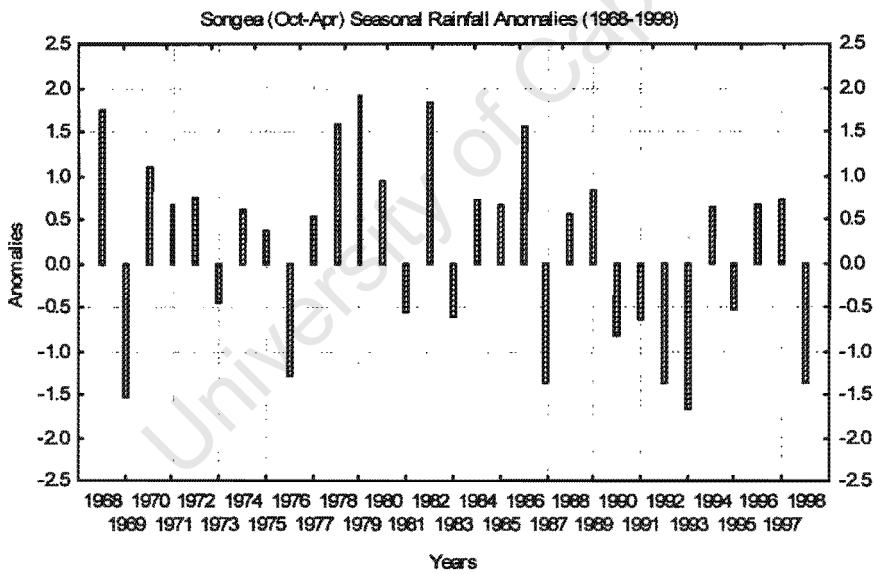


Figure 4.1 (b); Sumbawanga and Songea (Oct-Apr) Seasonal rainfall Time series



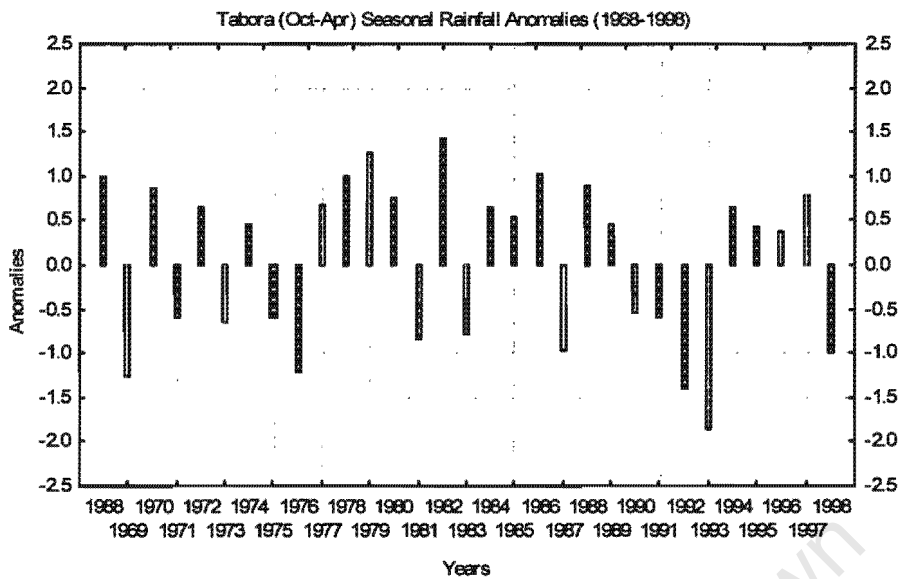
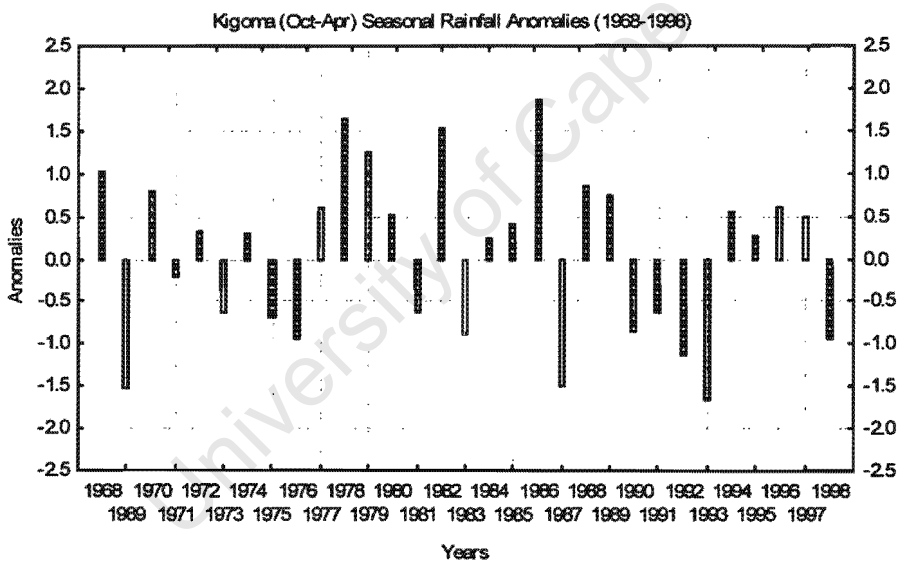


Figure 4.1 (c); Tabora and Kigoma (Oct-Apr) Seasonal rainfall Time series



## 4.2 Mean monthly composite anomaly evolution

This section discusses the composite anomaly evolution for the wet and dry years. The wet years used in the composite are 1968, 1970, 1978, 1979, 1982 and 1986, while the corresponding dry years are 1969, 1976, 1987, 1992, 1993 and 1998. Monthly plots corresponding to the onset, peak and withdrawal of the rainy season over western and southwestern Tanzania are shown.

#### 4.2.1 Wet years composite anomaly evolution

The wet composite in October [Figure 4.2.1(a)] indicates anomalously positive SST anomalies over the tropical western Indian Ocean, particularly east of Madagascar. Negative SST anomalies are apparent over the tropical southeast Indian Ocean. This SST anomaly pattern is reminiscent of the subtropical South Indian Ocean dipole suggested by Behera and Yamagata (2001) but only two of the years (1968, 1982) correspond to those identified by these authors. Over the Atlantic Ocean, negative SST anomalies are observed in the Gulf of Guinea and along the Angolan coast.

These negative anomalies are reminiscent of cool Benguela Nino events (Florenchie et al., 2003) which are forced by equatorial upwelling Kelvin waves and indeed the wind anomalies over the tropical Atlantic during July and August are suggestive of enhanced trades and generation of upwelling Kelvin waves.

During October, a strong lower tropospheric anticyclonic anomaly is evident over the western Indian Ocean. This circulation weakens the mean easterly flow over the equatorial North Indian Ocean (Fig.3.1.1a) and turns into a northerly anomaly on reaching the East African coast. Then anomalies imply a deceleration of the mean low-level southeasterly monsoonal flow over the western South Indian Ocean and therefore less moisture is expected for East Africa towards Central Africa. As a result, convergence occurs over western Tanzania. Another significant feature is a westerly anomaly from the tropical southeast Atlantic which extends across southern Angola, Zambia and the southern Congo basin towards Tanzania. These westerly anomalies converge over western Tanzania with easterlies from the tropical Indian Ocean.

At 200 hPa, the upper level cyclonic anomaly over Angola acts to strengthen the westerly mean flow (Fig.3.1.1a) from the tropical southeast Atlantic and Congo basin over the region. The low-level moisture convergence over western Tanzania is associated with positive latent heat flux anomalies and negative OLR anomalies over the region, which indicates increased evaporation and convection.

The composite velocity potential and divergent wind anomaly plots confirm this by indicating strong low-level convergence at 850hPa with associated anomalous upper level divergence. The composite zonal section of moisture flux anomaly along 20°E and 40°E provides further evidence of the convergence. Along 20°E, the zonal section of moisture flux indicates anomalous strong low-level westerlies between 5°S and 3°S with anomalous easterlies between 18°S and 6°S also between the equator and 4°N. These westerlies increase with height vertically up from the surface to 500hPa with maximum intensity at 700hPa level.

Along 40°E, low-level easterly anomalies are observed over most of the region with maximum between 24°S and 18°S, 11°S and 6°S and north of the equator. The longitude height section of moisture flux indicates a region of strong lower tropospheric westerly anomaly extending eastward to 35°E, and low-level easterly anomalies further east. At mid levels easterly anomalies are evident. The lower tropospheric westerly anomaly are centred at 850 and 700hPa beneath the easterly anomalies along 600hPa and 500hPa level. It is evident that anomalous westerly flow from the tropical southeast Atlantic located between 6°S and 3°S and easterlies from the tropical Indian Ocean between 9°S and 6°S are important in modulating the moisture flux from these two oceans into the region.

Moisture convergence over the region is consistent with positive anomaly value of rainfall apparent over western Tanzania during October.

In November [Figure 4.2.1(b)], negative SST anomalies in the South Atlantic intensify compared to the previous month while the Indian Ocean SST anomalies have weakened.

At 850hPa, an anticyclonic anomaly is apparent over the tropical South Indian Ocean which tends to weaken the mean easterly wind flow near 10°S (Fig.3.1.1b) toward the East African coast. Together with this, the westerly anomaly seen over the tropical southeast Atlantic Ocean at 700hPa acts to decelerate the flow for the Indian Ocean and weaken the export of moisture west out of Tanzania.

These lower tropospheric westerly anomalies converge locally over eastern Tanzania with weak anomalous northeasterlies from the tropical western Indian Ocean.

At 200hPa, southwesterly anomalies over the Mozambique Channel turn into southeasterly anomalies over Tanzania. This upper level pattern is favourable for convection to occur over the region since it implies upper level divergence. The composite velocity potential and divergent wind anomaly plots confirm the rainfall increase over the region by indicating a strong low level convergence anomaly zone to the west and east over Tanzania at 850hPa with associated anomalous wind divergence at the 200hPa level. This low level convergence over the region is consistent with the southeastward extent of large negative OLR anomalies, positive latent heat flux anomaly and increased rainfall.

The composite zonal section of moisture flux anomaly along 20°E portrays a similar pattern to October with the exception of stronger easterly anomaly between 15°S and 6°S and between the equator and 4°N. These anomalous easterlies are observed to incline vertically with height to 500hPa with maximum intensity at 850hPa level. Along 40°E, the lower tropospheric westerly anomaly between 3°S and equator is weaker than October while between 21°S and 15°S; these anomalies increase and extend from 850hPa to 500hpa. Compared to October, the easterlies anomalies strengthen and extend further southward from between 6°S and 15°S in November are apparent up to 500hPa. Strong westerly anomalies at 700hPa between Equator and 6°S along 20°E and easterly anomalies between 6°S and 15°S along 40°E can partly explain the moisture convergence over the region which leads to the rainfall increase over western Tanzania in November.

During December [Figure 4.2.1(c)], negative SST anomalies continue over the tropical South Atlantic with positive SST anomalies further south. In the Indian Ocean, the previous month's negative SST anomalies over the central region remain but positive anomalies are now apparent near the East African coast and in the east of this basin. The lower tropospheric anticyclonic anomaly over the central Indian Ocean is stronger than November and acts to weaken the easterly inflow from the Indian Ocean towards Tanzania. Another significant lower tropospheric feature at 700hPa is stronger westerly anomalies from the tropical southeast Atlantic over the Southern Congo basin. A further significant low-level feature is an anticyclonic anomaly observed to develop over south of Madagascar with associated southerly anomalies over Mozambique. At 200hPa, an anticyclonic anomaly becomes evident over central Africa.

This upper level anomaly, which is associated with anomalous easterly flow over Tanzania, is a favourable condition for the low-level convergence and convection since it suggests upper level divergence. Low-level convergence exists over Tanzania together with a large negative OLR anomaly and a large positive anomaly in latent heat flux. As a result, a large increase in rainfall over the mean is observed over Tanzania during December.

The velocity potential and divergent wind plots confirm the strong low-level convergence over almost all of Tanzania with associated anomalous divergence aloft. The zonal sections of moisture flux anomaly along 20°E and 40°E further illustrate this low-level moisture convergence over the region.

The zonal section of moisture flux anomaly along 20°E reveals a strong westerly anomaly centred near 700hPa between 3°S and the equator, while along 40°E weak easterly anomalies exist between 12°S and the equator. Taken together this, with the southward shift of the ITCZ over Southern Tanzania during this month, leads to strong moisture convergence over western and southwestern Tanzania and hence a substantial increase of rainfall in December.

During January [Figure 4.2.1(d)], negative SST anomalies strengthen in the subtropical and mid-latitude South Indian and South Atlantic Oceans. Weak positive anomalies are present further north in the tropical Indian Ocean. During this month, an anticyclonic anomaly develops over Angola at 850hPa, which acts to weaken the westerly mean flow [Fig. 3.1.1d] from the tropical southeast Atlantic across northern Angola towards the Congo basin.

Southwesterly anomalies over Tanzania imply a decelerating mean flow and low-level convergence. A broad cyclonic anomaly southeast of Madagascar at 850hPa leads to southerly anomalies over Zimbabwe, Mozambique and the Channel. This flow weakens at 700hPa and reverses at 200hPa indicating its baroclinic nature that enhances the easterly anomaly flow along 10°S at upper level from the tropical south Indian Ocean to the region.

This upper level feature with easterly anomalies near 10°S is a favourable condition for low-level convergence and rainfall increase over southwestern Tanzania since it implies upper level divergence. The moisture convergence over southwestern Tanzania, negative OLR anomalies and positive latent heat flux anomaly all suggest increased surface evaporation and increased precipitation as observed over the region.

Consistent with increased rainfall over the region, the velocity potential anomaly indicates low-level convergence anomaly over Tanzania with associated upper level divergent anomaly. The zonal section of moisture flux anomaly further illustrates this convergence over southwestern Tanzania by indicating westerly anomaly between 24°S and 15°S along 20°E and easterly anomaly between 15°S and 10°S along 40°E, consistent with the shift of the ITCZ over northern Mozambique during this month. The longitude height section of moisture flux anomaly indicates stronger lower tropospheric westerlies dominating eastward to about 36°E. This region inclines vertically up with height to 550hPa with maximum intensity at 700hPa level.

By February [Figure 4.2.1(e)], positive SST anomalies have developed over most of the tropical Indian Ocean with large negative anomalies over the subtropical South Atlantic and South Indian Ocean. The most significant lower tropospheric feature during this month is strengthening of the anticyclonic anomaly over Angola, which acts to reduce the inflow from the tropical southeast Atlantic into the region and weaken the easterly flow over Namibia.

The previous month's cyclonic anomaly southeast of Madagascar is no longer apparent and in fact an anticyclonic anomaly exists south of the Mozambique Channel. North of Madagascar, an easterly anomaly exists in the tropical western Indian Ocean towards the coast of Tanzania.

At 200hPa, westerly anomalies are observed to extend over the tropical Atlantic Ocean, Africa and the western Indian Ocean. This upper level anomaly suggests a weaker Walker circulation, upper level convergence and hence subsidence and decreased rainfall over Tanzania is observed. Consistent with the rainfall decrease over the western and southern Tanzania is a band of large positive OLR anomalies extending over the country from the western Indian Ocean and reduced evaporation from this oceanic region. The velocity potential anomaly plot illustrates stronger low-level divergent anomalies at 850hPa level with anomalous upper level convergence, again unfavourable for rainfall.

The zonal section of moisture flux anomaly along 20°E and 40°E supports this decrease of rainfall over the region by indicating westerly anomaly between 24°S and 18°S along 20°E and strong easterly anomalies between 21°S and 12°S along 40°E.

This convergence is located further south over Zambia and Mozambique and reflects the climatological position of ITCZ over those regions during this month consistent with rainfall decrease over Tanzania.

During March [Figure 4.2.1(f)], weak anomalies are evident over the tropical oceans while noticeable negative SST anomalies still prevail over the subtropical South Indian Ocean and Atlantic Oceans. The anticyclonic feature over Angola and Namibia remains prominent, and reduces inflow on its northern side from the tropical Southeast Atlantic. A strong cyclonic anomaly has developed northeast of Madagascar which weakens the easterly inflow into Tanzania from the tropical South Indian Ocean.

The previous month's anticyclonic anomaly south of Mozambique Channel has strengthened and shifted east slightly. Relative low-level convergence between the southeastern African and southwestern Indian Ocean anticyclonic anomalies is evident over southern Tanzania. This, together with the northward movement of the ITCZ over the region contributes to the increased rainfall seen during this month.

At 200hPa, the most pronounced feature is enhanced easterly anomaly over the tropical western Indian Ocean sweeping across East Africa towards the Atlantic Ocean. This upper level easterly anomaly suggests a stronger Walker circulation and favourable conditions for low level convergence and convection to occur over the region since it implies upper level divergence.

The low-level moisture convergence over the region is consistent with negative OLR anomalies over Tanzania and the Congo basin however the latent heat flux anomalies are relatively weak during this month. The velocity potential anomaly plot indicates a weak convergence over the region with increased convergence over the Indian Ocean at 850hPa level and an upper level divergent anomaly consistent with increased rainfall. The zonal sections of moisture flux anomaly along 20°E and 40°E also confirm this convergence over the region by showing lower tropospheric westerly anomalies between 6°S and 3°S along 20°E and strong easterlies centred at 850hPa and 700hPa along 40°E between 12°S and 6°S.

The longitude height section of moisture flux anomaly indicates a region of strong westerly anomaly to dominate over the region centred at 850hPa level and extend eastward to about 38°E. As a result, low-level moisture convergence exists over the region and increased rainfall occurs over southwestern Tanzania in March.

During April [Figure 4.2.1(g)], weak SST anomalies are present over the Indian Ocean while strengthened negative anomalies are still apparent in the South Atlantic. The significant pattern during this month is an anticyclonic anomaly north of Madagascar that enhances the easterly flow from the tropical western Indian Ocean towards Tanzania. This easterly flow converges over northern Tanzania with weak westerly anomalies from the Congo basin. The low level convergence over northern Tanzania together with negative OLR anomalies over much of East Africa and increased land surface evaporation over the region leads to the increased rainfall observed in this month.

The moisture evaporated at the Tanzanian coast as seen in latent heat flux anomaly and transported inland via easterlies (seen in 850hPa wind anomalies) contributes to the rainfall increase over the region in April. The velocity potential anomaly field indicates low level convergence and upper level divergent anomalies consistent with the increased rainfall. The zonal sections of moisture flux anomaly indicate lower tropospheric westerly anomalies between 3°S and the equator along 20°E and strong lower tropospheric easterly anomalies between 9°S and 3°S along 40°E that explain the low level convergence of the moisture and rainfall over the northern Tanzania in April.

During May [Figure 4.2.1(h)], the negative SST anomalies seen in the South Atlantic in March and April have contracted to the Benguela and Gulf of Guinea regions. Over the Indian Ocean, the west continues to show weak anomalies with more obvious negative anomalies in the east. During this month, a low level anticyclonic anomaly develops east of Somalia with a larger anticyclonic anomaly off the Tanzanian and Mozambique coasts. These anomalies enhance the mean southeasterly flow from the western Indian Ocean towards Tanzania.

At 200hPa, westerly anomalies persist over Tanzania and become a northwesterly anomaly over tropical western Indian Ocean. The weak negative OLR and positive latent heat flux anomalies over Tanzania are consistent with little change in rainfall from the mean over most of Tanzania during this month. May is the transition period towards the southwest (SW) monsoon over the Indian subcontinent and marks the end of the long rainy season over the northern Tanzania.

Velocity potential anomaly plots illustrate this transition period and show strong low level convergence anomaly over northern Tanzania and over Indian subcontinent at 850hPa level with associated upper level divergent anomaly. A summary of SST anomalies and circulation features associated with wet conditions over the western and southwestern Tanzania is provided in Table 1.

University of Cape Town

**Table 1: SST anomalies and circulation features associated with wet conditions over western and southwestern Tanzania**

INDIAN OCEAN	ATLANTIC OCEAN
<p><b>October:</b></p> <p><b>SST:</b> -Positive SST anomalies over tropical western Indian Ocean east of Madagascar.</p> <p>-Negative SST anomalies over tropical southeast Indian Ocean</p> <p>-Lower tropospheric anticyclonic anomaly over western Indian Ocean</p> <p>-Strong upper level westerly anomalies.</p> <p>-Enhanced negative OLR anomalies over western Tanzania, Zambia, Mozambique, Zimbabwe and southern Madagascar</p> <p><b>November:</b></p> <p>-Weak positive SST anomalies.</p> <p>-An anticyclonic anomaly over the south Indian Ocean.</p> <p>-Upper level southwesterly anomaly over the Mozambique Channel turn into southeasterly anomaly over Tanzania.</p> <p>-Negative OLR anomalies over Tanzania.</p>	<p><b>October:</b></p> <p><b>SST:</b> -Negative SST anomalies over the Gulf of Guinea and along the Angolan coast.</p> <p>-Lower tropospheric westerly anomaly from the tropical Southeast Atlantic ocean into Tanzania.</p> <p>-Upper level cyclonic anomaly over Angola acts to strengthen the westerly flow from the tropical Southeast Atlantic and Congo basin.</p> <p><b>November:</b></p> <p>-Negative SST anomalies over tropical south Atlantic.</p> <p>-Lower tropospheric westerly anomaly over tropical southeast Atlantic at 700hPa.</p>

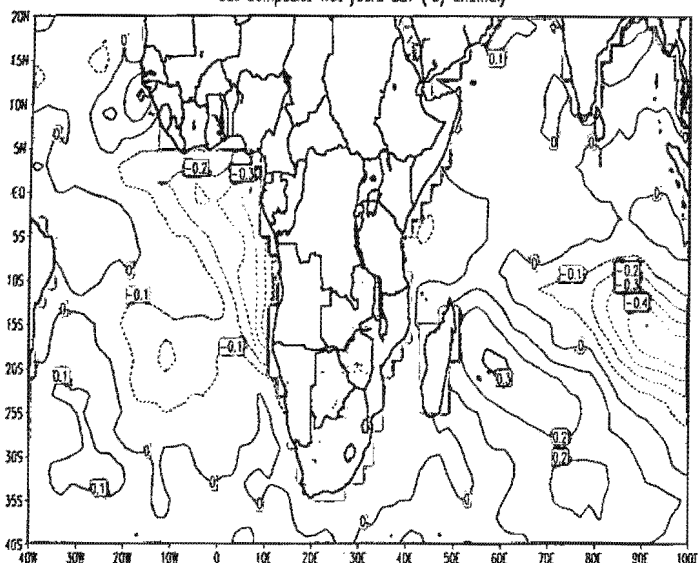
INDIAN OCEAN	ATLANTIC OCEAN
<p><b>December:</b></p> <ul style="list-style-type: none"> <li>-Positive SST anomalies over the East African coast and in the east of this basin.</li> <li>-Lower tropospheric anticyclonic anomaly over the central Indian Ocean</li> <li>-An anticyclonic anomaly over south of Madagascar with associated southerly anomalies over Mozambique.</li> <li>-Upper level anticyclonic anomaly over Central Africa with associated anomalous easterly flow over Tanzania.</li> <li>-Large negative OLR anomalies over Tanzania, western Indian Ocean and northeast of Madagascar.</li> </ul>	<p><b>December:</b></p> <ul style="list-style-type: none"> <li>-Negative SST anomalies over tropical South Atlantic with warm SST further south.</li> <li>-Westerly anomalies from the tropical Southeast Atlantic over the Southern Congo basin</li> </ul> <p><b>January:</b></p> <ul style="list-style-type: none"> <li>-Strengthened negative SST anomalies in the subtropical and mid-latitude South Atlantic.</li> <li>-Anticyclonic anomaly developing over Angola.</li> <li>-Westerly anomalies from the tropical Southeast Atlantic weakening.</li> </ul>

INDIAN OCEAN	ATLANTIC OCEAN
<p><b>January:</b></p> <ul style="list-style-type: none"> <li>- Negative SST anomalies in the subtropical and mid-latitude South Indian Ocean</li> <li>-Weak positive anomalies are evident further north in the tropical Indian Ocean.</li> <li>-A broad cyclonic anomaly southeast of Madagascar at 850hPa.</li> <li>-Upper level anticyclonic anomaly over Madagascar with associated easterly anomalies along 10°S.</li> <li>-Negative OLR anomalies over southern Tanzania, Mozambique and northeast of Madagascar.</li> </ul> <p><b>February:</b></p> <ul style="list-style-type: none"> <li>-Positive SST anomalies over most of the tropical Indian Ocean</li> <li>-Large negative SST anomalies over subtropical South Indian Ocean.</li> <li>-An anticyclonic anomaly south of the Mozambique Channel.</li> <li>-Easterly anomalies exists in the tropical western Indian Ocean</li> </ul>	<p><b>February:</b></p> <ul style="list-style-type: none"> <li>-Large negative SST anomalies over subtropical South Atlantic Ocean.</li> <li>-Weak positive SST anomalies near the Angolan coast.</li> </ul> <p><b>March:</b></p> <ul style="list-style-type: none"> <li>-Negative SST anomalies are still evident over the subtropical South Atlantic Ocean.</li> <li>-Anticyclonic feature over Angola and Namibia are apparent.</li> <li>-Westerly anomalies from the tropical Atlantic are shown.</li> </ul> <p><b>April:</b></p> <ul style="list-style-type: none"> <li>-Strengthened negative SST anomalies over South Atlantic Ocean</li> <li>-Weak westerly anomalies from the Congo basin are apparent</li> </ul>

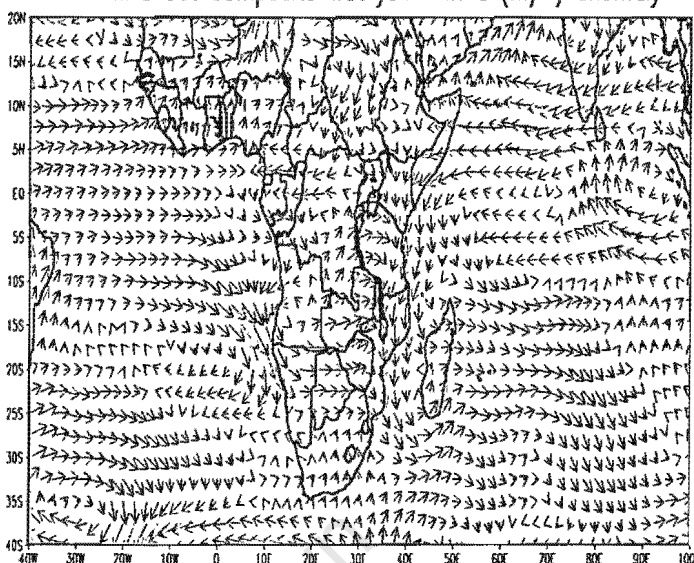
INDIAN OCEAN	ATLANTIC OCEAN
<p>-Upper level westerly anomalies over the tropical Atlantic, Africa and western Indian Ocean (weaker Walker circulation)</p> <p>-Stronger positive OLR anomalies over Tanzania and western Indian Ocean.</p> <p><b>March:</b></p> <p>-Weak positive SST anomalies over tropical western Indian Ocean and along the East African coast.</p> <p>-Negative SST anomalies over the subtropical South Indian Ocean.</p> <p>-A strong cyclonic anomaly developed over the northeast of Madagascar.</p> <p>-Upper level anomalies build up over tropical western Indian Ocean sweeping across East Africa to Atlantic Ocean.</p> <p>-Negative OLR anomalies over southern Tanzania, Zambia, Mozambique and Madagascar.</p>	<p><b>May:</b></p> <p>- Negative SST anomalies are still present over this ocean with large anomalies over Benguela and Gulf regions.</p> <p>-Anticyclonic anomaly over Angola and tropical Southeast Atlantic at 850hPa is evident.</p>

INDIAN OCEAN	ATLANTIC OCEAN
<p><b>April:</b></p> <ul style="list-style-type: none"> <li>-Weak positive SST anomalies are evident over Indian Ocean along the East African coast and to the South.</li> <li>-Anticyclonic anomaly over north of Madagascar</li> <li>-Large negative OLR anomalies over much of East Africa, Ethiopia and Somalia.</li> </ul> <p><b>May:</b></p> <ul style="list-style-type: none"> <li>-Negative SST anomalies are evident to the east of this Ocean while to the west weak anomalies are present.</li> <li>-Low-level anticyclonic anomaly seen to develop east of Somalia with large anticyclonic anomaly off the Tanzanian and Mozambique coasts.</li> <li>-Enhanced mean easterly flow from the western Indian Ocean towards Tanzania is apparent.</li> <li>-Negative OLR anomalies over coast of Tanzania and north of Madagascar.</li> </ul>	

Oct Composite Wet years SST (°C) anomaly

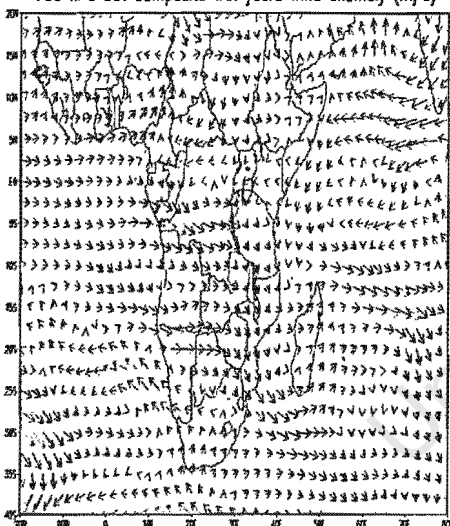


850 hPa Oct Composite Wet years wind (m/s) anomaly



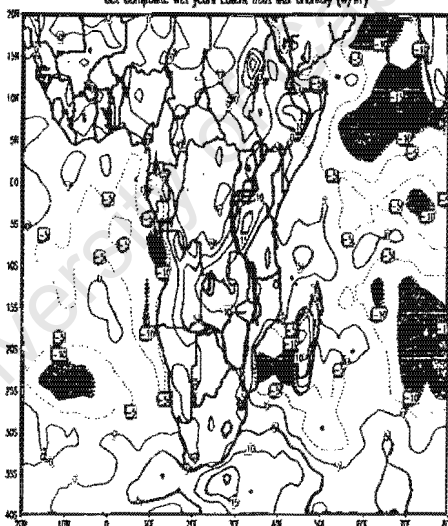
2

700 hPa Oct Composite Wet years Wind anomaly (m/s)

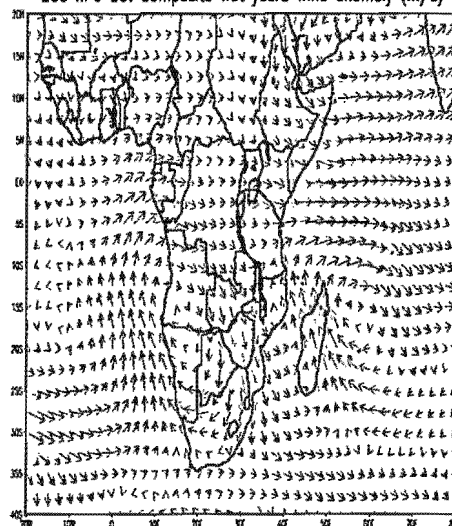


2

Oct Composite Wet years Latent heat flux anomaly (W/m²)



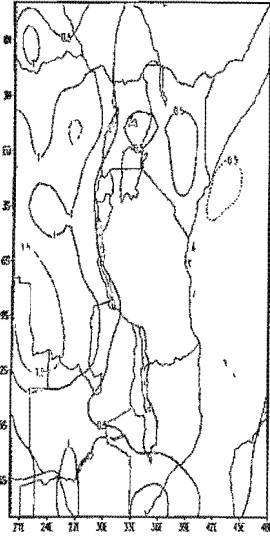
200 hPa Oct Composite Wet years Wind anomaly (m/s)



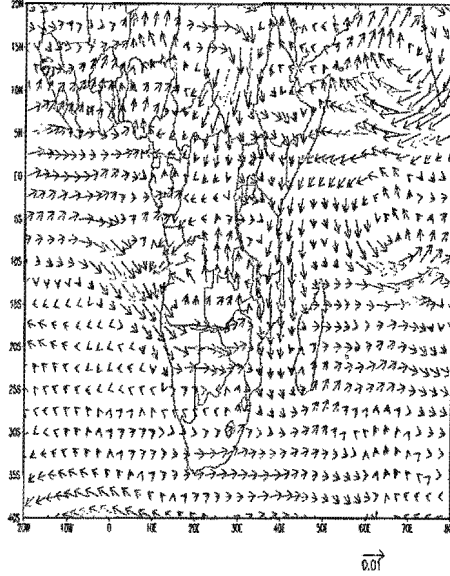
2

Figure 4.2.1(a) October wet composite anomaly; SST(contour interval 0.1°C ), wind at 850,700 and 200hPa (scale vector is shown at the bottom), latent heat flux (contour interval is 5 W/m<sup>2</sup>). Colour on wind vectors indicate their magnitude from low (purple) to high (red).

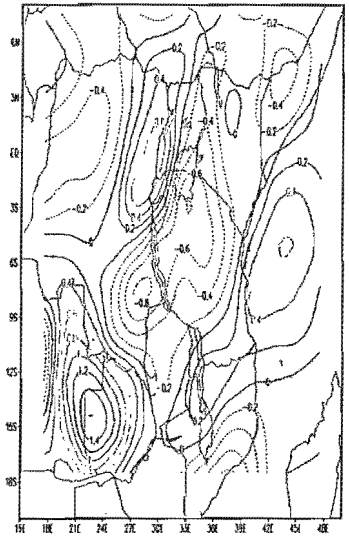
Oct Composite wet years precipitation (mm) anomaly



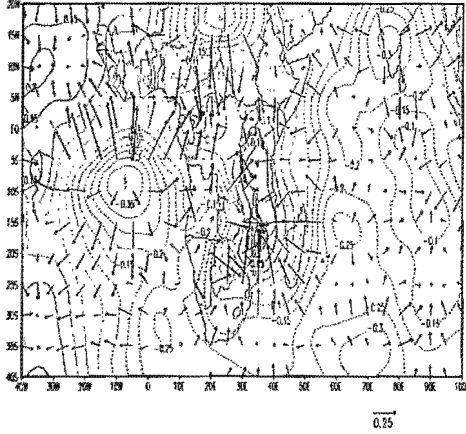
850 hPa Oct Composite wet years moisture flux anomaly



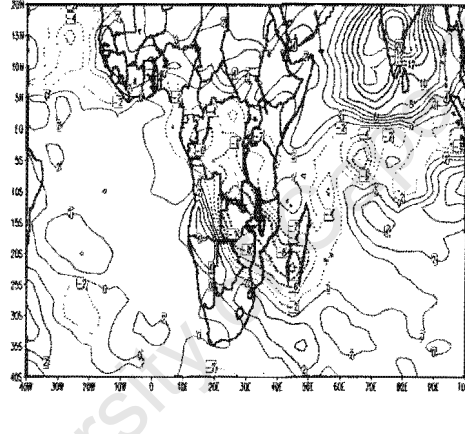
Oct 850 hPa Composite wet years moisture flux divergence



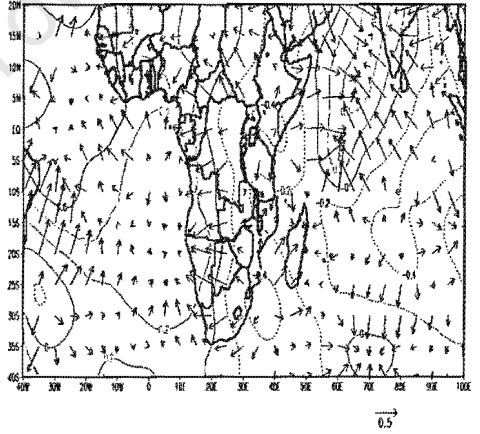
Oct 850 hPa Composite Wet VPotential and divergent wind anomaly



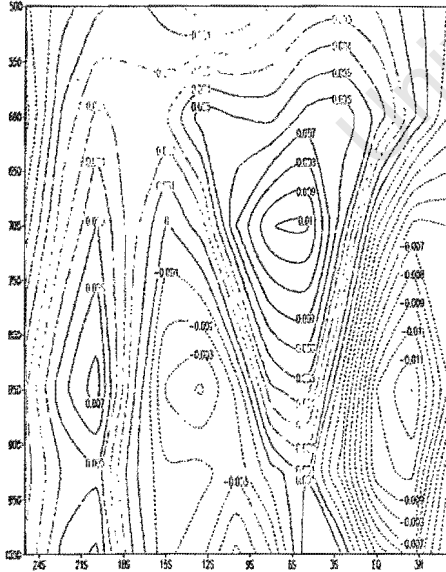
Oct Composite wet years OLR ( $Wm^{-2}$ ) anomaly



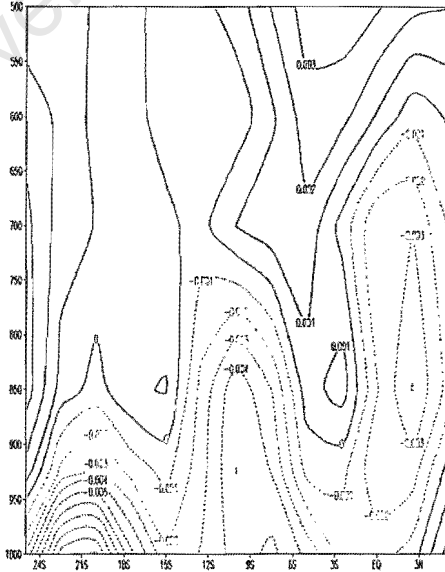
Oct 200 hPa Composite Wet VPotential and divergent wind anomaly



Oct Composite Wet years zonal moisture flux anomaly(20°)



Oct Composite Wet years zonal moisture flux anomaly(40°)



Oct Composite Wet years longitude height moisture flux anomaly (15-35°)

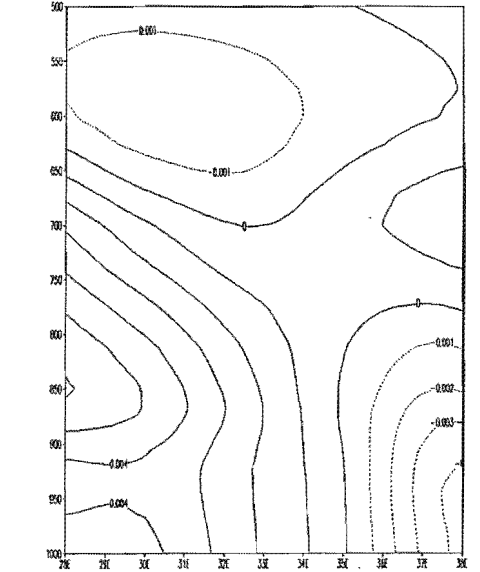
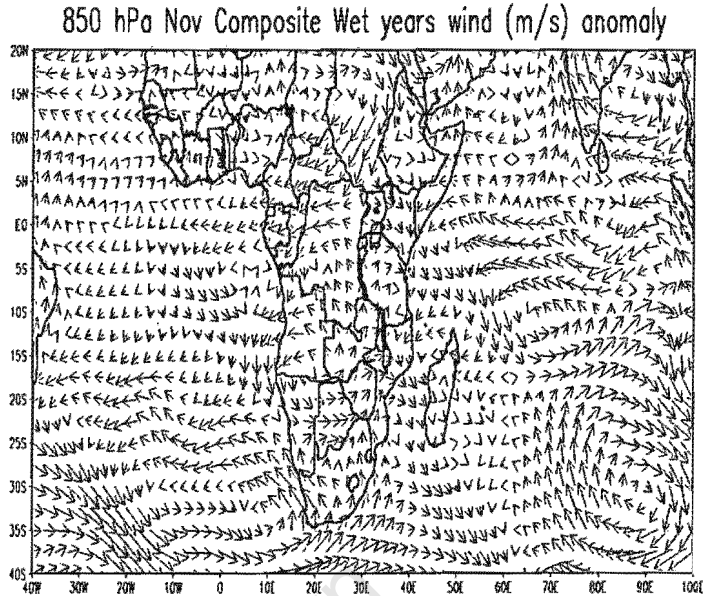
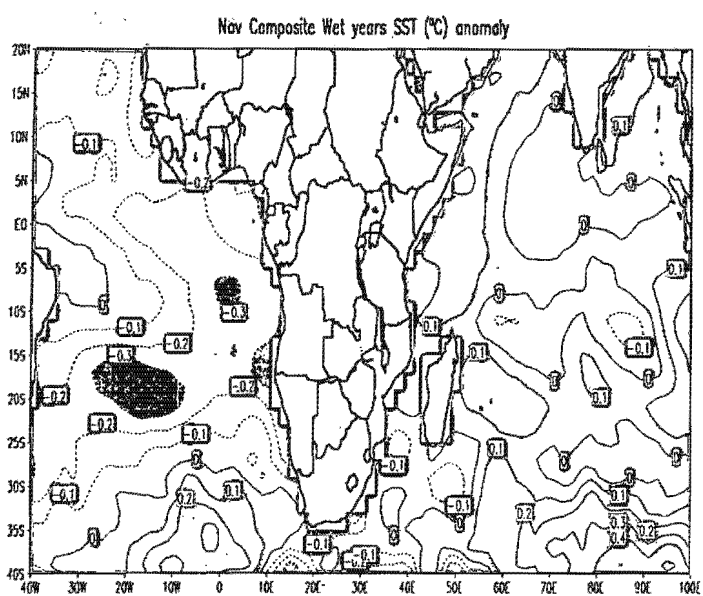
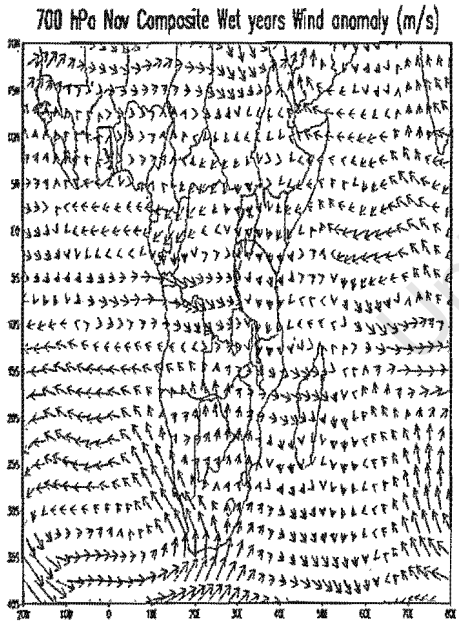


Fig. 4.2.1(a) cont..

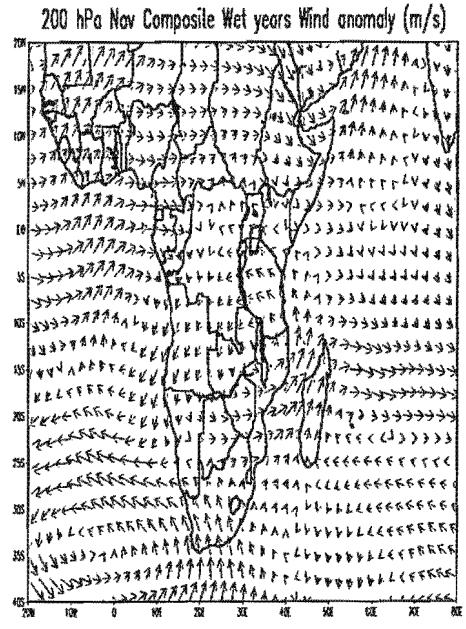
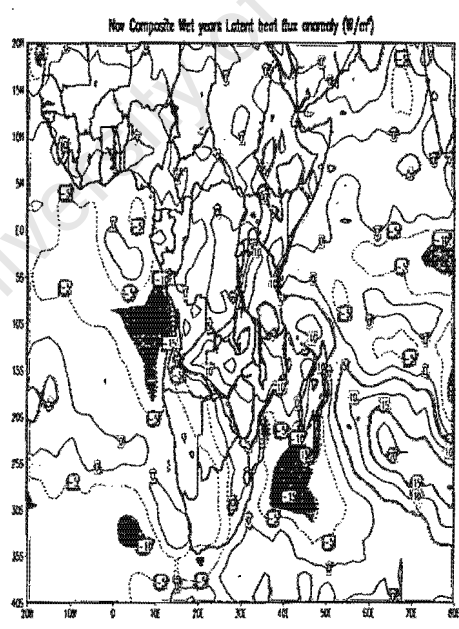
[Moisture flux in  $g/kg.ms^{-1}$  and scale vector is shown at the bottom of the figures; Divergent wind in  $10^{-6} s^{-1}$  and contour interval is  $0.2 \times 10^{-6} s^{-1}$ ; Velocity potential in  $10^{-6} m^2s^{-1}$  and contour interval is  $0.1 \times 10^{-6} m^2s^{-1}$ ; OLR (contour interval is  $5 Wm^{-2}$ ). Positive means westerlies and negative easterlies.



→  
2



→  
7



→  
3

Figure 4.2.1(b): as figure 4.2.1(a) above but for November

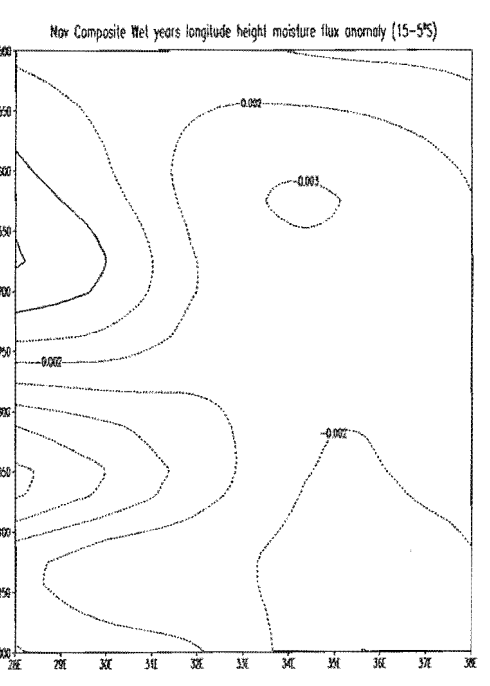
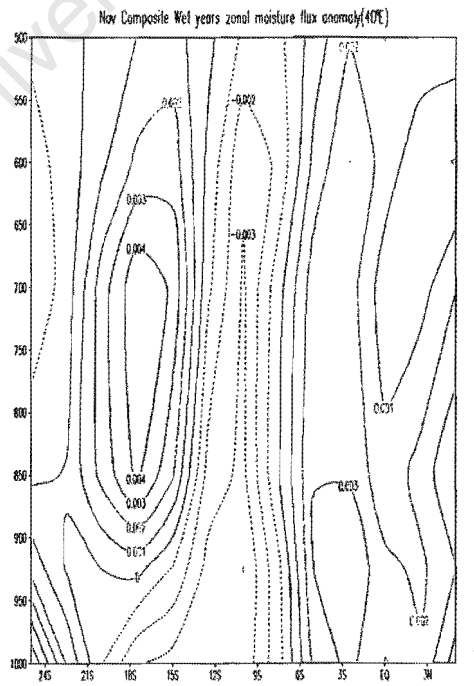
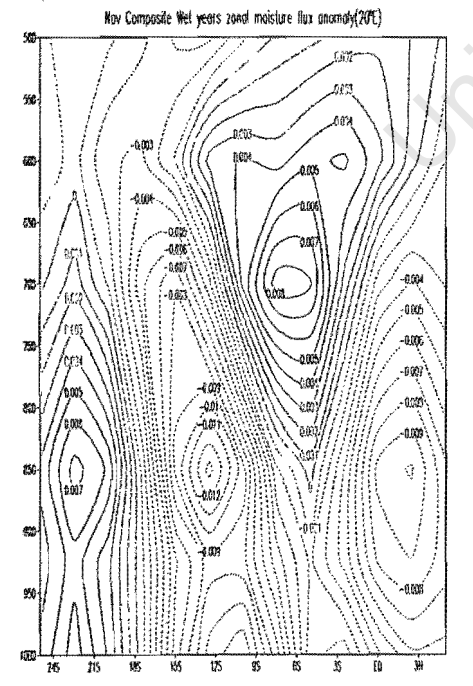
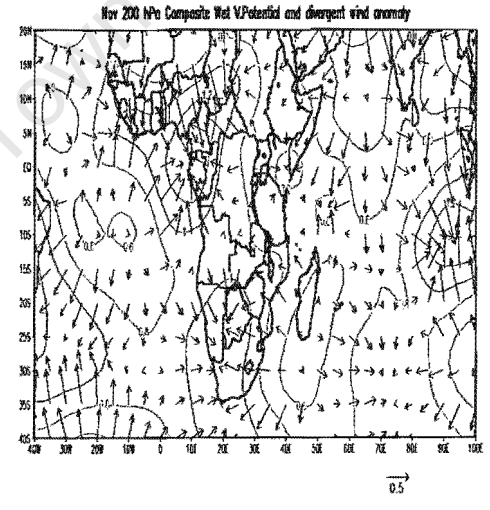
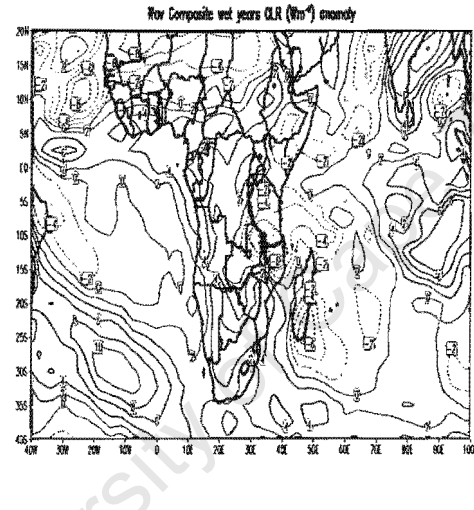
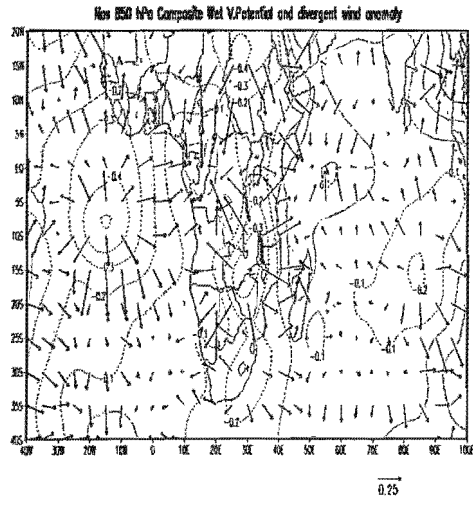
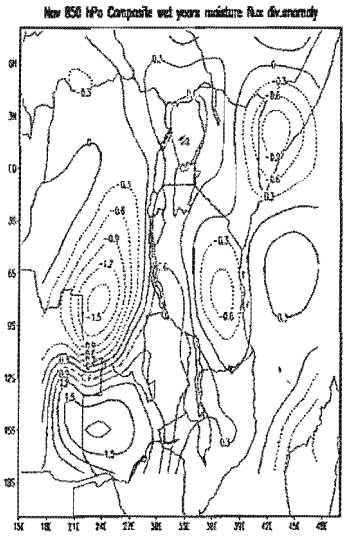
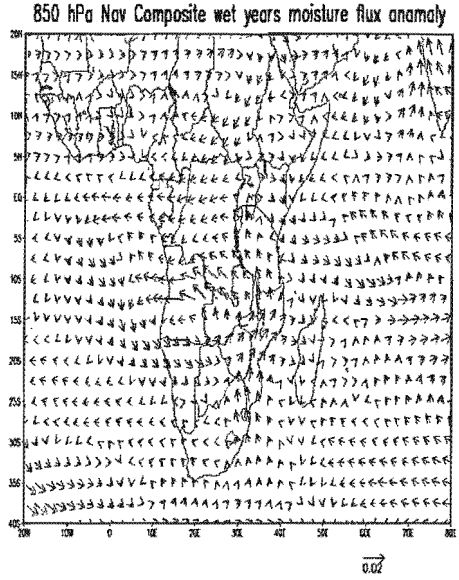
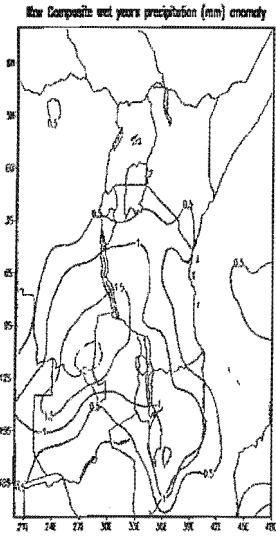


Fig. 4.2.1(b) cont..

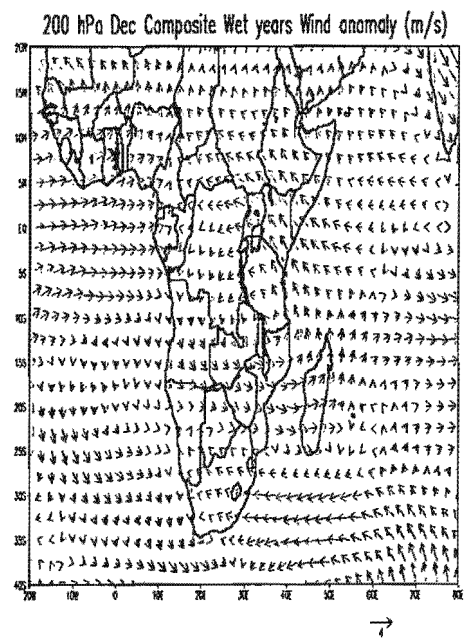
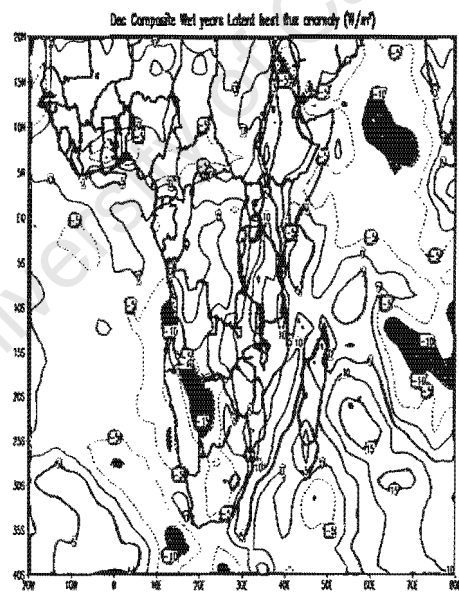
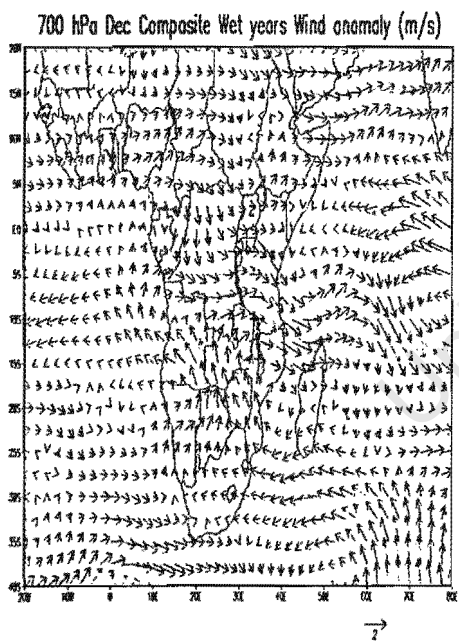
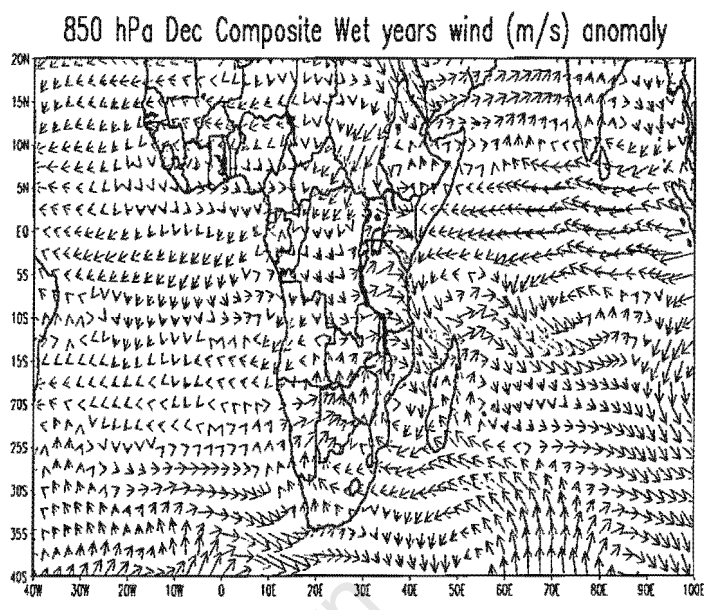
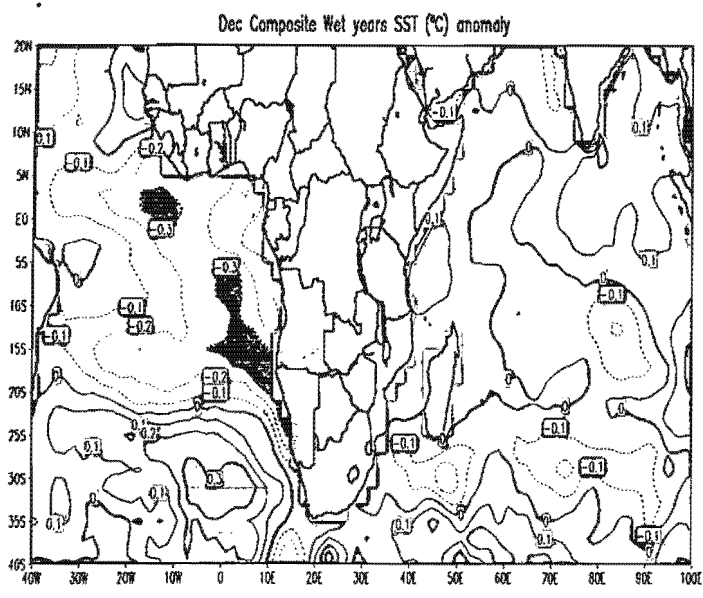
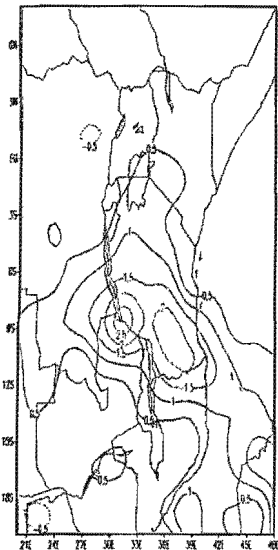
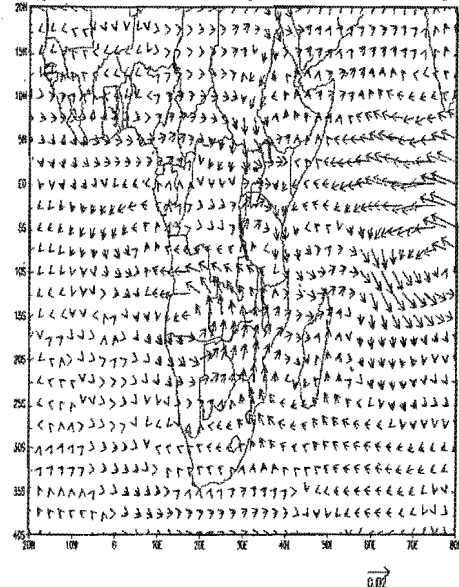


Figure 4.2.1(c): as figure 4.2.1(b) but for December

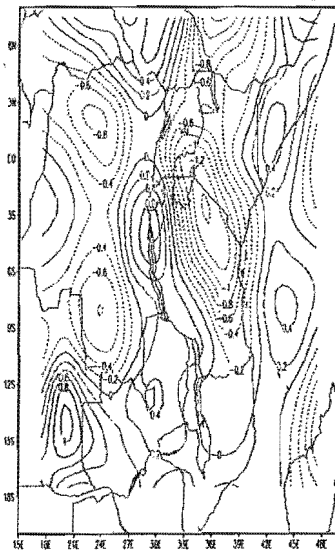
Dec Composite wet years precipitation (mm) anomaly



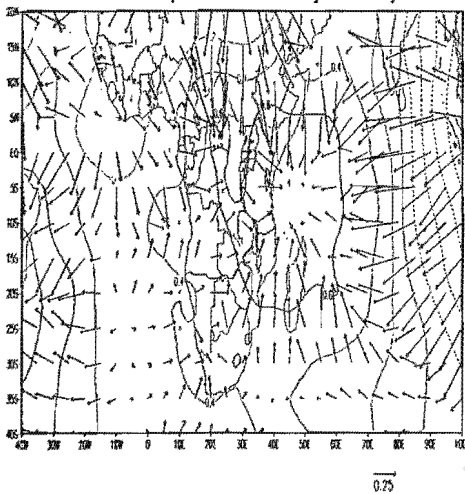
850 hPa Dec Composite wet years moisture flux anomaly



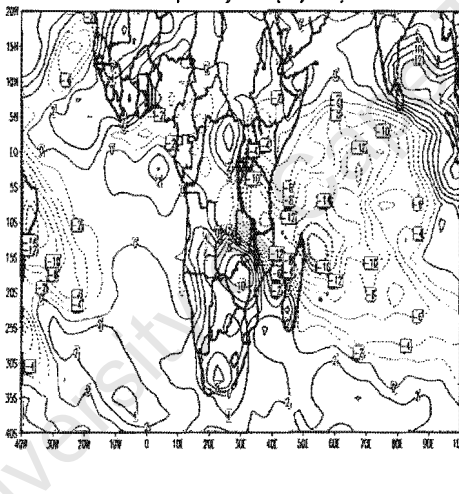
Dec 850 hPa Composite wet years moisture flux divergence



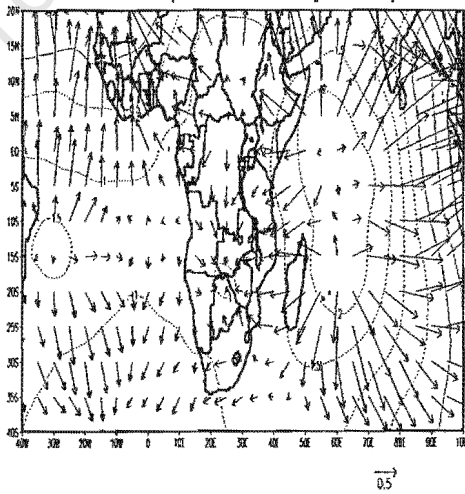
Dec 850 hPa Composite Wet V.Potential and divergent wind anomaly



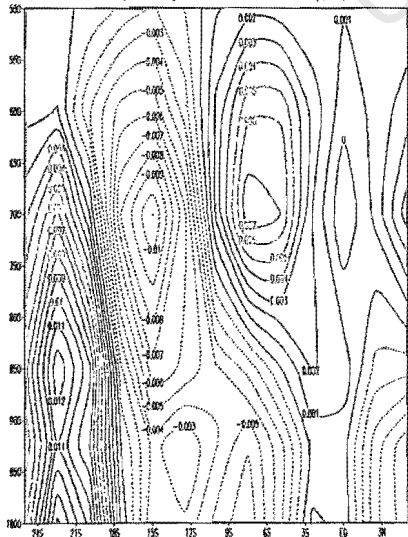
Dec Composite wet years QLR (Wm<sup>-2</sup>) anomaly



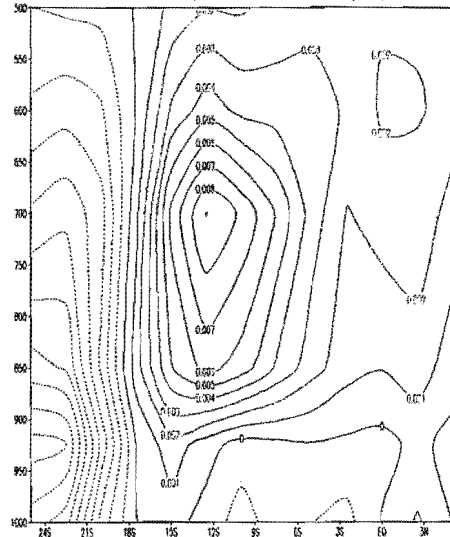
Dec 200 hPa Composite Wet V.Potential and divergent wind anomaly



Dec Composite Wet years zonal moisture flux anomaly(20E)



Dec Composite Wet years zonal moisture flux anomaly(40E)



Dec Composite Wet years longitude height moisture flux anomaly (15-5°S)

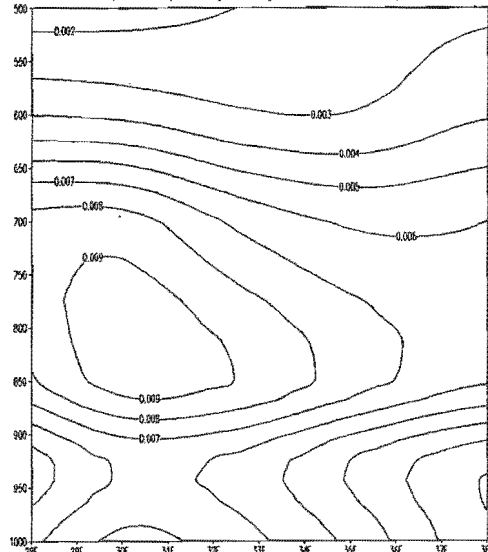
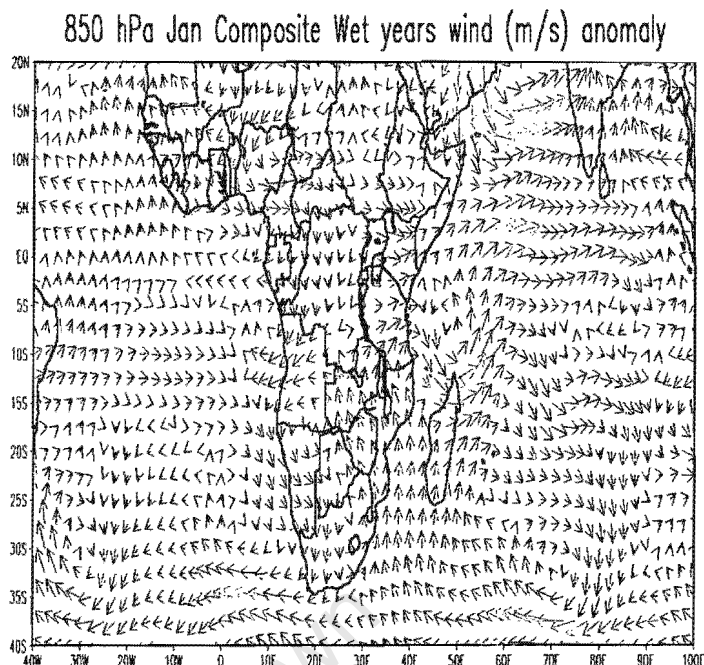
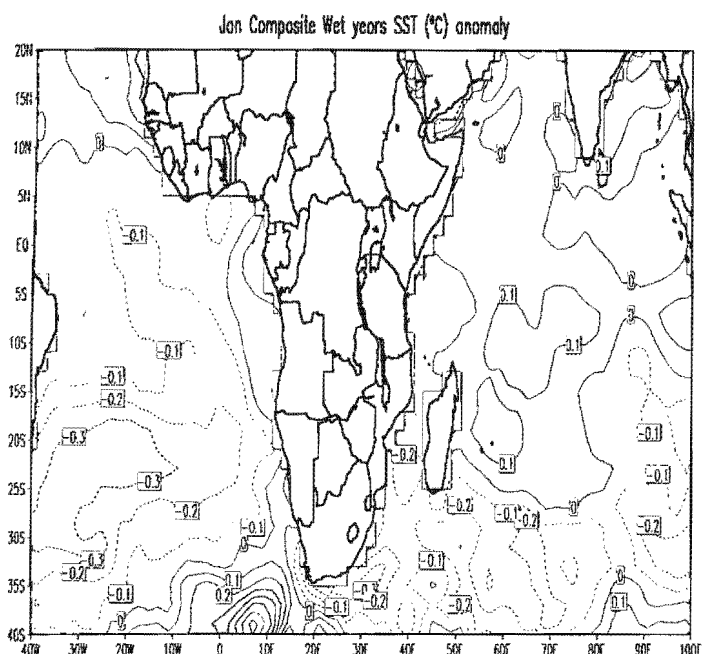
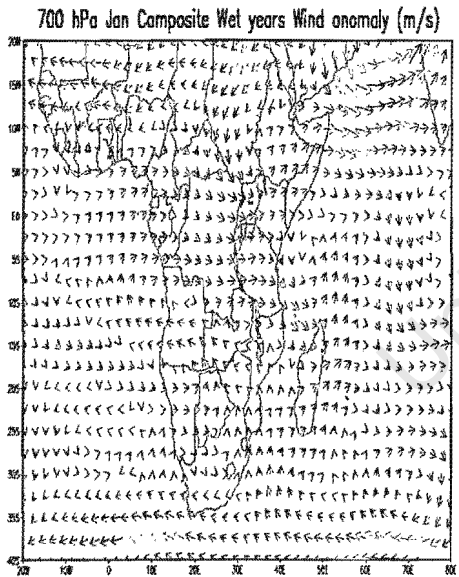


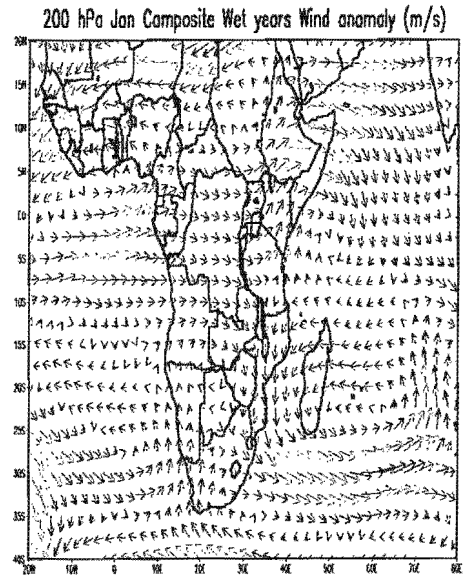
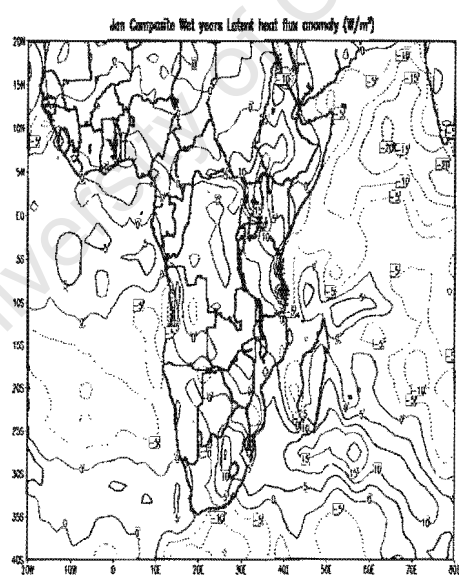
Fig.4.2.1(c) cont..



→  
2



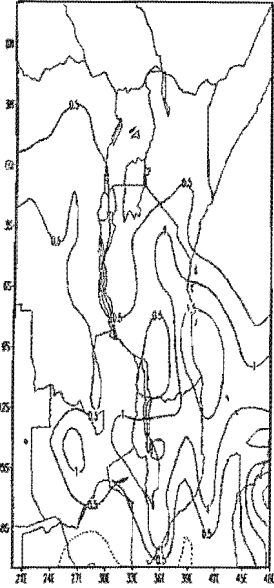
→



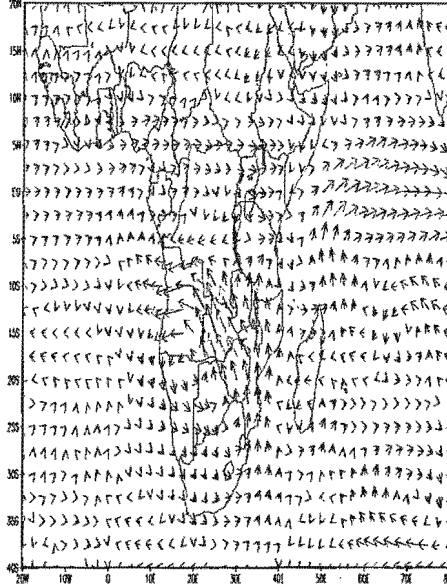
→

Figure 4.2.1(d): as figure 4.2.1(a) but for January wet composite anomaly

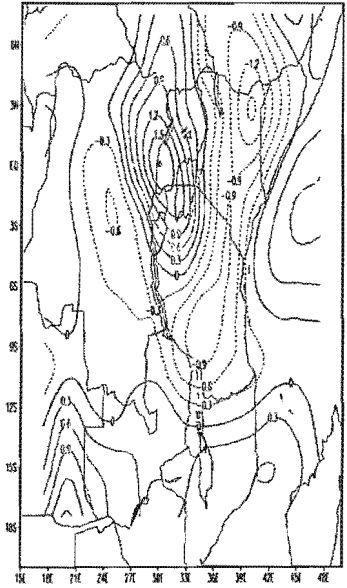
Jan Composite wet years precipitation (mm) anomaly



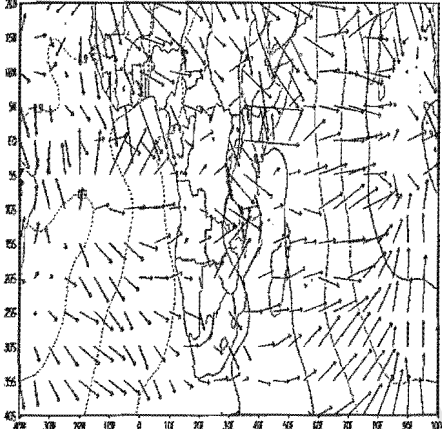
850 hPa Jan Composite wet years moisture flux anomaly



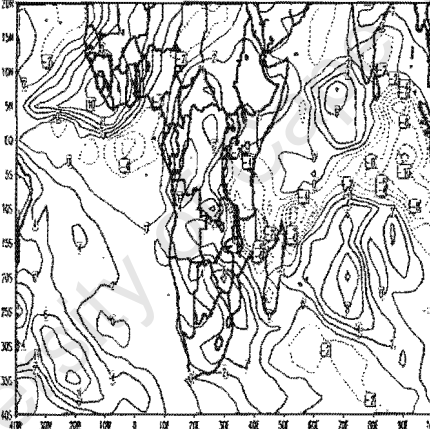
Jan 850 hPa Composite wet years moisture flux divergence



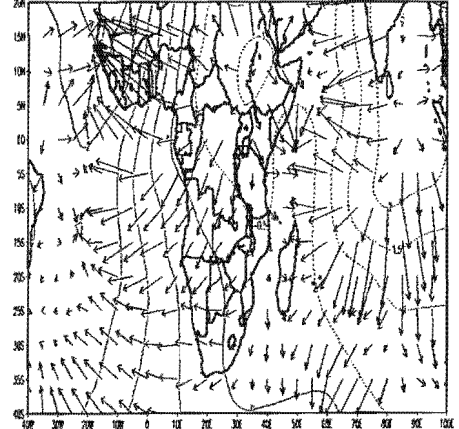
Jan 850 hPa Composite Wet V.Potential and divergent wind anomaly



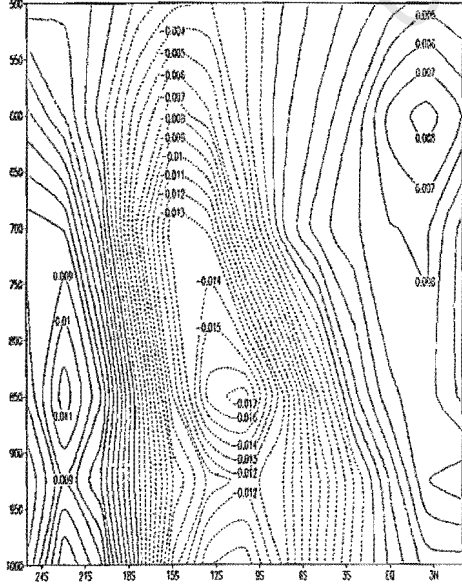
Jan Composite wet years QLR (Wm<sup>-2</sup>) anomaly



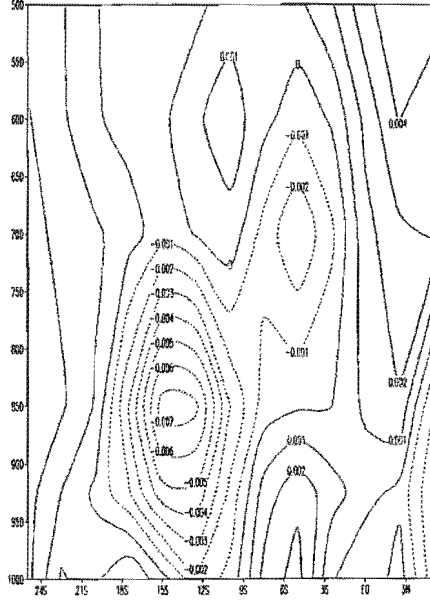
Jan 200 hPa Composite Wet V.Potential and divergent wind anomaly



Jan Composite Wet years zonal moisture flux anomaly(20E)



Jan Composite Wet years zonal moisture flux anomaly(40E)



Jan Composite Wet years longitude height moisture flux anomaly (15-5°S)

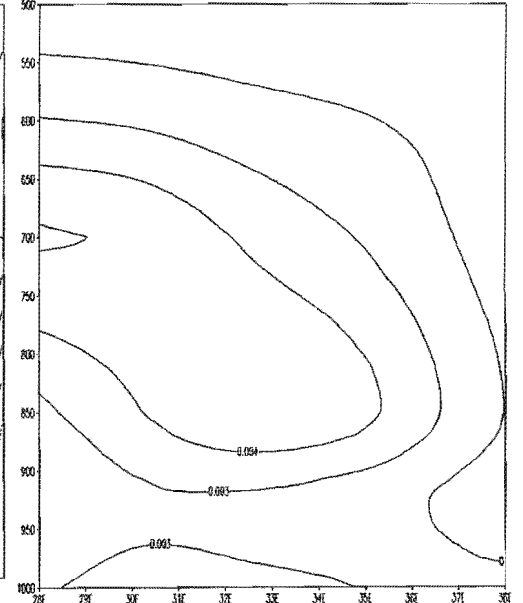
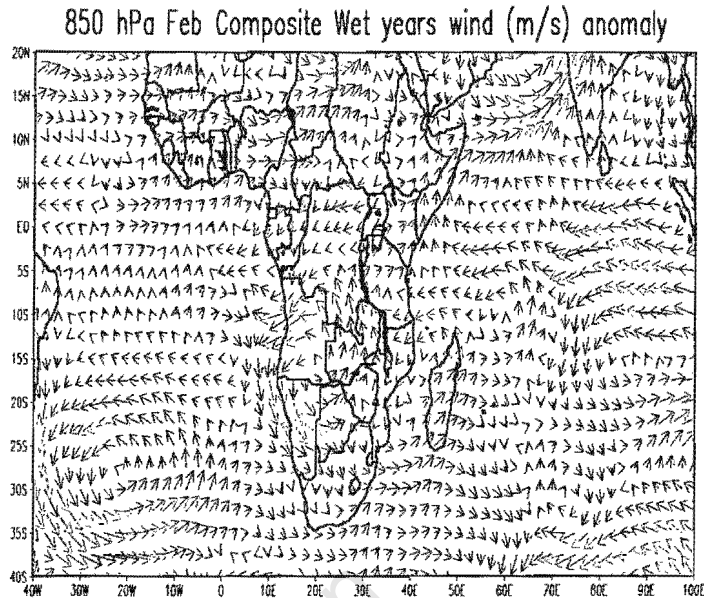
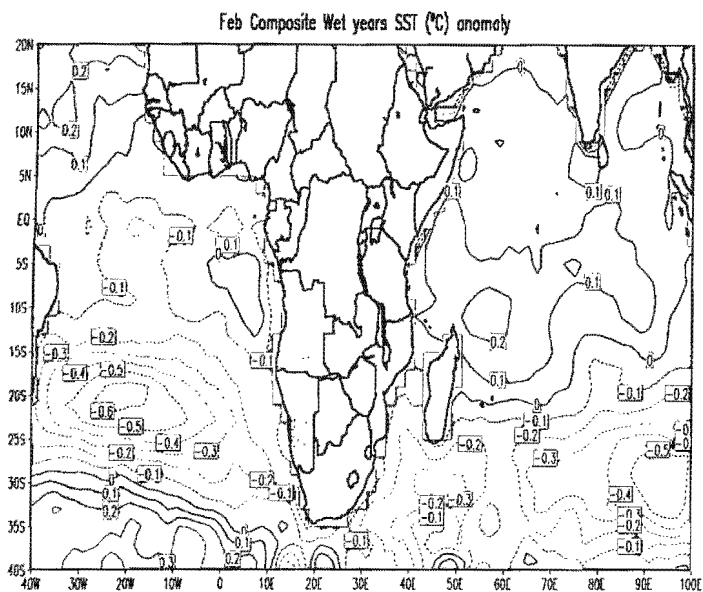


Fig. 4.2.1(d) cont..



2

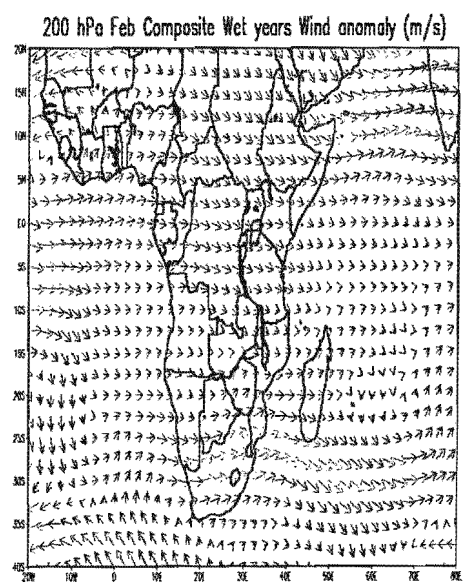
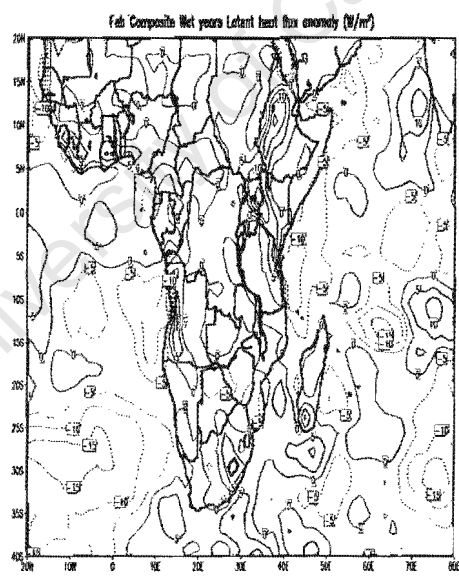
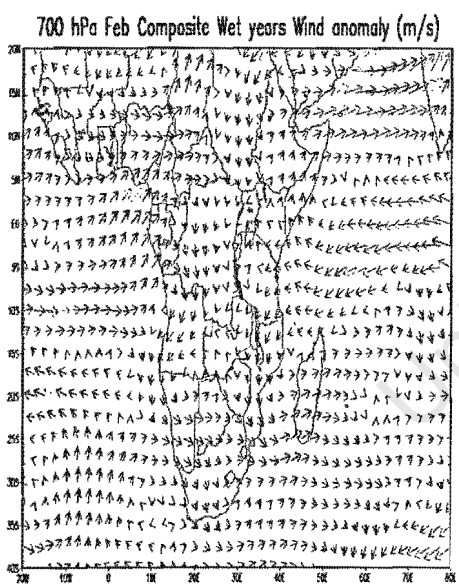
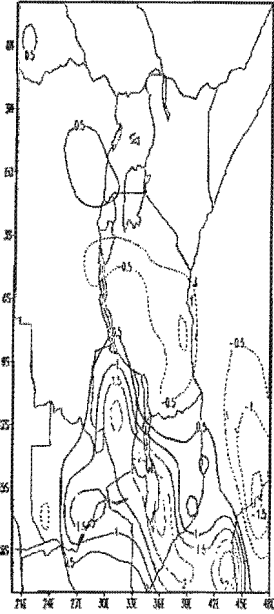
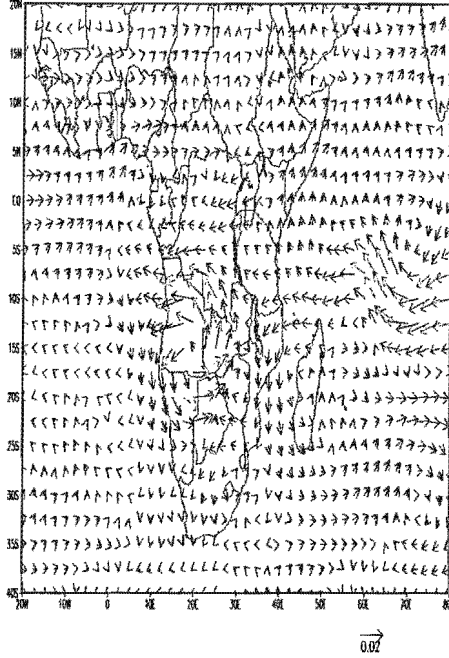


Figure 4.2.1(e): as figure 4.2.1(c) but for February

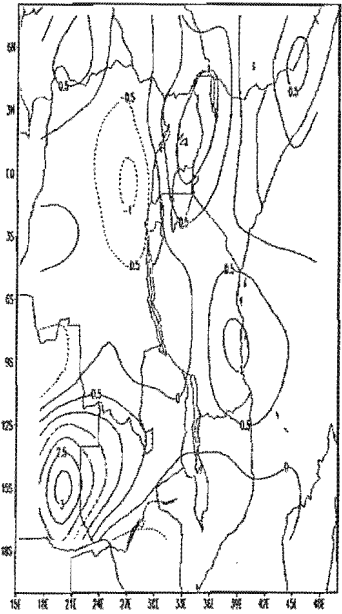
Feb Composite wet years precipitation (mm) anomaly



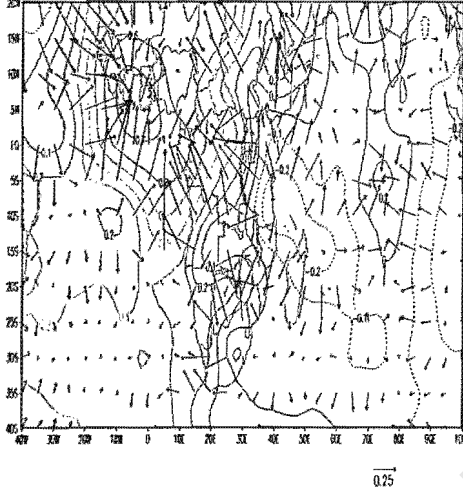
850 hPa Feb Composite wet years moisture flux anomaly



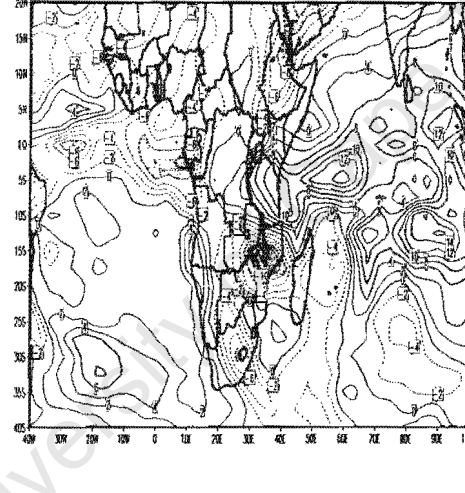
Feb 850 hPa Composite wet years moisture flux anomaly



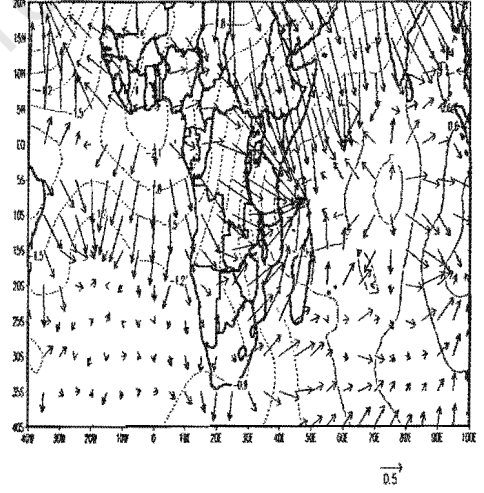
Feb 850 hPa Composite Wet V.Potential and divergent wind anomaly



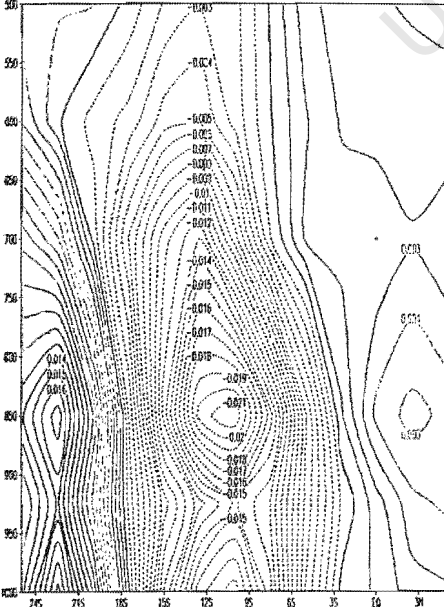
Feb Composite wet years (BLP) anomaly



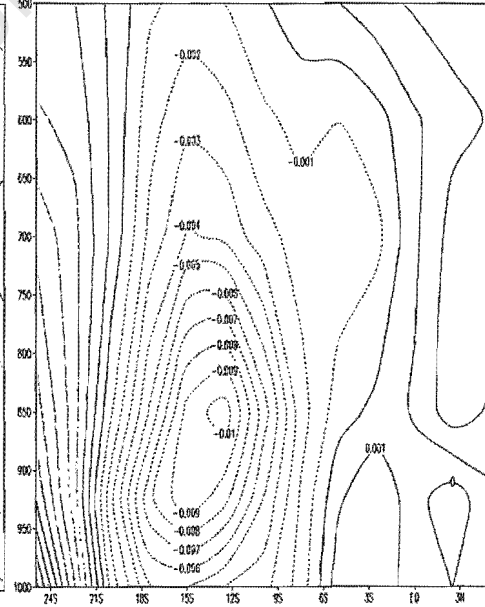
Feb 200 hPa Composite Wet V.Potential and divergent wind anomaly



Feb Composite Wet years zonal moisture flux anomaly(20E)



Feb Composite Wet years zonal moisture flux anomaly(40E)



Feb Composite Wet years longitude height moisture flux anomaly (15-5°S)

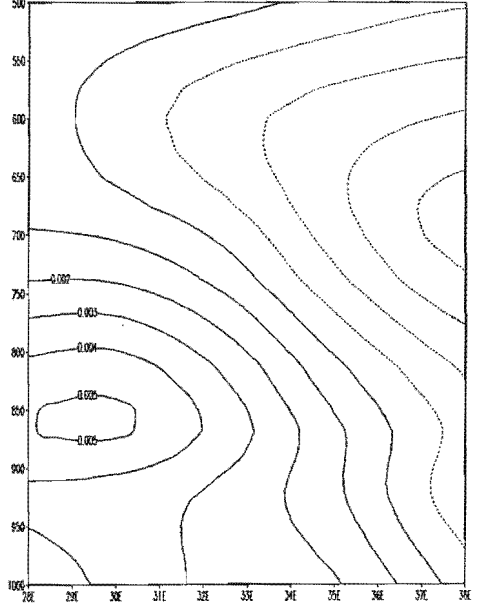
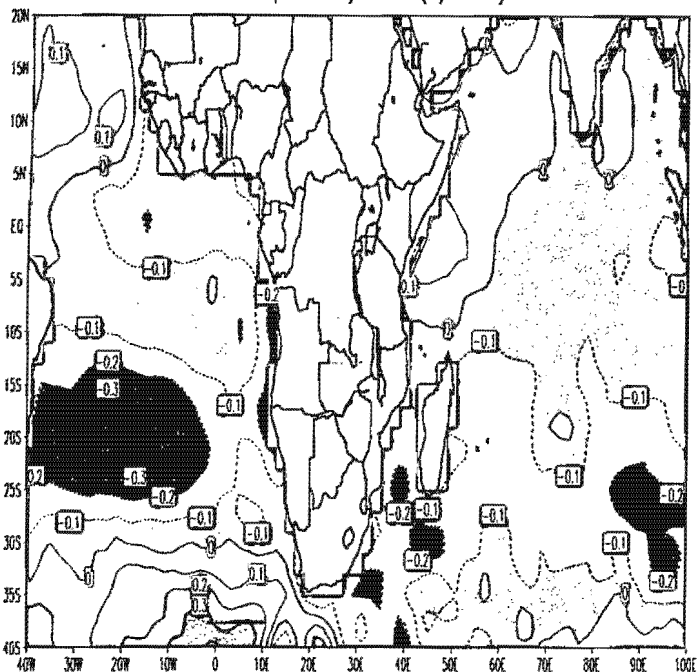
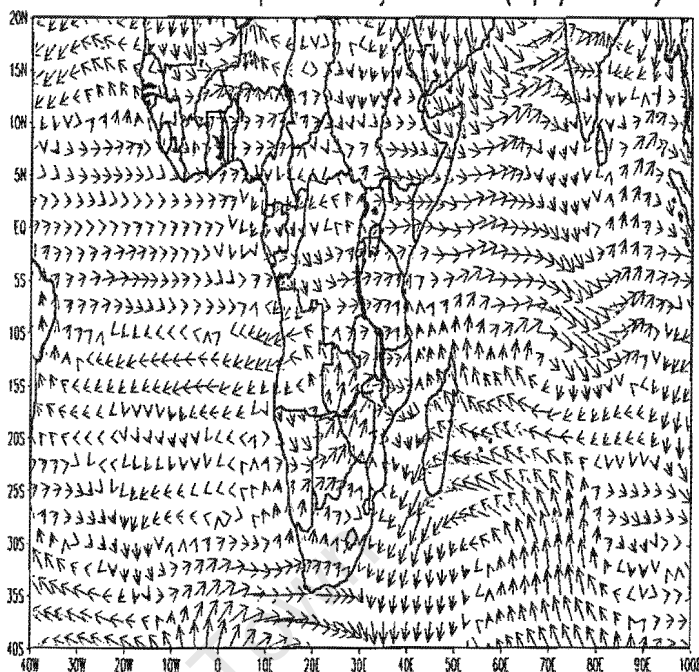


Fig 4.2.1(e) cont..

Mar Composite Wet years SST (°C) anomaly

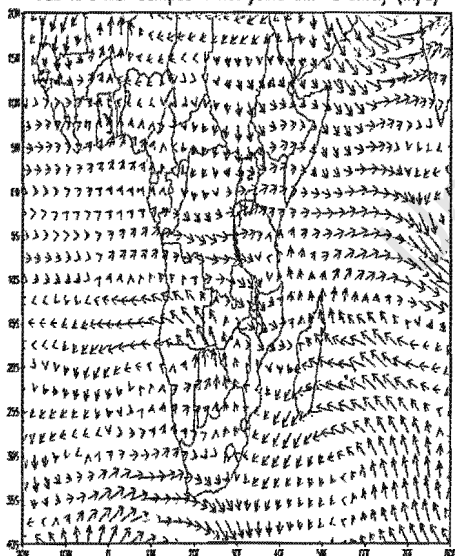


850 hPa Mar Composite Wet years wind (m/s) anomaly



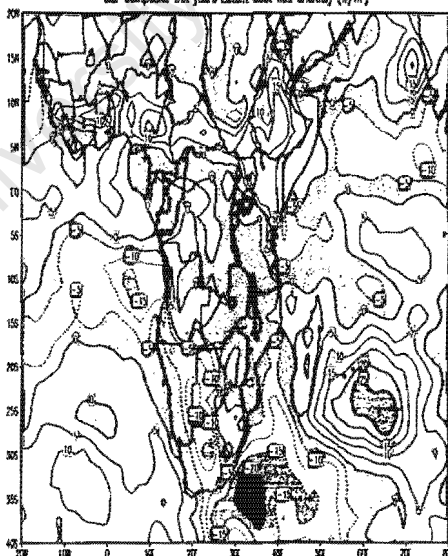
→

700 hPa Mar Composite Wet years Wind anomaly (m/s)

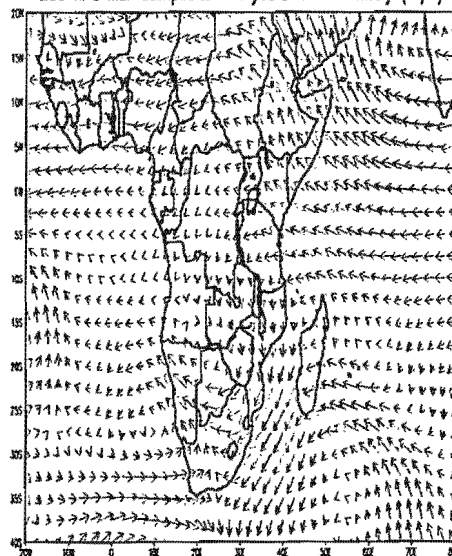


→

Mar Composite Wet years Latent heat flux anomaly (W/m²)



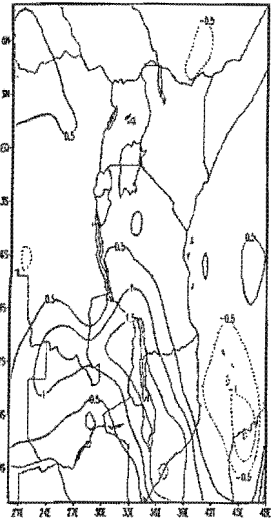
200 hPa Mar Composite Wet years Wind anomaly (m/s)



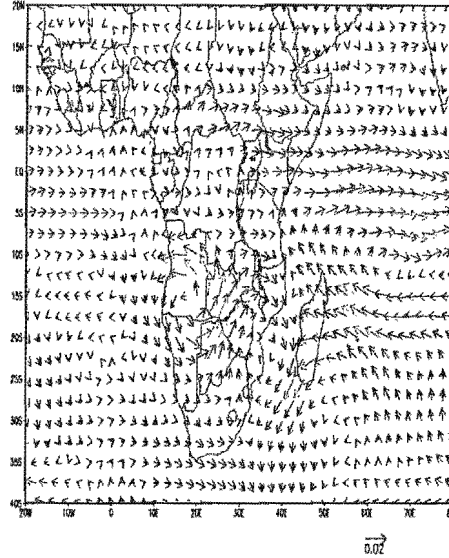
→

Figure 4.2.1(f); same as figure 4.2.1(a) but for March wet composite

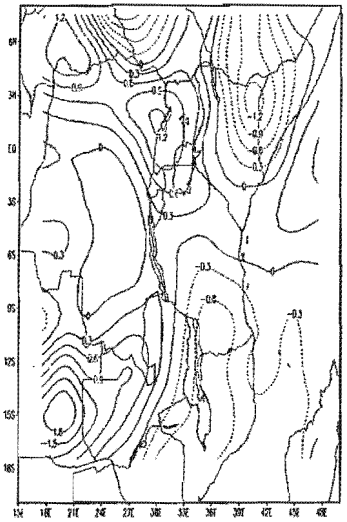
Mar Composite wet years precipitation (mm) anomaly



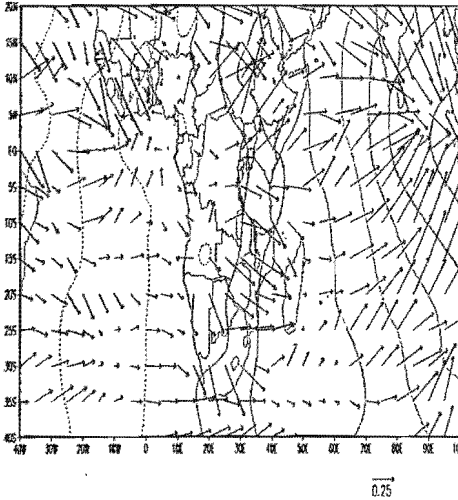
850 hPa Mar Composite wet years moisture flux anomaly



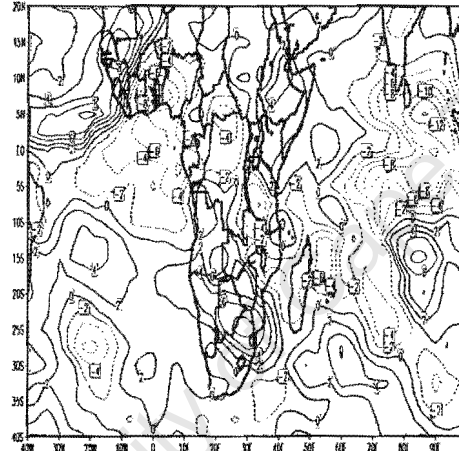
Mar 850 hPa Composite wet years moisture flux divergence anomaly



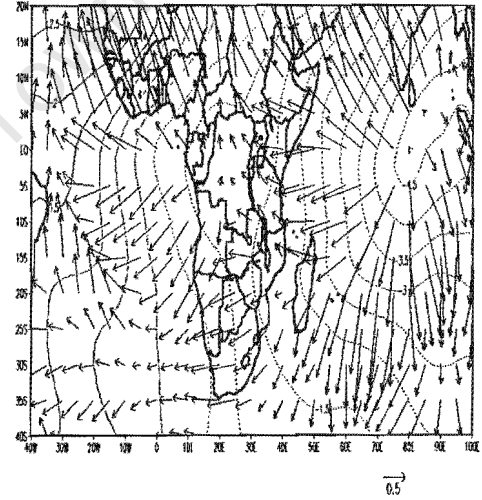
Mar 850 hPa Composite Wet VPotential and divergent wind anomaly



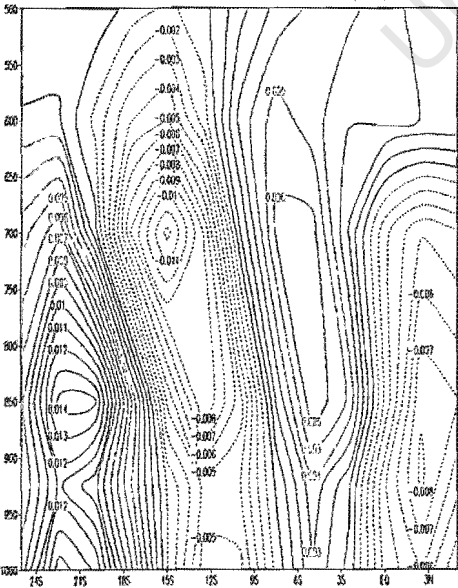
Mar Composite wet years QLR (Wm<sup>-2</sup>) anomaly



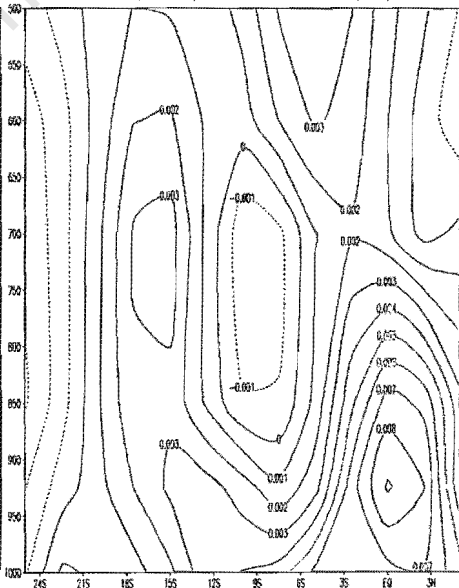
Mar 200 hPa Composite Wet VPotential and divergent wind anomaly

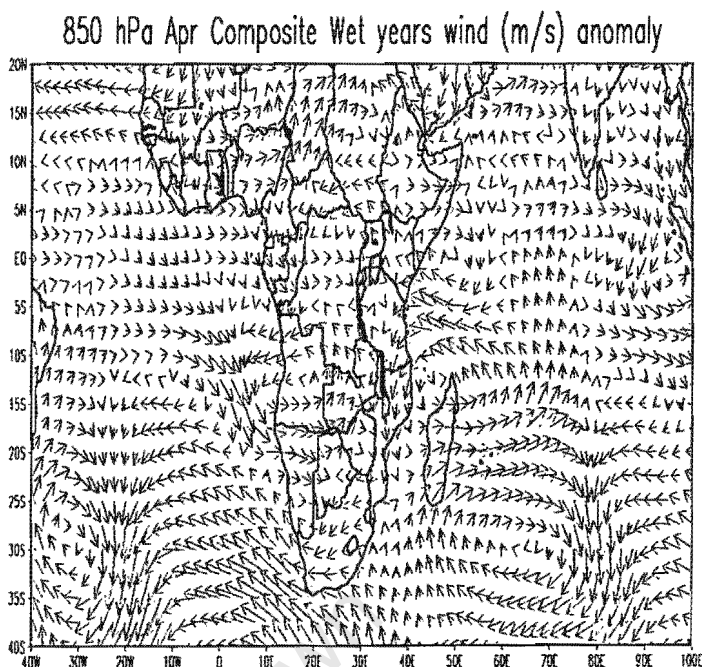
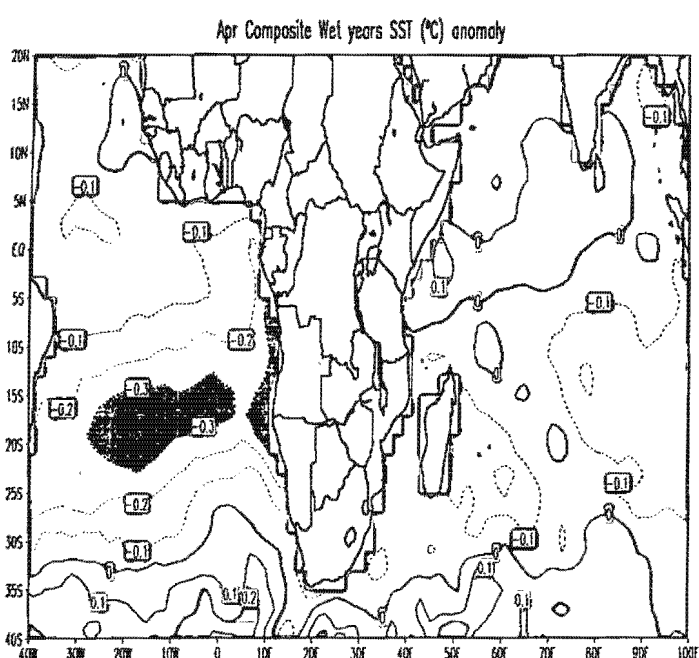


Mar Composite Wet years zonal moisture flux anomaly(20E)

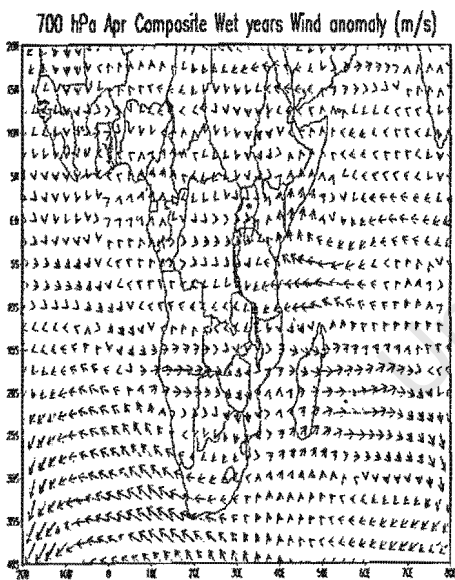


Mar Composite Wet years zonal moisture flux anomaly(40E)

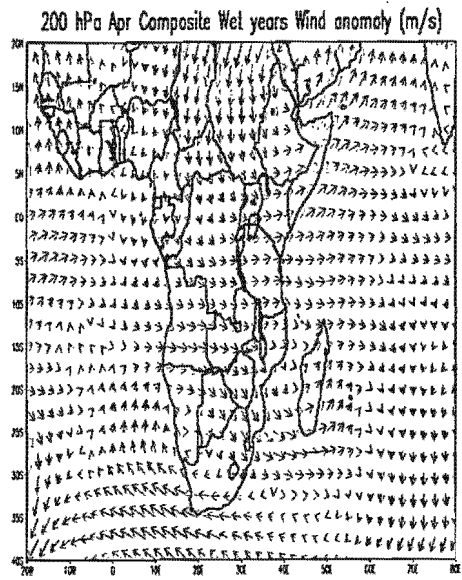
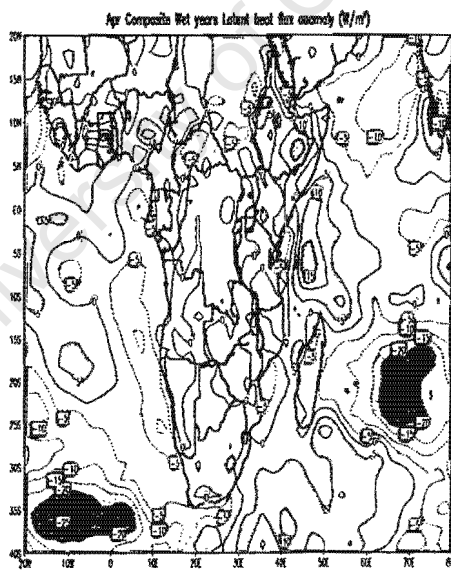




→  
2



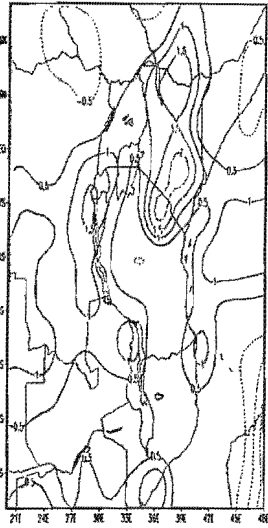
→



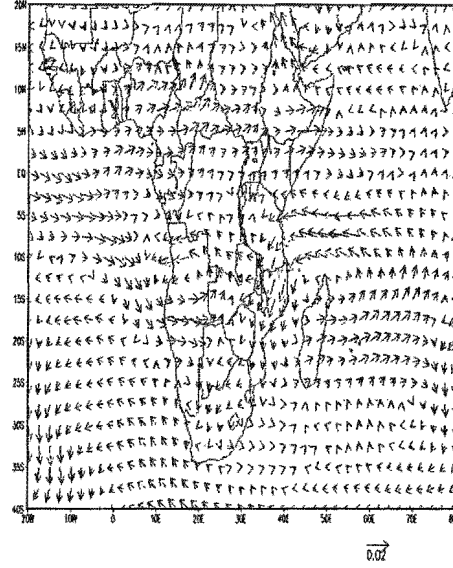
→  
6

Figure 4.2.1(g); same as figure 4.2.1(d) but for April

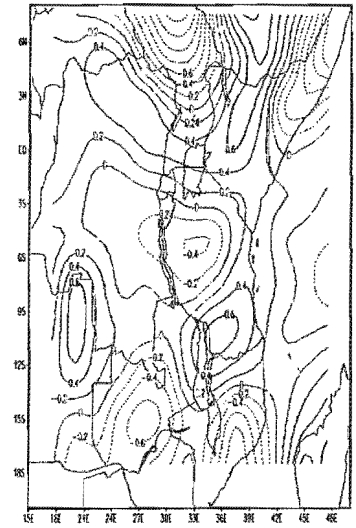
Apr Composite wet years precipitation (mm) anomaly



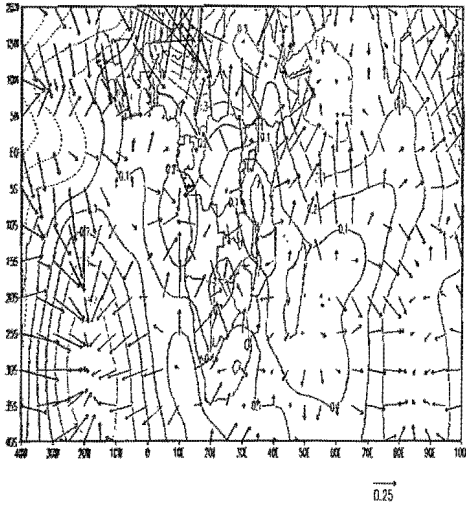
850 hPa Apr Composite wet years moisture flux anomaly



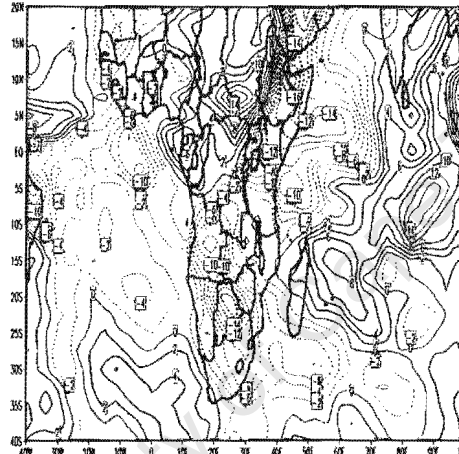
Apr 850 hPa Composite wet years moisture flux (hPa anomaly)



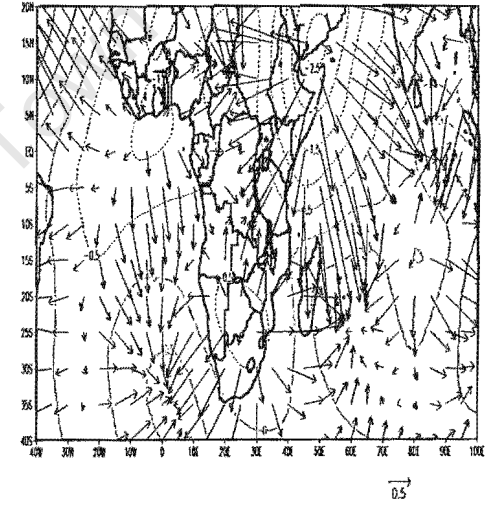
Apr 850 hPa Composite Wet V.Potential and divergent wind anomaly



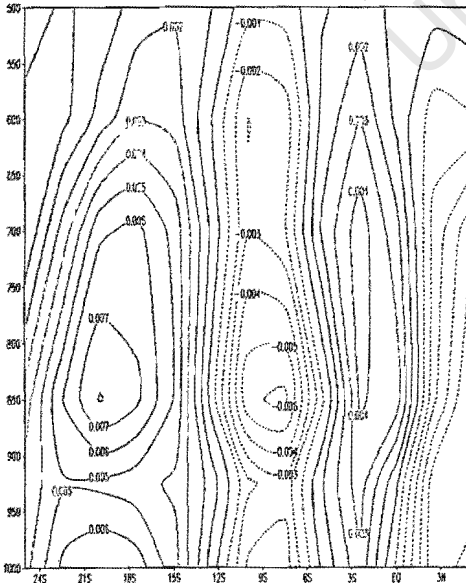
Apr Composite wet years QLR (Wm<sup>-2</sup>) anomaly



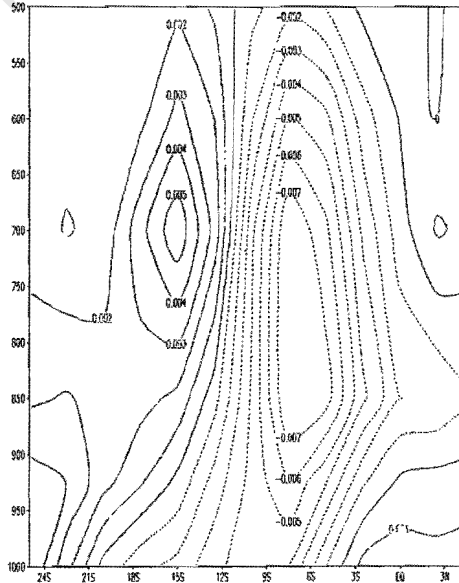
Apr 200 hPa Composite Wet V.Potential and divergent wind anomaly



Apr Composite Wet years zonal moisture flux anomaly(20E)



Apr Composite Wet years zonal moisture flux anomaly(40E)



Apr Composite Wet years longitude height moisture flux anomaly (15-5°S)

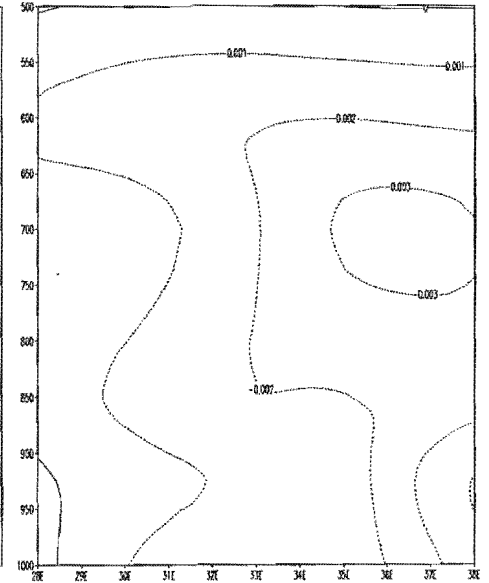


Fig. 4.2.1(g) cont..

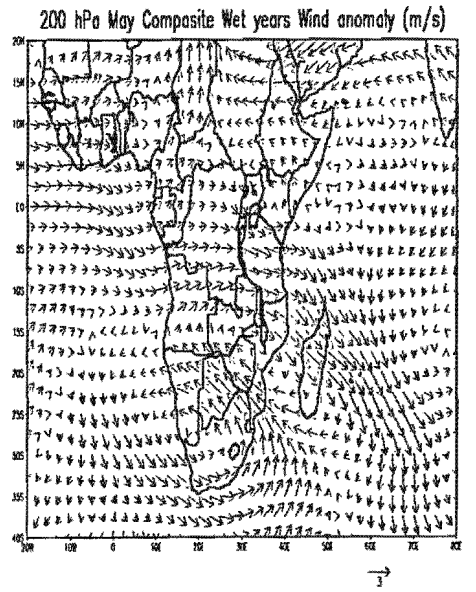
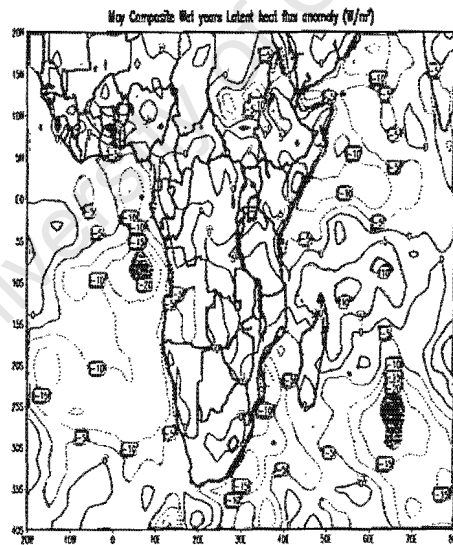
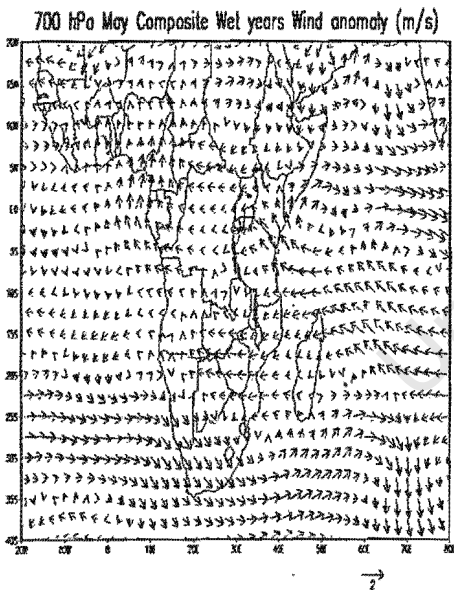
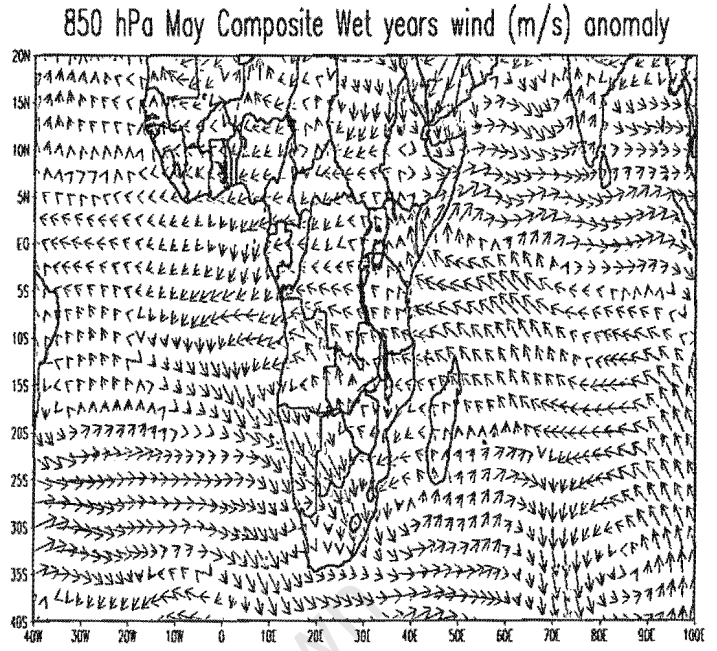
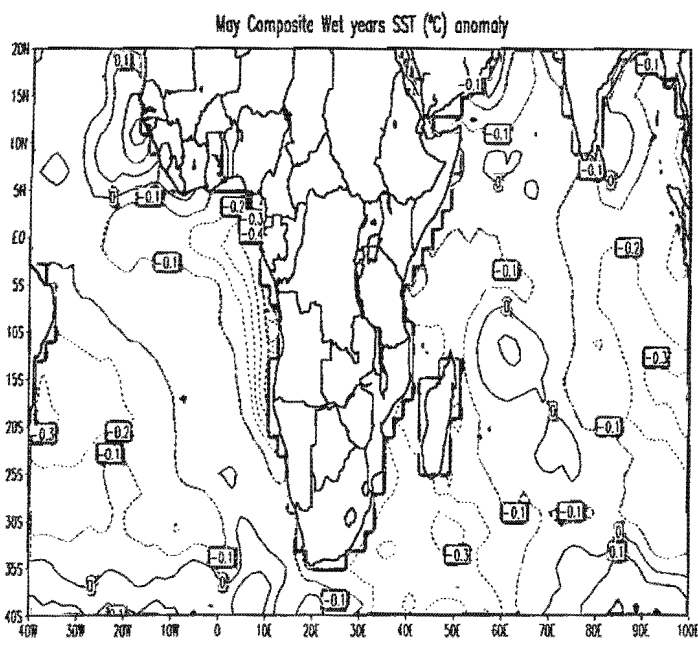
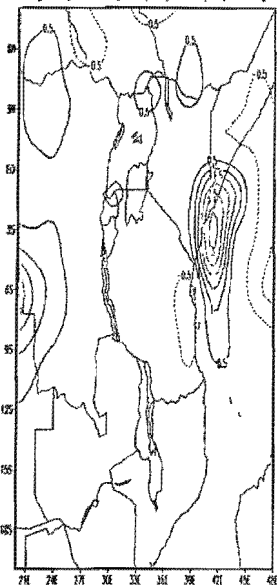
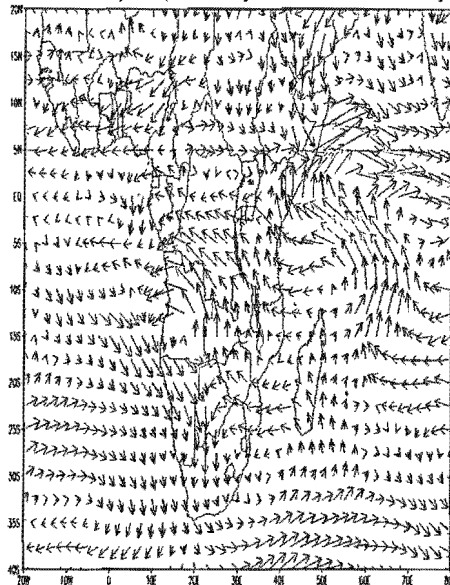


Figure 4.2.1(h); as figure 4.2.1(a) but for May wet composite

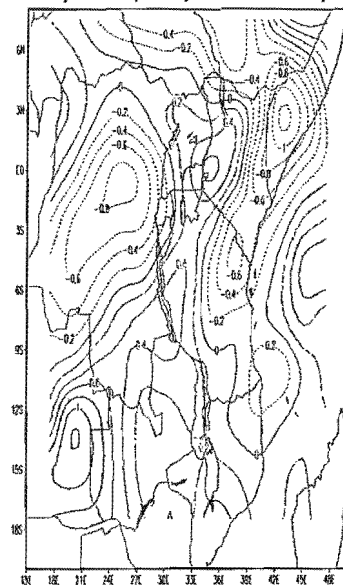
May Composite wet years precipitation (mm) anomaly



850 hPa May Composite wet years moisture flux anomaly

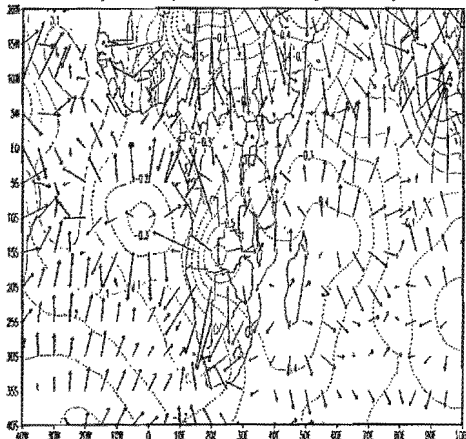


May 850 hPa Composite wet years moisture flux divergence



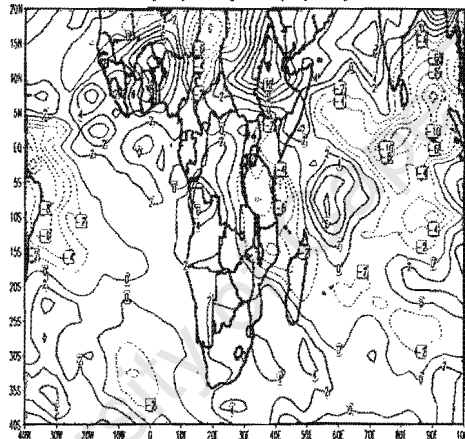
0.01

May 850 hPa Composite Wet V.Potential and divergent wind anomaly

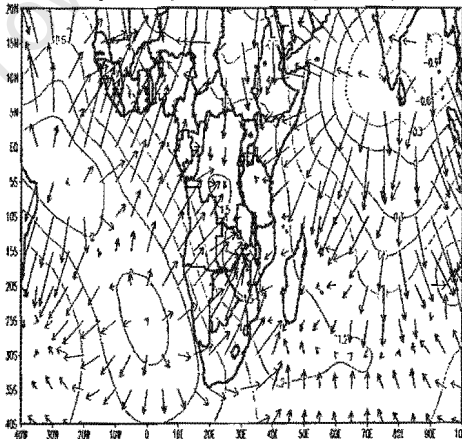


0.25

May Composite wet years QLR (Wm<sup>-2</sup>) anomaly

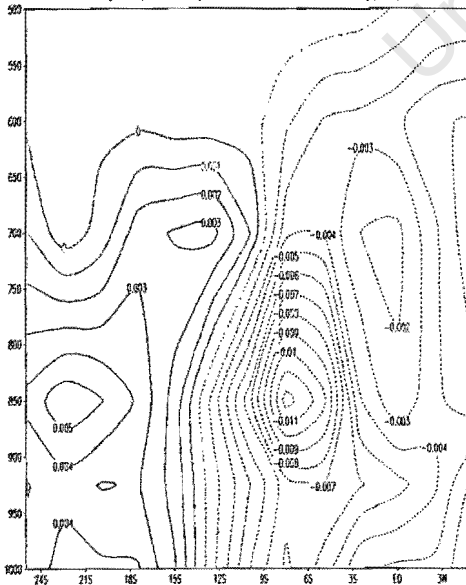


May 200 hPa Composite Wet V.Potential and divergent wind anomaly

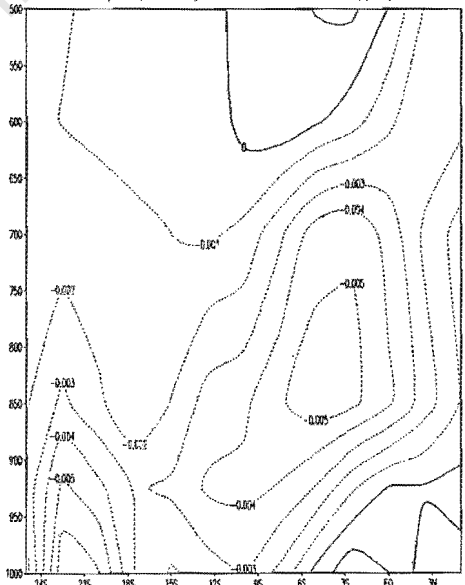


0.5

May Composite Wet years zonal moisture flux anomaly(20°E)



May Composite Wet years zonal moisture flux anomaly(40°E)



May Composite Wet years longitude height moisture flux anomaly (15-5°S)

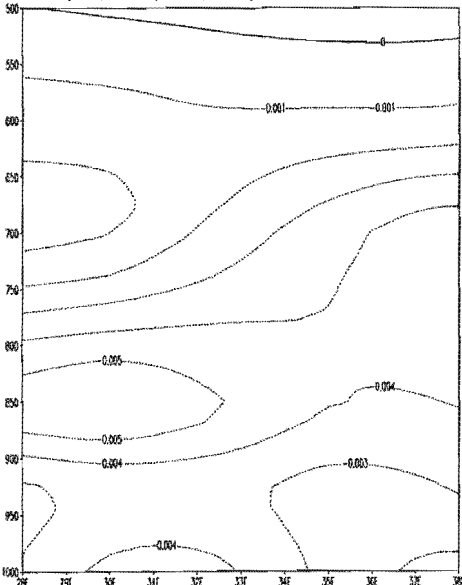


Fig.4.2.1(h) cont..

#### 4.2.2 Dry years composite anomaly evolution

In this section, the composite anomaly evolution for the dry years are discussed. The dry years used in the composite are 1969, 1976, 1987, 1992, 1993 and 1998.

During October [Figure 4.2.2(a)], weak positive SST anomalies exist over the tropical western and central Indian Ocean. Negative SST anomalies over southwestern and subtropical Indian Ocean are evident. Over the Atlantic Ocean, positive SST anomalies are shown over subtropical South Atlantic and negative SST anomalies across the tropical South Atlantic.

During this month, a lower tropospheric anticyclonic anomaly is apparent over the tropical western Indian Ocean leading to southerly anomalies over Somalia and westerly anomalies over northern Mozambique and southern Tanzania. Another prominent lower tropospheric feature is a cyclonic anomaly over the tropical southeast Atlantic Ocean / southwestern African region which weakens the mean easterly flow across tropical southern Africa during this period. This feature together with that over the Indian Ocean act to reduce the influx of moisture into eastern Tanzania. Low-level divergence exists over most of Tanzania which together with positive OLR anomalies and negative latent heat flux anomalies over this region, indicate, suppressed evaporation and convection.

At 200 hPa, a cyclonic anomaly is observed to develop over East Africa and the neighbouring regions, with associated westerly anomalies over Tanzania. This upper level feature is unfavourable for convection to occur over the region since it implies upper level convergence and subsidence.

The velocity potential anomaly plots confirm the decrease of rainfall over western Tanzania by indicating a strong low-level divergence at 850hPa over Tanzania with an associated upper level convergent anomaly.

Further evidence of the divergence is shown by the zonal section of moisture flux anomaly along 20°E which indicates strong westerly anomalies between 15°S and 3°S and easterly anomalies to the south between 24°S and 18°S. Along 40°E, strong westerly anomalies are evident between 18°S and 3°S and can partly explain the low level moisture divergence over the region consistent with substantial rainfall decrease over western Tanzania in October. The longitude height section of moisture flux anomaly indicates low level westerly anomalies across the region with relative maximum in the far west and east respectively.

During November [Figure 4.2.2(b)], the weak positive SST anomalies over the tropical western and central Indian Ocean continue with increased positive SST anomalies over subtropical South Indian Ocean. Over the Atlantic Ocean, positive SST anomalies exist over the tropical Southeast Atlantic and negative anomalies further north. During this month, a cyclonic anomaly over the tropical southeast Atlantic and an anticyclonic anomaly over the midlatitude southwestern Indian Ocean and a cyclonic anomaly over the tropical Indian Ocean are apparent. These anomalies weaken the mean easterly flow across tropical southern Africa, and reduce the flux of moisture into the region from the Atlantic and South Indian Oceans.

The cyclonic anomaly over the tropical central Indian Ocean acts to weaken the northeast monsoon flow over the Indian Ocean. In turn, low-level diffluent flow is evident over western Tanzania and the neighbouring regions in November. At 200hPa, a cyclonic anomaly is evident over East Africa. This upper level feature is associated with westerly anomalies over Tanzania which is unfavourable for convective rainfall because it implies the upper level convergence and subsidence. The large positive OLR and negative latent heat flux anomalies over Tanzania indicate suppressed evaporation and reduced convection and hence decreased precipitation over western Tanzania in this month.

The velocity potential anomaly plot confirms the reduced moisture over western Tanzania by indicating a strong low-level divergence over almost the entire East Africa at 850hPa with upper level convergent anomaly. The zonal sections of moisture flux anomaly along 20°E and 40°E support the rainfall decrease over western Tanzania by showing strong westerly anomalies centred at 850hPa between 15°S and the equator along 20°E while along 40°E, westerly anomalies are evident between 9°S and equator extending vertically up from 850hPa to 500hPa level.

In December [Figure 4.2.2(c)], positive SST anomalies are observed to decrease over the tropical western Indian Ocean and the negative anomalies east of Madagascar strengthen. Over the South Atlantic Ocean, positive SST anomalies decrease in intensity and contract in area compared to the previous month with large negative SST anomalies now apparent over the tropical South Atlantic.

The lower tropospheric cyclonic anomaly over the central tropical Indian Ocean strengthens compared to November and acts to weaken the northeast monsoon from the tropical western Indian Ocean towards Tanzania. Another significant feature is a cyclonic anomaly over northern Angola and a northwesterly over southern Africa, which tends to shift the moisture further south.

The anticyclonic anomaly southeast of Madagascar together with the cyclonic anomaly further north acts to weaken the mean easterly flow from the tropical south Indian Ocean and leads to low-level moisture divergence over eastern Tanzania. The rainfall decrease over western and southwestern Tanzania is consistent with large negative anomalies of latent heat flux and positive OLR anomalies over the region which indicates weaker evaporation and convection in December.

The velocity potential anomaly plot confirms this decrease by indicating a strong low-level divergence over Tanzania at 850hPa with an associated upper level convergent anomaly. Further evidence of the reduced moisture over the study region is illustrated by the zonal section of moisture flux anomaly along 20°E which shows westerly anomalies between 15°S and 9°S. Along 40° E, low level easterly anomalies between 15°S and 9°S are evident. These distributions leads to low-level convergence of moisture further south over Zambia consistent with rainfall increase there and a decrease over Tanzania during this month.

During January [Figure 5.2.2(d)], positive SST anomalies strengthen in the South Indian Ocean as well as in the subtropical South Atlantic Ocean. Negative SST anomalies are observed to develop over the tropical South Atlantic Ocean and over the western Indian Ocean near the coast of Tanzania. The most notable lower tropospheric feature during this month is zonally extensive anticyclonic anomaly over the South Indian Ocean, which tends to enhance the easterly mean flow towards northern Madagascar and the northeasterly monsoonal flow towards northern Tanzania and Kenya. On the other side of Africa, the anticyclonic anomaly over Angola is also present and weakens the low level flux of moisture from the tropical southeast Atlantic into the region.

At 200hPa, weak westerly anomalies are observed over Tanzania, this feature becomes stronger over the western Indian Ocean and may be associated with a weaker Walker circulation which is unfavourable for low-level convection since it reflects upper level convergence. The rainfall decrease seen over southwestern Tanzania during this month is consistent with the positive OLR anomalies and negative latent heat flux anomalies over this region.

The velocity potential anomaly plot confirms this decrease with strong low-level convergence over central Africa at 850hPa. The zonal sections of moisture flux anomaly along 20°E and 40°E further illustrate the reduced moisture over southwestern Tanzania. Along 20°E, lower tropospheric westerly anomalies are observed to retreat further north between 9°S and 3°S while along 40°E, strong lower tropospheric easterly anomalies dominate between 12°S and 6°S.

These patterns explain moisture convergence to the north (northwestern Tanzania and Kenya) and divergence to the south consistent with rainfall decrease over southwestern Tanzania in January.

During February [Figure 4.2.2(e)], positive SST anomalies strengthen over the South West Indian Ocean while over the tropical South Atlantic Ocean, negative SST anomalies exist. Strong low-level easterly anomalies exist over the tropical Indian Ocean and over East Africa. Over the northwestern Indian Ocean, the anomaly has a southerly component. Taken together, this represents a weakening of the Northeast monsoon towards East Africa, consistent with decreased rainfall over the southwestern Tanzania in February. On the other side of Africa, the Angola low is seen to be stronger and shifting further south. As a result, the flux of moisture from the tropical southeast Atlantic is located further south during this month.

At 200hPa, westerly anomalies are evident over Tanzania and the rest of East Africa consistent with a weaker Walker circulation and reduced rainfall. The velocity potential anomalies are weakly convergent at all levels which confirms the rainfall decrease over Tanzania during this month. The zonal sections of moisture flux anomaly along 20°E reveals strong low level westerly anomalies between 15°S and 9°S with easterlies to the south while along 40°E, westerly anomalies are evident between 18°S and 12°S with easterly anomaly to the north of this flow. This distribution indicates moisture divergence consistent with rainfall decrease over the region during February.

In March [Figure 4.2.2(f)], positive SST anomalies in the South West Indian Ocean extended towards Tanzania i.e. north of Madagascar while over the tropical South Atlantic Ocean, negative SST anomalies continue.

During this month, a lower tropospheric anticyclonic anomaly is apparent over western Indian Ocean and acts to weaken the mean easterly anomalies towards Madagascar and southern Tanzania but strengthen the mean flow towards Kenya and Somalia. Another low-level feature is the cyclonic anomaly over Angola which acts to strengthen the westerly inflow from the tropical southeast Atlantic towards Southern Zambia, Angola and Namibia.

Low-level divergent flow is evident over western and southwestern Tanzania consistent with the reduced rainfall. More evidence of the rainfall decrease in the region is provided by the velocity potential anomaly plot, which indicates low-level divergence over Tanzania at 850hPa with associated upper level divergent anomaly.

Along 20°E, westerly anomalies exist between 15°S and equator with easterly anomalies to the south of this flow between 24°S and 18°S. This pattern with the westerly anomalies between 15°S and 9°S along 40°E further illustrates the moisture divergence over the region consistent with the rainfall decrease in March.

During April [Figure 4.2.2(g)], the positive SST anomalies over the central and southwestern Indian Ocean weaken. Negative SST anomalies develop over the northwestern Indian Ocean. Over the tropical Atlantic Ocean, negative SST anomalies strengthen relative to March.

An anticyclonic anomaly over the western tropical Indian Ocean and a cyclonic anomaly over Angola are evident at 850hPa. These anomalies act to weaken the mean flow of easterlies from the western Indian Ocean and across Southern Africa towards the tropical southeast Atlantic and as a result, divergent flow exists over most of Tanzania. This diffluent flow over the study area is also reflected by weak positive OLR anomalies over most of East Africa which suggest reduced convection consistent with a rainfall decrease during this month. Large negative OLR anomalies exist over the warm SST anomaly northeast of Madagascar with increased rainfall there.

At 200hPa, westerly anomalies are present over East Africa consistent with a weaker Walker circulation leading to reduced rainfall over the region. The velocity potential anomaly plot confirms the reduced rainfall over the region in April by indicating relative low-level divergence over Tanzania at 850hPa with associated upper level convergence anomaly. Along 20°E, westerly anomalies to the north exist between 15°S and 6°S with easterly anomalies to the south between 24°S and 18°S. Westerly anomalies exist between 15°S and 3°S along 40°E. This pattern can explain the low level divergence of the moisture over the region consistent with a significant rainfall decrease in April.

During May [Figure 4.2.2(h)], the positive SST anomalies over the Indian Ocean strengthen to the west and south while in the South Atlantic Ocean, the negative SST anomalies increase compared to the previous month. During this month, an intense lower tropospheric anticyclonic anomaly is evident over the western Indian Ocean. This anomaly is more or less opposite in direction to the mean flow suggesting a weaker ITCZ over East Africa and reduced inflow of moisture from the tropical South West Indian Ocean. These anomalies converge near Lake Victoria with westerly anomalies from the Congo basin leading to a rainfall increase there.

At 200hPa, westerly anomalies across tropical East Africa strengthen, implying a weak Walker circulation and hence low level divergence and reduced rainfall over western Tanzania. This reduction of rainfall over western Tanzania is consistent with the velocity potential anomaly plot, which indicates relative divergence over Tanzania at 850hPa and an upper level convergent anomaly.

The zonal section of moisture flux anomaly along 20°E indicates westerly anomalies between 12°S and 9°S with easterly anomalies south and north of this flow while along 40°E, westerly anomalies dominate between 24°S and the equator. This pattern leads to low-level divergent flow over southern and eastern Tanzania and reduced rainfall. A summary of SST anomalies and circulation features associated with dry conditions over the western and southwestern Tanzania is presented in Table 2 below.

A one-sided t-test is used to identify areas where SSTs are significantly different from climatology at 95% significance level. Shading indicates anomalies that are statistically significant at the 95% level. During the wet years, significant negative anomalies are seen from October to May over the South Indian Ocean and the central South Atlantic Ocean. During dry years, there appear to be weak but significant positive anomalies over the subtropical Southeast Indian Ocean, but these may not be of much significance to western and southwestern Tanzanian rainfall (Appendix 3 and 4). It is however noted that latent heat flux (LHF), outgoing longwave radiation (OLR), moisture flux and wind circulation over the adjacent Atlantic and Indian oceans may be important to rainfall variability for the October/April season over the study area.

t-values are calculated using 
$$t = \frac{\bar{d}}{S/\sqrt{n}}$$

where  $n$  is the size of the sample,  $\bar{d} = \sum d_i/n$  is the mean difference,  $d_i$  represent the  $i$ th realization of the rainfall difference and  $S = \sqrt{\sum (d_i - \bar{d})^2 / (n-1)}$  is the sample variance of the observed differences. This statistic has a t - distribution with  $n - 1$  degree of freedom. If the absolute value of t-value exceeds 2.015, the anomaly is significantly different at the 95% confident level (von Storch and Zwiers, 1999).

**Table 2:** SST anomalies and circulation features associated with dry conditions over western and southwestern Tanzania

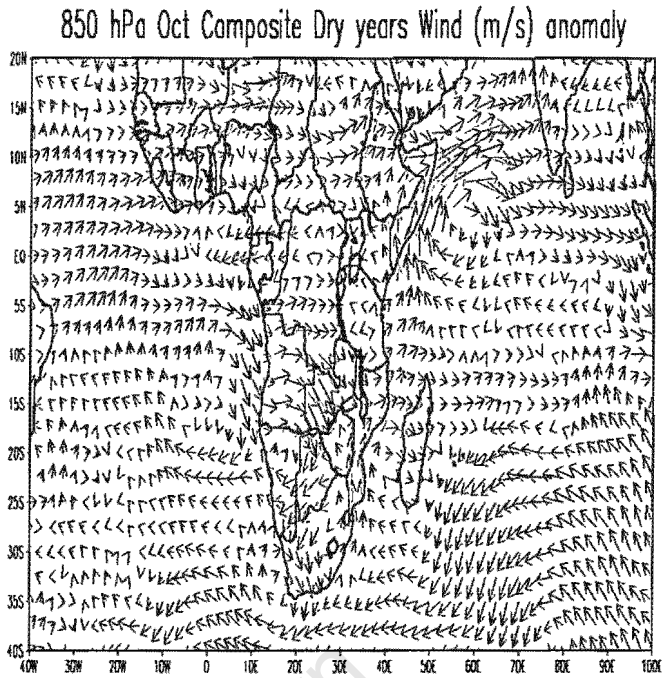
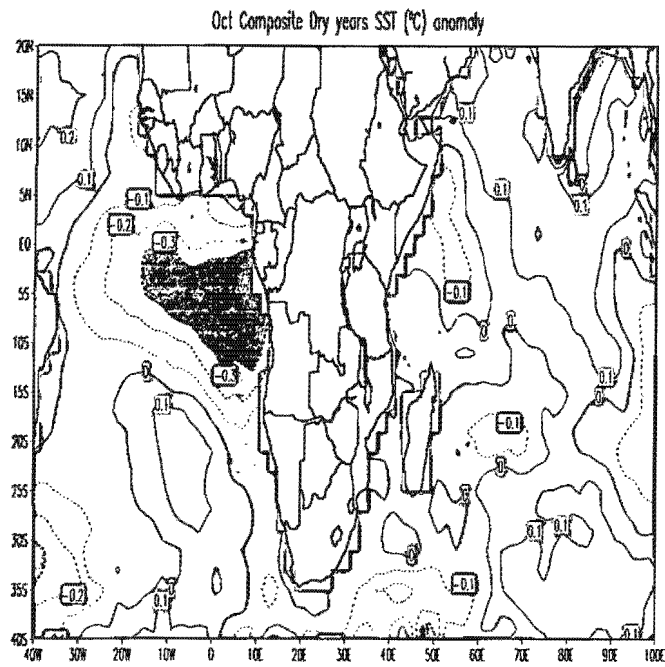
INDIAN OCEAN	ATLANTIC OCEAN
<p><b>October:</b></p> <ul style="list-style-type: none"> <li>-Weak positive SST anomalies over tropical western and central Indian Ocean</li> <li>-Negative SST anomalies are evident over southwestern and subtropical Indian Ocean</li> <li>-Lower tropospheric cyclonic anomaly over the tropical western Indian Ocean</li> <li>-Southeasterly anomaly over Mozambique and Tanzania.</li> <li>-Upper level Cyclonic anomaly developing over East Africa and the neighbouring regions with westerly anomalies over Tanzania</li> <li>-Positive OLR anomalies are evident over most of Tanzania, Kenya and Uganda.</li> </ul> <p><b>November:</b></p> <ul style="list-style-type: none"> <li>-Weak positive SST anomalies over the tropical central Indian Ocean continue.</li> </ul>	<ul style="list-style-type: none"> <li>-Negative SST anomalies across the tropical South Atlantic</li> <li>-Positive SST anomalies are shown over subtropical South Atlantic</li> <li>-Cyclonic anomaly over the tropical Southeast Atlantic and southwestern African region</li> </ul> <p><b>November:</b></p> <ul style="list-style-type: none"> <li>-Positive SST anomalies exist over the tropical Southeast Atlantic.</li> <li>-Cyclonic anomaly over the tropical Southeast Atlantic</li> </ul> <p><b>December:</b></p> <ul style="list-style-type: none"> <li>-Positive SST anomalies decrease intensity compared to the previous month with large negative SST anomalies over tropical South Atlantic.</li> </ul>

INDIAN OCEAN	ATLANTIC OCEAN
<p>with increased positive SST anomalies over subtropical South Indian Ocean.</p> <p>-Cyclonic anomaly over the tropical Indian Ocean and anticyclonic anomaly over the mid latitude Southwestern Indian Ocean are apparent.</p> <p>-Cyclonic anomaly over the tropical central Indian Ocean.</p> <p>-Upper level cyclonic anomaly over East Africa with associated westerly anomalies over Tanzania.</p> <p>-Positive OLR anomalies are evident over Tanzania, southwest of Madagascar, Kenya and Uganda.</p> <p><b>December:</b></p> <p>-Positive SST anomalies over the tropical western Indian Ocean decreases</p> <p>-Negative SST anomalies east of Madagascar persist.</p>	<p>-An anticyclonic anomaly over Angola and northwesterly anomaly over southeastern Africa are evident.</p> <p><b>January:</b></p> <p>-Positive SST anomalies strengthen in the subtropical South Atlantic Ocean</p> <p>-Negative SST anomalies over the tropical South Atlantic</p> <p>-Anticyclonic anomaly over Angola persists.</p> <p><b>February:</b></p> <p>-Negative SST anomalies over tropical South Atlantic Ocean persist.</p> <p>-Angola low strengthens and shifts further south.</p>

INDIAN OCEAN	ATLANTIC OCEAN
<p>-Lower tropospheric cyclonic anomaly over the central tropical Indian Ocean strengthen</p> <p>-Northeast monsoon flow from the tropical western Indian Ocean to Tanzania weakens</p> <p>-Anticyclonic anomaly southeast of Madagascar with cyclonic anomaly further north.</p> <p>-Positive OLR anomalies over Tanzania, Madagascar and western Indian Ocean</p> <p><b>January:</b></p> <p>-Positive SST anomalies strengthen in the South and central Indian Ocean.</p> <p>-Negative SST anomalies over western Indian Ocean and along the coast of Tanzania are apparent.</p> <p>-Zonally extensive anticyclonic anomaly over South Indian Ocean</p> <p>-Enhanced mean easterly flow towards Madagascar and Northeasterly flow</p>	<p><b>March:</b></p> <p>-Negative SST anomalies over the tropical South Atlantic maintained.</p> <p>-Cyclonic anomaly over Angola is apparent.</p> <p><b>April:</b></p> <p>- Negative SST anomalies over the tropical South Atlantic strengthen relative to March.</p> <p>-Cyclonic anomaly over Angola present.</p> <p><b>May:</b></p> <p>-Negative SST anomalies in the south Atlantic increase compared to April.</p>

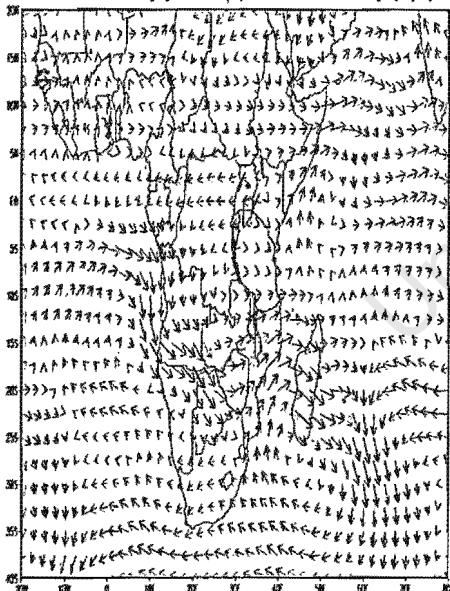
INDIAN OCEAN	ATLANTIC OCEAN
<p>towards northern Tanzania and Kenya.</p> <ul style="list-style-type: none"> <li>-Weak upper level westerly anomalies over Tanzania which become stronger over western Indian Ocean (weaker Walker circulation)</li> <li>-Weak Positive OLR anomalies over Tanzania (subsidence)</li> </ul> <p><b>February:</b></p> <ul style="list-style-type: none"> <li>-Strengthened positive SST anomalies over southwest Indian Ocean.</li> <li>-Strong low-level easterly anomalies over the tropical Indian Ocean and over East Africa.</li> <li>-Weakening of the northeast monsoon towards East Africa.</li> <li>-Upper level westerly anomalies are evident over Tanzania and the rest of East Africa (weaker Walker circulation).</li> </ul> <p><b>March:</b></p> <ul style="list-style-type: none"> <li>- Positive SST anomalies strengthen in the tropical Indian Ocean</li> <li>-Lower tropospheric anticyclonic anomaly over western Indian Ocean.</li> </ul>	

INDIAN OCEAN	ATLANTIC OCEAN
<p data-bbox="175 311 766 400">-Positive OLR anomalies over Tanzania, Kenya and Uganda.</p> <p data-bbox="175 477 263 510"><b>April:</b></p> <ul style="list-style-type: none"> <li data-bbox="175 533 766 621">-Positive SST anomalies over the central and southwestern Indian Ocean weaken.</li> <li data-bbox="175 643 766 732">-Negative SST anomalies developing over northwestern Indian Ocean.</li> <li data-bbox="175 754 766 898">-An anticyclonic anomaly over western tropical Indian Ocean at 850hPa is apparent</li> <li data-bbox="175 920 766 1119">-Upper level westerly anomalies are present over East Africa consistent with weak Walker circulation and reduced rainfall.</li> <li data-bbox="175 1141 766 1229">-Weak positive OLR anomalies over most of East Africa</li> </ul> <p data-bbox="175 1307 247 1340"><b>May:</b></p> <ul style="list-style-type: none"> <li data-bbox="175 1362 766 1451">-Positive SST anomalies over Indian Ocean strengthen to the west and south.</li> <li data-bbox="175 1473 766 1605">-Intense lower tropospheric anticyclonic anomaly is evident over East Africa and western Indian Ocean.</li> <li data-bbox="175 1628 766 1716">-Stronger upper level westerly anomalies across tropical East Africa.</li> </ul>	



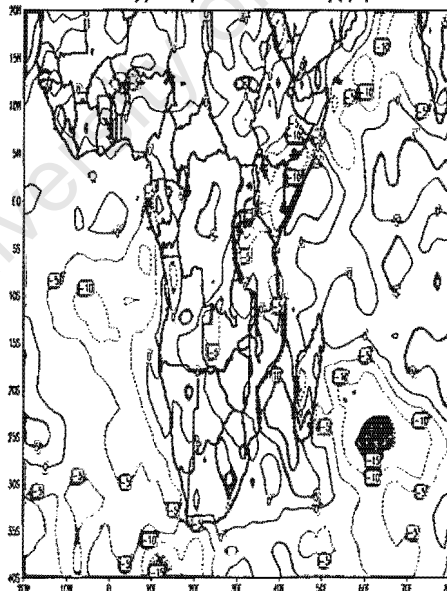
→

700 hPa Oct Dry years composite Wind anomaly (m/s)

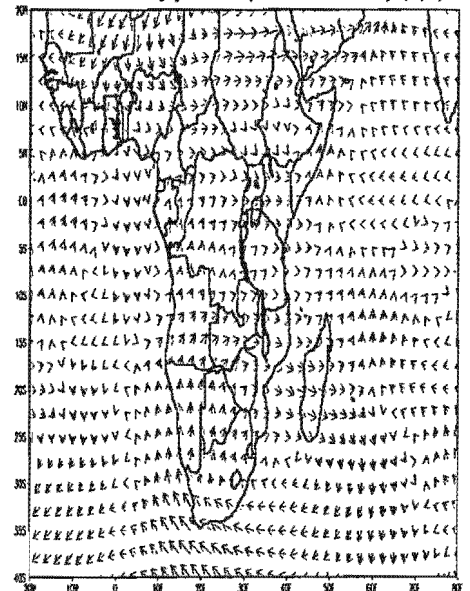


→

Oct Dry years Composite Latent heat flux anomaly (W/m²)



200 hPa Oct Dry years composite wind anomaly (m/s)



→

Figure 4.2.2(a) October dry composite anomaly; SST(contour interval 0.1°C), wind at 850,700 and 200hPa (scale vector is shown at the bottom), latent heat flux (contour interval is 5 W/m²). Colour on wind vectors indicate their magnitude from low (purple) to high (red).

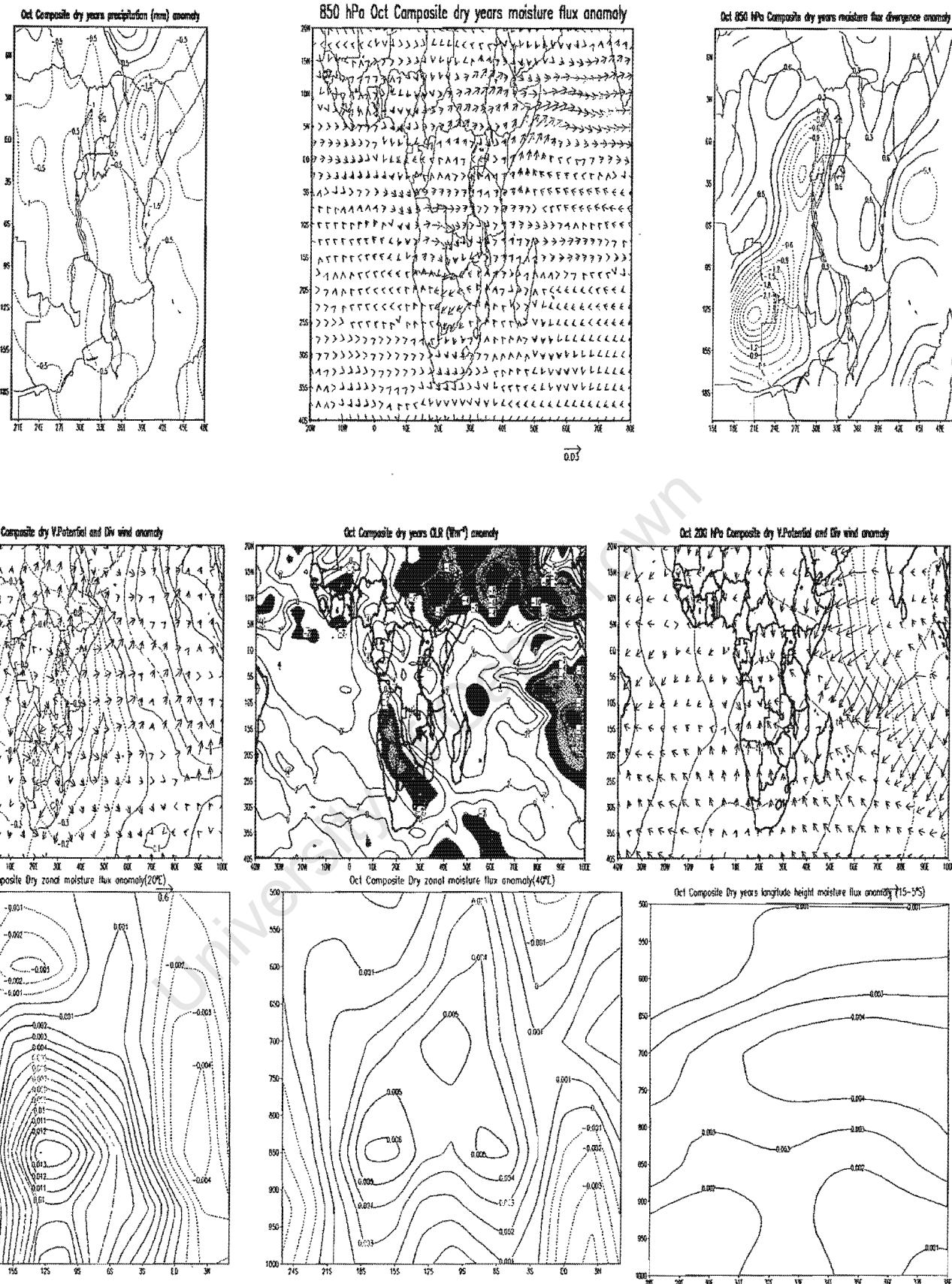
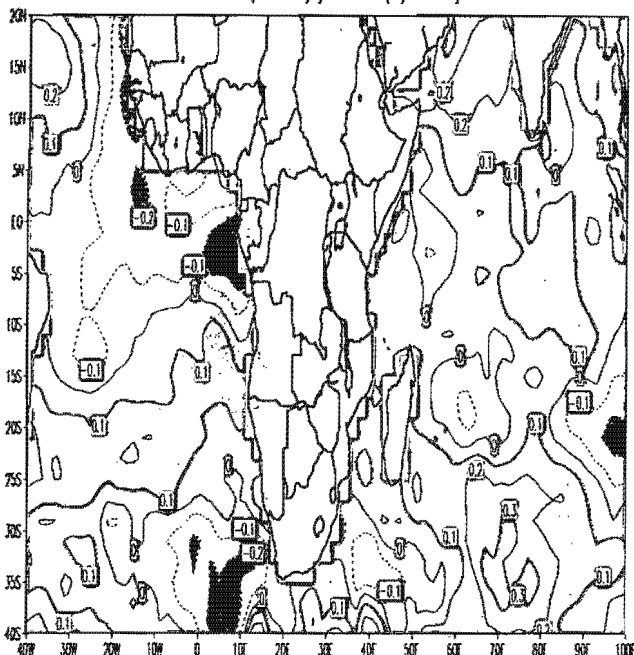


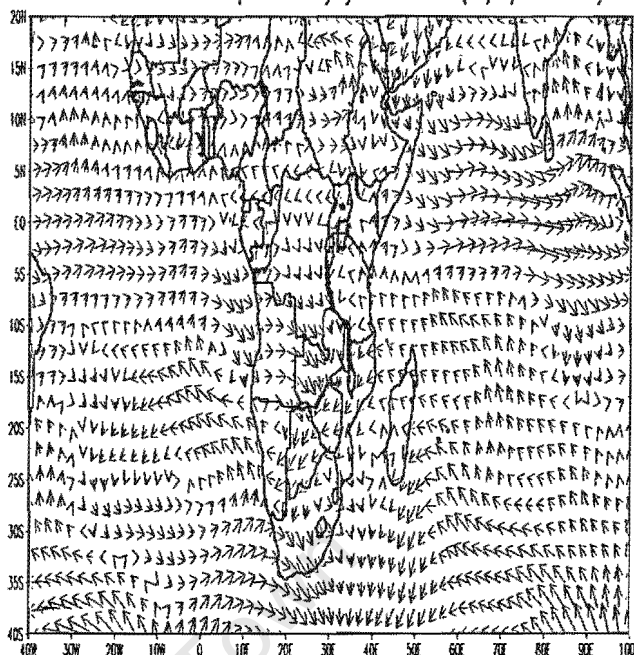
Fig.4.2.2(a) cont..

[Moisture flux in  $\text{g/kg}\cdot\text{ms}^{-1}$  and scale vector is shown at the bottom of the figures; OLR (contour interval is  $5 \text{ Wm}^{-2}$ ); Divergent wind in  $10^{-6} \text{ s}^{-1}$  and contour interval is  $0.2 \times 10^{-6} \text{ s}^{-1}$ ; Velocity potential in  $10^{-6} \text{ m}^2\text{s}^{-1}$  and contour interval is  $0.1 \times 10^{-6} \text{ m}^2\text{s}^{-1}$ ]. Positive means westerlies and negative easterlies.

Nov Composite Dry years SST (°C) anomaly

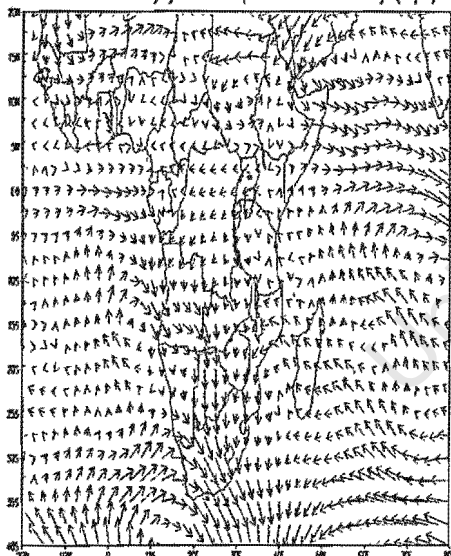


850 hPa Nov Composite Dry years Wind (m/s) anomaly



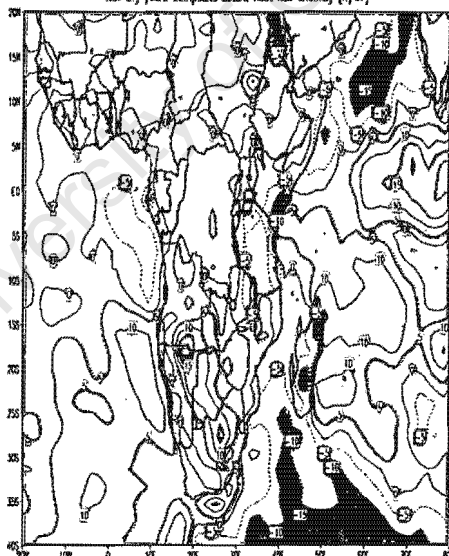
3

700 hPa Nov Dry years composite Wind anomaly (m/s)

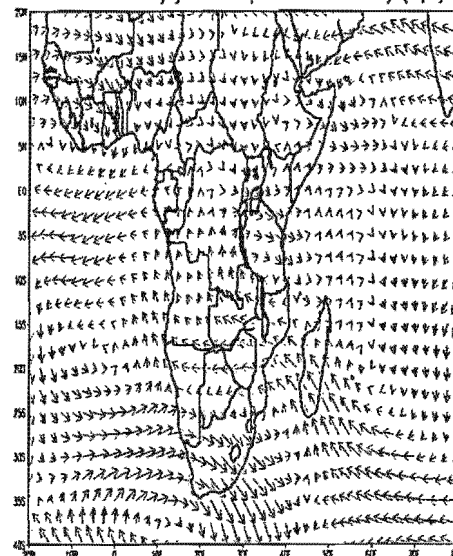


2

Nov Dry years Composite Latent heat flux anomaly (W/m²)



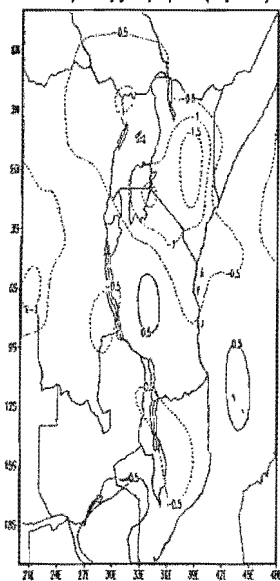
200 hPa Nov Dry years composite wind anomaly (m/s)



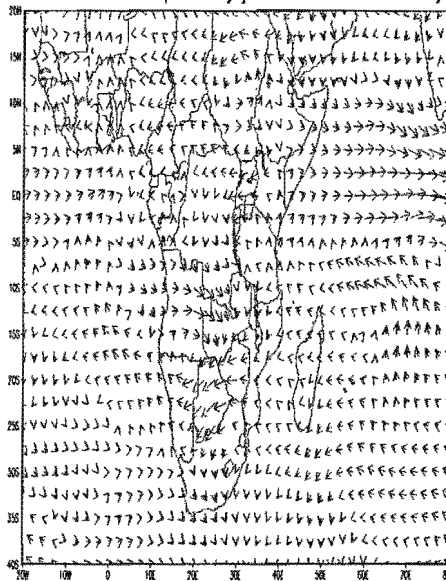
3

Figure 4.2.2(b); as figure 4.2.2(a) but for November dry composite

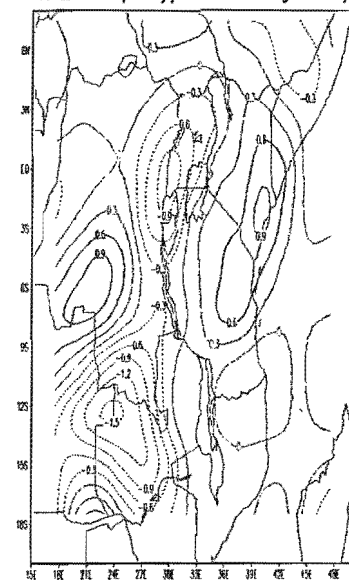
Nov Composite dry years precipitation (mm) anomaly



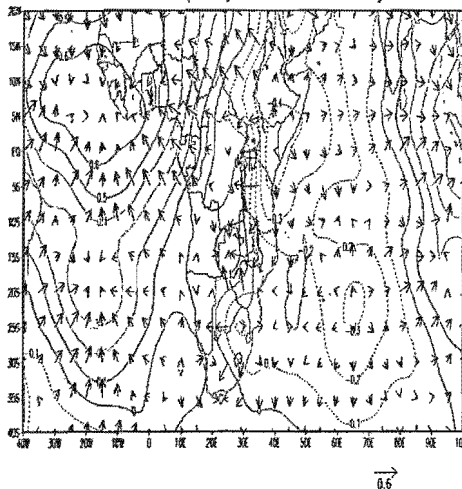
850 hPa Nov Composite dry years moisture flux anomaly



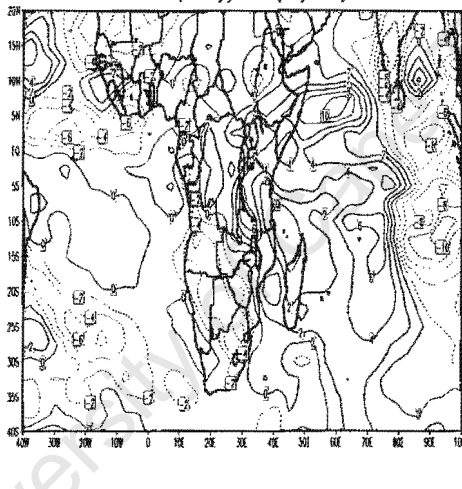
Nov 850 hPa Composite dry years moisture flux divergence anomaly



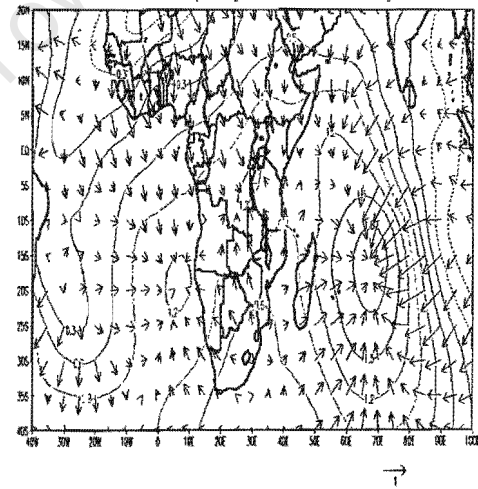
Nov 850 hPa Composite dry V.Potential and Div wind anomaly



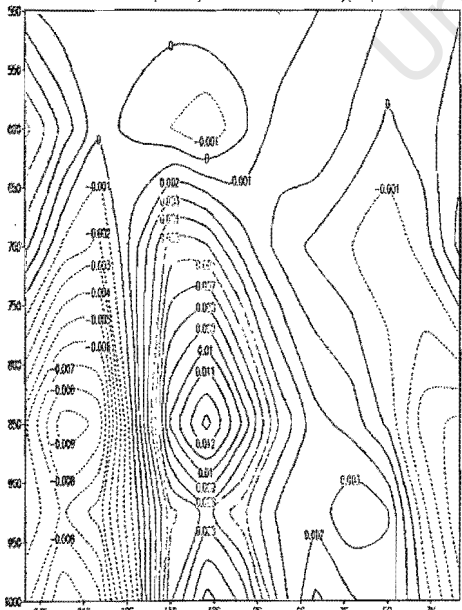
Nov Composite dry years CLR ( $Wm^{-2}$ ) anomaly



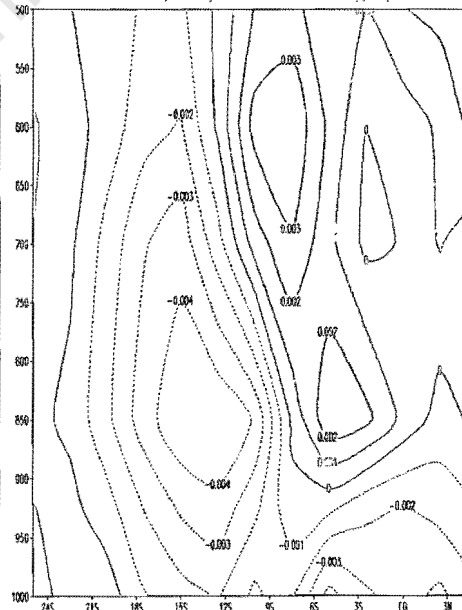
Nov 200 hPa Composite dry V.Potential and Div wind anomaly



Nov Composite Dry zonal moisture flux anomaly(20°C)



Nov Composite Dry zonal moisture flux anomaly(40°C)



Nov Composite Dry years longitude height moisture flux anomaly (15-5°S)

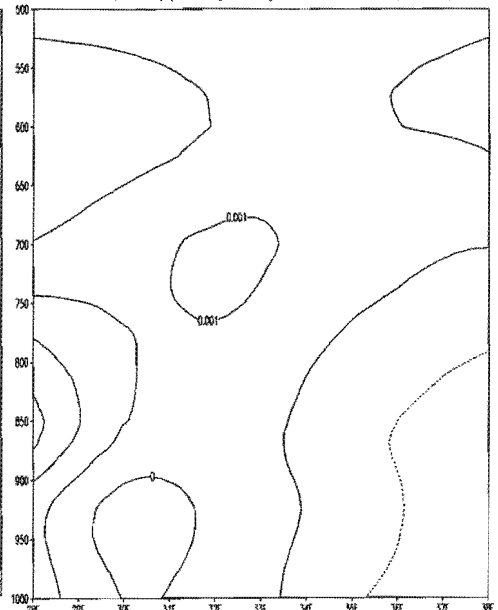
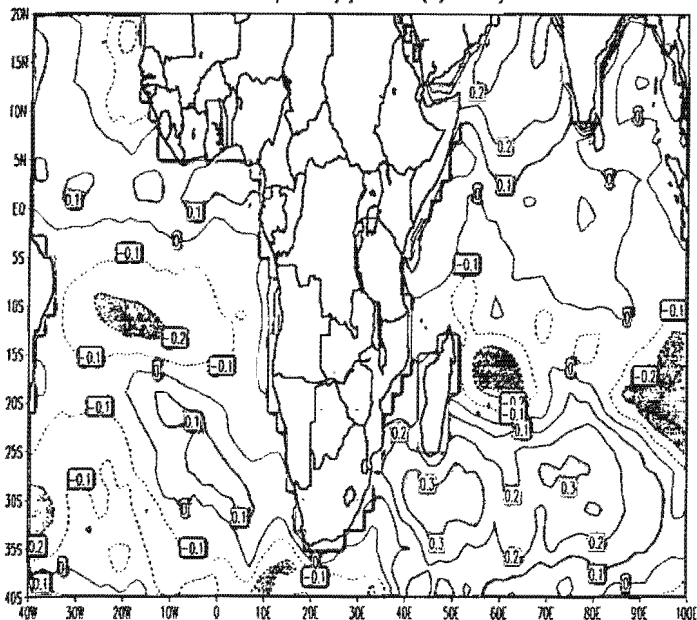
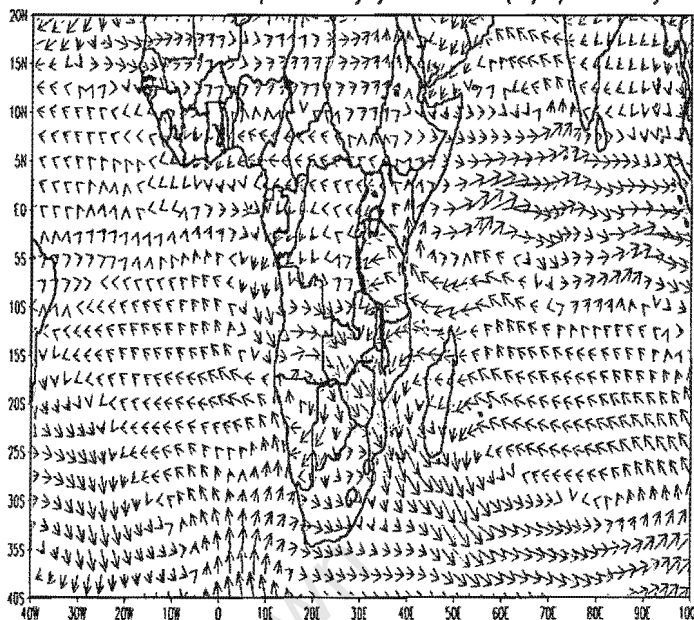


Fig.4.2.2(b) cont..

Dec Composite Dry years SST (°C) anomaly

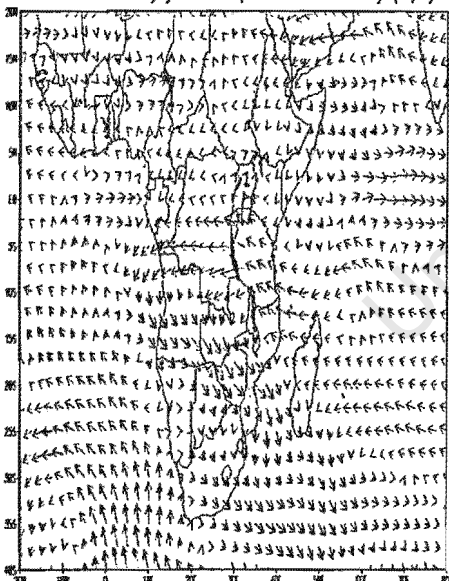


850 hPa Dec Composite Dry years Wind (m/s) anomaly



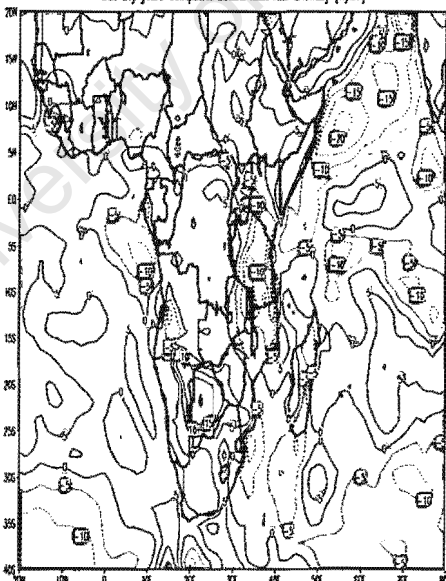
→  
3

700 hPa Dec Dry years composite Wind anomaly (m/s)

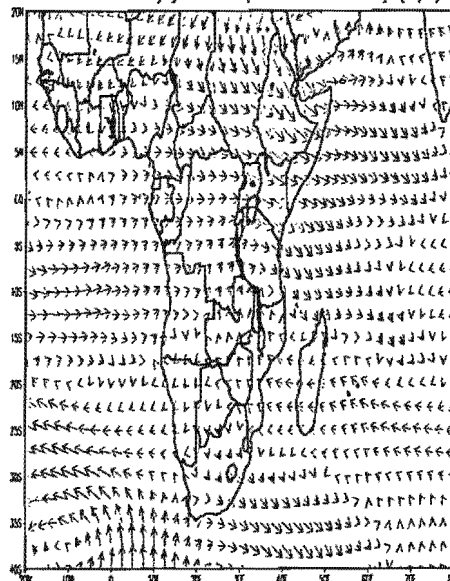


→  
3

Dec Dry years Composite Latent heat flux anomaly (W/m²)



200 hPa Dec Dry years composite wind anomaly (m/s)

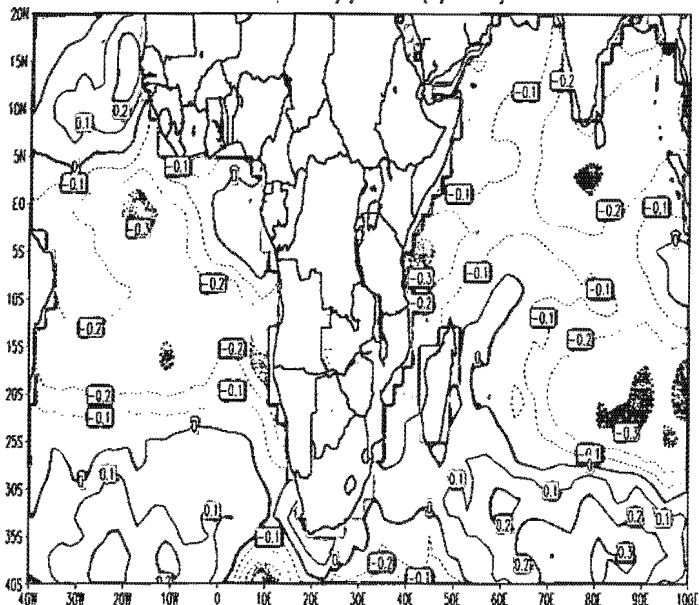


→  
3

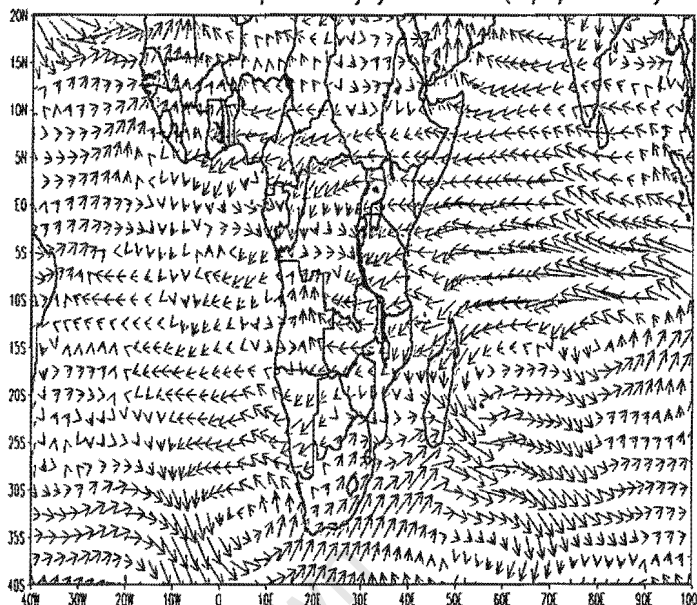
Figure 4.2.2(c); like figure 4.2.2.(b) but for December



Jan Composite Dry years SST (°C) anomaly

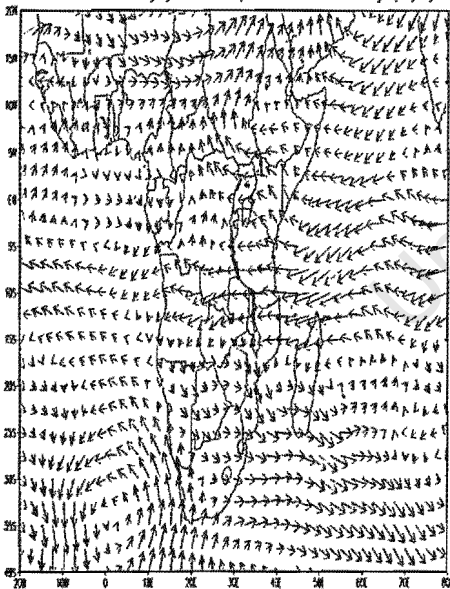


850 hPa Jan Composite Dry years Wind (m/s) anomaly



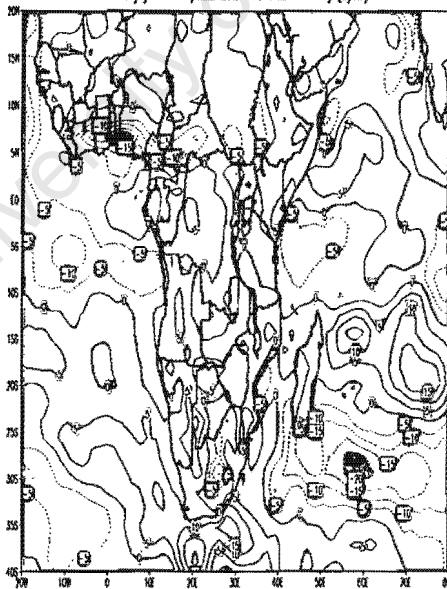
→

700 hPa Jan Dry years composite Wind anomaly (m/s)

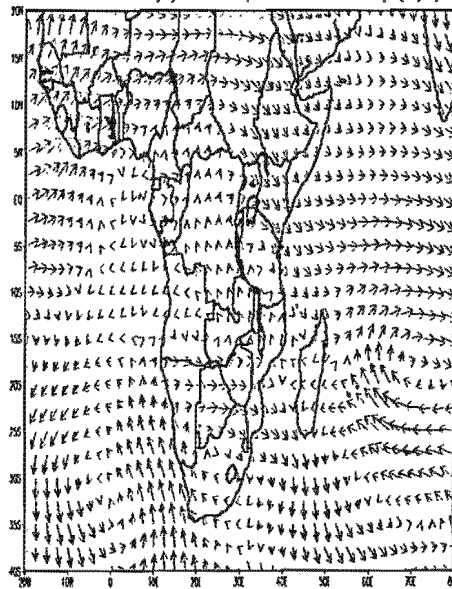


→

Jan Dry years Composite Latent heat flux anomaly (W/m²)



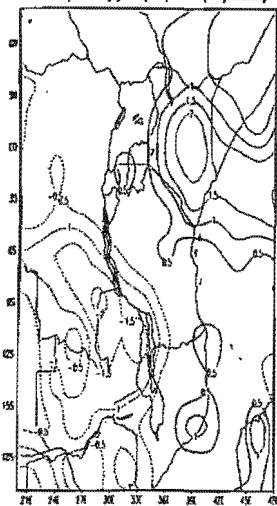
200 hPa Jan Dry years composite wind anomaly (m/s)



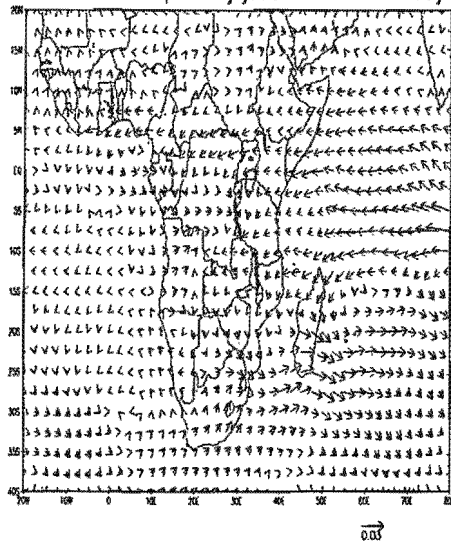
→

Figure 4.2.2(d); as figure 4.2.2(c) but for January

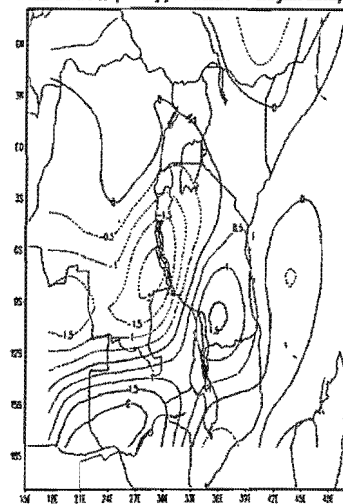
Jan Composite dry years precipitation (mm) anomaly



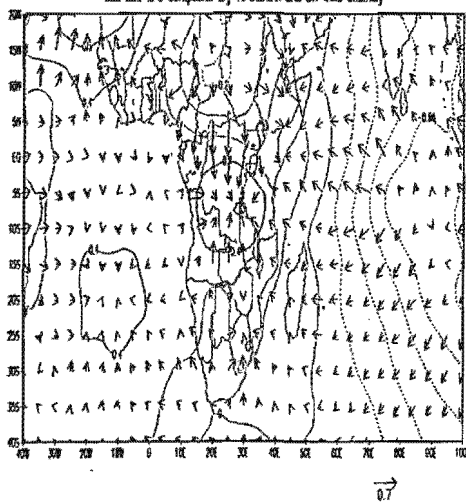
850 hPa Jan Composite dry years moisture flux anomaly



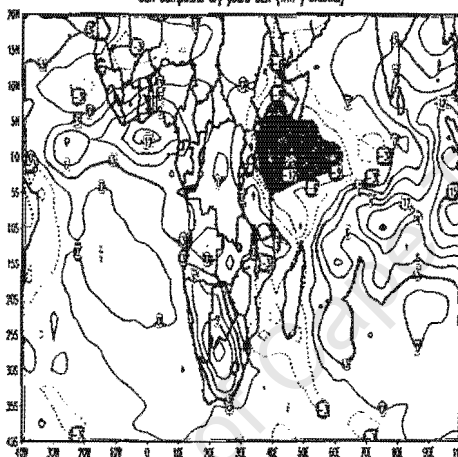
Jan 850 hPa Composite dry years moisture flux divergence anomaly



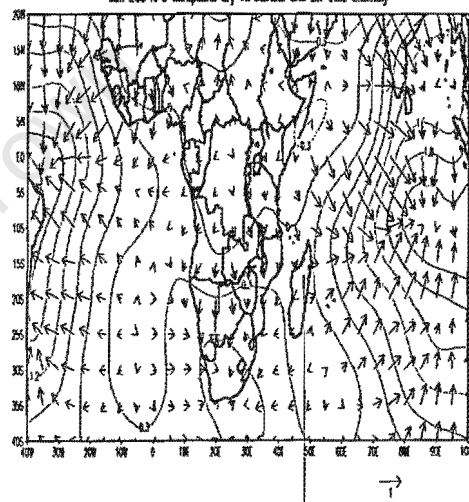
Jan 850 hPa Composite dry VPotential and the wind anomaly



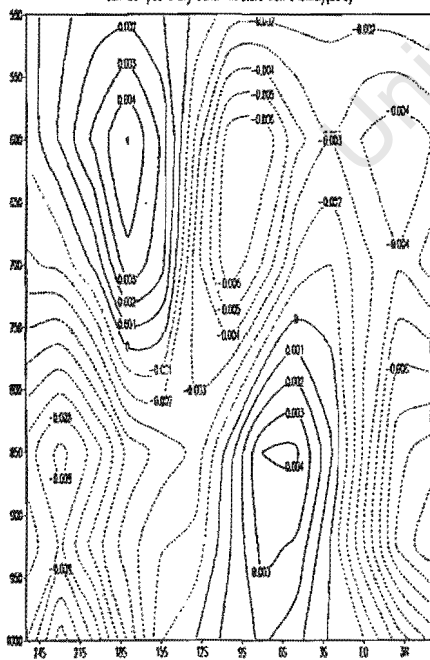
Jan Composite dry years QLR (W/m²) anomaly



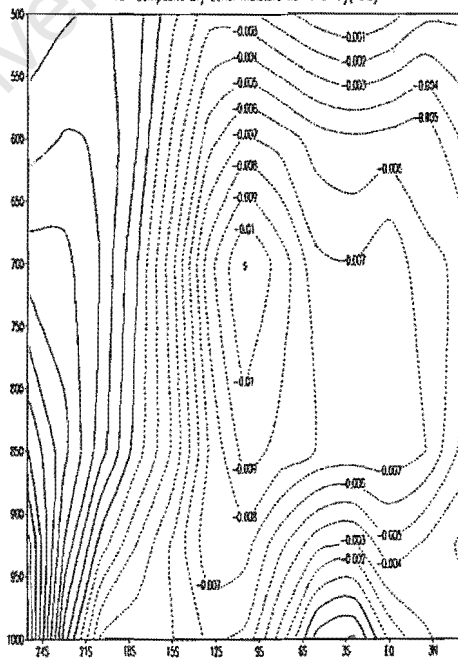
Jan 200 hPa Composite dry VPotential and the wind anomaly



Jan Composite Dry zonal moisture flux anomaly(20%)



Jan Composite Dry zonal moisture flux anomaly(40%)



Jan Composite Dry years longitude height moisture flux anomaly (15-5°S)

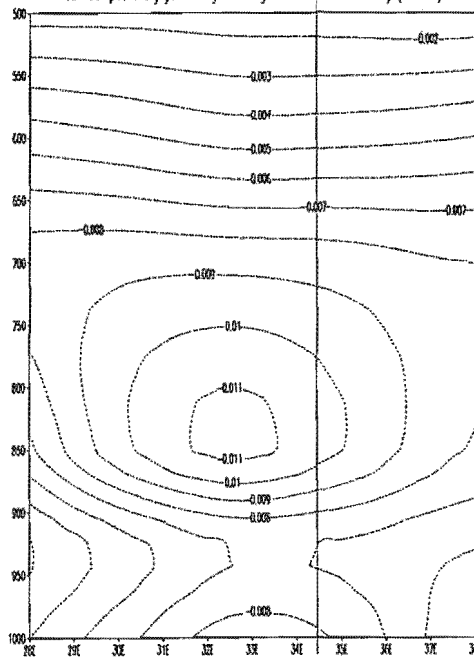


Fig. 4.2.2(d) cont..

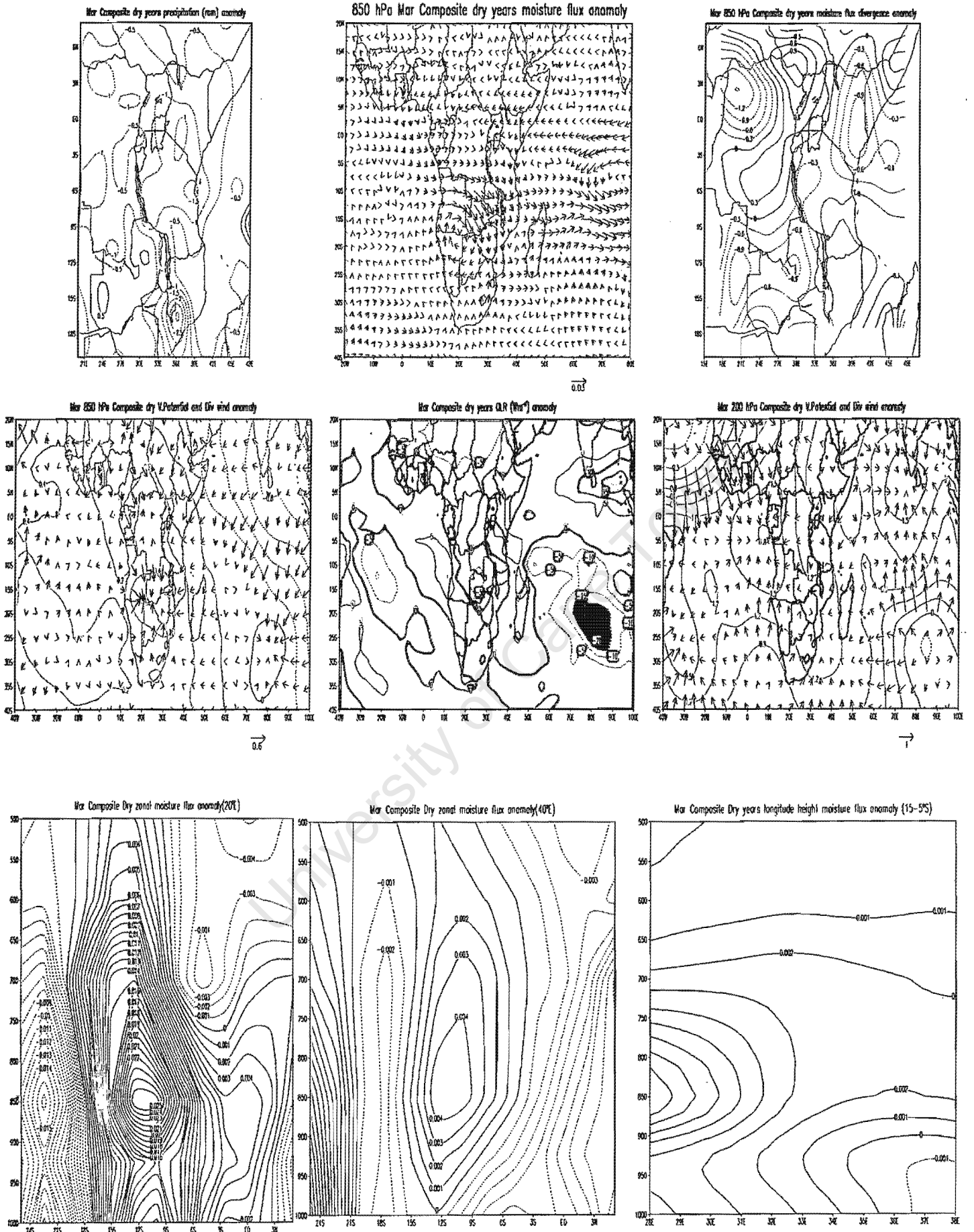
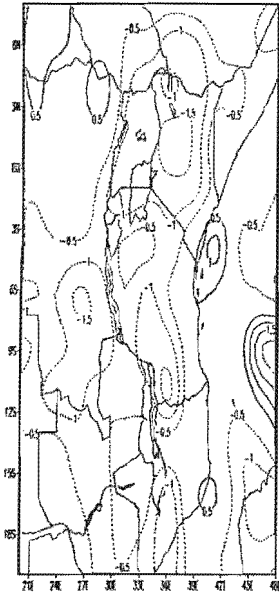
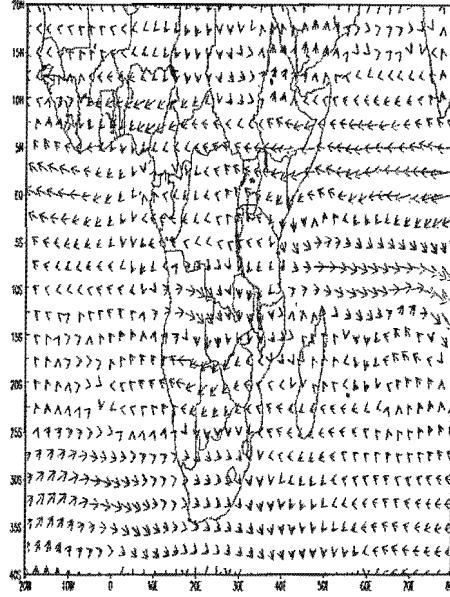


Figure 4.2.2(f) cont..

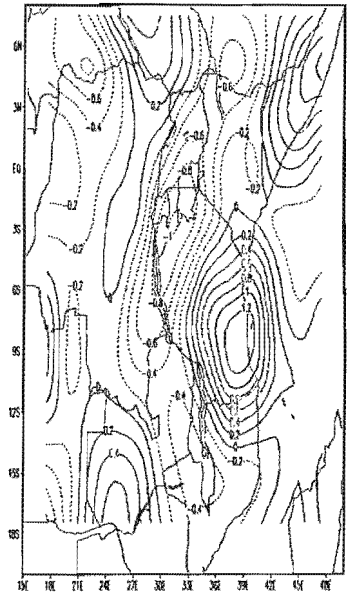
Apr Composite dry years precipitation (mm) anomaly



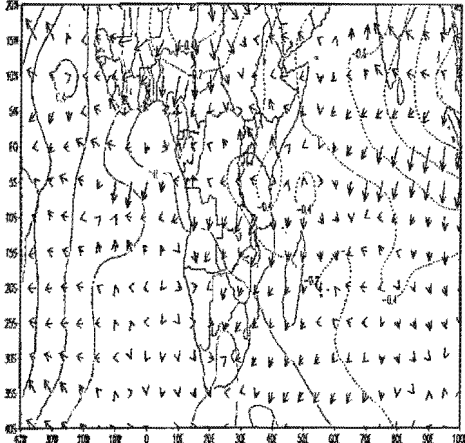
850 hPa Apr Composite dry years moisture flux anomaly



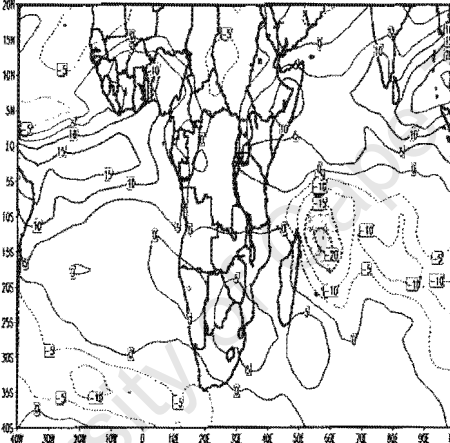
Apr 850 hPa Composite dry years moisture flux divergence anomaly



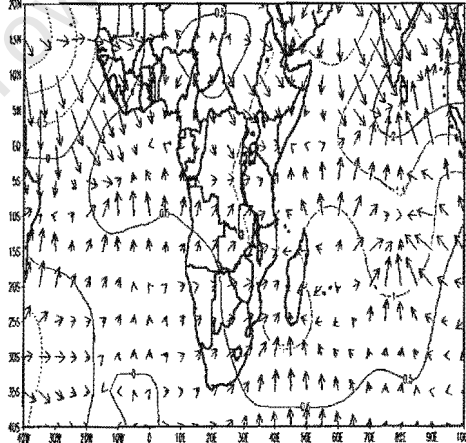
Apr 850 hPa Composite dry V.Potential and Div wind anomaly



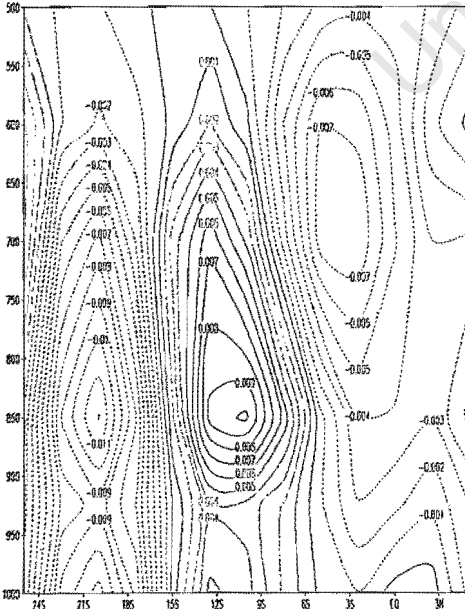
Apr Composite dry years OLR (Wm<sup>-2</sup>) anomaly



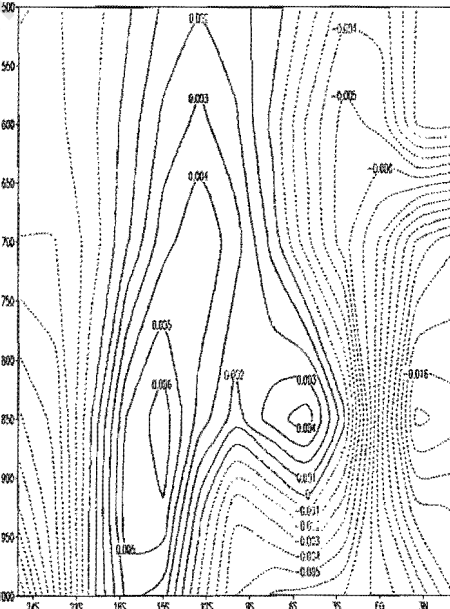
Apr 200 hPa Composite dry V.Potential and Div wind anomaly



Apr Composite Dry zonal moisture flux anomaly(20°E)



Apr Composite Dry zonal moisture flux anomaly(40°E)



Apr Composite Dry years longitude height moisture flux anomaly (15-5°S)

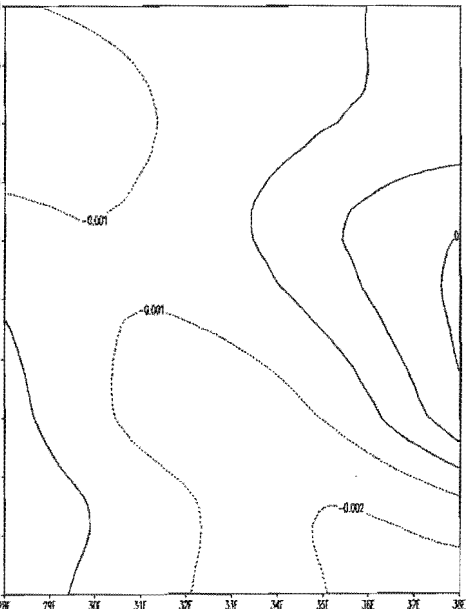
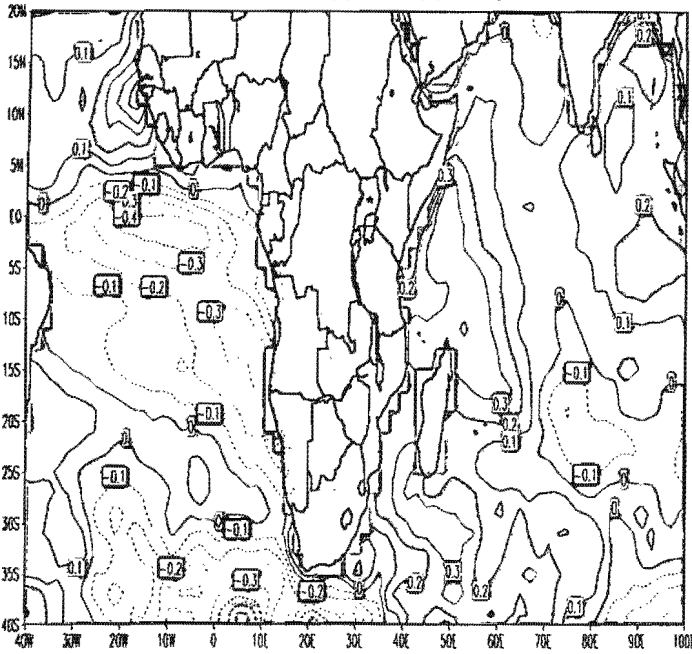
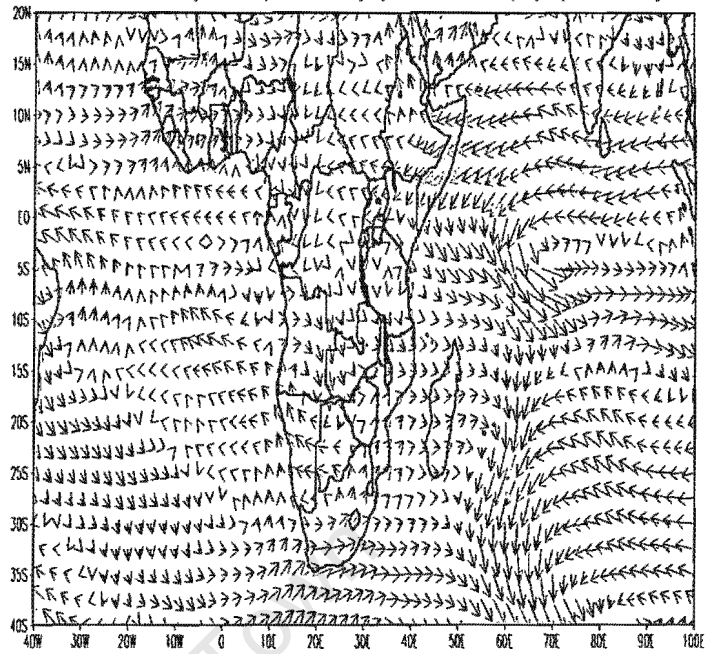


Fig. 4.2.2(g) cont..

May Composite Dry years SST (°C) anomaly

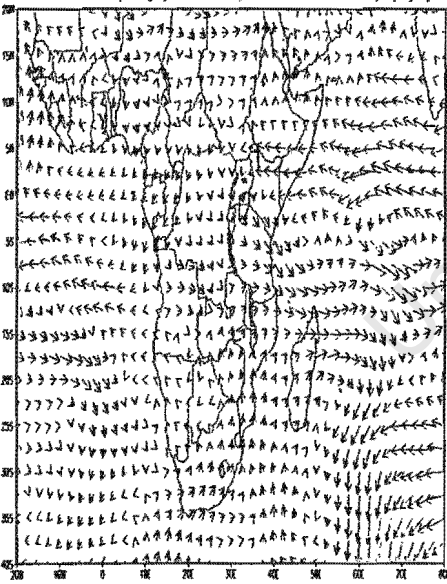


850 hPa May Composite Dry years Wind (m/s) anomaly



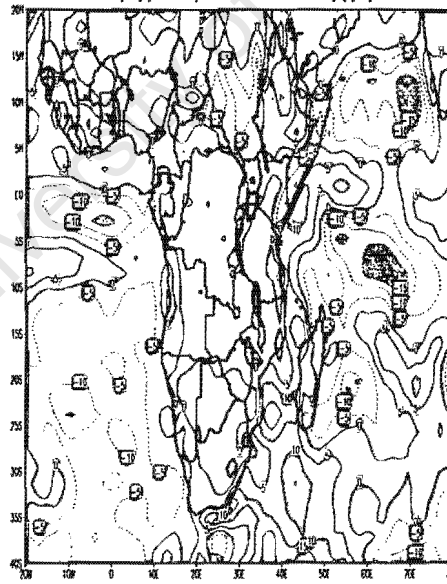
→  
3

700 hPa May Dry years composite Wind anomaly (m/s)

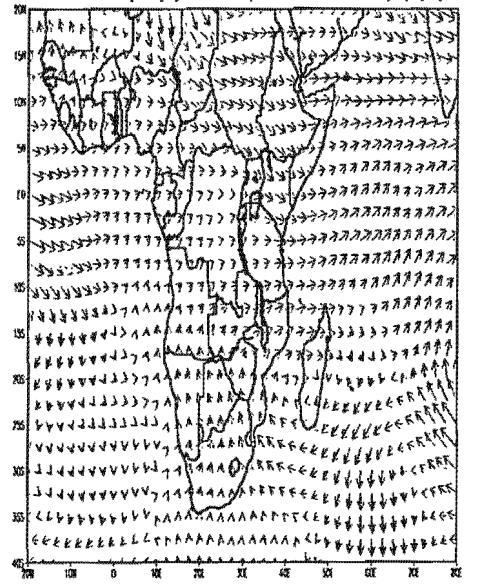


→  
2

May Dry years Composite Latent heat flux anomaly (W/m²)



200 hPa May Dry years composite wind anomaly (m/s)



→  
5

Figure 4.2.2(h); as figure 4.2.2(a) but for May dry composite



## **CHAPTER 5**

### **5.0 Intra seasonal variability**

Intra-seasonal oscillations in the atmosphere are generally defined as fluctuations with periods longer than a week but shorter than a season (Madden and Julian, 1972). A recent study of Zimbabwean rainfall by Makarau (1995) observed intra-seasonal oscillations with two cycles, 10 to 25 and 40 to 50 days. Intra-seasonal oscillation studies which relate to tropical Africa and its adjacent oceans include that of Zhu and Wang (1993), who found a prominent centre of action in the central Indian Ocean with variability in convection on a 30 to 60 day time scale. Madden and Julian (1972) discovered a 40 to 50 day oscillation in the equatorial region. In their pioneering work, they described the oscillations as global-scale eastward propagating oscillations along the equator. Levey (1993) found a 20-30 day oscillation over Southern Africa and noted that of 175 convective systems achieving status over this region; 50% propagated eastwards, 21% were stationary, 18% had an ambiguous pattern and the rest propagated westward.

To further investigate the intra-season rainfall variability for the wet and dry years over western and southwestern Tanzania, pentad (5-day) mean rainfall from the CMAP dataset (Xie and Arkin, 1997) was used. This dataset covers the period 1979–2002 at pentad resolution and it has a spatial resolution of  $2.5^{\circ} \times 2.5^{\circ}$ . To diagnose the mechanisms underlying intra-seasonal circulation over the study region, OLR and NCEP pentads of zonal wind component at 850 and 200hPa levels were used. In this analysis the pentad (5-day) mean were based on the CMAP daily rainfall data period ranging from 1979-1999. The pentad series started with pentad 48 (September) and ended with pentad 108 (June).

Anomalous wet and dry years chosen for this analysis are among those delineated from the spatially rainfall index in Chapter 2 for further detailed study. Wet years selected are Oct1979/May 1980, Oct1982/May83 and Oct1986/May87 while dry years are Oct1987/May88, Oct1992/May93, Oct1993/94 and Oct1998/May99 (OLR and CMAP data is not available prior to 1979)

### **5.1 Methodology:**

To investigate the intra-seasonal variability for the wet and dry spells over the region of study, an area-averaged index of CMAP pentad (5-day) mean rainfall at (29-37°E, 11.5-4.75°S) was created. Latitude-time sections of CMAP precipitation along 29-37°E were plotted to observe the evolutions of wet and dry spells circulations over the region during the onset period and withdrawal of the rains. Longitude-time section (Hovmoller) plots of OLR anomalies and zonal wind components at 850 and 200hPa levels were used to identify zonally propagating features over 15-5°S.

Visual inspection was used to determine when there was a 'sudden increase' and 'sudden decrease' of rainfall in each particular year. The pentad corresponding to the sudden increase and sudden decrease of rainfall were regarded as approximate pentad of the onset and withdrawal respectively.

### **5.2 Results for pentad (5-day) analysis**

Figure 5.2 (a-h) presents the CMAP pentad averaged rainfall time series, latitude-time section of CMAP precipitation, longitude-time section (Hovmoller) of OLR and zonal wind component at 850hPa and 200hPa anomaly plots for the wet and dry years over the study region.

It is evident from the CMAP averaged rainfall time series plots that the onset of wetter than average seasons over western and southwestern Tanzania occurs during the pentad range of 57-58 (mid October) while the pentad 97 –101 (late April to May) marks the end (withdrawal) of the season. For the drier than average seasons, it is evident from the plots that the onset occurs around pentad 60-66 (November) i.e. one month later compared to those of wet years, while the pentad marking the withdrawal occurs around pentad 90-96 (late March to April) [Table 3].

Wet years			Dry years		
Year	Pentad and dates of the rain onset	Pentad and dates of withdraw of the rains	Year	Pentad and dates of the rains onset	Pentad and dates of withdraw of the rains
1979	57 (12-15 Oct.)	97 (30 Apr. to 03 May)	1987	58 (17 –19 Oct.)	90 (26–28 March)
1982	58 (17-19 Oct)	100 (20-23 May)	1992	63 (11-13 Nov.)	92 (31Mar-03 Apr.)
1986	57 (12-15 Oct.)	101 (25-27 May)	1993	60 (27-29 Oct)	93 (4-6 Apr.)
			1998	65 (26-28 Nov.)	96 (25-29 Apr.)

Table 3: Mean pentad and dates of the onset and withdraw of the rains for wet and dry years over western and southwestern Tanzania.

The latitude-time section indicates that during 1979/1980 [Figure 5.2(b)] the rains started in pentad 57 (October) over western Tanzania and increased in intensity later in pentad 66 (November). Rains then spread over southwestern Tanzania from this pentad 66. Strong wet spells occurred in pentad 71 (December), 86 (March) and pentad 94 (April). Rains started to withdraw from the study region in pentad 97 (early May). Early in the season, wet spells propagated from south to north whereas after pentad 78 wet spells tended to occur simultaneously over the country.

The 1982/1983 season [Figure 5.2(c)] was wetter than 1979/1980, and the rains began over western Tanzania in pentad 58 (mid October). Strong wet spells during this season occurred in pentad 67 (early December), 72 (end of December), pentad 79 and 82 (February) and pentad 89 (March). Thereafter, rains continue with decreasing intensity but ongoing variability and started to withdraw in pentad 100 (late May). Again, wet spells tended to propagate from south to north earlier in the season.

During the 1986/1987 [Figure 5.2(d)] wet season, rains over western Tanzania commenced in pentad 57 (October) and increased in intensity later in pentad 67 (November). During this season, wet spells had greater intensity compared to 1979/80 and 1982/83, although the 1982/83 wet spells were evenly distributed throughout the season. The strong wet spells in 1986/87 occurred in pentad 69 (December), pentads 74, 76, 78 all in January and pentad 82 and 84 in March. After pentad 84, rains reduced over the study region and started to withdraw in pentad 101 (early June).

During the dry season of 1987/88 [Figure 5.2(e)], some rain occurred very early in pentad 54 (early October) followed by significant dry spell in pentad 57 and 61/2. Weak wet spells are evident during this season with two strong wet spell occurring in pentad 78 in January and 89 in March. Other weak wet spells experienced in pentad 74 in January and pentad 81 in February. Rains began to withdraw over the region in pentad 90 (early April). Unlike that of wetter than average year, wet spells early in the season appear to propagate southwards.

Another dry season is 1992/93 [Figure 5.2(f)], for which rains started in pentad 63 (November). Only one intense wet spells (85 in February) is evident. Weaker wet spells occurred at regular intensity through the season. The rains started to withdraw in pentad 92(early April).

The 1993/94 season [Figure 5.2(g)] was relatively dry, onset occurred in pentad 60 with dramatic increase in intensity during pentad 75. During this season, a large number of dry spells occurred at the beginning of the season. Relatively strong wet spells occurred in pentad 75 (January), pentad 80 and 83 in March. After pentad 83,rains weakened in intensity and start to withdraw in pentad 93 (early April).

In 1998/99 [Figure 5.2(h)], the rainy season started in pentad 65 (late November) with an extended dry period observed from pentad 54 to pentad 64. During this season significant wet spells were experienced in pentad 77 and pentad 78 in February, pentad 88 (March), pentad 91 and 93 (April). Pentad 96 marked the end of the rainy season in 1998/9.

Year	Pentad	Phase speed eastward propagation
1979/80	83-85	1.5 m/s
1982/83	71-73	1.5 m/s
1986/87	94-96	1.5 m/s
1987/88	94-96	3.0 m/s
1992/93	81-83	2.5 m/s
1993/94	72-74	4.0 m/s
1998/99	55-57	2.3 m/s

Table 4: Phase speed propagation of OLR anomalies for wet and dry seasons

The longitude-time (Hovmoller) plots of OLR and zonal wind anomalies at 850 and 200hPa reveal alternating positive and negative propagating features. The eastward propagating negative and positive OLR anomalies are evident in most wet and dry years although early in some seasons westward propagation is apparent (e.g. 1998/99). The non-propagating pattern of negative and positive OLR anomaly values could be associated with the ITCZ. Positive and negative zonal wind anomaly values are shown to propagate eastward as well as westward.

Some of the propagating OLR anomalies are seen to originate west of 20°E and continue east to 40°E while others seem to originate between 20-40°E and continue beyond 60°E. It is evident that most large negative OLR anomalies are found east of 30°E while west of 30°E, anomalies are relatively smaller.

This indicates that convection tends to occur over the East coast and the adjacent western Indian Ocean consistent with other studies (e.g. Levey, 1993; Rui and Wang, 1990). Eastward propagating anomalies have different phase speeds in different years. Sometimes the features move slowly then become stationary and resume propagating in the same direction (e.g. 1979/80 and 1993/94).

The longitudes and corresponding pentads of contours (5 to 10  $\text{Wm}^{-2}$ ) of OLR anomalies in the Hovmoller plot are identified, and used to calculate the phase speed from the slope of the propagating features (Mpeta and Jury, 2001). These speeds are listed in Table 4.

During the wet seasons, the eastward propagation speed is slower than the dry seasons imply the correlation remains over Tanzania for longer.

The elevated land surface and low-level meridional monsoon flow may interfere with propagation across Africa. It has been found that areas of strong convection lie just down stream of low-level westerly anomalies (Rui and Wang, 1990, Knutson and Weickmann, 1987).

During the wet years the mean speed of eastward propagating features is 1.5m/s while during the dry years is about 3 m/s. The slower speed of the eastward propagation of OLR anomalies is consistent with the strong convective activities observed to occur over the region during the wet seasons. In contrast, the greater speed of propagation suggests a reduced convection and rainfall experienced during the dry periods. Westward propagating features are found during dry years east of 40°E while during the wet years eastward propagation west of 40°E is clear.

It is evident that the eastward negative OLR anomaly values are consistent with wet spells observed over the study region for both wet and dry years, while the dry spells are linked with positive OLR anomaly values.

It is apparent that the area of negative OLR anomalies (strong convection) correspond well with areas of positive (westerly) anomaly values at 850hPa and negative (easterly) anomaly values at 200hPa level, while strong dry spells are corresponding with positive OLR anomaly values consistent with negative (easterly) anomaly values at 850hPa and positive (westerly) anomaly values at 200hPa level. This seems to agree with the previous observations (e.g. Rui and Wang, 1990, Knutson and Weickmann, 1987, Hendon and Liebmann, 1990).

During the wet years, large negative OLR anomaly values tend to be located between 20 and 35°E with anomalous westerly flow at 850hPa occurring across the continent from 10°E to the tropical western Indian Ocean. This indicates that the convective precipitation over western and southwestern Tanzania may be associated with a flux of moisture from the tropical southeast Atlantic and Congo basin followed by weak easterlies flow from tropical western Indian Ocean.

During dry seasons, large positive OLR anomalies are evident over about 30-50°E as well as negative (easterly) anomalies at 850hPa and positive (westerly) anomaly flow at 200hPa level. Westward propagating features are evident during these periods.

This suggests that the weakened convection over western and southwestern Tanzania is associated with anomalous easterly flow from the tropical western Indian Ocean at 850hPa and westerly anomaly flow at 200hPa level. These results are also consistent with those of monthly composite anomaly evolutions for wet and dry seasons discussed in Chapter 4 of this thesis.

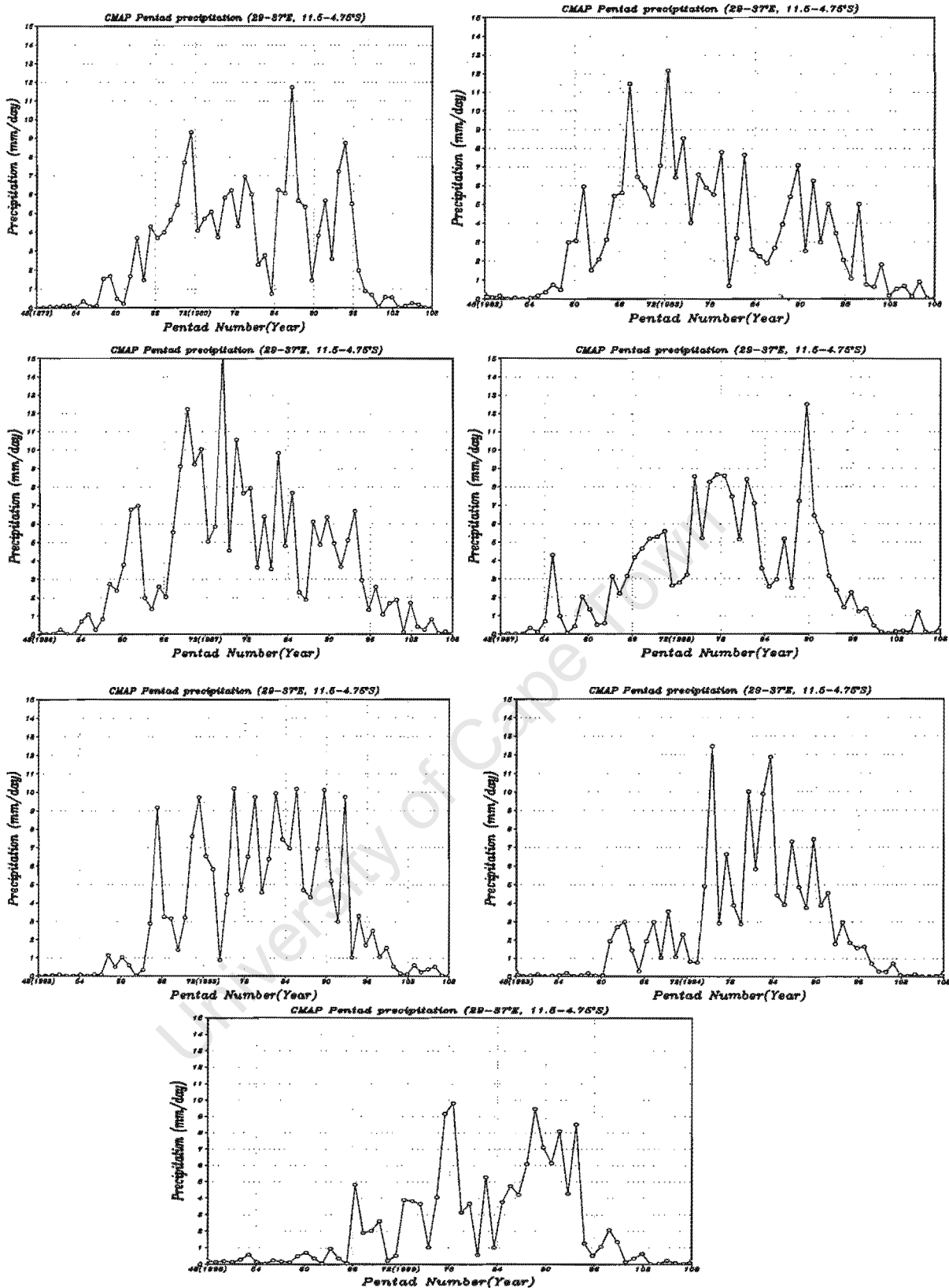
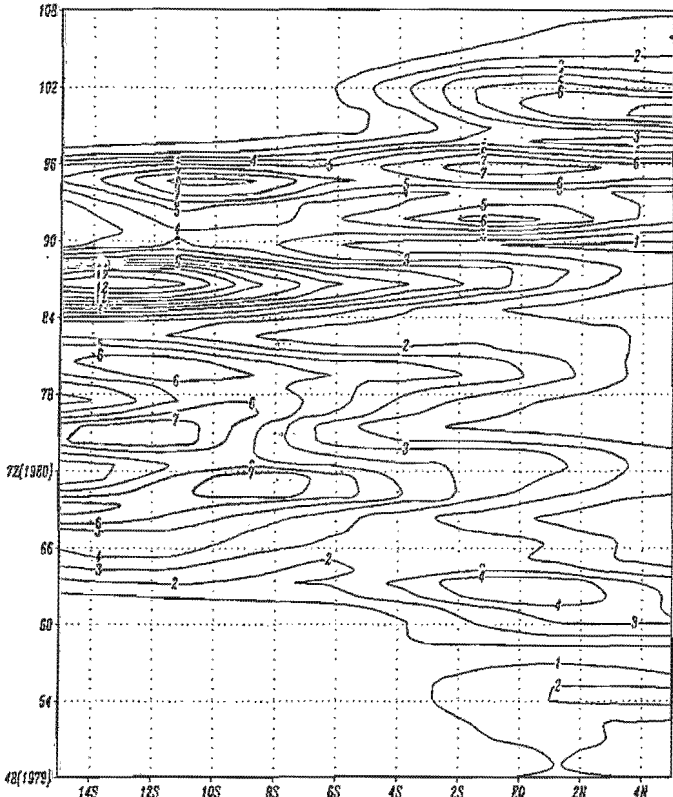
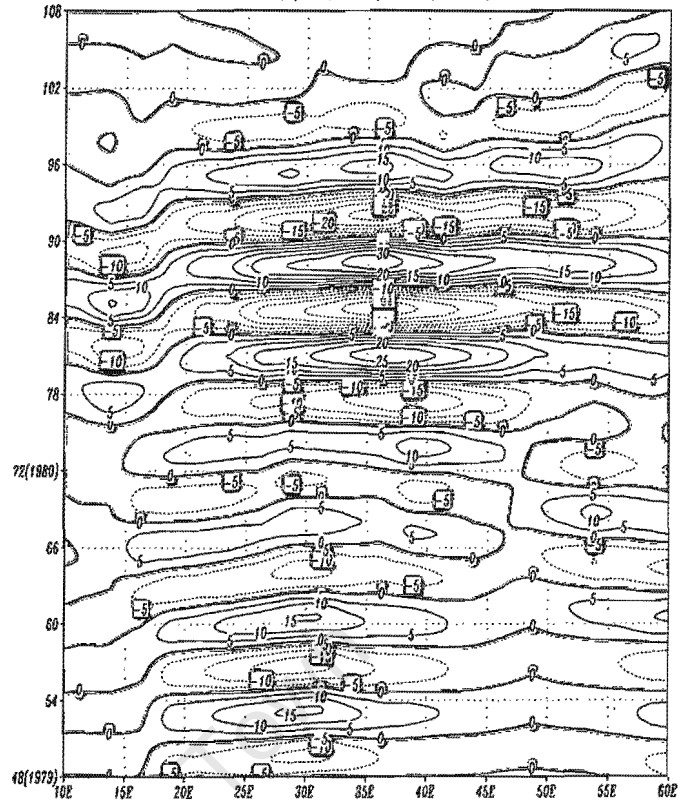
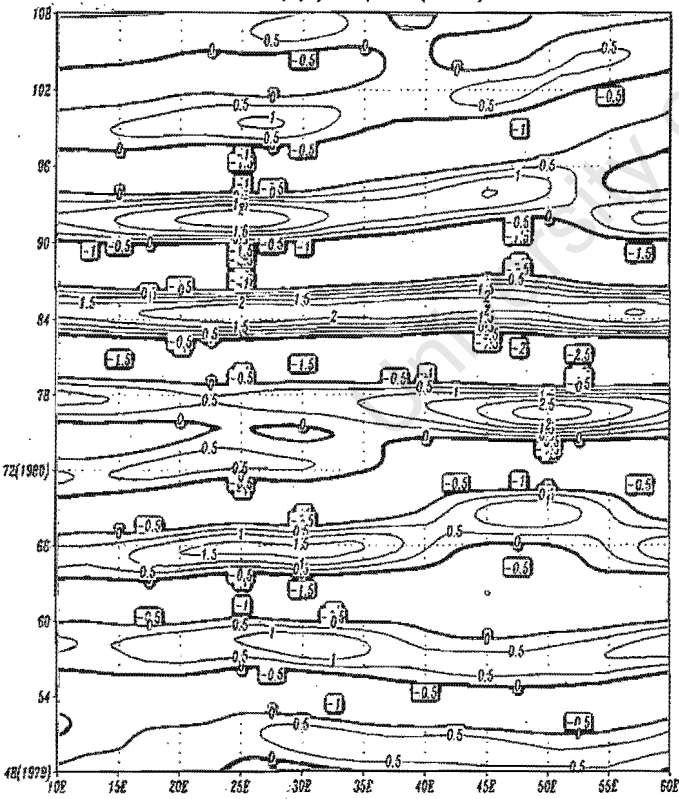


Figure 5.2(a): Area averaged Time series of pentad (5-day) CMAP rainfall over western and southwestern Tanzania

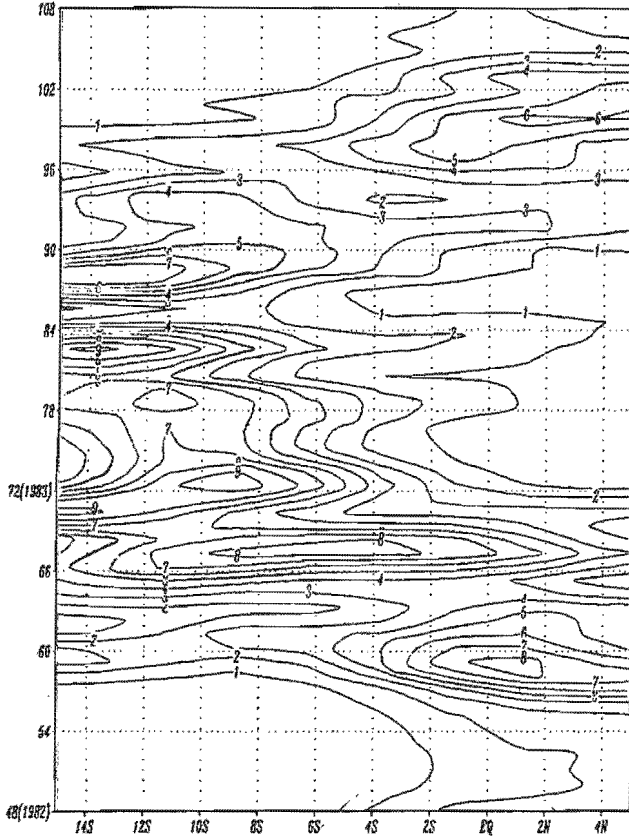
CMAP Pentad precipitation (29-37°E)

OLR ( $W/m^2$ ) 1979/1980 (15-5°S)

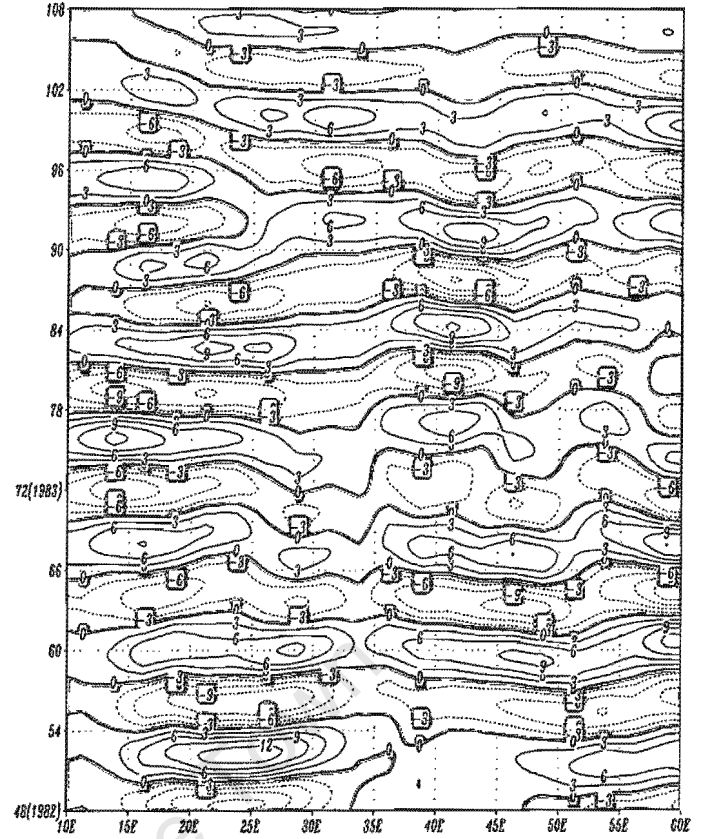
U850(m/s) 1979/1980 (15-5°S)



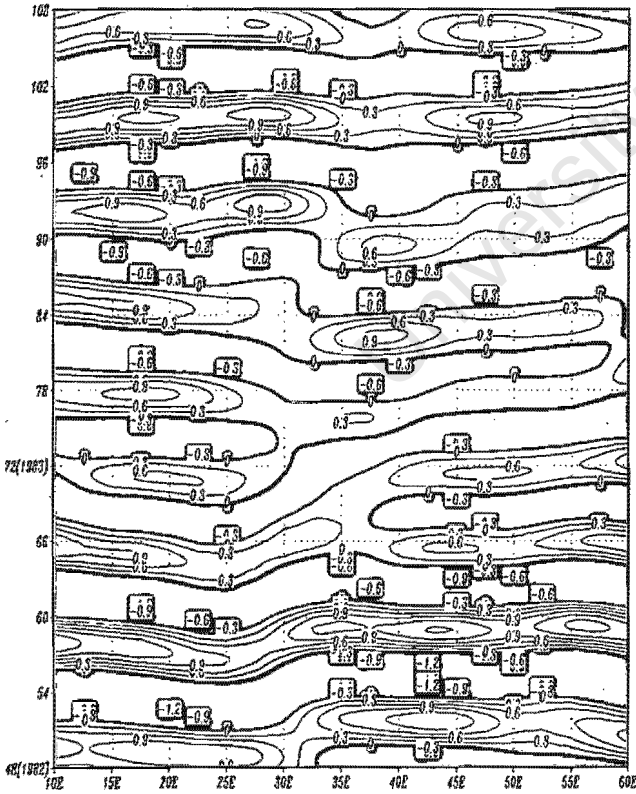
CMAP Pentad precipitation (29-37E)



OLR ( $W/m^2$ ) 1982/1983 (15-5'S)



U850(m/s) 1982/1983 (15-5'S)



U200(m/s) 1982/1983 (15-5'S)

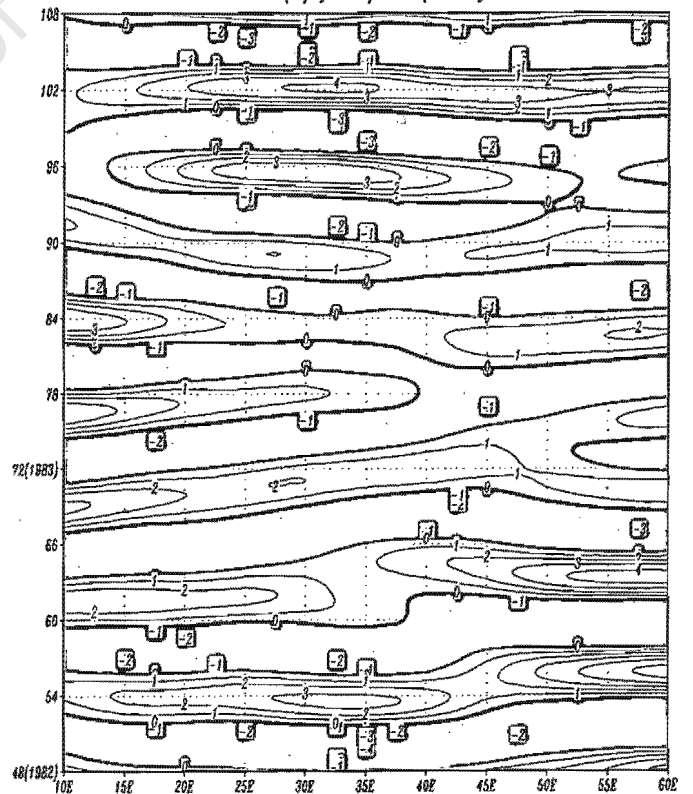
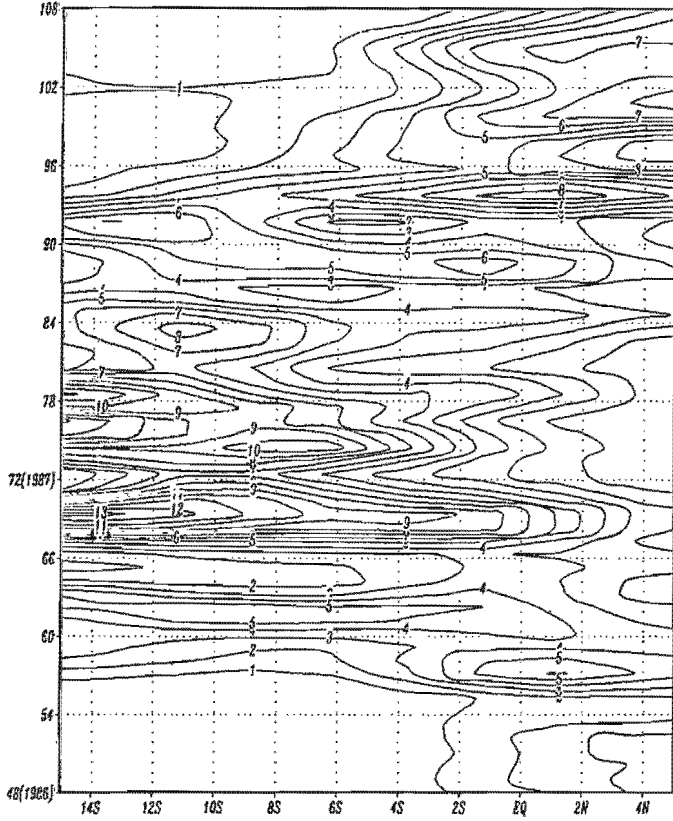
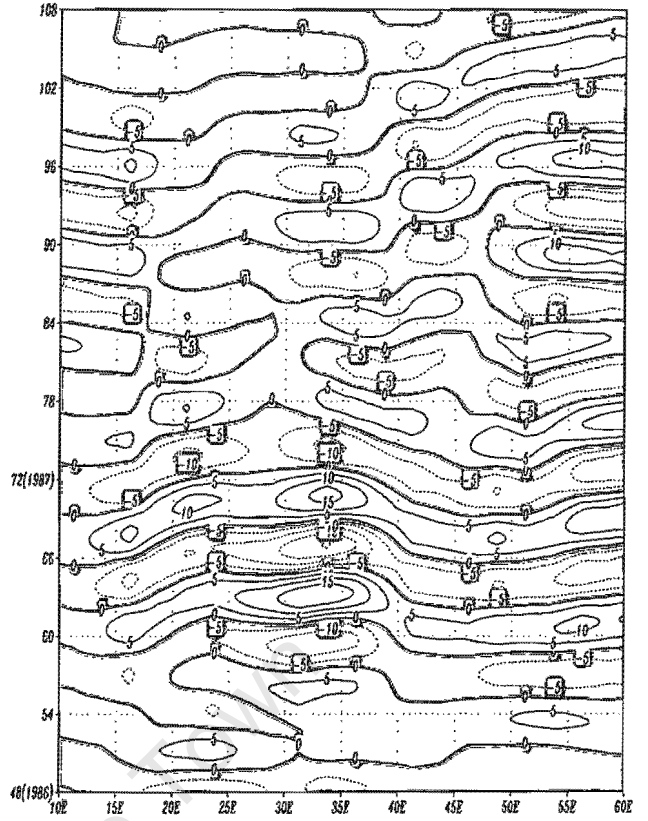


Figure 5.2(c): same like fig.5.2(b) but for 1982/83

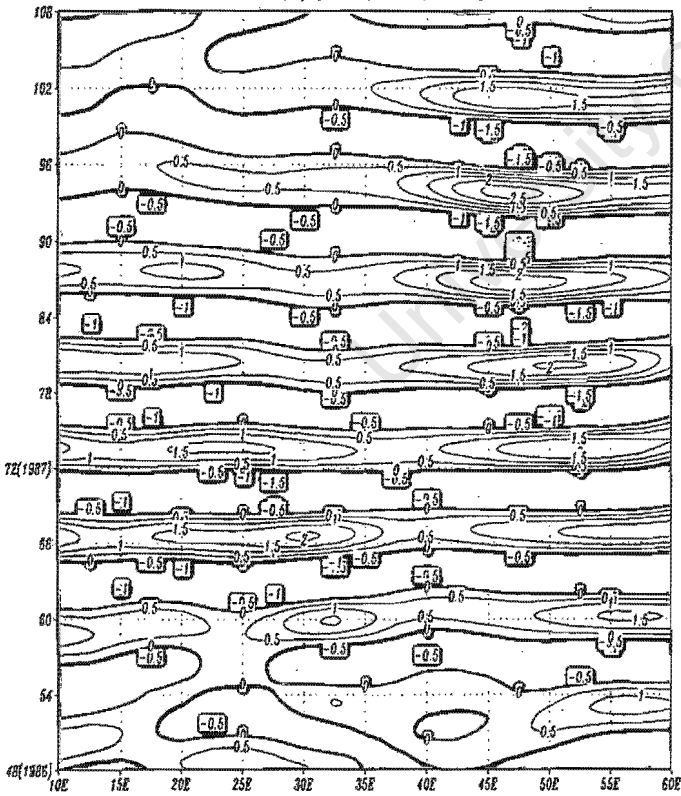
CMAP Pentad precipitation (29-37°E)



OLR ( $W/m^2$ ) 1986/1987 (15-5°S)



U850(m/s) 1986/1987 (15-5°S)



U200(m/s) 1986/1987 (15-5°S)

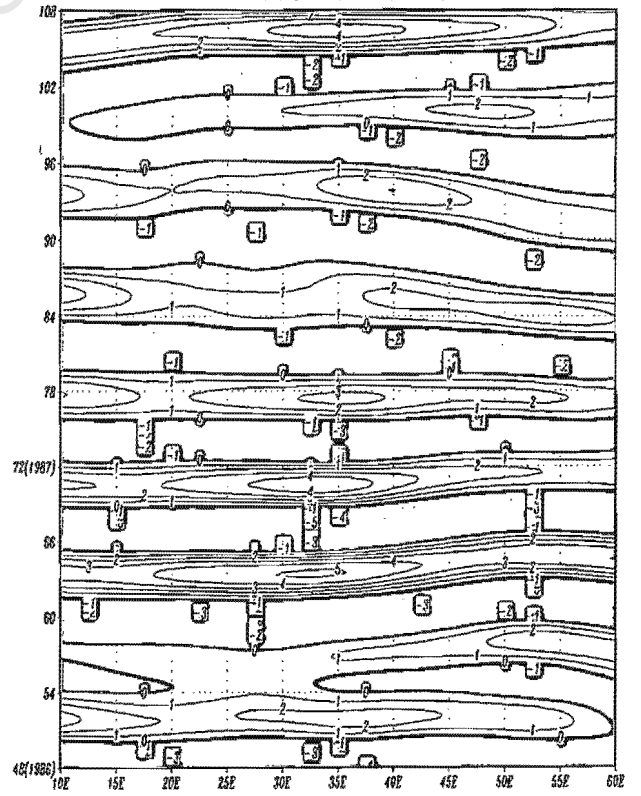
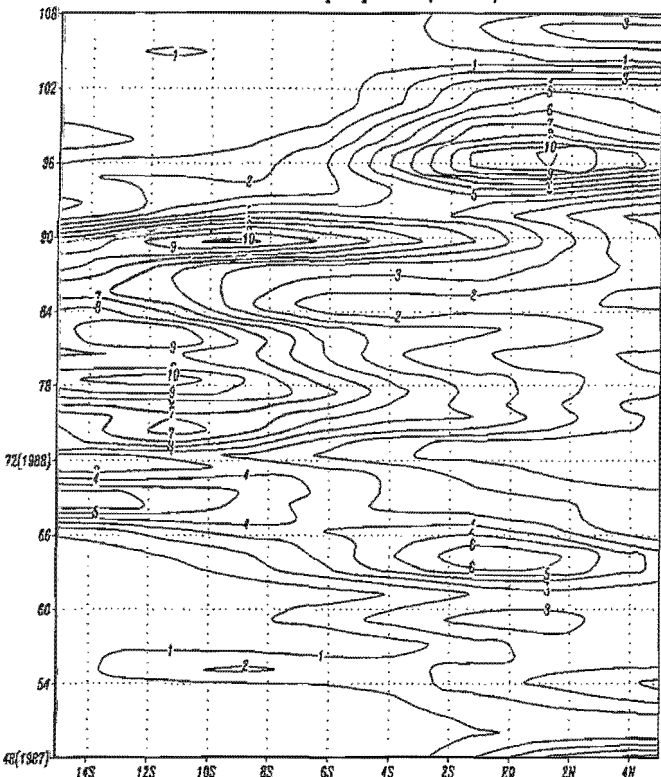
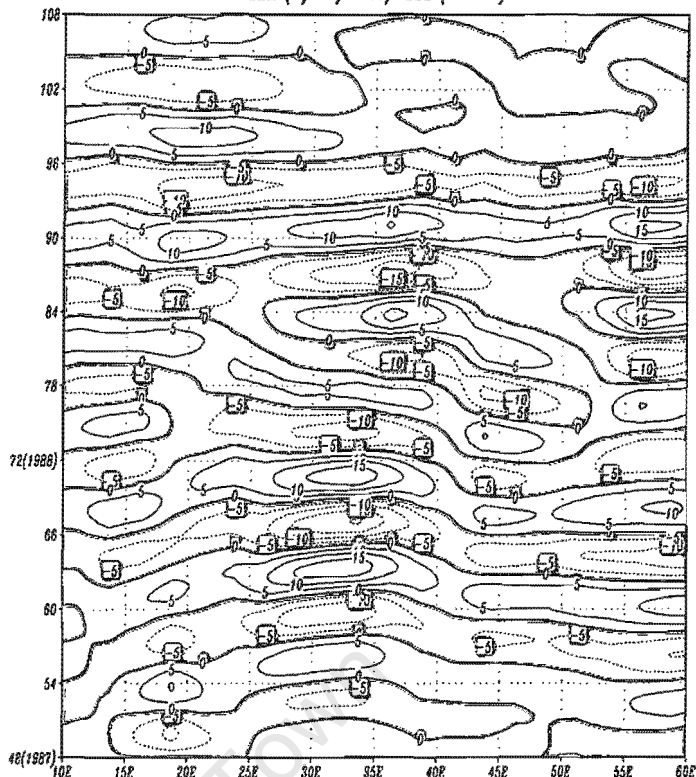


Figure 5.2(d): same like fig. 5.2(c) but for 1986/87

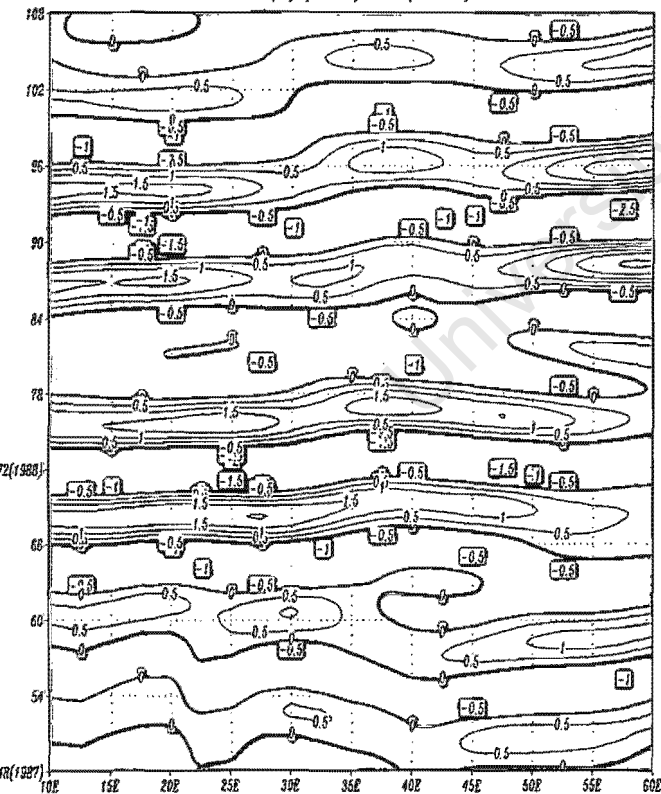
CMAP Pentad precipitation (29-37E)



OLR ( $W/m^2$ ) 1987/1988 (15-5°S)



U850(m/s) 1987/1988 (15-5°S)



U200(m/s) 1987/1988 (15-5°S)

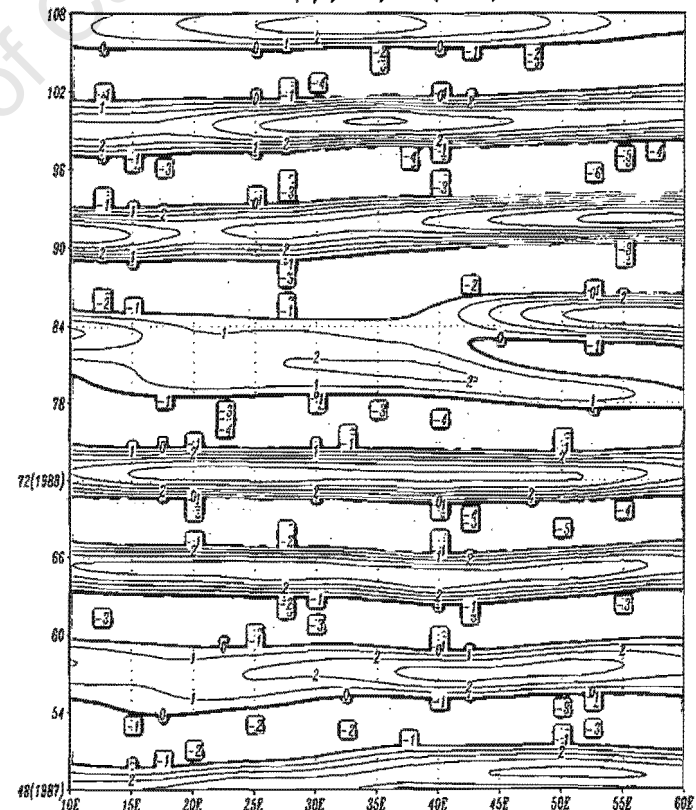


Figure 5.2(e): for 1987/88

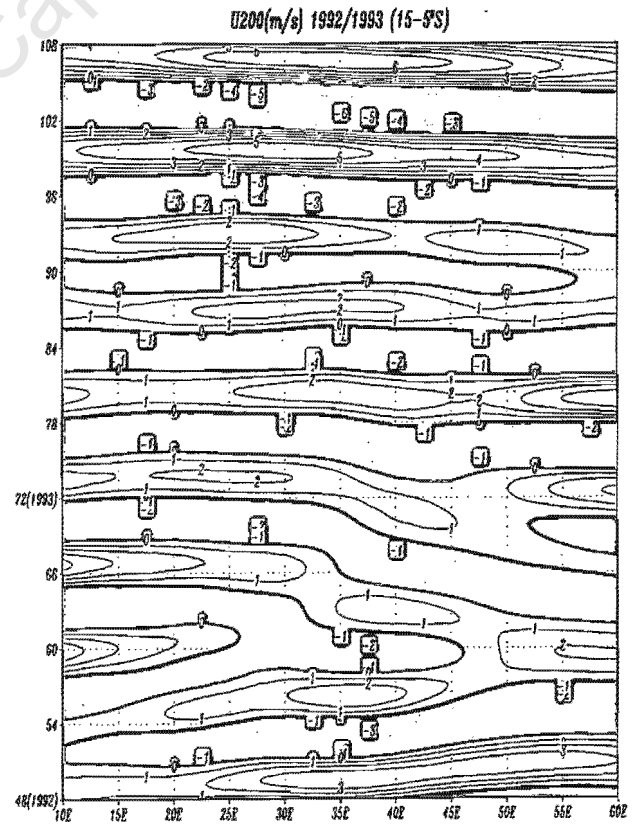
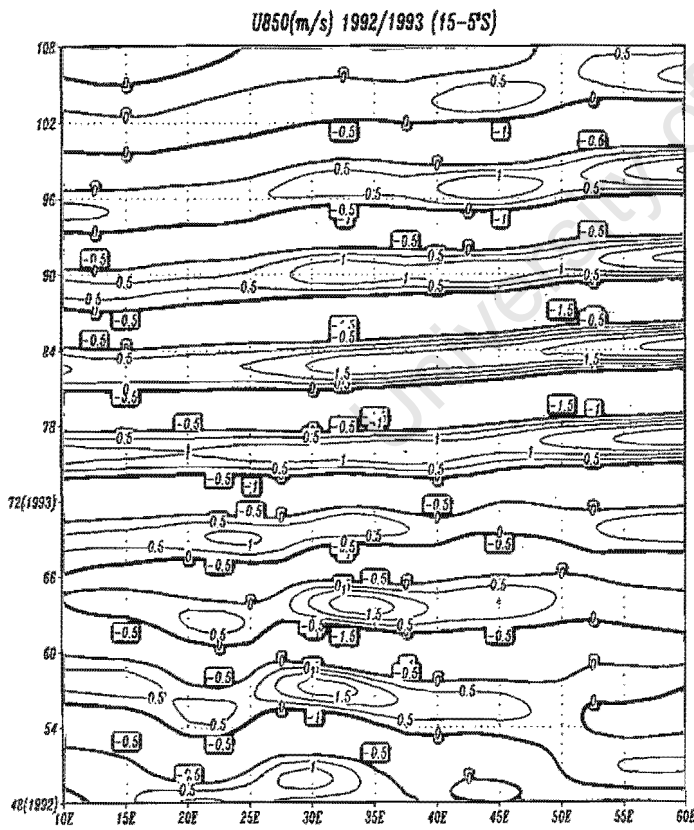
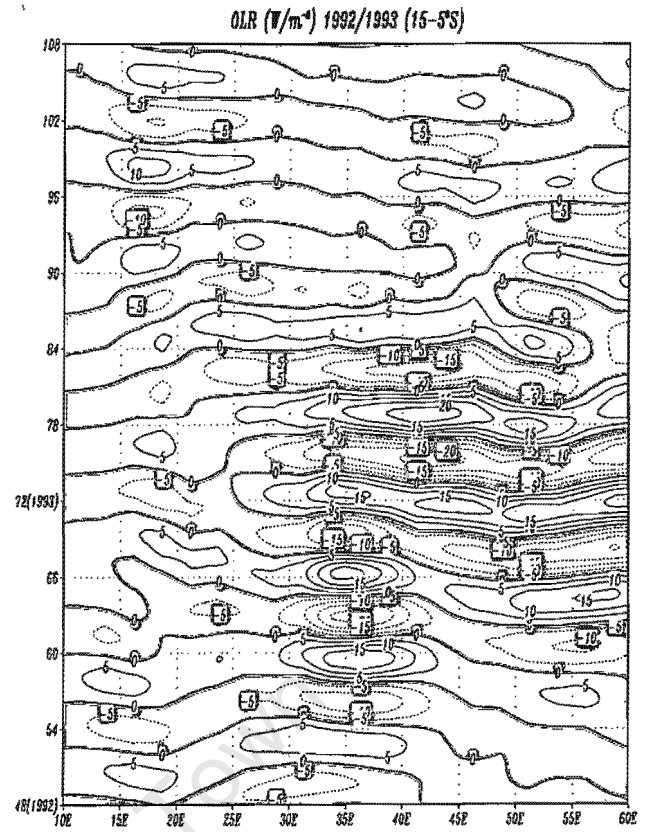
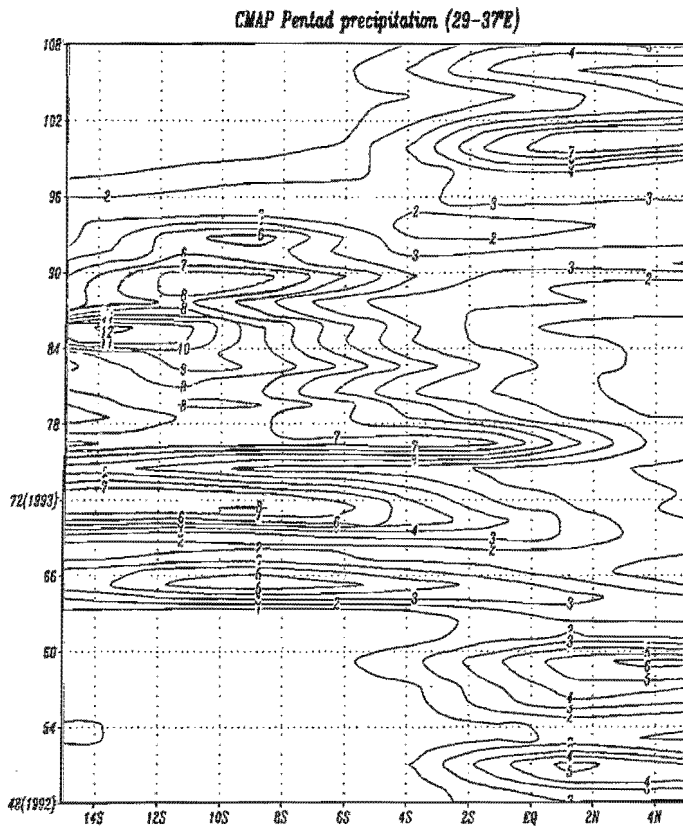
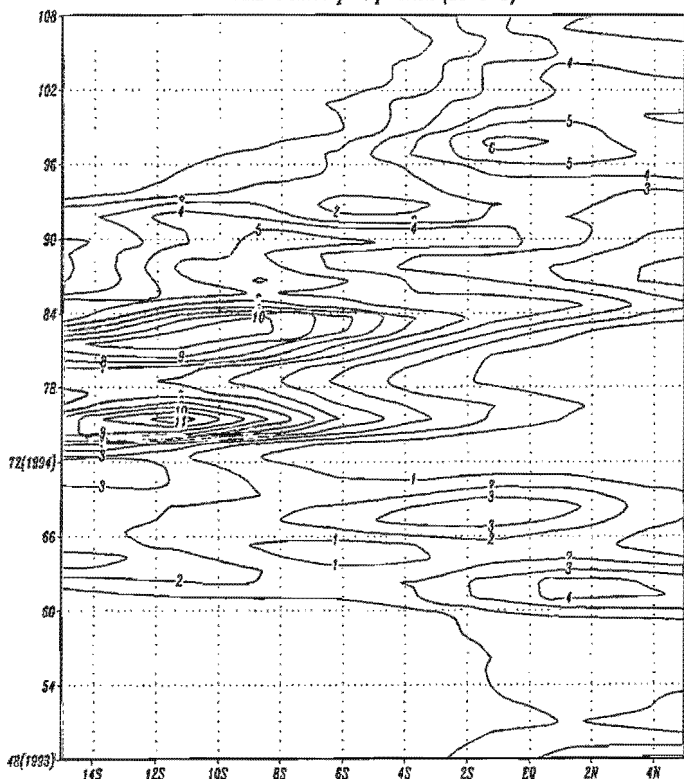
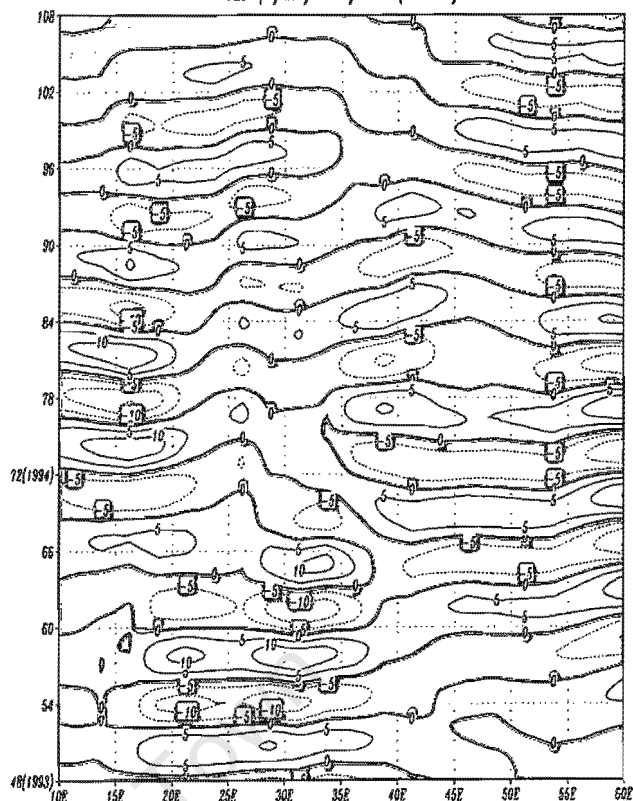


Figure 5.2(f): for 1992/93 season.

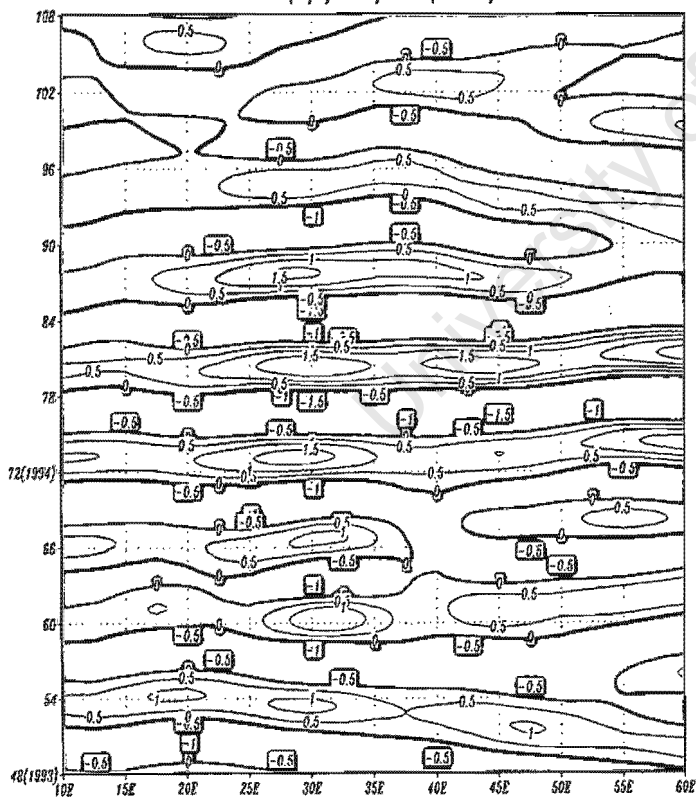
CMAP Pentad precipitation (29-37E)



OLR ( $\text{W/m}^2$ ) 1993/1994 (15-5°S)



U850(m/s) 1993/1994 (15-5°S)



U200(m/s) 1993/1994 (15-5°S)

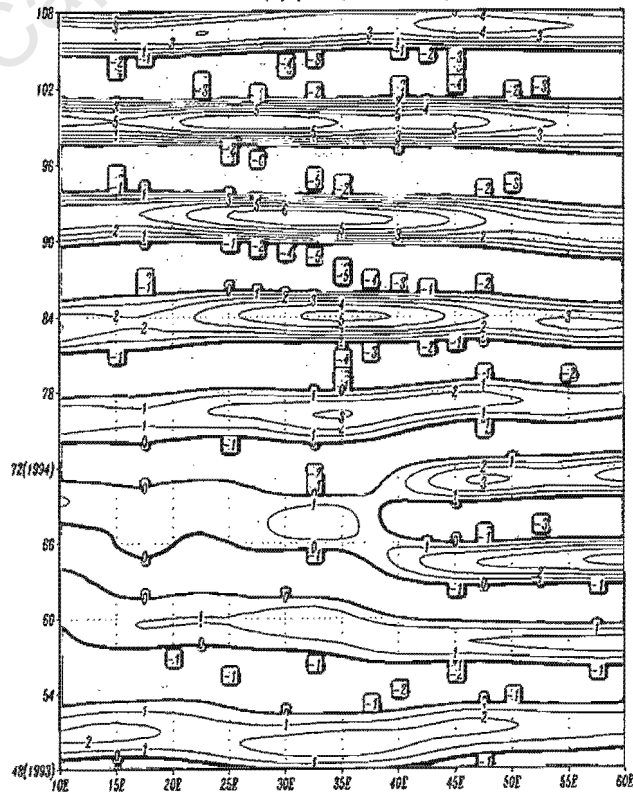


Figure 5.2(g): for 1993/94 season

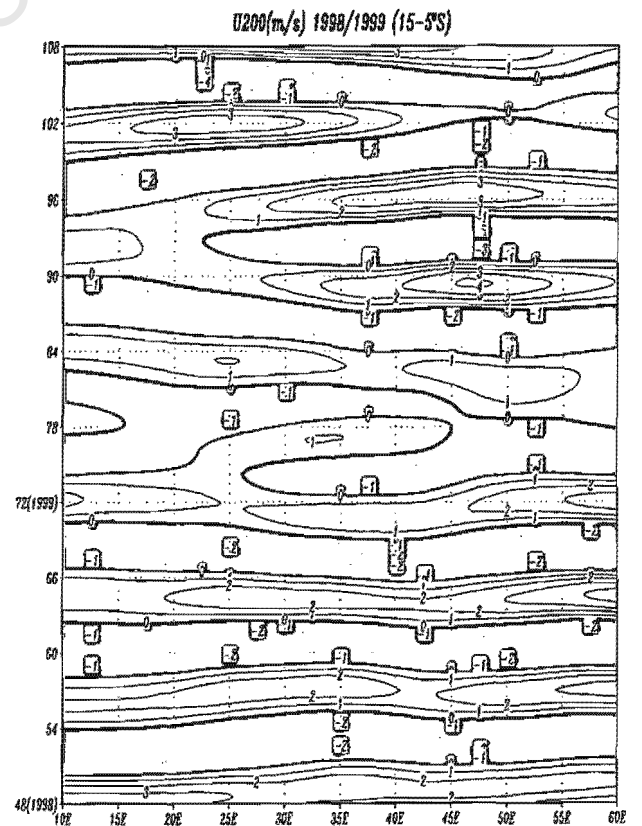
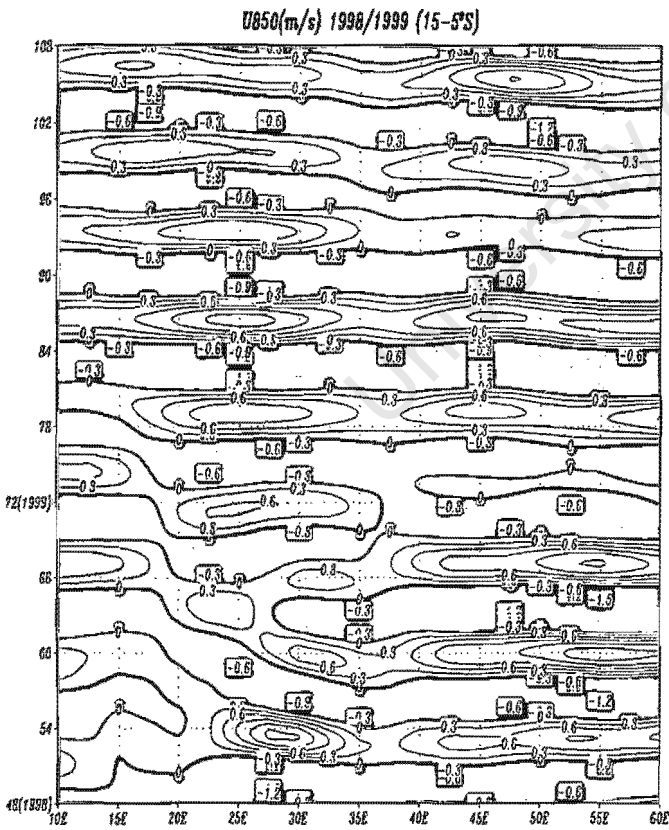
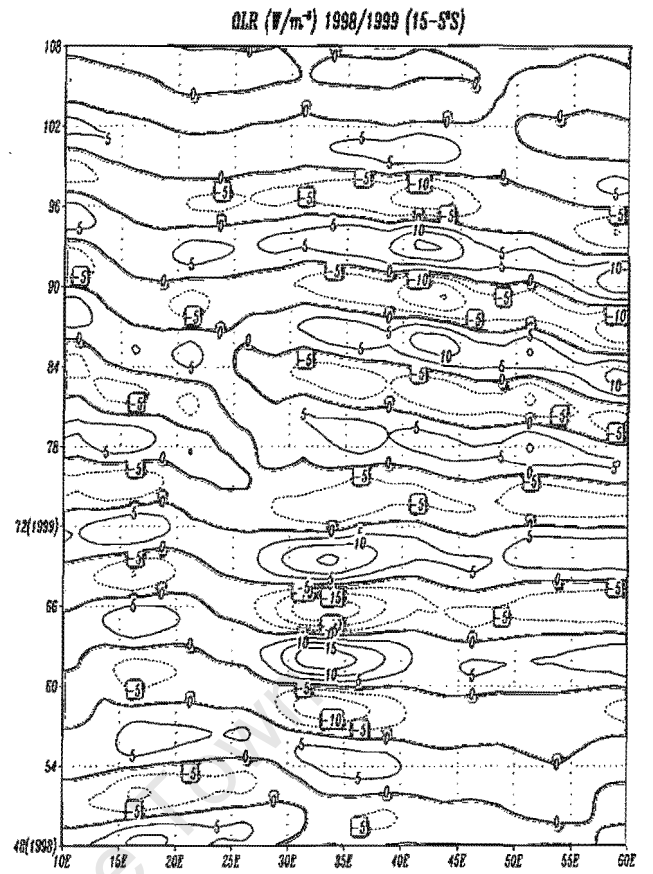
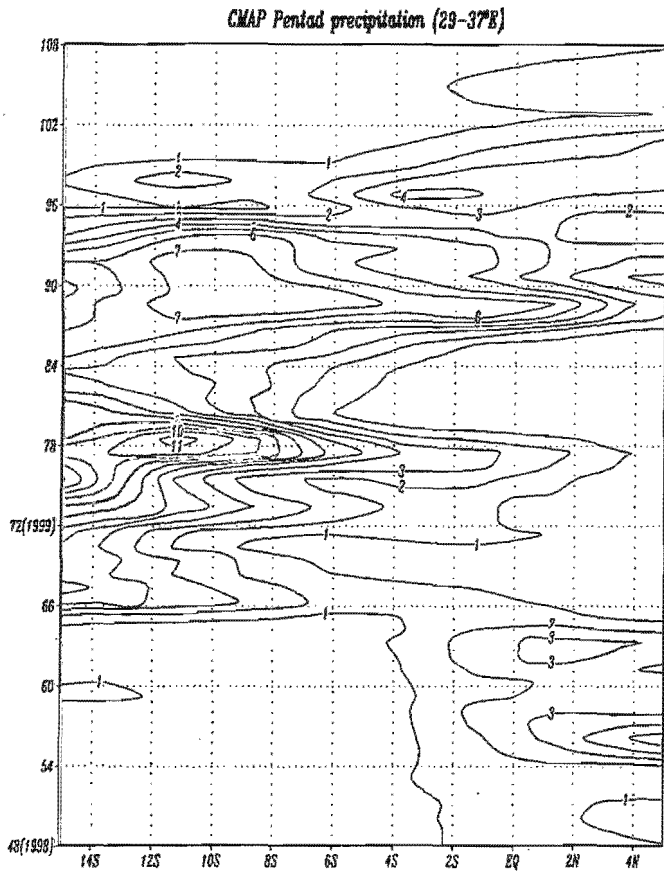


Figure 5.2(h): same like fig.5.2(b) but for 1998/99 season

## **CHAPTER 6: Summary and conclusions**

In this thesis, potential linkages between the monsoon regions of Indian and Atlantic Oceans and seasonal rainfall variability in western and southwestern Tanzania are investigated. This region has one prolonged rainy season (uni-modal) from the November to April, June to September is the dry season while October and May are transition months.

A number of different topographic features, soil and vegetation characteristics, lake effects (local water bodies), local wind regimes and interactions associated with meso-scale circulations and large-scale weather systems may also affect the various parts of the region. Kigoma and Sumbawanga over the Western area report higher rainfall mainly due to moisture advection from Congo basin coupled with Lake Tanganyika effects. Mbeya and Songea over southwestern Tanzania may receive increased rain due to orographic effects associated with the mountainous ranges of Livingstone, Ufipa and Lake Malawi. However, some stations like Iringa may receive less rain due to rain shadow effects.

In Chapter 3, the mean monthly climatological patterns for various fields (i.e. sea surface temperature (SST), winds, latent heat fluxes, outgoing long wave radiation (OLR), velocity potential and divergent wind, moisture flux and precipitation) are discussed. It is evident that the convective activity over the study region is associated with the movement of the ITCZ as it moves south and north of the equator with overhead sun. Moisture tends to converge in the vicinity of this ITCZ.

In Chapter 4, the mean monthly composite anomaly evolutions for the wet and dry years are investigated. It is evident from this chapter that the SST anomalies do not appear to show an obvious influence on the rainfall anomalies over western and southwestern Tanzania. It may be that atmospheric circulation anomalies which cause the rainfall variability over the region, also drive the changes in SST.

The results from this chapter reveal that during the wet years, lower tropospheric westerly anomalies build up over the tropical southeast Atlantic Ocean and over the Congo basin while easterly anomalies build up over the tropical western Indian Ocean. Associated with these anomaly flows are the cyclonic anomaly over Angola, which acts to enhance westerly flow from these regions to Tanzania while the anticyclonic anomaly over central Indian Ocean tends to weaken the mean easterly wind flow from this ocean towards East Africa. Although modulations to the Angola low led to enhanced westerlies and convergence early in the season, in February and March of the wet seasons, an anticyclonic anomaly develops over this region which acts to weaken the westerly mean flow from the tropical southeast Atlantic across northern Angola towards the Congo basin into Tanzania.

During the wet years, positive latent heat flux and negative OLR anomalies over the region are evident which indicate the increased evaporation and convection consistent with significant rainfall experienced during the wet seasons. At 200hPa, the wet composite reveals anomalous strong easterlies build up over western Indian Ocean, which indicates a favourable condition for low-level convergence and convection since it implies upper level divergence.

This upper level feature also suggests a stronger Walker circulation consistent with rainfall increase during these seasons. The velocity potential and divergent wind anomaly reflects strong low-level convergence over Tanzania at 850hPa with associated upper level divergence during the wet seasons.

During the dry years, lower tropospheric easterly anomalies build up over the central and western Indian Ocean, and at upper levels strong westerly anomalies build up over the tropical southeast Atlantic Ocean. The strong upper level westerly anomalies implies a weaker Walker circulation and are unfavourable for low-level ascent and convection since it indicates upper level convergence and subsidence.

During the dry seasons a cyclonic anomaly over the tropical southeast Atlantic and anticyclonic anomaly over southwestern Indian Ocean are evident. These circulations weaken the westerly and mean easterly flow across the tropical southern African regions and reduce the flux of moisture into the region from the nearby oceans. The cyclonic anomaly over the tropical central Indian Ocean acts to weaken the northeast monsoon flow across the western Indian Ocean. Positive OLR and negative latent heat flux anomalies are apparent during the dry seasons which reflect reduced evaporation and convection consistent with rainfall decrease during these seasons. Velocity potential and divergent wind anomaly show a strong low-level divergence over Tanzania at 850hPa and upper level convergent anomaly.

In Chapter 5, the Intra-seasonal rainfall variability for the wet and dry years over western and southwestern Tanzania was investigated. During wet seasons rains began earlier in mid October and withdraw later, sometimes in May to early June, whilst the dry seasons, rains commence later and withdraw early (Table 3). During wet years, rains are evenly distributed over the region throughout the season while for the dry seasons, an extended dry period occurs early after the onset of the rains.

Agrarian-based communities have developed in the monsoon regions because of abundant solar radiation and precipitation, the two essential ingredients for successful agriculture. The agricultural practices over Tanzania have traditionally tied strictly to the annual cycle of monsoons, although the regularity of the monsoon would seem to be ideal for agricultural communities over the region; any small variations in the timing and quality of seasonal rainfall have the potential for significant consequences, such as droughts and floods.

Economic development in Tanzania depends largely on the climate-driven agricultural sector, which in turn is highly vulnerable to variability in rainfall amount and distribution. Accurate seasonal, inter-annual and intra-seasonal climate monitoring and forecasting could therefore contribute to improved planning and the management of climate sensitive activities, involving agricultural and water resources, hydroelectric power supply and tourism. It is hoped that this thesis contributes towards better understanding of the inter annual and intra-seasonal variability of rainfall over Tanzania which will assist in improving forecasting.

## References

- Alusa, A.L and Mushi, M.T, 1973:** A study on the onset, duration and cessation of the rains in East Africa, Reprints, *International Meteorological Meeting, Nairobi, 1974, pp.133-140.*
- Allan, R.J, Lindesay, J.A and Reason, C.J.C, 1995:** Multi-decadal in the climate system over Indian Ocean region during the austral summer. *J.Climate, 8 1953-1873*
- Anyamba, E.K, 1983:** On the monthly Mean lower tropospheric circulation and anomalous circulation during the 1961/62 floods in East Africa. M.Sc Thesis, Department of Meteorology, University of Nairobi, pp. 240
- Asnani, G.C, 1993:** Tropical Meteorology. Noble Printers, Pune India, pp. 1202
- Atwoki, K, 1975:** A factor analytic approach for the delimitation of the rainfall regions of Uganda, *Eas. African Geogr. Rev, 13, 9-36.*
- Barring, 1988:** Regionalization of daily rainfall in Kenya by means of common factor analysis, *J. Climatol. , 8, 371-389.*
- Behera, S.K and Yamagata, T, 2001:** Subtropical SST dipole events in the southern Indian Ocean. *Geophys. Res. Lett., 28, 327-330.*
- Cadet, D.L, 1985:** The southern Oscillation over the Indian Ocean. *J.Climate, 5,189-212.*

**Camberlin, P, 1995:** June-September rainfall in northeastern Africa and atmospheric signals over the tropics: A zonal perspective. *Int.J.Climatology*, **15**, 773-783.

**Camberlin, P. and Wairoto, J.G, 1997:** Intraseasonal wind anomalies related to wet and dry spells during the long and short rainy seasons in Kenya, *Theor. Appl. Climatol.* **58**, 57-69.

**Charney, J.G, 1975:** Dynamics of deserts and drought in the Sahel. *Quart. J.Roy.Meteor.Soc.*, **101**, 193-202.

**Charney, J.G and Shukla J, 1981:** Predictability of monsoons. In *Monsoon Dynamics*, Lighthill M.J.Pearce RP (eds). Cambridge University Press, pp, 99-109.

**D'Abreton, P.C and Lindesay, J.A, 1993:** Water vapour transport over southern Africa during wet and dry early and late summer months. *Int.J. Climatology*, **13**,151-170.

**East African Meteorological Department (EAMD), 1963;** Climate Seasons of East Africa, East African Meteorological Department Report No.8, 4pp.

**Findlater J, 1971:** Mean monthly airflow at low levels over the western Indian Ocean. *Geophysical Memoirs.* **115**, HMSO, London.

**Florenchie, P, Lutjeharms, J.R.E, Reason C.J.C, Masson S and Rouault, M, 2003:** The source of Benguela Ninos in the South Atlantic Ocean. *Geophys. Res. Lett.* , **30**,10,1505,doi: 10.1029/2003GL017172.

**Folland, C.K, 1983:** Regional –Scale interannual variability of climate. A northwest European perspective. *Met. Mag.*, **112**, 163-187.

**Griffiths, J.F, 1959:** Climatic zones of East Africa. *E.Afr. Agric. J.*, **23(3)**, 179-185.

**Hastenrath S, Nicklis A and Greischar L, 1993.** Atmospheric hydrospheric mechanisms of climate anomalies in the western equatorial Indian Ocean. *J.Geophys Res*, Vol.**98**, 20219-20235

**Hendon H.H and Liebmann, G, 1990:** The intraseasonal (30-50) oscillation of the Australian summer monsoon. *J.Atmos. Sci.* **47(24)**: 2904-2923.

**Hirst, A.C and Hastenrath, S, 1993:** Atmosphere-ocean mechanisms of climate anomalies in the Angola tropical Atlantic sector. *J.Phys. Oceanogr.*, **13**, 1146-1157.

**Holland, G.J, 1986:** Interannual variability of the Australian summer monsoon at Darwin; 1952-82. *Mon.Wea.Rev.* **114**, 594-604.

**Hyden, L, 1999:** Meteorological Droughts and rainfall variability in the Lesotho Lowlands. M.Sc. Thesis. Royal Institute of Technology Stockholm, Sweden.

**Janowiak, J.E, 1988:** An investigation of interannual rainfall variability in Africa. *J.Climate*, **1**, 240-255.

**Johnson, D.H and Morth, H.T, 1961:** Forecasting research in East Africa (E.A.M.D). *Memoirs*, **3**, No.9, 57 pp.

**Jury, M.R, 1992:** A climatic dipole governing the interannual variability of convection over the SW Indian Ocean and SE Africa region. *Trends in Geographical Research*, **1**, 165-172.

**Jury, M.R, McQueen, C.A and Levey, K.M, 1994:** SOI and QBO signals in the African region. *Theor.Appl.Climatol.*, **50**, 103-115.

**Jury, M.R, Parker, B.A, Raholijao, N and Nassor, A, 1995:** Variability of summer rainfall over Madagascar: climatic determinants at interannual scales. *Int.J.Climatology*, **15**, 1323-1332.

**Kabanda, T.A, 1995.** Seasonal and Intra-seasonal dynamics and precursors of rainfall over northern Tanzania. M.Sc. thesis Department of Oceanography, University of Cape Town. South Africa.

**Kabanda, T.A and Jury M.R, 1999;** Interannual variability of short rains over Northern Tanzania. *Climate Research*. **13**; 231-241.

**Kalnay E, Kanamitsu M, Kistler R, Collins W, Deaven D, Gandin L, Iredell M, Saha S, White G, Woolen J, Zhu Y, Leetmaa A, Reynolds R, Chelliah M, Ebisuzaki W, Higgins W, Janowiak J, Mo KC, Popelewski C, Wang CJ, Jenne R, and Joseph, D, 1996;** The NCEP/NCAR 40-years reanalysis project. *Bull. Am. Meteorol Soc.*, **77**: 437-471.

**Khromov, S.P, 1957:** The geographical distribution of the monsoon. Petermanns Geogr.Mitt. **101**, 234-237.

**Knutson, T.R and Weickmann, K.M, 1987:** 30-60 day atmospheric-circulations, composite life cycles of convection and circulation anomalies. *Mon. Weather Rev.* **115**: 1407-1436.

**Krishnamurti, T.N and Bhalme H.H, 1976:** Oscillation of monsoon system, part1: Observational aspects; *J.Atmos.Sci.* **33**, 1937-1954.

**Lamb, P.J and Pepler, R.A, 1992:** Further case studies of tropical Atlantic surface Atmospheric and Oceanic patterns associated with sub Saharan drought, *J. of Clim.* , **5**, 476-488.

**Levey, K.M, 1993:** Intraseasonal oscillations of convection over southern Africa. MSc. Thesis, University of Cape Town, Cape Town, South Africa. 226pp.

**Madden, R.A and Julian, P.R, 1971:** Determination of 40-50 day oscillation in the zonal wind in Tropical Pacific. *J.Atmos.Sci.*, **28**, 702-708.

**Madden, R.A and Julian, P.R, 1972:** Description of global-scale circulation cell in the tropics with a 40-50 day period. *J.Atmos.Sci.* **29**, 1109-1123.

**Makarau, A, 1995:** Intra-seasonal oscillatory models of the southern Africa summer circulation. PhD thesis, University of Cape Town, South Africa, 321 pp.

**Mason, S.J and Tyson P.D, 1992:** The modulation of sea surface temperature and rainfall associations over southern Africa with solar activity and the quasi-biennial oscillation. *Journal of Geographical Research* **97**: 5847-5856.

**Matarira, C.H and Jury, M.R, 1992** Contrasting meteorological structure of intraseasonal wet and dry spells in Zimbabwe, *J.Climatol.*, **12**, 165-176.

**Minja, W.S.M, 1982:** The weather anomalies during the northern summer of 1972 and 1978. In proceedings of the technical conference on climate. WMO / OMM. No.596. World Meteorological Organisation, Geneva pp.195-208

**Mpeta, E. and Jury, M, 2001;** Intra-seasonal convection structure and evolution over tropical East Africa. *Climate research vol.17*: 83-92.

**Mhita M.S, 1990;** The analysis of rainfall data for agriculture in Tanzania; Tanzan. Met.Res.Pub. (T.M.R.P), **2**(90), pp.61

**Mukabana, J.R. and Pielke, R.A, 1996;** Investigating the influence of synoptic-scale monsoonal winds and mesoscale circulations on diurnal weather patterns over Kenya using a mesoscale numerical model. *Mon.Wea.Rev.* **124**,224-243.

**Murakami T, Long-Xun C, Xie A.N and Shretha, M.L, 1986:** Eastward propagation of 30-60 day perturbations as revealed from outgoing longwave radiation data. *J. Atmos.Sci.* **43**(10): 961-971.

**Murakami, T, 1988:** Intraseasonal atmospheric teleconnection patterns during the northern hemisphere winter. *J.Clim.* **1:** 117-131.

**Murakami, T and Sumathipala, W.L, 1989.** Westerly bursts during the 1982/83 ENSO, *J.Climate*, **2**, 71-85.

**Mutai, C.C, Ward, M.N and Colman, A.W, 1998.** Towards the prediction of the East Africa short rains based on sea surface temperature- atmosphere coupling. *Int.J.Climatol.* **18:** 975-997

**Nakamura, K, 1968:** Equatorial westerlies over East Africa and their climatological significance, Tokyo Metropolitan University *Geographical Reports*, **3**, 43-61.

**Nassor, A, 1994:** Monsoon surges, tropical cyclones and extreme rainfall events in NW Madagascar. MSc thesis, University of Cape Town. South Africa.

**Nicholson, S.E and Chervin, R.M, 1983:** Recent rainfall fluctuations in Africa interhemispheric teleconnections. Variations in the Global Water budget, Eds: A street- Perrott, M.Beran and R.Rateliffe, D.Reidel, Dordrecht, 221-238.

**Nicholson, S.E and Nyenzi, B.S, 1990.** Temporal and spatial variability of sea surface temperature in the tropical Atlantic and Indian Oceans. *Archives for Meteorology, Geophysics and Bioclimatology, Series A* **42:** 1-17.

**Nicholson, S.E, 1996a:** A review of climate dynamics and climate variability in Eastern Africa. In the limnology, climatology and Paleoclimatology of the East African lake, T.C.Johnson and E. Odada (Eds), Gordon and Breach, Amsterdam, 57-78.

**Nieuwolt, S, 1978:** Rainfall and drought frequencies in East Africa, *Erkunde* **32**: 81-88.

**Nigam S and Shen H, 1993;** Structure of oceanic and atmospheric low-level variability over the tropical Pacific and Indian Oceans. Part1: COADS observations. *Bull. Am. Meteorol. Soc.* **74**: 657-676.

**Nyenzi, B.S, 1988:** Equatorial zonally moving disturbances which contributed to the East African long rains of March to May 1979, in WAMEX Related Research and Tropical Meteorology in Africa, *WMO, TMRP, Geneva*, **28**, 270-271.

**Nyenzi, B.S, 1990:** Inter-annual variability in the Atlantic and Indian Oceans and its relationship to the southern oscillations. TOGA scientific oscillation Conference Hawaii, U.S.A.

**Nyenzi, B.S, 1992:** An analysis of interannual variability of rainfall over East Africa. *J.African.Meteor.Soc.* **1**,57-79.

**Ogallo L.J, 1988:** Relationships between Seasonal rainfall in East Africa and southern oscillation. *J.Climatology*.**8**. 31-43.

**Ogallo L.J, 1989:** The spatial and temporal patterns of the East African Seasonal rainfall derived from Principal component Analysis. *J. Climatology*. **9**. 145-167.

**Okoola, R.E, 1996:** Space-Time characteristics of the ITCZ over equatorial Eastern Africa during anomalous rainfall years. PhD. Dissertation, Dept. of Meteorology, University of Nairobi, Kenya.

**Park C and Schubert S.D, 1993:** Remotely forced intraseasonal oscillations over the tropical Atlantic. *J.Atmos. Sci.***50:** 89 -103.

**Ramage, C.S, 1971:** Monsoon Meteorology. Academic Press, 391 pp.

**Ramage, C.S and Raman, C.R.V, 1972:** Meteorological Atlas of the International Indian Ocean Expedition Vol.2: Upper Air, National Science Foundation, Washington, D.C. , NSF-IIOE-3, pp. 97 (Charts No.1-21)

**Reason, C.J.C and Mulenga, H, 1999;** Relationship between South African rainfall and SST anomalies in the Southwest Indian Ocean. *Int.J.Climatol.* **19.** 1652-1673.

**Reason, C.J.C, Allan, R.J, Lindsay, J.A and Ansell, T.J, 2000;** ENSO and climatic signals across Indian Ocean basin the global context: Part 1, Inter-annual composite patterns. *Int.J.Climatol.***20.** 1285-1327.

**Reason, C.J.C, 2001:** Subtropical Indian Ocean SST dipole events and southern African rainfall; *Geographical Res. letters*, vol. **28**, 2225-2227.

**Ropelewski, C.F and Halpert, M.S, 1987:** Precipitation patterns associated with El Nino/ Southern Oscillation. *Mon.Wea.Rev.* **115**, 1606-1626.

**Rui, H and Wang, B, 1990;** Development characteristics and Dynamic structure of Tropical Intraseasonal convection Anomalies, *J.Atmos.Sci.*, **47**, 357-379.

**Saji, N.H, Goswami, B.N, Vinayachandran P.N and Yamagata, T, 1999.** A dipole mode in the tropical Indian Ocean. *Nature*, **401**, 360-363.

**Semazzi, F.H.M, Mehta, V and Sud, Y.C, 1988:** An investigation of the relationship between sub-Saharan rainfall and global sea surface temperatures. *Atmosphere-Ocean*, **26**, 118-138.

**Semazzi, F.H.M, Burns, B, Lin N.H and Schemm, J.K, 1996.** A GCM study of the teleconnections between the continental climate of Africa and global sea surface temperature anomalies. *Journal of climate*, **9**: 2480-2497.

**Smith, T.M, Reynolds, R.W, Livezey, R.E and Stokes, D.C, 1996:** Reconstruction of historical Sea Surface temperature using empirical orthogonal functions. *J.Clim*, **9**, 1403-1420.

**Von Storch, H and Francis W. Z, 1999:** Statistical Analysis in climate Research, Cambridge Univ.press, pp. 113-114.

**Ward, M.N, 1992:** Provisionally corrected surface wind data, worldwide ocean atmosphere surface fields and Sahelian rainfall variability. *J.Climatol.* **5**, 454-475.

**Ward, M.N and Hoskins, B.J, 1996;** Near-surface wind over the global ocean 1949-88. *J.Climate*, **9**, 1877-1895.

**Webster PJ, 1987.** The elementary monsoon. In Monsoons, Fein J, Stephens P (eds). J.Wiley and Sons: New York; 3-32.

**Webster PJ, Na VOM, Palmer TN, Shukla J, Tomas RA, Yanai M and Yasunari T, 1998;** Monsoons: processes, predictability, and the prospects for prediction. *Journal of Geophysical Research* **103**: 14451-14510.

**Webster, P.J, Loschnigg, J.P, Moore, A.M and Leben, R.R, 1999:** The Great Indian Ocean warming of 1997-1998; evidence of coupled oceanic-atmospheric instabilities. *Nature*, **401**, 6751, 356-360.

**Yasunari, T, 1991:** The monsoon year – a new concept of the climatic year in the tropics. *Bull.Amer.Meteor.Soc.* **72**, 1331-1338.

**Xie P and Arkin, P.A, 1997:** Global precipitation: A 17-year monthly analysis based on gauge observations, satellite estimates and numerical model outputs. *Bull. Americ. Met. Soc.* **78**, 2539-2558.

**Zhu, B and Wang, B, 1993:** The 30-60 day convective seesaw between the tropical Indian and western pacific oceans. *J.Atmos.sci.* **50**, 184-199.

## Appendix

### Derived parameters

#### 1.0 Moisture flux

The horizontal moisture flux for a given level can be obtained from the product of specific humidity and horizontal wind vector. In the tropics, the bulk of the horizontal transport of moisture takes place below 700hPa (e.g. Newell et al 1972). The lower tropospheric wind field can therefore, determine most of the moisture transport. Previous studies (e.g. Goddard and Graham, 1999) observed 850hPa level to be the most representative of the behaviour of the vertical integrated moisture flux over East Africa. In this study the 850hPa level is used as well for analyses of moisture flux over the region.

#### 2.0 Divergence and velocity potential

There is a useful decomposition of the horizontal wind field into distinct contributions: uniform translation, horizontal divergence, vorticity and deformation. Bluestain (1992, pp87-113) describes these and provides ways of computing their magnitude. The physical properties of the horizontal two-dimensional wind fields ( $V$ ) can be described by considering the rotational and irrotational terms, also known as nondivergent and divergent respectively.

$$\text{That is: } \mathbf{V} = \mathbf{V}\psi + \mathbf{V}\chi \quad (1)$$

where  $\psi$  is the stream function (rotational) part of the wind, while  $\chi$  is the velocity potential (irrotational). The divergence is of importance because it controls the evolution of the wind field and resultant dynamics through the vorticity equation. Only in the presence of horizontal divergence (Bluestein, 1992, pp. 87-113) will there be vertical motion and the possibility of the release of latent heat from the moisture flux.

## Appendix 2

The contribution to the velocity field from pure divergence can be singled out for further description. Divergence is defined (Bluestein, 1992) as

$$\frac{\partial u}{\partial x} + \frac{\partial v}{\partial y} = \delta = \nabla_h \cdot \mathbf{V} \dots \dots \dots (2)$$

$u$  = zonal wind component

$v$  = meridional wind component

$x$  = longitudinal distance

$y$  = latitudinal distance

The subscript (h) means that derivatives are computed on a horizontal surface.

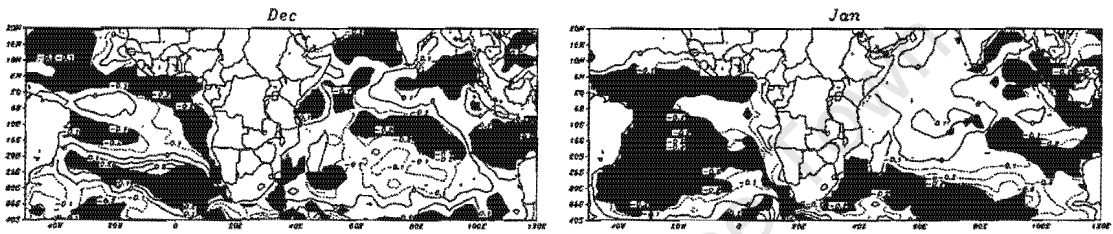
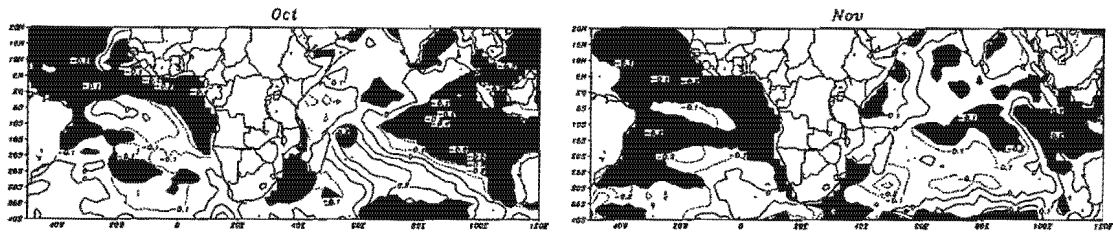
Velocity potential of pure divergent field, is defined as follows:  $\mathbf{V} = -\nabla_h \chi$  while

$\nabla_h \cdot \mathbf{V} = -\nabla_h^2 \chi = \delta$  which is the divergent contribution to the total wind field. The isolines of this pure divergence field have vector rates of change, which are the divergent contribution of the wind field.

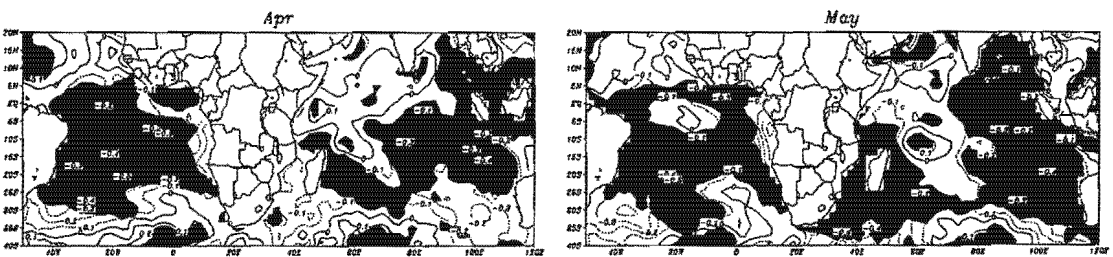
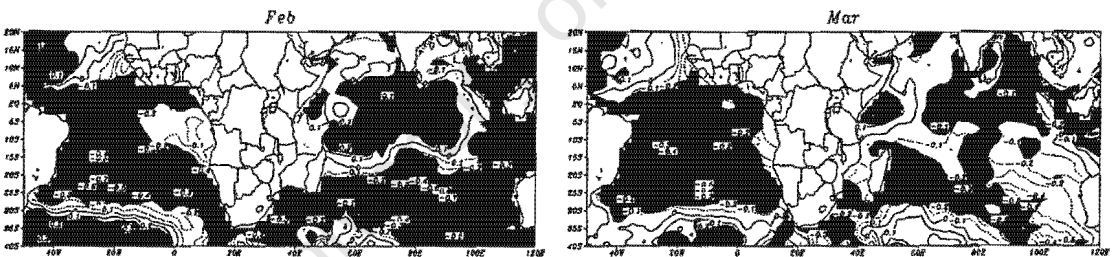
University of Cape Town

Appendix 3

Wet years Composite SST Anomaly



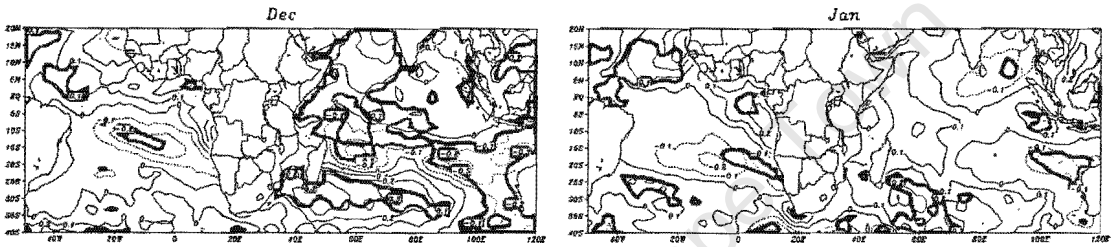
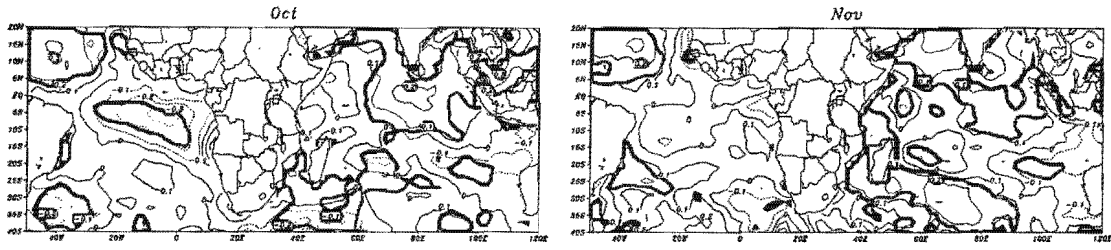
Wet years Composite SST Anomaly



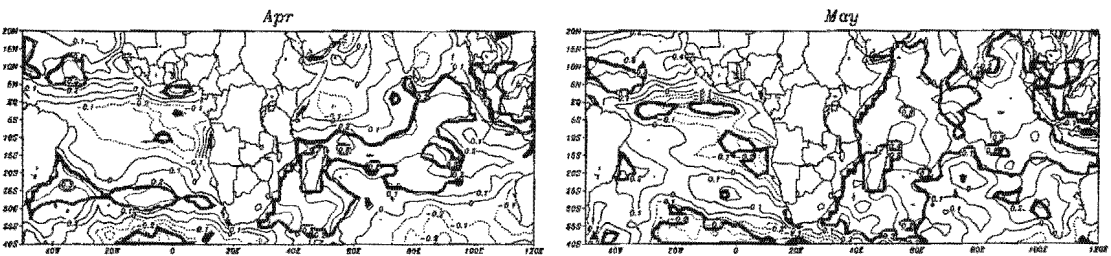
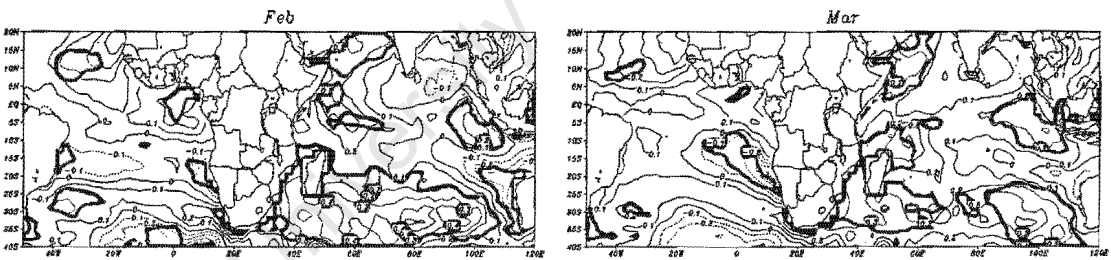
t-test for the wet composite SST anomalies

# Appendix 4

## Dry years Composite SST Anomaly



## Dry years Composite SST Anomaly



t-test for the dry composite SST anomalies